Department of Chemical and Energy Engineering

Synthesis, Optimization, and Kinetic Studies of Sulfonated Palm Biomass Magnetic Biochar Catalyst for Biodiesel Production Using Used Cooking Oil

Mohd Nurfirdaus Bin Mohiddin

0000-0003-0994-7332

This thesis is presented for the Degree of
Doctor of Philosophy
of
Curtin University

July 2023

DECLARATION

To the best of my knowledge and belief this thesis contains no material previously published by any other person except where due acknowledgment has been made.

This thesis contains no material which has been accepted for the award of any other degree or diploma in any university.

Signature: ……..

Date: ……25th July 2023……..

ABSTRACT

Biodiesel has recently gained popularity as an alternative biofuel to substitute fossil fuel. Biodiesel's global demand has increased significantly over the last decade. The continuous rise in demand requires new technology to produce biodiesel more efficiently and environmentally. Current biodiesel technology mainly produces biodiesel from the transesterification of edible crop oils. Due to ethical issues related to the utilization of edible oils, inedible oil is deemed as a promising feedstock because it will eliminate the 'food versus fuel feedstock' problem created by edible plant oils. In order to eliminate the need for cultivation for inedible oil plants, waste oil such as used cooking oil (UCO) is seen as an attractive feedstock for biodiesel production. The usage of UCO as feedstock is also an environmental way to dispose of waste. A catalyst is usually used to expedite the biodiesel transesterification reaction. Turning oil palm waste such as palm kernel shell (PKS), an oil palm frond (OPF), and empty fruit bunch (EFB) into biochar catalyst for biodiesel production is both economically and environmentally attractive. Oil palm solid wastes have high carbon content and usually dispose of in a landfill or turned into boiler fuel. The usage of oil palm waste as a biodiesel transesterification catalyst reduces the amount of oil palm waste disposed of in the landfill, at the same time it creates another value-added product from the waste. In transesterification of biodiesel, heterogeneous catalyst separation through centrifugation and filtration requires high energy and long time. Sulfonated magnetic biochar catalyst (SMBC) utilization can enhance the catalyst separation process and reusability. As SMBC utilization is still on the laboratory scale and studies on the utilization of SMBC in biodiesel production are still limited, many aspects are still unknown. Knowing the kinetics of biodiesel production using SMBC is beneficial for designing and scaling up biodiesel production on an industrial scale. Hence, this study includes the kinetic studies specifically designed for the magnetic catalyst. This research is addressing the abovementioned research gaps. In this research, SMBC was synthesized from PKS, OPF, and EFB and then characterized via FESEM, EDX, BET, TGA, FTIR, neutralization titration, and VSM. Based on these characterization results, the most suitable biomass for SMBC synthesis is EFB. The optimum SMBC synthesis parameters were acquired using the Taguchi method. The optimum parameters for the SMBC synthesis are at $FeCl_3 \cdot 6H_2O$ concentration of 1.5M, carbonization temperature of 800 °C and H_2SO_4 concentration of 2.5M. The synthesized catalyst was used to produce biodiesel from UCO. Biodiesel production parameters were studied using the central composite design-based response surface method (RSM-CCD). The optimized reaction parameters which are at a catalyst loading of 10.12 wt%, methanol to oil molar ratio of 28, reaction temperature of 70°C, and reaction time of 8 h gave a maximum yield

of 95.87%. The catalyst was reused for five cycles to determine its reusability. After five cycles, the biodiesel yield dropped to 70.16%. Biodiesel production via transesterification of UCO using SMBC synthesized from EFB at the optimized condition is reported to conform to the pseudo-irreversible first-order kinetic with an activation energy of 31.77 kJ mol^{-1}. Finally, this research has successfully investigated the optimized SMBC synthesis, reaction and mechanism of producing biodiesel from UCO, as well as its reaction kinetics.

ACKNOWLEDGEMENTS

All praise and gratitude to Allah, the Most Gracious and Most Merciful for His blessing and the strength gave to me to complete this research.

I would like to express my deepest gratitude and appreciation to my principal supervisor, Dr. Tan Yie Hua and my co-supervisor, Dr. Jibrail Kansedo for their valuable guidance and support throughout this research. My appreciation also goes to my associate supervisors, Assoc. Prof. Dr. Mubarak Mujawar of Universiti Teknologi Brunei, and Prof. Lee Keat Teong of Universiti Sains Malaysia, who have provided me with valuable help and support.

I would like to acknowledge all laboratory technicians and technical officers of the Chemical and Energy Engineering Department, Faculty of Engineering and Science, Curtin University Malaysia who have provided me with valuable help and support.

My deepest gratitude also goes to Ministry of Education, Malaysia for their generous financial support under Fundamental Research Grant Scheme (FRGS/1/2019/TK10/CURTIN/03/1), and Curtin University Malaysia for providing the Curtin Sarawak Higher Degree Research Fee Waiver.

Last but not the least, my warmest gratitude goes to my parents, Mohiddin bin Narawi and Habibah binti Boret as well as my siblings, my friends, and my fellow postgraduates in Curtin University Malaysia. Their kind help and moral supports assisted me in completing this research.

TABLE OF CONTENT

Page

LIST OF FIGURES

Page

LIST OF TABLES

Page

LIST OF ABBREVIATION

AD	Acid density
Al_2O_3	Aluminium oxide
Am^2/kg	Mass magnetization
ANOVA	Analysis of variance
ASTM	American Standards for Testing Materials
ATR	Attenuated Total Reflectance
BET	Brunauer- Emmett-Teller
Bi_2O_3	Bismuth(III) oxide
BJH	Barrett-Joyner-Halenda
$C_2HF_3O_2$	Trifluoroacetic acid
$C_4H_4O_6HK$	Potassium hydrogen tartrate
C_4SO_3H	Butyl carbon chain
Ca	Calcium
$Ca(OCH_3)_2$	Calcium methoxide
$CaCO_3$	Calcium carbonate
CaO	Calcium oxide
$CaTiO_3$	Calcium titanate
$CaZrO_3$	Calcium zirconate
CC	Catalyst concentration
CCD	Central composite design
CeO_2	Cerium(IV) oxide
CO	Carbon monoxide
Co	Cobalt
CO_2	Carbon dioxide
CPO	Crude palm oil
CT	Carbonization temperature
DOE	Design of experiment
DTA	Differential thermal analysis
EDX	Energy Dispersive X-Ray

EU	The European Union
FAAE	Fatty acid alkyl ester
FAME	Fatty acid methyl ester
FC	$FeCl_3 \cdot 6H_2O$ concentration
Fe	Iron
$Fe_2(SO_4)_3$	Iron(III) sulfate
Fe_3O_4	Iron(II, III) oxide
$FeCl_3$	Iron(III) chloride
$FeCl_3 \cdot 6H_2O$	Iron (III) chloride hexahydrate
FeO(OH)	Iron(III) oxide-hydroxide
FESEM	Field emission scanning electron microscope
FFA	Free fatty acid
FOG	Fats, oils and grease / waste oil
FTIR	Fourier transform infrared
G	Gauss
GOM	Government of Malaysia
h	Hour
H_2SO_4	Sulfuric acid
$H_3PW_{12}O_{40}$	Phosphotungstic acid
HC	Sulfuric acid concentration
H_c	Coercivity
HPA	Heteropolyacid
HTC	Hydrothermal carbonization
I_2	Iodine
K_2CO_3	Potassium carbonate
K_2CO_3	Potassium carbonate
KF	Potassium fluoride
kg oil/ha	Kilogram of oil per hectare
KNO_3	Potassium nitrate
KOH	Potassium hydroxide

La_2O_3	Lanthanum oxide
LHHW	Langmuir-Hinshelwood-Hougen-Watson
M	Molarity (mol per liter)
M:O	Methanol to oil ratio
m^2/g	Squared meter per gram
mg KOH/g	Milligram of KOH equivalent per gram
MgO	Magnesium oxide
min	Minute
MM	Mass saturation magnetization
mmol/g	Millimole per gram
MPOB	Malaysian Palm Oil Board
MT	Metric tonne
Na_2SiO_3	Sodium silicate
NaOH	Sodium hydroxide
NaX	Zeolite X
nm	Nanometer
NO_x	Nitrogen oxides
OPF	Oil palm frond/fibre
OPW	Oil palm waste
PIFO	Pseudo irreversible first order
PISO	Pseudo irreversible second order
PKS	Palm kernel shell
PRSO	Pseudo reversible second order
RP	Reaction period
RSM	Response surface method
RT	Reaction temperature
SA	BET surface area
SD	Standard deviation
SFC	Specific fuel consumption
SMBC	Sulfonated magnetic biochar catalyst

SN	Signal to noise
SO_2	Sulfur dioxide
SO_3	Sulfur trioxide
SO_3CF_3	Triflate anion
SO_x	Sulphur oxides
sp.	Species
$Sr_3Al_2O_6$	Strontium aluminate
TGA	Thermogravimetric analysis
TiO_2	Titanium dioxide
UCO	Used cooking oil
UK	The United Kingdom
vol:vol	Volume ratio
VSM	Vibrating sample magnetometer
WO_3	Tungsten trioxide
wt%	Weight percentage
ZnO	Zinc oxide
ZnSe	Zinc selenide
$Zr_{0.7}H_{0.2}PW_{12}O_{40}$	Zirconiumdodecatungstophosphate
ZrO_2	Zirconium dioxide
σ_s	Mass saturation magnetization

CHAPTER 1
INTRODUCTION

1.1 Background

1.1.1 Fossil Fuel Detriment

The current global consumption of fossil fuels is increasing steadily as a result of the growing global population and energy demand (Zohuri and McDaniel 2021). Petroleum plays a huge role in powering our accommodation and transportation. The modern exploitation of petroleum began as early as the 19th century (Chisholm 2018). The adverse environmental effect was constantly associated with petroleum use. The carbon dioxide (CO_2), carbon monoxide (CO), nitrogen oxides (NO_X), and sulfur oxide (SO_X) gases, which are produced from the combustion of fossil fuels, are termed 'greenhouse gases' because of their effect on global warming (Ljupkovic et al. 2014). These gases are toxic and will form acid rain when reacted with atmospheric water (Mat Yasin et al. 2017). Acid rain can cause damage to buildings and reduce the pH value of soil and small bodies of water, disrupting the natural vegetation and living organisms in the vicinity (Hughes 2017). Unsustainable petroleum consumption and non-renewability intensified the progress of various alternative modes of fuel transportation. Biofuel, energy produced from renewable sources, can reduce the dependability towards petroleum and at the same time tackle the environmental problem possessed by petroleum combustion. According to the International Energy Agency, transportation fueled by petroleum accounted for 92.16% in 2015. However, biofuel only fueled 2.81% of the world's transportation (International Energy Agency 2017).

Our dependence on ever-depleting fossil fuels is alarming. It became evident when the oil glut hit the world in 2012, the production of biodiesel keeps on increasing despite the falling crude oil price, where biodiesel's price previously more favorable when the price of crude oil was high (Naylor and Higgins 2017). Biodiesel is one of the most popular and promising alternative energy in reducing our dependence on fossil fuels. The environmentally friendly aspect of biodiesel makes it an excellent choice for an alternative source of energy. Biodiesel produces cleaner exhaust emissions in the form of lower soot, hydrocarbon, and CO compared to petrodiesel (Y. Zhang et al. 2022; J. Liu et al. 2023). Biodiesel has become one of the most preferred biofuels for the transportation sector due to its biodegradability and less toxicity exhaust gas emission (Y.-A. Chen et al. 2019; Wong et al. 2022). However, the major drawback of biodiesel is its cost (Kirubakaran and Arul Mozhi Selvan 2018).

1.1.2 Biodiesel in Malaysia

Biodiesel is primarily produced from palm oil in Malaysia (Nambiappan 2018). Biodiesel development in Malaysia began as early as 1981. Malaysian Palm Oil Board (MPOB) is the main driver behind all palm oil based biodiesel research and development all around Malaysia (Malaysian Biodiesel Association 2023). In 2007, the Biofuel Industry Act was passed by the Malaysian parliament. The act provides legislation over the biodiesel blending mandate and the licensing of downstream activities. The Biofuel Industry Act 2007 dictates the compulsory blending of biodiesel blending for commercial diesel. B5 blending was planned to be implemented in 2008 but was delayed until 2011 due to high crude palm oil prices (Naylor and Higgins 2017). The production of biodiesel prior to the 2011 introduction of the B5 mandate was mainly for export (including re-export) and non-road use (Malaysian Biodiesel Association 2018). The mandatory blending ratio for biodiesel in Malaysia has been increasing steadily since 2011. With this increment, domestic biodiesel production also increases. The Malaysian annual biodiesel production in 2011 was 173 kilo-metric-tons (kMT) increased significantly to 1,423 kMT in 2019 (Unnithan 2022). Biodiesel production was significantly increased from 2011 onwards due to the introduction of the biodiesel blending mandate in 2011 (Mahayuddin et al. 2022). The Malaysian biodiesel blending mandate has increased steadily from B5 in 2011 to the current B10 in 2019 (Attorney General's Chambers of Malaysia 2019). The proposed B20 blending mandate nationwide from the year 2020 was postponed indeterminately. On the other hand, Langkawi, Labuan, and Sarawak have adopted the B20 blending from the year 2020 (Unnithan 2022). The export of biodiesel was somewhat inconsistent due to the varying demand by the importing countries such as China, the United Kingdom (UK), and Japan, especially from countries in the European Union (EU), which are the major export destination of Malaysian biodiesel (Wahab 2022).

1.1.3 Biodiesel Production

Biodiesel is a fuel consisting of long-chain fatty acids and mono-alkyl esters produced from vegetable oils or animal fats (ASTM International 2020). There are various ways to produce biodiesel, such as esterification (Rokhum et al. 2022), interesterification (Akkarawatkhoosith et al. 2020), and transesterification (Hazrat et al. 2022). Esterification is usually used to produce biodiesel from high acid-value oil feedstock (Rokhum et al. 2022). Interesterification can produce biodiesel as well as other high-value by-products instead of glycerol (Akkarawatkhoosith et al. 2020). However, transesterification is the most common and preferred method to produce biodiesel. This process produces biodiesel of excellent

quality. Its overall operation cost is relatively lower compared to other biodiesel production methods, owing to the simplicity of the production reaction (Atabani et al. 2012; D. Singh et al. 2020).

Biodiesel production needs triglyceride from oil or fat feedstock and alcohol feedstock. Biodiesel is conventionally produced from edible vegetable oil and animal fat (Mathew et al. 2021). These high-quality feedstocks comprise most of biodiesel production cost. One of the reasons for such a high price is the competition for edible oil between biofuel producers and the food industry. This situation creates food security as a result of the increase in the non-food usage of agricultural products (Dey et al. 2021). A non-edible and inexpensive alternative feedstock for biodiesel production has been the focus of a number of studies in recent times including non-edible fats, oils and grease (FOG) such as animal fats (Yari et al. 2022), used cooking oil (UCO) (Takase 2022), yellow or brown grease (Bashir et al. 2020), and sludge oil (Abdulhussein Alsaedi et al. 2022) that can absolutely become the feedstock of choices in order to avoid competition for feedstock with the food industry. These types of waste are readily available from municipal and industrial waste (N. P. L. Tran et al. 2019). UCO may contain up to 20% FFA. However, 1% to 9% content of FFA is normally observed. Meanwhile, waste yellow or brown grease contains up to 80% FFA (Ghosh and Halder 2022). Low FFA content is vital in order to increasing the biodiesel production rate and reducing unwanted soap formation. In this case, UCO is a much better biodiesel feedstock due to its low content of FFA (J. Zhang 2017). Alcohol is another feedstock needed for biodiesel production. The types of alcohol used for biodiesel production can influence its properties. Although longer-chain alcohols such as butanol (Musil et al. 2018), tert-butanol, and isopropanol (Likozar and Levec 2014) usage as biodiesel alcohol feedstock has been studied, their low conversion rate keeps researchers interest in short-chain alcohol such as methanol and ethanol (Mahdi et al. 2023). The lower cost of methanol production is also one of the factors making it a favorable choice for industrial biodiesel production.

Catalysts for biodiesel production are categorized into three types: homogeneous, heterogeneous, and enzyme (Karmakar and Halder 2019). Homogeneous catalysts can be further classified into two types: homogeneous base catalysts (Al-Humairi et al. 2022) and homogeneous acid catalysts (Guldhe et al. 2017). Homogeneously catalyzed transesterification is the most favorable process for producing biodiesel due to its low energy consumption and simplicity (Al-Humairi et al. 2022). However, it does have a number of drawbacks. Homogeneous catalysts are almost impossible to recover after the reaction. This has led to the disposal of the catalysts and by-product problems as most conventional homogeneous catalysts

are not biodegradable (Ghosh and Halder 2022). Reusing a homogeneous catalyst is impossible in this sense. The solution to these problems can be overcome by using a heterogeneous catalyst. Heterogeneous catalysis has been widely studied for the reason that it is easier to separate and reuse if needed (Ghosh and Halder 2022). The heterogeneous catalyst can be produced from a renewable source, such as industrial waste materials (Mardhiah et al. 2017). Similar to homogeneous catalysts, heterogeneous catalysts can be further classified into two categories; heterogeneous base catalysts (Bargole et al. 2021) and heterogeneous acid catalysts (Yu et al. 2021). Heterogeneous catalysts can be synthesized from various material sources such as waste shells (Mohd Nurfirdaus Mohiddin et al. 2020), biomass ash (Gouran et al. 2021), biochar (Yameen et al. 2023), and activated carbon (S. H. Y. S. Abdullah et al. 2017). In recent times, biomass-derived heterogeneous catalysts have caught the interest of researchers around the globe. The idea of turning industrial by-products into a catalyst for biodiesel production is economically and environmentally attractive (Cheng and Li 2018). One such material used for a catalyst precursor is biochar. Biochar is naturally extremely porous and has a high specific surface area (Yameen et al. 2023). Both of these characteristics make biochar a suitable material for a catalyst precursor (Kastner et al. 2012). The abundance of alkali and alkali earth metal elements in biochar and its ash was also reported as giving good catalytic activity for biodiesel transesterification (Shan et al. 2018). Biochar has been impregnated with ferrite ions in order to make it ferromagnetic and enhance the catalyst separation process and reusability (Rahimi et al. 2021). Magnetic catalyst requires lower energy for catalyst-product separation compared to other non-magnetic catalysts (H. Li et al. 2021). In addition, conventional heterogeneous catalyst also is harder to separate in high viscosity product and takes longer time compared to magnetic catalyst (F. Zhang et al. 2016). The amount of magnetic catalyst that could be recovered after a reaction is higher compared to non-magnetic catalysts. As high as 96% of used catalyst can be recovered when a magnetic catalyst is employed (F. Zhang et al. 2015). A magnetic catalyst also yielded more than 90% biodiesel after 7 cycles of reaction (P. Guo et al. 2012). All in all, sulfonated magnetic biochar catalyst (SMBC) is still in the laboratory research stage. The industrialization of this technology will need more studies, especially in the area of reaction mechanisms and process optimization (Tamjidi et al. 2021). This can be achieved by studying the relationship between the physicochemical properties of the catalyst and its catalytic activity.

1.2 Research Problem Statement

Biodiesel has received great demand all over the world due to its benefits for the environment. It also reduces the overall consumption of fossil fuels. Most conventional biodiesels are produced from edible vegetable oil. This makes biodiesel economically unattractive as competition is induced between biodiesel producers and the edible oil industry. Therefore, studies have searched for some alternative inexpensive and sustainable feedstocks (Ambat et al. 2018). Inedible plant oil has been studied as an oil feedstock for biodiesel production. However, this oil source needs cultivation and extraction processes (B. Abdullah et al. 2019). Another inedible oil source, UCO, is readily available as a waste. Its application as an oil feedstock for biodiesel production is environmental and economic (Nahas et al. 2023).

A catalyst is used in order to expedite the biodiesel-producing transesterification reaction. Homogeneous catalysts such as NaOH and potassium hydroxide (KOH) are typically used. However, this type of catalyst has limitations. A homogeneous catalyst cannot be separated post-reaction, which means it can only be used once. Soap formation due to water washing after the reaction is also a problem associated with the homogeneous catalyst. On the other hand, a heterogeneous catalyst can overcome these limitations. The major difference between a homogeneous catalyst and a heterogeneous catalyst is a heterogeneous catalyst can be separated from other reactants or products, while a homogeneous catalyst cannot be separated. This means a heterogeneous catalyst can be easily separated and reused to minimize soap formation, and some studies suggested that it eliminated saponification altogether (Mardhiah et al. 2017). Nonetheless, the time and energy used for heterogeneous catalyst separation through centrifugation and filtration after transesterification can be decreased further by impregnating ferrite ions onto the catalyst. This impregnation resulted in the catalyst becoming ferromagnetic and can be separated easily by attracting it with an external magnetic field. This attribute is very useful for separating the catalyst from a viscous fluid. In an industrial sense, magnetizing the catalyst will simplify the separation process and reduce the biodiesel separation cost (P. Guo et al. 2012). Nevertheless, no study has investigated the optimum synthesis parameters for magnetic catalyst, and only few have conducted kinetic study using magnetic catalyst in biodiesel production.

Oil palm plantations generate a considerable amount of waste. Palm kernel shells (PKS), oil palm fronds (OPF), and empty fruit bunches (EFB) are examples of biomass wastes that are usually disposed of in a landfill or burned as boiler fuel (Prasertsan and Prasertsan 1996). When exposed to water in the landfill, PKS, OPF, and EFB react with water and bacteria to produce methane gas, which is one of the greenhouse gases (Liew et al. 2018). The landfill

disposal cost for oil palm waste is also astronomical in some countries owing to the fact that this type of waste is difficult to decompose (Prasertsan and Prasertsan 1996). PKS, OPF, and EFB have a high content of carbon (Liew et al. 2018). For this, it usually undergoes pyrolysis or gasification and turns into biochar (Sadhukhan et al. 2018). Biochar and its ash have one of the best physical properties in terms of catalytic activity and highly specific surface area (Cheng and Li 2018). The abundance of alkali and alkali earth metal elements in biochar and its ash was also reported as giving good catalytic activity for biodiesel transesterification (Shan et al. 2018). Catalyst synthesized from biochar costs relatively lower compared to homogeneous catalyst. At the same time, it is also a sustainable source of catalyst as the synthesis converts industrial waste into a functional catalyst (Cheng and Li 2018).

Additionally, the reaction mechanism and kinetics of biodiesel transesterification from UCO catalyzed by SMBC have not been studied yet. Knowing the reaction's kinetic model is important to select the best parameters for the reaction process and forecasting the product yield in order to increase the energy process and cost efficiency (Opara and Oh 2022). This step is crucial in order to translate the biodiesel production process from laboratory-scale to industrial scale (Tien Thanh et al. 2022). Therefore, this research investigates the synthesis of PKS, OPF, and EFB into SMBC and its employment in producing biodiesel from UCO.

1.3 Research Questions

The following research questions are addressed in order to deal with the research gaps:

i. What are the characteristics and the synthesis parameters of the magnetic catalyst synthesized from biochar?
ii. What are the optimum synthesis parameters of the magnetic catalyst synthesized from biochar?
iii. What is the relationship between the reaction parameters of SMBC-catalyzed transesterification and the biodiesel yield, and how reusable and regenerative is the SMBC?
iv. What are the characteristics of the biodiesel produced from UCO using SMBC?
v. How do the reaction mechanism and kinetics of the transesterification using SMBC?

1.4 Aim and Objectives

This study aims to understand the SMBC synthesis, reaction, and separation mechanism in producing biodiesel from used cooking oil. This can be achieved through several specific objectives, as follow:

i. To synthesize and characterize the sulfonated magnetic biochar catalyst from PKS, OPF, and EFB.
ii. To optimize the synthesis of the sulfonated magnetic biochar catalyst from PKS, OPF, and EFB.
iii. To study the catalytic activity, regeneration, and reusability of the sulfonated magnetic biochar catalyst in optimized biodiesel production from used cooking oil.
iv. To characterize the biodiesel produced from used cooking oil using sulfonated magnetic biochar catalyst.
v. To investigate the mechanism and kinetics of magnetic biochar-catalyzed biodiesel production.

1.5 Significances

The results and outcomes of this research will contribute to society and green catalysis research. This research provides a better understanding of the synthesis and characteristics of SMBC produced from different biomass materials. The optimization of the SMBC synthesis gives further insight into the best parameters to produce SMBC of the highest quality. Besides that, by studying the catalytic activity and reusability of SMBC in biodiesel production from UCO, the integration of SMBC for industrial biodiesel production can be realized. The characterization of the biodiesel produced using SMBC ensures that the biodiesel meets industrial standards. Moreover, this research also investigates the kinetics of UCO biodiesel production using SMBC. The kinetics study is important for designing the scale-up.

The outcomes of this research will benefit the biofuel and oil palm industry in several ways. The usage of UCO as biodiesel feedstock will create an alternative solution for this type of waste instead of being disposed of. The utilization of oil palm biomass-based biochar reduces the amount of biomass waste from the agriculture industry going to landfill. The employment of a magnetic catalyst will reduce energy consumption during the catalyst-biodiesel separation and wastewater generation for biodiesel production. All this will translate into lower capital and production expenditure for the biofuel and oil palm industries and better waste management practices.

From the social point of view, this research will create more job opportunities as a direct effect of the technological advancement of biodiesel production. Apart from that, this advancement will also improve the economic standards of current workers by benefiting from the increased productivity of the industry.

1.6 Scope of Study

i. In this research, PKS, OPF, and EFB were converted into SMBC. The produced catalyst was characterized. SMBC was synthesized using a series of processes, i.e. impregnation – pyrolysis – sulfonation. The characterization of SMBC was carried out using field emission scanning electron microscope (FESEM), energy dispersive X-ray (EDX), Brunauer – Emmett – Teller (BET), thermogravimetric analysis (TGA), Fourier transform infrared (FTIR), neutralization titration, and vibrating sample magnetometer (VSM).

ii. The optimum parameters of SMBC synthesis were obtained via process optimization using Taguchi method. Three parameters or the factors studied in this method are the concentration of ferric chloride hexahydrate ($FeCl_3 \cdot 6H_2O$) used for biomass impregnation, the carbonization temperature for pyrolysis, and the concentration of sulfuric acid (H_2SO_4) for the catalyst sulfonation. Based on published literature, the concentration of $FeCl_3 \cdot 6H_2O$ and H_2SO_4 investigated in this method was between 1.5M and 2.5M. While the carbonization temperature of the biomass was between 600°C and 800°C. The responses considered for the Taguchi method are SMBC's BET specific surface area, acid density, and mass saturation magnetization.

iii. Transesterification process parameters to convert UCO into biodiesel were studied. The parameters that were studied are catalyst loading, methanol–oil molar ratio, reaction temperature, and reaction period. The optimization of these parameters was carried out using the response surface methodology – central composite design (RSM – CCD) module of Design-Expert version 12 software. The range on which the parameters were studied was based on the values of optimized transesterification parameters of published literature. The catalyst concentration was studied between 4 and 16 wt%, methanol–oil molar ratio was studied between 10 and 30, reaction temperature was studied between 50 and 70 °C, and reaction period was studied between 2 and 10 hours. The response used for this method was the biodiesel yield. The reusability of the SMBC without regeneration was studied for five cycles. Other parameters that might influence the biodiesel yield, such as reaction pressure, stirring rate, and stirring mode, were not studied but kept constant.

iv. The characterization of the biodiesel produced was done and compared based on methods designated by ASTM D6751 and EN 14214 biodiesel standards. The studied properties were flash point, density at 15°C, specific gravity, API gravity at 60°C, kinematic viscosity at 40°C, cetane index, cloud point, and pour point. In addition, the

fatty acid profile of the biodiesel was acquired using gas chromatograph (GC) fitted with mass spectrometer detector (MSD).

v. Kinetic study was carried out on the transesterification reaction by investigating the effect of reaction temperature and time. Three reaction kinetic models were proposed based on mostly reported kinetic models from published literature, i.e. pseudo-irreversible first order kinetic, pseudo-irreversible second order kinetic, and pseudo-reversible second order kinetic. The reaction temperature investigated in this study ranged between 50°C and 70°C. Meanwhile, the reaction time was investigated between 5 and 480 min. The kinetic study carried out in this research only limited to the transesterification step in biodiesel production.

1.7 Thesis Layout

Chapter 1 (Introduction) lays the background of the research along with the research problem statement, aim and objectives of the research, significance, and the scope of the research.

Chapter 2 (Literature Review) assesses published literature and basic principle, which are related to the current research. The results and outcomes of these works of literature are reviewed. This chapter ends with the research gap for this research.

Chapter 3 (Methodology) describes the experimental procedures and methods for catalyst and biodiesel synthesis, catalyst and biodiesel characterization, catalyst reusability study, and the reaction mechanism study.

Chapter 4 (Results and Discussion) shows and discusses results from the synthesis and characterization of catalyst and biodiesel.

Chapter 5 (Conclusion) presents the conclusion of this research. Future recommendations are also included in this chapter.

CHAPTER 2
LITERATURE REVIEW

2.1 Overview

This chapter presents the published literature that was viewed and discussed in this research. Section 2.2 introduces biodiesel as an alternative biofuel. Section 2.3 discusses the literature on the subject of biodiesel production by transesterification. Section 2.4 presents the literature regarding the feedstock for biodiesel production. Section 2.5 presents the literature on the subject of the catalysts for biodiesel production. Section 2.6 presents the literature regarding process modeling and optimization. Section 2.7 presents the literature with respect to the effect of transesterification parameters on biodiesel yield. Section 2.8 discusses the literature that performed kinetic studies on transesterification. Finally, Section 2.9 presents the summary and research gap.

2.2 Biodiesel as Fuel

The term "biodiesel" had been used prior to 1988, and the first use of the word "biodiesel" as an article keyword was by Wang in the Taiyangneng Xuebao, a Chinese technical paper in 1988 (Knothe et al. 2010). The work on biodiesel started in 1937 through a Belgian patent by C. G. Chavanne (University of Brussels). The Belgian patent 422,877 was granted on 31st August 1937. The patent describes the acid-catalyzed transesterification of palm oil into ethyl esters, which are then used as diesel fuel. The patent also mentioned other oils and methyl esters (Knothe et al. 2010). In modern times, biodiesel is one of the many biofuels commonly used in the world. It is comprised of vegetable oils or animal fats derived from mono-alkyl esters of long chain fatty acids (ASTM International 2020). Biodiesel can be produced from various types of plant oils and animal fats; Thus, the physical and chemical properties of biodiesel vary from one feedstock to another (Tamjidi et al. 2021). Currently, two industrial standards are commonly referred to and abided by biodiesel producers to ensure the biodiesel produced meets the market quality. The standards are ASTM International (ASTM) D6751 (ASTM International 2020), which is mainly used in the USA, and EN 14214 (European Committee for Standardization 2010), which is mainly used in the EU (Mat Yasin et al. 2017). Apart from these two standards, Malaysian biodiesel manufacturers must abide by the Malaysian standard for biodiesel, MS 2008:2014 (Department of Standards Malaysia 2014). The summary of the property requirement by all three of the standards is shown in Table 2.1.

Table 2.1: B100 biodiesel property requirements by various international standards.

Property	**ASTM D6751**	**EN 14214**	**MS 2008:2014**
Flash point	min 130.0°C	min 101°C	min 120°C
Water and sediment	max 0.050 % vol	n/a	n/a
Kinematic viscosity, 40°C	1.9 – 6.0 mm^2/s	3.50 – 5.00 mm^2/s	3.50 – 5.00 mm^2/s
Sulfated ash content	max 0.020 % mass	max 0.020 % mass	max 0.020 % mass
Sulfur content	max 0.0015 % mass (Grade S15) max 0.05 % mass (Grade S500)	max 10.0 mg/kg	max 10.0 mg/kg
Copper strip corrosion	max No.3	Class 1	Class 1
Cetane number	min 47	min 51	min 51
Cloud point	-3 – 12°C	n/a	n/a
Carbon residue	max 0.050 % mass	max 0.30 % mass	n/a
Acid number	max 0.80 mg KOH/g	max 0.50 mg KOH/g	max 0.50 mg KOH/g
Free glycerin	0.020 % mass	max 0.02 % mass	max 0.02 % mass
Total glycerin	0.240 % mass	max 0.25 % mass	max 0.25 % mass
Phosphorus content	max 0.001 % mass	max 4.0 mg/kg	max 4.0 mg/kg
Distillation temperature	max 360°C	n/a	n/a
FAME content	n/a	min 96.5 % mass	min 96.5 % mass
Density at 15°C	n/a	860 – 900°C	860 – 900°C
Water content	n/a	max 500 mg/kg	max 500 mg/kg
Total contamination	n/a	max 24 mg/kg	max 24 mg/kg
Oxidation stability	n/a	min 6.0 hours	min 10.0 hours
Iodine value	n/a	max 120 g iodine/100 g	max 110 g iodine/100 g
Linolenic acid methyl ester	n/a	max 12.0 % mass	max 12.0 % mass
Polyunsaturated methyl esters	n/a	max 1.00 % mass	max 1 % mass

Table 2.1 continued.

Methanol content	n/a	max 0.20 % mass	max 0.20 % mass
Monoglyceride content	n/a	max 0.80 % mass	max 0.70 % mass
Diglyceride content	n/a	max 0.20 % mass	max 0.20 % mass
Triglyceride content	n/a	max 0.20 % mass	max 0.20 % mass
Group I metals (Na+K)	n/a	max 5.0 mg/kg	max 5.0 mg/kg
Group II metals (Ca+Mg)	n/a	max 5.0 mg/kg	max 5.0 mg/kg
Cold filter plugging point	n/a	n/a	max 15°C
References	(ASTM International 2010)	(European Committee for Standardization 2010)	(Department of Standards Malaysia 2014)

Biodiesel generally has a higher density than petrodiesel (Hanif et al. 2018). The long carbon chains of biodiesel give an attribute to its density. The greater the carbon number, the denser the biodiesel will be. The higher density of biodiesel could cause an increase in ignition delay and inferior fuel atomization (D. Singh et al. 2021). High-density biodiesel is also reported to emit a high amount of particulate matter and have incomplete hydrocarbon combustion. Nevertheless, these problems can be reduced by blending biodiesel with petrodiesel before using it to fuel a diesel engine in order to bring down the density value (Abdalla 2018).

The flammability of a fuel is defined by its flash point. The flash point is the minimum temperature at which a fuel starts to ignite. Flash point requirement doubles as a means to limit the amount of alcohol unreacted in a finished biodiesel fuel (ASTM International 2010). The flash point value of biodiesel has no effect on its combustion quality. Nonetheless, a flash point is regarded as vital in order to consider the storage, transportation, and handling methods of biodiesel fuel (Kolobeng et al. 2022; Zaharin et al. 2017).

Biodiesel acid value can be used as an indicator to quantify biodiesel quality (Changmai et al. 2021). The acid value of biodiesel is usually obtained and reported from the amount of KOH needed to neutralize the biodiesel sample, commonly in terms of mg KOH/g of sample. The acid value can indicate the quality of biodiesel by way of the value rises when the biodiesel

quality drops (Saluja et al. 2016). Another reason why a lower acid value is much preferred is that it lowers the chances of corrosion of the fuel supply line in a vehicle (Sakthivel et al. 2018).

The heating value of a fuel is a characteristic that corresponds directly to the amount of energy contained within the fuel. It is also known as the calorific value or heat of combustion (Abdalla 2018; Fassinou et al. 2010). The heating value is the quantity of heat discharged for the combustion of one gram of fuel to give off CO_2 and H_2O at its initial temperature and pressure (Fassinou et al. 2011). The heating value of biodiesel is commonly lower than that of petrodiesel. Biodiesel is usually blended with petrodiesel to increase the heating value to meet the requirement for vehicle use. The heating value of the biodiesel-petrodiesel blend falls between biodiesel and petrodiesel (M. M. Hasan and Rahman 2017). High percentage biodiesel blends with low heating value have been studied to have higher fuel consumption and lower power output (Ismail et al. 2014; Reddy et al. 2018; E. S. Tan et al. 2017).

Biodiesel has a high potential to become fully sustainable and renewable if the feedstock from which it is produced is managed appropriately and environmentally. Biodiesel is also biodegradable and non-toxic to both terrain and aquatic environments. The high flash point and low volatility of biodiesel make it safer to handle. Because its features are similar to petrodiesel, it can be used for the current infrastructure with little to no modification. The usage of biodiesel was reported to give little harmful gas emissions and improve engine lubricity (Mahmudul et al. 2017).

2.3 Biodiesel Production

Although biodiesel is a remarkable fuel, it still has some shortcomings. Improper usage and management of land in obtaining feedstocks might defeat biodiesel's status as a sustainable fuel. Biodiesel renewability can be challenged through the energy input required for production During engine tests in several studies, biodiesel was reported to increase fuel consumption, decrease overall power output, raise NOx emission, and show corrosion potential in the engine's fuel system. Above all, the largest obstacle for biodiesel is its overall production cost. The highest proportion of its production cost is for the feedstock (Firth 2014; Mat Yasin et al. 2017). Most conventional biodiesel produced from edible vegetable oil drives the high price of feedstock and disrupts food security (Abdulhussein Alsaedi et al. 2022; Hredzak and Le 2012).

2.3.1 Esterification

Esterification is usually used to produce biodiesel from high acid value oil feedstock (Rokhum et al. 2022). One mole of free fatty acid interacts with one mole of alcohol to create

one mole of biodiesel and one mole of water in the comparatively simple esterification reaction, as shown in Figure 2.1, where R_1 is a long-chain hydrocarbon, sometimes called fatty acid chains. As an endothermic process, the esterification process can be strongly impacted by certain operational factors, such as the temperature of the reaction, the amount of catalyst, and the oil-to-alcohol ratio. Mass transfer resistance, which refers to the immiscibility characteristic of glycerides and alcohol, may be overcome using a variety of techniques, including arduous mechanical agitation, supercritical conditions, microwave, ultrasonic, and hydrodynamic cavitation (Ahmed and Huddersman 2022).

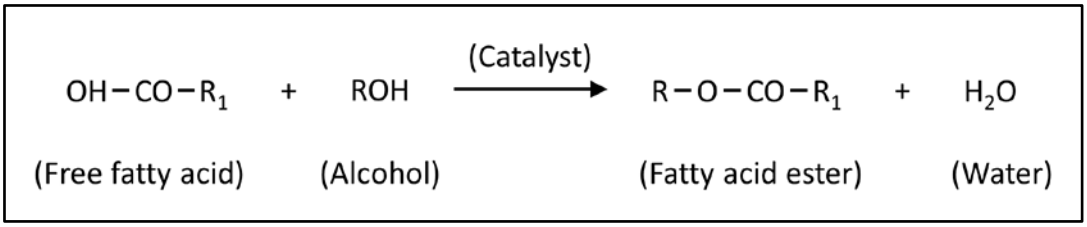

Figure 2.1: Esterification of free fatty acid.

2.3.2 Interesterification

Interesterification of triglycerides uses methyl acetate instead of methanol. It offers a possible substitute for transesterification since triacetin is produced instead of glycerol. During interesterification, one mole of triglyceride needs three moles of methyl acetate to synthesize one mole of triacetin and three moles of alkyl esters, as shown in Figure 2.2, where R_1, R_2, and R_3 are long-chain hydrocarbons, sometimes called fatty acid chains (Estevez et al. 2019). Triacetin, a valuable medicinal and cosmetic component, which also functions as an anti-knocking fuel additive that enhances combustion qualities in biodiesel blends, is created as a byproduct of using methyl acetate for interesterification (Akkarawatkhoosith et al. 2020). As a result, the FAME/triacetin combination may be utilized directly as fuel (Esan, Olabemiwo, et al. 2021).

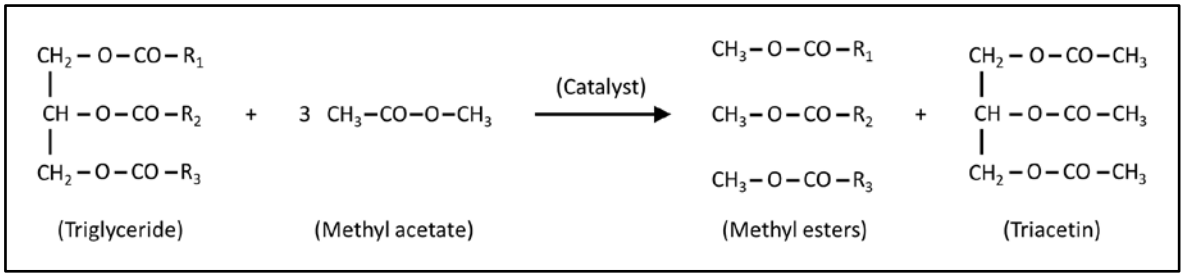

Figure 2.2: Interesterification of triglyceride and methyl acetate.

2.3.3 Transesterification

Transesterification, known as alcoholysis, is the most prominent and commonly used process to produce biodiesel. The transformation of vegetable oils and animal fats into biodiesel is aided by an appropriate catalyst in the presence of alcohol (Hazrat et al. 2022), and methanol is very widely used (Kirubakaran and Arul Mozhi Selvan 2018). Transesterification can be further categorized by the type of catalyst used in the process: homogeneous catalyst, heterogeneous catalyst, and enzymatic catalyst (Kirubakaran and Arul Mozhi Selvan 2018). Each catalyst used for biodiesel production has its own advantages and disadvantages, which are discussed in Section 2.5. Figure 2.3 shows a simplified overall reaction of transesterification (Leung et al. 2010).

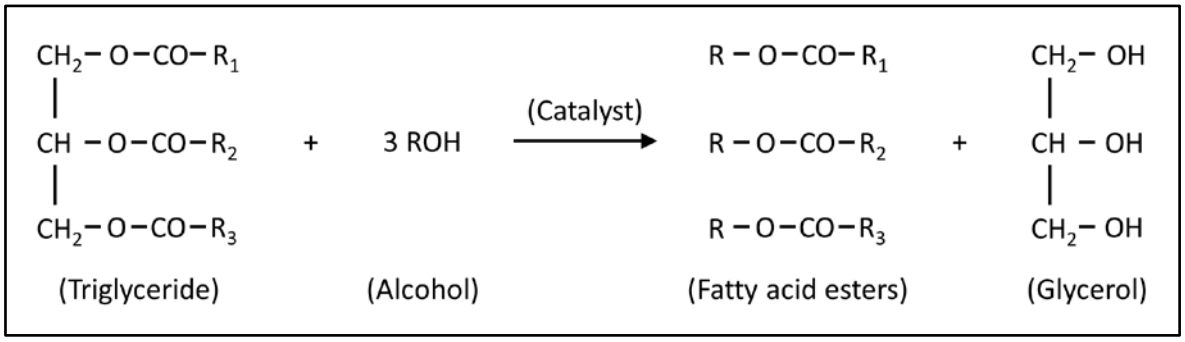

Figure 2.3: Transesterification of triglycerides.

Transesterification is generally favored by the industry due to its simplicity. The overall biodiesel production cost through transesterification also relatively lower than other production methods (Tamjidi et al. 2021). Transesterification needs low energy input and is very versatile in terms of feedstock types. Its reaction time is also relatively lower than other production methods (Ganesan et al. 2021). Some of the drawbacks of producing biodiesel through transesterification relative to other production methods are lower conversion rate, high likelihood of soap formation as shown in Figure 2.4 (Williams 2015), sensitivity to water and free fatty acid (FFA) content of the feedstock, and a large amount of wastewater production depending on the type of catalyst used (Ganesan et al. 2021; Y. H. Tan et al. 2015). Table 2.2 shows the summary of the advantages and disadvantages of each biodiesel producing process.

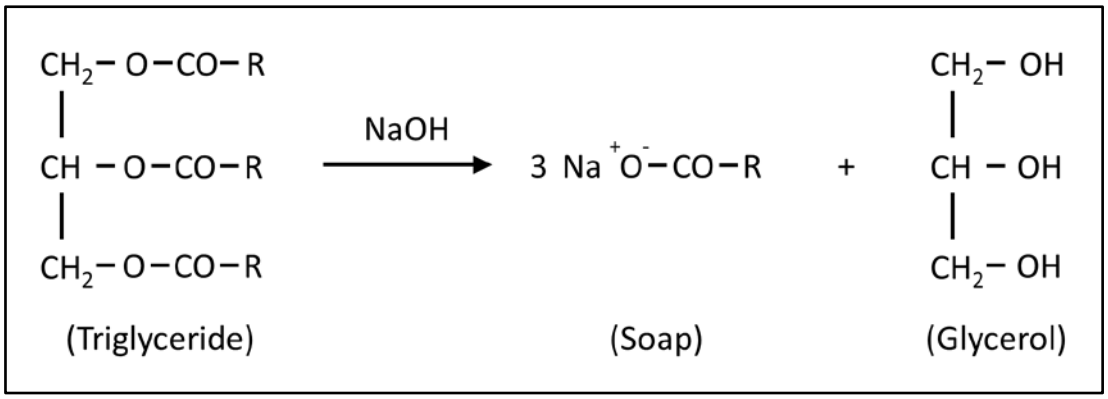

Figure 2.4: Saponification of triglycerides.

2.3.4 Other Reactions

Various different techniques for producing biodiesel have been developed in recent times. They are pyrolysis (Teoh et al. 2022), microemulsion (Shen et al. 2020), dilution (Tamjidi et al. 2021), and catalytic cracking (Laksmono et al. 2013). Pyrolysis, known as thermal cracking, is a conversion process through which heat is applied to reactants and catalyst without the use of oxygen (Teoh et al. 2022). The microemulsion process uses an immiscible liquid in the range of 0.001 – 0.15 µm that is mixed with a solvent such as methanol and vegetable oil resulting in a reduced viscosity mixture (Shen et al. 2020). Dilution or direct blending is a process of mixing petrodiesel directly with highly viscous vegetable oils and animal fats, which decrease once they are blended with petrodiesel resulting in improved spray characteristics of the fuel (Tamjidi et al. 2021). Catalytic cracking combines a chemical reaction and product separation in a single-step process, throughout which methanol is in a state of vapor, resulting in separated products through distillation due to the difference in their volatility. This process has been reported as consuming less energy and producing a high yield (Laksmono et al. 2013). Nonetheless, most of these techniques do not produce fatty acid alkyl esters (FAAE), which is the recognized form of biodiesel by all biodiesel standards.

Table 2.2: Advantages and disadvantages of various biodiesel production methods. *Source*: Data from (Ambat et al. 2018).

Methods	Advantage	Disadvantage
Esterification	• Suitable for industrialized production • Fuel properties are comparable to diesel	• Lengthy reaction time • High reaction parameters are required
Interesterification	• High valued by-product • Fuel properties are comparable to diesel	• Relatively higher cost feedstock instead of alcohol is required
Transesterification	• Suitable for industrialized production • Fuel properties are comparable to diesel	• Conversion efficiency • High cost • Catalyst reusability • Applicability for feedstocks with water and high free fatty acid content depends on the type of catalyst used
Pyrolysis	• Simple • Pollution free process	• High temperature is required • Expensive apparatus are required • Low purity due to intolerable amount of carbon residues • Does not produce FAAE
Microemulsion	• Simple process	• High viscosity • Poor volatility • Poor stability
Dilution	• Simple process	• Incomplete combustion • Carbon formation in engine • Does not produce FAAE
Catalytic distillation	• Easy product separation	• Conversion rate as well as solvent usage for post-treatment depends on catalyst recovery • Does not produce FAAE

2.4 Feedstock for Biodiesel Production

Biodiesel is produced from natural and organic matter, whereby the oil or lipid from either plants or animals is the source for biodiesel production in the presence of alcohol. The commonly used oil feedstocks for biodiesel production are plant oil from soybean, rapeseed,

and palm oil (Ambat et al. 2018). These oil feedstocks are categorized as the first generation feedstock. Four generations of oil feedstock for biodiesel production are first, second, third, and fourth generations feedstocks (R. A. Lee and Lavoie 2013; D. Singh et al. 2020). The alcohol feedstock for biodiesel production can be categorized into three; primary alcohol, secondary alcohol, and tertiary alcohol. The category of alcohol dictates by the number of carbon atoms bonded to the carbon atom bonded with a hydroxyl group (Reusch 2023).

2.4.1 First Generation Oil Feedstock

The first generation feedstocks are mainly extracted from edible crop oil or biomass (D. Singh et al. 2020). Some examples of first generation feedstocks are rapeseed, palm, sunflower, and soybean oil. The first generation feedstocks are widely used feedstock because of their availability to support the biodiesel demand sufficiently (Kirubakaran and Arul Mozhi Selvan 2018). The extensive use of first generation feedstocks has a negative impact on the food price. The competition between the food industry and the fuel industry drives a price war for feedstocks and can cause food insecurity (Gaurav et al. 2019). Edible oil markets are generally more profitable than the fuel market, making the production of biodiesel from first generation feedstocks, to some extent, cost-ineffective. The need for intensive plantation of feedstock crops results in environmental problems. Food insecurity, water scarcity, soil degradation, deforestation, and biodiversity loss are some examples of environmental problems created by the first generation feedstock plantations (Jayakumar et al. 2017; Shah et al. 2018). Table 2.3 shows studies that employed first generation feedstocks for biodiesel production.

Table 2.3: Biodiesel production from first generation feedstock.

Feedstock	FFA content (mg KOH/g)	Catalyst	CC (wt%)	M:O	RT (°C)	RP	Yield (wt%)	Reference
Canola oil	n/a	CaO·MgO	5	9:1	65	2 h	99.1	(Temur Ergan et al. 2022)
Canola oil	n/a	H_2SO_4	5	10:1	150	6 h	84.6	(Jaroszewska et al. 2022)
Canola oil	n/a	KOH	1.05	275:1	60	6 h	80	(Haagenson et al. 2010)
Canola oil	n/a	Na-CaO/MgO dolomites	6	12:1	65	7 h	97.46	(Murguía-Ortiz et al. 2021)
Canola oil	n/a	Na-K doped CaO	3	9:1	50	3 h	97.6	(Khatibi et al.)
Canola oil	3.07	NaOH	3	6.5:1	70	2 h	85	(Hariprasath et al. 2019)
Canola oil	n/a	$ZnO/BiFeO_3$	4	15:1	65	6 h	95.43	(Salimi and Hosseini 2019)
Cashew oil	5.4	NaOH	3	6.5:1	70	2 h	55	(Hariprasath et al. 2019)
Crude palm oil	6.9	H_2SO_4	5	40:1	95	9 h	97	(Crabbe et al. 2001)
Palm kernel oil	1.23	CaO	4	8:1	65	3 h	86	(Tarigan et al. 2017)
Palm oil	n/a	Cu-TiO2	3	20:1	45	45 min.	90.93	(De and Boxi 2020)
Palm oil	n/a	Grafted polypropylene-NaOH	0.5	200:1 (Ethanol)	66	3 h	91.6	(Maleki et al. 2022)
Palm oil	0.957	KOH	2.5	40:1	65	1 h	80	(Soly Peter et al. 2021)
Palm oil	n/a	Solid mixed rare earth catalysts	3	20:1	200	3 h	99.57	(Duangdee et al. 2022)

Table 2.3 continued.

Palm oil	n/a	TiO_2–ZnO	0.92	6:1	60	5 h	92.2	(Madhuvilakku and Piraman 2013)
Palm oil	n/a	Zn-Ce/Al_2O_3	8.19	18.53:1	66.12	3 h	99.44	(T. Qu et al. 2021)
Palm-sesame oil blend	n/a	KOH	1	9:1	25	40 min.	96.14	(Mujtaba et al. 2021)
Palm-sesame oil blend	n/a	KOH	0.7	60:1 (v/v)	25	38.96 min.	96.61	(Mujtaba et al. 2020)
Rapeseed oil	n/a	Activated carbon	2	12:1	130	24 h	80	(Rechnia-Gorący et al. 2020)
Rapeseed oil	n/a	Calcined dolomite	5.24	13.71:1 (Butanol)	110	8 h	94.55	(Gaide et al. 2022)
Rapeseed oil	n/a	Calcined waste filter cake	9.1	9:1	59.2	47 min.	96.5	(Nježić et al. 2023)
Rapeseed oil	n/a	Calcined waste filter cake	10	9:1	60	1 h	97.9	(Krstić et al. 2022)
Rapeseed oil	0.2	Guanidine catalyst	1.8	6.2:1	60	80 min.	96.5	(Racar et al. 2023)
Sesame oil	n/a	$KAlSiO_4$	5	6:1	75	3 h	97.6	(Mahloujifar and Mansournia 2021)
Soybean oil	n/a	$Al_2O_3/ZrO_2/WO_3$	4	40:1	175	60 min.	100	(Rezaei et al. 2013)
Soybean oil	n/a	Co doped Fe2O3eCaO nanocatalyst	3	16:1	70	2.5 h	98.2	(Xia et al. 2022)
Soybean oil	n/a	Mo-KIT-6 catalyst	3	20:1	150	3 h	68.51	(Cardoso et al. 2022)
Soybean oil	n/a	Nano-MgO on TiO_2	0.1	18:1	225	60 min.	95	(Mguni et al. 2012)

Table 2.3 continued.

Soybean oil	0.4	$Sr_3Al_2O_6$	1.3	25:1	60	61 min.	95.7	(Rashtizadeh et al. 2014)
Soybean oil	n/a	Tetraethylammonium arginine	20	10:1	100	1 h	98.4	(X. Wang et al. 2022)
Soybean oil	n/a	Zn Al hydrotalcite catalyst	5	4:1	140	2 h	77	(Shrivastava et al. 2023)
Soybean oil	0.9762	$ZrO_2/C_4H_4O_6HK$	6	16:1	60	2 h	98.03	(Qiu et al. 2011)
Sunflower oil	0.06	Calcined waste scallop seashells	10	12:1	65	4 h	97	(Nahas et al. 2023)
Sunflower oil	n/a	Ca-Mg-Al	2.5	15:1	60	6 h	95	(Dahdah et al. 2020)
Sunflower oil	0.11	CaO Nanoparticles/NaX Zeolite	10	6:1	60	6 h	93.5	(Luz Martínez et al. 2011)
Sunflower oil	n/a	ChOH	2	10:1	65	30 min.	95	(Lima et al. 2022)
Sunflower oil	n/a	KI/Al_2O_3	2.5	15:1	65	4 h	99.99	(Marinković et al. 2022)
Sunflower oil	n/a	MgO	5	9:1	70	6 h	94.3	(Dehghani and Haghighi 2019)

CC = Catalyst Concentration, **M:O** = Methanol to oil ratio, **RT** = Reaction Temperature, **RP** = Reaction Period

2.4.2 Second Generation Oil Feedstock

Most non-edible second generation feedstocks come from various sources (R. A. Lee and Lavoie 2013). Some of them are derived from waste cooking oil, grease, waste animal fats, and non-edible plant oil. Less plantation land is required by the non-edible plant crops, and it can be cultivated through mixed crop cultivation. According to Hums, Cairncross, and Spatari (2016), the usability of waste as the source of second-generation feedstock is capable to solve two problems: reduction of landfill area and reduction of toxic gases emission from petrodiesel. Compared to the first-generation feedstocks, there are significantly cheaper prices recorded by these feedstocks. Yang et al. (2012) and Sakthivel et al. (2018) reported that better fuel quality (relative to the first-generation feedstocks), for example, cleaner, non-corrosive, and higher cetane numbers, were produced from biodiesel of the second-generation feedstocks. Despite that, past scholars outlined a few shortcomings in the biodiesel produced from the second-generation feedstocks. First, low yield and substandard fuel quality of the produced biodiesel are recorded (Alptekin and Canakci 2011). Second, Shah et al. (2018) reported problems such as poor cold flow fuel properties, bio-security concerns on feedstocks from animals and insufficient technologies for commercial-scale production.

Some species of oil-bearing plants, such as *Azadirachta indica* (Neem), *Calophyllum inophyllum* (Bintangor), *Jatropha curcas* (Jatropha), and *Pongamia pinnata* (Karanja), are suitable for use as biodiesel feedstocks (Mohibbe Azam et al. 2005). Since these oil plants are cultivated in their natural habitat, their oil will be present all year. This would ensure that biodiesel feedstock is available at all times (Wan Ghazali et al. 2015; Arumugam and Ponnusami 2019). Biodiesel made from the oil of non-edible plants is said to have properties identical to biodiesel made from the first-generation feedstock. Furthermore, biodiesel made from non-edible plant oil is low in sulfur and aromatics. This contributes to dropping the amount of toxic exhaust gases emitted into the atmosphere (No 2011). Despite the fact that non-edible plants like jatropha, neem, and karanja provide a large amount of oil, they still fall short of the first generation feedstock. Jatropha, neem, and karanja produce 1590, 2670, and 2250 kg oil/ha, respectively. Oil palm and coconut, on the other hand, produce 5000 and 2670 kg oil/ha, respectively (Wan Ghazali et al. 2015). Biodiesel made from non-edible plant oil has high density, viscosity, and carbon residue while having good pollution characteristics. Due to incomplete combustion, these properties have led the biodiesel to emit more particulate matter and NO_x. (D. S. Kim et al. 2018; No 2011). Nevertheless, more studies have been conducted in recent years on genetically engineered oil plants. The modification made to the plant's major

genes by its expression, overexpression, or suppression improved the plant's oil content, quality, and composition (Salehi Jouzani et al. 2018; Yang‡ et al. 2016; Y. Chen et al. 2015; J. Qu et al. 2012).

Waste oil (FOG) is usually found in the form of used cooking oil (UCO), yellow or brown grease, animal fat, and soapstock (a by-product of vegetable oil refining) (Math et al. 2010). They can be acquired from the waste produced domestically and industrially. According to Math, Kumar, and Chetty (2010), the production of global FOG amasses approximately millions of tons annually. However, the disposition of FOG through domestic and stormwater drains presents huge health and environmental problems. Oxygen dissolution is prevented by the presence of an oil layer on top of river water (Jafari 2010). This poses a threat to the lives of aquatic flora and fauna. According to Jafari (2010), oxygen demand in a specific body of water is increased by the mixture of chemical, oil and water. This causes it to become poisonous to marine life. Furthermore, there is a fear that aquatic animals and plants ingested or absorbed the carcinogenic compounds yielded by the FOG. As a consequence, these aquatic lives can potentially transmit the compounds to humans through the food chain process, thus creating serious health problems (Marjadi and Dharaiya 2010). These problems can be mitigated through the utilization of FOG as a feedstock for biodiesel. Compared to the much more expensive vegetable oil, the low cost of FOG is favorable to the feedstock for biodiesel. Generally, feedstock for biodiesel production uses higher quality food-grade vegetable oil i.e. palm oil, rapeseed oil, and soybean oil. This creates a food security problem because the producers of vegetable oil have to choose the option of using the vegetable oil for food supply or biodiesel production (N. P. L. Tran et al. 2019). The problem can be potentially avoided through the utilization of FOG as a biodiesel feedstock. Khan et al. (2019) suggest that the lower cost of biodiesel feedstocks is preferred to the petrodiesel in the market. However, the FOG contains a high percentage of FFA. This causes the formation of soap (or saponification) during the production process via base catalysis. Saponification inhibits biodiesel production and also reduces its yield. Furthermore, it prevents biodiesel, glycerol, and wash water from being easily separated (Yaakob et al. 2013). To mitigate this problem, a two-step process is usually conducted in producing biodiesel from high FFA feedstock. The first step is to convert FFA into esters through acid catalysis. The second step is transesterification through base catalysis (Yaakob et al. 2013). Table 2.4 shows past research that employed waste and non-edible oil as a biodiesel feedstock.

Table 2.4: Studies utilizing waste and non-edible oil as a feedstock for biodiesel.

Feedstock		FFA content (mg KOH/g)	Catalyst	CC (wt%)	M:O	RT (°C)	RP	Yield (wt%)	Reference
Waste Cooking Oil	Waste cooking oil	13.58	La^{3+}/ZnO-TiO_2 photocatalyst	4	12:1	35	3 h	96.14	(M. Guo et al. 2021)
	Waste cooking oil	n/a	Calcined waste scallop seashells	10	12:1	65	4 h	97	(Nahas et al. 2023)
	Waste frying oil	3.9	Magnetic graphene oxide	10	8:1	60	90 min.	94	(Rezania et al. 2021)
	Waste cooking oil	n/a	Calcined cow bone	8.5	1:2.25 (vol:vol)	63.1	60 s.	99.24	(Mohadesi et al. 2021)
	Waste cooking oil	2.7	Sulfonated carbon microsphere	10	10:1	110	10 h	89.6	(T. T. V. Tran et al. 2016)
	Waste cooking oil	1.23	Calcined scallop shell	5	6:1	65	2 h	86	(Sirisomboonchai et al. 2015)
	Waste cooking oil	n/a	CaO-MgO	3	7:1	75	6 h	98.95	(Tahvildari et al. 2015)
Grease	Grease interceptor	19.9	$Fe_2(SO_4)_3$	1	20:1	50	48 h	93	(Montefrio et al. 2010)
	Brown grease	n/a	H_2SO_4	5.95	1:1.44 (wt:wt)	65	2 h	99.7	(Bashir et al. 2020)

Table 2.4 continued.

	Grease	42.4	Phosphotungstic acid-poly(glycidylmethacrylate)-magnetic nano particles	4	33:1	122	24 h	96	(Zillillah et al. 2014)
	Scum of grease trap	167.4	H_2SO_4	1.5	9:1	70	3 h	95.3	(J. P. Oliveira et al. 2017)
	Sludge lipid	129.5	[Methyl imidazolium-C_4SO_3H][SO_3CF_3]	7	10:1	100	5 h	90	(Olkiewicz et al. 2016)
Animal Fats	Chicken fat	5.33	H_2SO_4	35	30:1	65	3.41 h	90.2	(Odetoye et al. 2021)
	Chicken fat	1.72	KOH	0.5	4:1	60	60 min.	96	(M. N. Mohiddin et al. 2018)
	Chicken fat	n/a	*Turritella terebra* shell CaO	4	12:1	60	90 min.	94.03	(Mohd Nurfirdaus Mohiddin et al. 2020)
	Beef tallow	1.8	KOH	1.5	6:1	65	3 h	96.4	(da Cunha et al. 2009)
	Pork lard	0.67	KOH	1.26	7.5:1	65	20 min.	98.6	(Jeong et al. 2009)
	Duck fat	0.56	KOH	0.5	6:1	65	3 h	97	(Chung et al. 2009)
	Heckel fish oil	1.9	KOH	0.5	6:1	32	60 min.	96	(Fadhil and Ali 2013)

Table 2.4 continued.

	Goat tallow	8.4	H_2SO_4	59.93	31.88:1	69.97	150 min.	96.7	(Chakraborty and Sahu 2014)
Soapstock	Soybean soapstock	153.72	Lipase enzyme	0.4	4:1	37	48 h	76	(Ferrero et al. 2020)
	Soapstock oil	81.9	Lipase enzyme	4	5:1	45	10 h	95.2	(E. Su and Wei 2014)
	Soybean soapstock	111.8	Lignin-derived carbonaceous catalyst	7	9:1	70	5 h	97	(F. Guo et al. 2012)
	Soybean soapstock	194.62	*Burkholderia cepacia*	12	3:1	50	31 h	93	(Soares et al. 2013)
	Soybean soapstock	19.9	KOH	0.1	20:1	25	60 min.	81	(Haas and Scott 1996)
Non edible oils	Jatropha oil	16.52	Lithium ion impregnated CaO	5	12:1	65	2 h	>99	(Kaur and Ali 2011)
	Karanja oil	6.77	Lithium ion impregnated CaO	5	12:1	65	60 min.	>99	(Kaur and Ali 2011)
	Rubber seed oil	10.35	Sodium metasilicate	9	9:1	65	40 min.	97	(Roschat et al. 2017)
	Neem oil	n/a	Copper doped zinc oxide	10	10:1	55	60 min.	97.18	(Gurunathan and Ravi 2015)
	Jatropha oil	13.6	CaO/La_2O_3	4	24:1	65	6 h	86.51	(Teo et al. 2015)

Table 2.4 continued.

Jatropha oil	27.86	Bi_2O_3–La_2O_3	2	15:1	150	4 h	93	(Rabiah Nizah et al. 2014)
Jatropha oil	29.85	CaO-Al_2O_3	0.1	5:1	100	3 h	82.3	(Hashmi et al. 2016)
Pongamia oil	n/a	Fe/ZnO	12	10:1	55	55 min.	93	(Baskar et al. 2016)
Attalea speciosa oil	0.6	Co(II) ions adsorbed chitosan	1.64	5:1	70	3 h	86.65	(R. B. da Silva et al. 2008)
Madhuca indica oil	22.9	CaO	2.5	8:1	65	150 min.	97	(B. Singh et al. 2011)

CC = Catalyst Concentration, **M:O** =Methanol to oil ratio, **RT** = Reaction Temperature, **RP** = Reaction Period

2.4.3 Third Generation Oil Feedstock

Third generation feedstocks originate from algal biomass. Two types of algae are macroalgae and microalgae (Shah et al. 2018). Algae need less area to grow and are environmentally friendly. They only need ample sunlight, water, CO_2, and sometimes, nutrients, to grow. As they consume CO_2 to grow, they can become one way to mitigate air pollution by reducing greenhouse gas. It was estimated that 1.8 kg of CO_2 is consumed in order to produce 1 kg of algal biomass (Zhou et al. 2014). Some algae have productivity in terms of oil content. Chlorella species can produce oil as much as 70% of their dry weight (Liang et al. 2009). Some microalgae contain oil of more than 80% of their dry weight. To put it into perspective, sunflower contains 55% of oil, and oil palm contains only 50% of oil per dry weight. As with the feedstock from the previous generations, third generation feedstocks also come with some drawbacks. The production of algae needs a large amount of water. In some countries, water is scarce or in a frozen state for the most part of the year. Thus, algae cultivation is challenging in those countries (R. A. Lee and Lavoie 2013). Also, the technology required to cultivate algae is relatively new. Scaling up and industrializing algae biodiesel currently is difficult, and existing technology is very expensive (Shah et al. 2018). Table 2.5 shows studies that employed third generation feedstock in biodiesel production. Figure 2.5 shows the types, advantages, and disadvantages of each feedstock generation (Hajjari et al. 2017; Shah et al. 2018; D. Singh et al. 2020). By taking into consideration all the requirements, advantages, and disadvantages of all feedstock types, the future of biodiesel production is perceived as not fully relying on a single type of feedstock only but rather a combination of all generations of feedstocks. The selection process for a biodiesel feedstock might include climate, plant availability, technology, market stability, and government policy (Varkkey et al. 2018).

Table 2.5: Biodiesel production from third generation feedstock.

Feedstock	FFA content (mg KOH/g)	Catalyst	CC (wt%)	M:O	RT (°C)	RP	Yield (wt%)	Reference
Algae biomass	69.85	H_2SO_4	79.7	220:1	65	2 h	83	(Haas and Wagner 2011)
Algal lipid	n/a	$Ca(OCH_3)_2$	3	30:1	80	150 min.	99	(Teo et al. 2016)
Algal oil	n/a	CaO	1.25	9:1	55	60 min.	96.3	(Siva and Marimuthu 2015)
Aurantiochytrium	96.3	Lipase enzyme (Novozyme 435)	30	5:1	50	12 h	90	(K. H. Kim et al. 2016)
Chaetoceros gracilis	n/a	H_2SO_4	15.8	988:1	80	20 min.	82	(Wahlen et al. 2011)
Chlorella microalgae	n/a	NaOH	1	12:1	75	6 min.	96	(Martinez-Guerra et al. 2014)
Chlorella pyrenoidosa	n/a	H_2SO_4	23.4	154:1	90	2 h	95	(P. Li et al. 2011)
Chlorella sp.	n/a	Lipase enzyme (Novozyme 435)	30	6:1	35	60 min.	47.5	(Al-Ameri and Al-Zuhair 2019)
Chlorella vulgaris	6.37	H_2SO_4	35	600:1	60	20 h	97	(Velasquez-Orta et al. 2012)
Chlorella vulgaris	3.8	KF/CaO	12	8:1	60	45 min.	93.07	(Ma et al. 2015)
Rhodosporidium toruloides	n/a	H_2SO_4	9.3	868:1	70	20 h	98	(B. Liu and Zhao 2007)
Scenedesmus sp.	30	WO_3/ZrO_2	4	60:1	50	20 min.	71	(Guldhe et al. 2014)
Spirulina microalgae	n/a	KOH	4.85	2:1	25	60 min.	86	(Xu and Mi 2011)

CC = Catalyst Concentration, **M:O** = Methanol to oil ratio, **RT** = Reaction Temperature, **RP** = Reaction Period

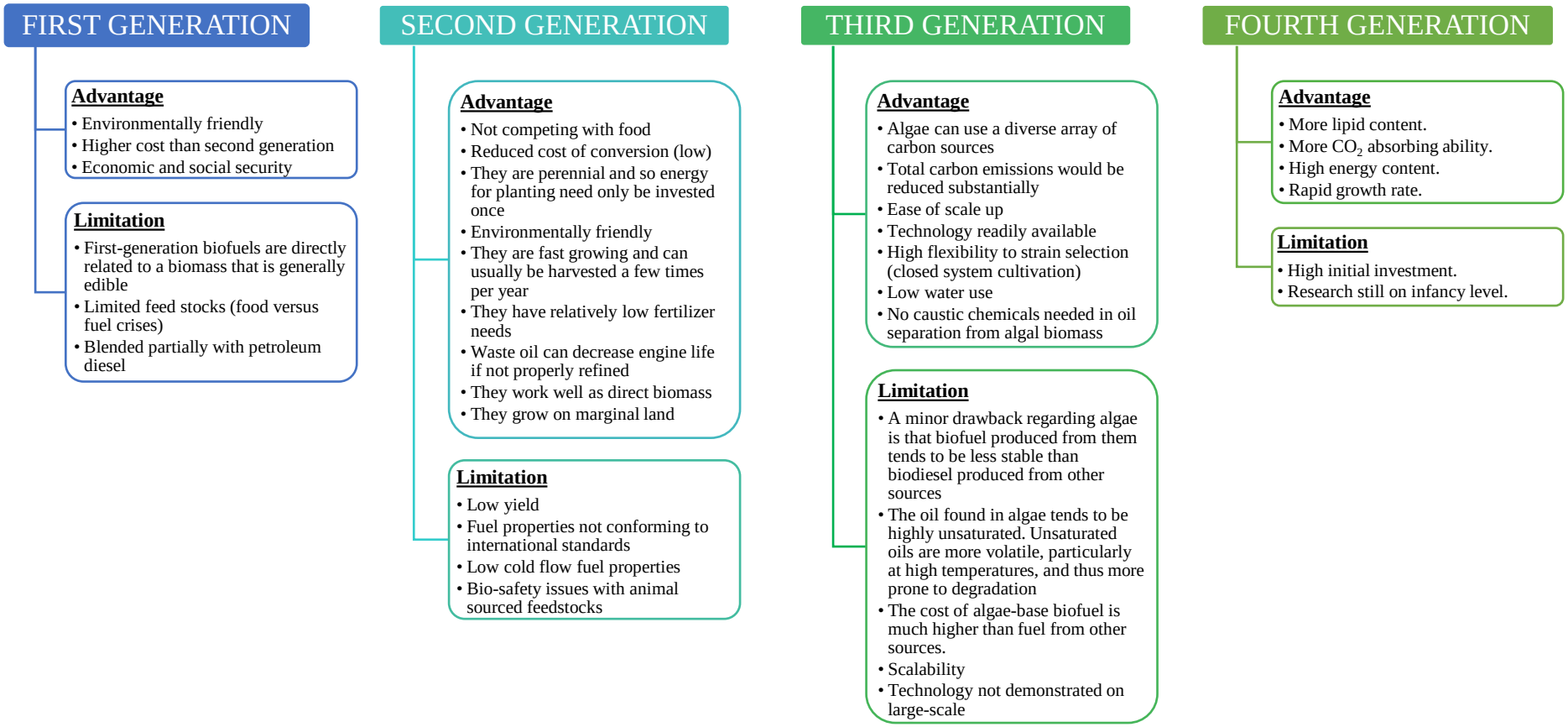

Figure 2.5: Biodiesel feedstocks classification, its advantages, and disadvantages. *Sources*: Figure reproduced from (Hajjari et al. 2017; Shah et al. 2018; D. Singh et al. 2020).

2.4.4 Fourth Generation Oil Feedstock

The recent development of synthetic biology has opened the path for the fourth generation feedstock. A renewable and economic biodiesel feedstock may be developed by incorporating the purpose-designed biological system and solar energy (D. Singh et al. 2020; Dutta et al. 2014). The fourth generation biodiesel feedstock can be produced through one or a combination of three means; (i) purpose-designed photosynthetic microorganisms, (ii) the production combination of photovoltaics and microbial fuel, and/or (iii) synthetic cell production (Ambaye et al. 2021; Aro 2016). A recent development in genetic engineering opens up the possibility of designing a crop plant or any microorganism with increased yield output or increased robustness so that it can grow in adverse conditions which it had never withstood before (Chellamuthu et al. 2022). However, the industrialization of fourth generation feedstock is not yet feasible due to its relatively higher intricacy and capital investment (Shokravi et al. 2021). There are also apprehensions about its possibility to affect the environment and health negatively since the technology is relatively recent (B. Abdullah et al. 2019).

2.4.5 Alcohol Feedstock

Methanol, ethanol, propanol, and butanol are among the several types of alcohols used in the manufacturing of biodiesel (Gotovuša et al. 2022; Gaide et al. 2022; Likozar and Levec 2014). Alcohol can be categorized into primary alcohol, secondary alcohol, and tertiary alcohol. The terminology denotes the number of carbon atoms attached to the saturated carbon bearing the hydroxyl group (Reusch 2023).

Methanol and ethanol are two examples of primary alcohol with shorter hydrocarbon chains that are frequently used in the process of biodiesel production because they are more reactive, environmentally friendly, and less expensive than other types of alcohol (Mahdi et al. 2023). In contrast, longer hydrocarbon chains (propanol and butanol), secondary alcohol (isobutanol and sec-butanol), and tertiary alcohol (tert-butanol) produce less biodiesel despite having a higher rate of reaction (Musil et al. 2018; Y. Sun et al. 2014; Günay et al. 2019).

Although methanol is relatively less expensive compared to ethanol, it is more dangerous and harmful to humans than ethanol (Y. Sun et al. 2014). Furthermore, ethanol is a more ecologically friendly alcohol made from renewable resources and is less toxic than methanol. Methanol can be detrimental to the active sites of enzymes and may quickly deactivate the performance of enzyme catalysts (Andrade et al. 2019). However, one of the

drawbacks of utilizing ethanol is the creation of emulsion during the separation from the product (Danane et al. 2022).

The synthesis of biodiesel utilizing methanol as the reactant offers improved activity, higher stability, and a simpler separation procedure (Mahdi et al. 2023). Nevertheless, the proper methanol concentration for biodiesel synthesis is vital for improved catalytic activity and yields since too much methanol has a detrimental impact on catalyst function (Lokman et al. 2014).

2.5 Catalyst for Biodiesel Production

Biodiesel can be produced with or without the aid of a catalyst. Non-catalytic biodiesel production usually requires a longer reaction period and higher reaction temperature and pressure than a catalytic biodiesel production reaction (Azad et al. 2016). A catalyst's purpose is to expedite the rate of conversion in a certain reaction. Three types of catalysts for biodiesel production are acid, base, and enzyme (Boey et al. 2011). Figure 2.6 shows the classification of catalysts for biodiesel production (Chouhan and Sarma 2011). Acid and base types of catalysts can be further distinguished through either their homogeneity or heterogeneity. A homogeneous catalyst is a catalyst that dissolves and forms a mixture of uniform appearance with the reactants. A heterogeneous catalyst, on the other hand, forms either a suspension or visible physical phases with other reactants. The biggest difference between a homogeneous and a heterogeneous catalyst is that a heterogeneous catalyst can be mechanically separated from other reactants or the finished product through filtration or centrifugation, while a homogeneous catalyst cannot (Ophardt 2003). This property makes heterogeneous catalysts reusable and, to some extent, unaffected by the high FFA content of a feedstock. Nonetheless, the reaction rate of heterogeneously-catalyzed biodiesel production is relatively lower compared to a homogeneously-catalyzed one.

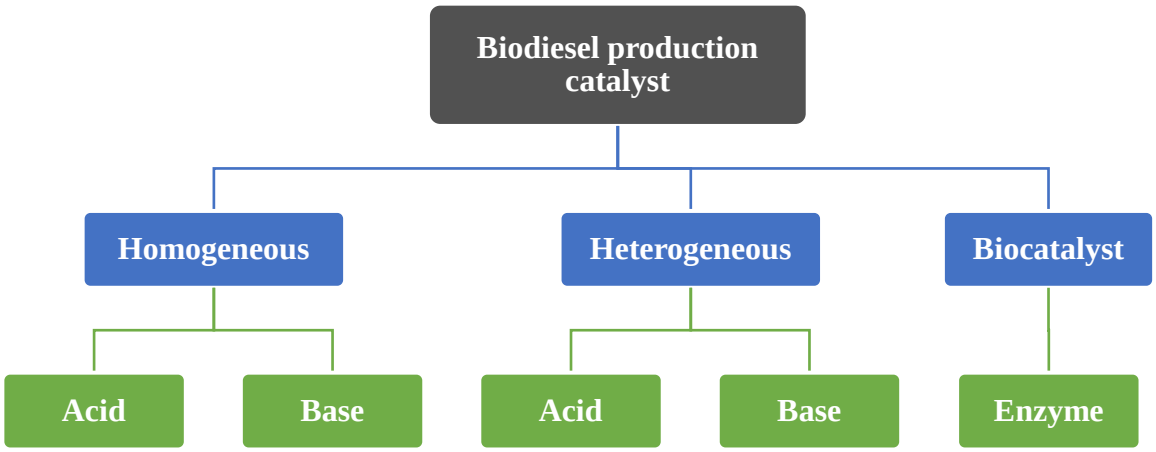

Figure 2.6: Biodiesel production catalyst classification. *Source*: Figure reproduced from (Chouhan and Sarma 2011).

2.5.1 Homogeneous Catalysts

Base homogeneous catalyst is the most used catalyst for industrial biodiesel production. This owes to the high reaction rate of the process catalyzed by this catalyst. Some examples of base catalysts are sodium hydroxide, potassium hydroxide, sodium methoxide, and potassium methoxide (Boey et al. 2011). Base-catalyzed transesterification is approximately 4,000 times faster than acid-catalyzed transesterification (Williams 2015). However, a base catalyst is relatively more expensive and prone to produce soap in the presence of FFA and water. Acid homogeneous catalyst is widely used for a process prior to transesterification in order to reduce the FFA content of a feedstock. This process is usually termed as feedstock pre-treatment. The process is insensitive to FFA and water content (Mardhiah et al. 2017). Thus, an acid catalyst is usually used in conjunction with a base catalyst. Both organic and inorganic acids can be used for transesterification. Sulfuric acid is the most used acid catalyst for transesterification. An acid catalyst is relatively inexpensive and very reactive compared to a base catalyst. It can convert low-cost feedstock that usually contains high FFA and water content without any saponification problem. Nevertheless, the acid catalyst is corrosive to the equipment. As highly-concentrated acid is dangerous, catalyst storage and handling are difficult and risky. Acid catalyst also produces biodiesel at a slower rate compared to base catalyst. This is the main reason why it is seldom used by the industry for transesterification (Williams 2015).

2.5.2 Heterogeneous Catalyst

Heterogeneous catalysts have captivated researchers because of their potential in saving chemical and time consumption, which can be accomplished because the catalysts and the final products are easily separable because of their high selectivity (Al-Jammal et al. 2016). A heterogeneous catalyst is also non-corrosive, reusable (Molaei Dehkordi and Ghasemi 2012), and less susceptible to water and FFA, compared to a homogeneous catalyst (Uprety et al. 2016). Both acidic heterogeneous catalysts and basic heterogeneous catalysts can be used for transesterification. The choice of using a suitable type of catalyst may depend on the value of the FFA contents of the feedstock used (Mansir et al. 2018). Since a heterogeneous catalyst is reusable, it can be adopted for batch and continuous reaction systems (Chopade et al. 2013). Some examples of acidic heterogeneous catalysts are ZnO/I_2, ZrO_2/SO_2^{-4}, TiO_2/SO_2^{-4}, niobic acid, sulfated zirconia, Amberlyst-15, and Nafion-NR50. While some examples of basic heterogeneous catalysts are CaO, $CaTiO_3$, $CaZrO_3$, $CaO\text{-}CeO_2$, $CaMnO_3$, $Ca_2Fe_2O_5$, KOH/Al_2O_3, KOH/NaY. Al_2O_3/KI, ETS-10 zeolite, and alumina/silica supported K_2CO_3 (Leung et al. 2010).

A heterogeneous catalyst has a limitation on the mass transfer as a result of the solid-liquid two-phase reaction. Reaction parameters are usually higher for heterogeneous catalysts compared to homogeneous catalysts for the purpose of obtaining a high biodiesel yield (Thitsartarn and Kawi 2011). Contrasted to a homogeneous catalyst, a heterogeneous catalyst has fewer active catalytic sites, resulting in a lower biodiesel yield (Mansir et al. 2018). Presently, researchers are turning towards bifunctional heterogeneous catalysts that can perform both esterification and transesterification at the same time. This type of catalyst could save time, material, and production costs (Farooq et al. 2013).

2.5.2.1 Biochar Catalyst

Biochar is solid formed from a thermochemical reaction of biomass and any organic carbonaceous materials under limited oxygen condition (X. Sun et al. 2020). Biochar has porous structure and was reported to have high surface area (64 to 795 $m^2\ g^{-1}$) (Babinszki et al. 2021; X. Sun et al. 2020). These properties made it the perfect material as a catalyst for biodiesel production. Biochar can be produced from any biomass (Awogbemi and Kallon 2023). However, the biomass composition and the biochar synthesis method dictates the final biochar yield and properties (Chi et al. 2021). Biochar has been synthesized from various raw materials, mostly derived from agricultural waste such as shell (Zama et al. 2017), straw (Kavindi and Lei 2019), bagasse (J. S. Silva et al. 2018), husk (Vieira et al. 2020), peels

(Awogbemi et al. 2022), and oil palm waste (OPW) (Lawal et al. 2021). More than 60% of biochar is made of carbon, between 10 and 35% from oxygen, an average of 10% of hydrogen and nitrogen, and a trace amount of sulfur (Awogbemi and Kallon 2023). Depending on the type of biomass, these elemental contents may vary.

The biochar production method also influences the biochar properties. Generally, biochar can be produced through either pyrolysis, gasification or hydrothermal carbonization (HTC) as the main product or by-product. Pyrolysis is the most favored method to produce biochar as it produce higher biochar yield compared to other methods (Chi et al. 2021). In pyrolysis, biomass is heated at high temperatures while being subjected to minimal oxygen or an inert gas environment (such as nitrogen) in order to cause its thermal decomposition. Biomass undergoes pyrolysis, when its organic components are thermally broken down into a vapor phase and a residue solid phase (i.e., biochar) is left behind. In the vapor phase, polar and high-molecular-weight molecules are cooled to form bio-oil, while non-condensable gases like H_2, CH_4, C_2H_2, CO, and CO_2 remain gaseous (J. Lee et al. 2019). Depending on the operational conditions, most notably the heating rate, pyrolysis may be broken down into two broad categories: fast and slow pyrolysis (G. Su et al. 2022). The temperatures required for fast pyrolysis range from 400 to 600 °C, and the heating rates must be greater than 300 °C min^{-1}. Additionally, the vapor residence time must be less than 10 seconds. In addition to producing biochar with a yield ranging from 15 to 30 wt%, fast pyrolysis primarily creates bio-oil. Biochar is most commonly made using slow pyrolysis due to its higher solid product yield of 35 to 50 wt%. The temperatures and heating rates for this method range from 300 to 800 °C at 5 to 10 °C min^{-1}. The residence period during slow pyrolysis varies from a few minutes to several hours (Safarian 2023).

Syngas, biochar, biohydrogen, CH_4, value-added chemicals like ammonia, methanol, and other byproducts like CO, and CO_2 are all compounds that can be produced through gasification. Gasification is a method for breaking down carbonaceous materials and lignocellulosic biomass into simpler and more useful compounds (Ajorloo et al. 2022). Utilizing this method is a practical approach to waste management and conversion for the creation of biochar, biohydrogen, syngas, biomethane, and other valuable compounds (Dafiqurrohman et al. 2022). The method requires a reaction temperature of above 700 °C and a controlled environment with a suitable gasifying agent. There are four distinct reaction stages that constitute gasification, which are drying, pyrolysis, combustion, and reduction (You et al. 2018). It is common for there to be no clear demarcation points between these stages, as they frequently run concurrently. Steam, air, oxygen, carbon dioxide, and combinations of these are

all commonly used as gasifying agents (Yepes Maya et al. 2021). Nevertheless, due to its low price and abundant supply, air is utilized in most cases. There is an improvement in biomass conversion rate, product composition, heating value, and physicochemical qualities of the biochar and other produced gases when gasifying agents are used (You et al. 2018).

When compared to other thermochemical processes used to make biochar, hydrothermal carbonization, also known as wet torrefaction, has a high conversion efficiency, needs no pre-drying stage of feedstock, and operates at lower temperatures (Iwuozor et al. 2023). It takes place in water at a temperature ranging from 180 to 300 °C for anywhere between five minutes and 12 hours (Qin et al. 2022). The process is carried out in a subcritical water environment, where the vapor pressure of water varies with the reaction temperature. In its subcritical state, water remains liquid despite being under pressure, and it functions as a nonpolar solvent. The organic components of biochar's feedstock are water-soluble under these circumstances (Ponnusamy et al. 2020; Pauline and Joseph 2020). Biochar (the solid phase), bio-oil (the liquid phase), and minor amounts of gases are the three primary products of hydrothermal carbonization (Pauline and Joseph 2020). Process operating parameters are strongly correlated with the distribution of the three phases and the qualities of each product. Biochar may be produced at a yield of 40 – 70 wt% using hydrothermal carbonization (Safarian 2023). Nevertheless, freshly created biochar is a two-phase slurry, which means that it must first go through a number of procedures to remove excess water before it can be put to use. These steps include mechanically compressing the biochar, sifting it, and drying it with heat or the sun (J. Lee et al. 2019).

Several studies investigating the usage of heterogeneous acid catalysts synthesized from biochar have been carried out on biodiesel production using biochar. Dehkhoda, West, and Ellis (2010) used biochar pretreated with sulfuric acid as a catalyst for rapeseed oil biodiesel. Biodiesel yield and catalyst reusability capacity are highly-dependent on the biochar’s surface area and acid density. High acid density and catalyst surface area resulted in a higher biodiesel yield. Acid density can be increased by elongating the sulfonation time during the catalyst synthesis (Dehkhoda et al. 2010). The effectiveness of a biochar catalyst has also been related to the particle strength, hydrophobicity, and density of the sulfonic acid groups on the biochar surface. As biochar is considered a type of heterogeneous catalyst, it is easily separable from the biodiesel product and reusable. This trait is desirable for cost-saving reasons (Kastner et al. 2012). Dong et al. (2015) have studied biodiesel production from microalgae using a sulfonated biochar catalyst. The study has discovered that catalyst degradation can be avoided by removing chlorophyll and phospholipids from the biodiesel

feedstock of crude microalgal oil. The biochar catalyst also showed excellent catalyst-product separation and reusability. It was reported to have high reactivity for up to ten production cycles (T. Dong et al. 2015). Table 2.6 shows some of the research using biochar as a catalyst for biodiesel production.

Table 2.6: Biodiesel production from biochar catalyst.

Catalyst precursor	Catalyst synthesis parameters	Biodiesel feedstock	CC (wt%)	M:O	RT (°C)	RP	Reusability	Yield (wt%)	Reference
Peanut shell	Carbonized at 450°C, 15h, sulfonated with H_2SO_4 at 200°C, 10h.	Cottonseed oil	2	9:1	85	2 h	50.3% on 5th cycle	90.2	(D. Zeng et al. 2014)
Biochar	Activated with KOH at 675°C, sulfonated with SO_3 at 150°C, 15h.	Canola oil and oleic acid mixture	5	10:1	150	3 h	29% on 2nd cycle	48.1	(Dehkhoda and Ellis 2013)
Carbonized vegetable oil asphalt	Sulfonated with concentrated H_2SO_4 at 210°C, 10h.	Cottonseed oil and oleic acid mixture	0.2	16.8:1	220	4.5 h	97% on 5th cycle	94.8	(Shu et al. 2010)
Glucose	Carbonized at 400°C, 5h, sulfonated with H_2SO_4 at 150°C, 10h.	Calophyllum inophyllum oil	7.5	30:1	180	5 h	50.3% on 5th cycle	99	(Dawodu et al. 2014)
Oat hull	Carbonized at 600°C, 3h, sulfonated with H_2SO_4 at 140°C, 30min, microwave assisted.	Waste cooking oil	10	10:1	140	30 min.	33% on 6th cycle	75	(González et al. 2017)
Coconut shell	Carbonized at 422°C, 4h, sulfonated with concentrated H_2SO_4 at 100°C, 15h.	Palm oil	6	30:1	60	6 h	n/a	88.15	(Endut et al. 2017)
Palm kernel shell	Calcined at 800°C, 2h.	Sunflower oil	3	9:1	65	6 h	3 cycles	99	(Kostić et al. 2016)
Chicken manure	Carbonized at 350°C.	Waste cooking oil	n/a	20:1	350	n/a	n/a	95	(Jung et al. 2018)
Pig meat and bone meal	Carbonized at 650°C, KOH activated, K_2CO_3 alkalized.	Palm oil	5	7:1	65	150 min.	84% on 10th cycle	98.2	(S. Wang et al. 2017)

CC = Catalyst Concentration, **M:O** = Methanol to oil ratio, **RT** = Reaction Temperature, **RP** = Reaction Period

2.5.2.2 Magnetic Catalyst

A heterogeneous catalyst requires less energy and hassle for its separation from any reaction products compared to a homogeneous catalyst. This fact has captured the interest of many studies nowadays. Nonetheless, ordinary techniques of separation for heterogeneous catalysts, such as filtration and centrifugation, still proved to be problematic due to the difficulty and sluggish recovery (F. Zhang et al. 2016; P. Guo et al. 2012). To overcome this problem, ferromagnetism was introduced with the heterogeneous catalyst. This magnetic catalyst can be separated by attracting it to a magnetic force, which is usually induced by an external magnetic field (Krishnan et al. 2021). Ferromagnetism can become magnetic in the presence of a magnetic field and maintain its magnetic properties after the magnetic field is removed. Some examples of ferromagnetic materials are iron and nickel. A magnetic field refers to the area in which the effect of the magnetic force can be observed (H. R. Khan 2003; Givord and Takabatake 2016). Magnetic separation was reported to recover more catalysts and has better separation between catalyst and product, especially with a highly viscous product. The magnetic catalyst was recorded to be 70% faster in catalyst recovery compared to the non-magnetic catalyst. For an iron-doped magnetic catalyst, the addition of the ferrite ions assisted in increasing the porosity and surface area of the catalyst (P. Guo et al. 2012; W. J. Liu et al. 2013).

The synthesis of magnetic catalysts mostly involves multiple combinations of processes. Generally, a reagent containing ferrite ions was used for impregnation prior to catalyst carbonization and functionalization. In a typical synthesis process, iron (III) oxide-hydroxide was formed via ferric chloride hydrolyzation prior to its transformation into FeO(OH). Carbonization was then carried out towards the $FeCl_3$-impregnated catalyst precursor at a high temperature. FeO(OH) was reduced during carbonization due to the production of reducing agents, such as hydrogen, carbon, and carbon monoxide during the process. The resulting compound was magnetite or iron (II, III) oxide, Fe_3O_4, which gave the catalyst its ferromagnetism (Hu et al. 2015; W. J. Liu et al. 2013). Ferrite ion compounds were also reported to assist in pore formation during the carbonization process. In some cases, they also escalate the pore formation significantly due to the dehydration or decomposition of said compounds, such as $FeCl_3$, Fe_3O_4, and FeO(OH) (Atkinson et al. 2011).

A magnetic catalyst for biodiesel production was successfully synthesized from glucose in a study by F. Zhang, Fang, and Wang (2015). They began by preparing Fe/C magnetic core through hydrothermal precipitation. The precursor for the catalyst was then recoated

hydrothermally to prevent Fe_3O_4/Fe leaching during the sulfonation process. Pyrolysis of the catalyst precursor was carried out prior to the sulfonation using H_2SO_4. The magnetic catalyst showed great magnetism at 14.4 Am^2/kg and a significantly high acid density of 2.79 mmol/g. Biodiesel production from jatropha oil was tested using the magnetic catalyst. A maximum biodiesel yield of 90.5% was reported when optimized reaction parameters of 24:1 methanol-to-oil molar ratio, 10 wt% catalyst loading, 200 °C reaction temperature, and 10 hours reaction period were used. The biodiesel yield remained high even after three cycles, with 96.3% of the catalyst amount successfully recovered (F. Zhang et al. 2015).

In another study by F. Zhang et al. (2016), a magnetic base catalyst was synthesized from bamboo-derived biochar and nickel supported Na_2SiO_3. The ferromagnetism of the catalyst was provided by the nickel embedded into the bamboo biochar. The catalyst was synthesized by, firstly, impregnating the support precursor. Then, calcination was done to the support precursor before it was subjected to activation by the catalyst solution. The catalyst precursor was then calcined again into the finished magnetic catalyst. The mass saturation magnetization of the catalyst was reported to be 15.7 Am^2/kg, while its basicity was reported to be 3.18 mmol/g. The magnetic catalyst demonstrated good catalytic activity. The biodiesel yield from soybean oil was reported to be optimized at 98.1%. Optimized biodiesel production parameters were 7 wt% catalyst loading, 9:1 methanol to oil ratio, reaction temperature of 65°C, and reaction period of 100 minutes. The magnetic catalyst was successfully reused for five cycles, with 85.6% of the magnetic catalyst recovered by the end of the fifth cycle (F. Zhang et al. 2016).

Han et al. (2016) carried out a study on the production of the heteropolyacid catalyst supported with a magnetic cellulose microsphere. The cellulose microsphere was created from cotton and given its ferromagnetism by Fe_3O_4 particles via co-precipitation. The magnetic heteropolyacid catalyst was then synthesized by immobilizing $H_3PW_{12}O_{40}$. The immobilization of the heteropolyacid has increased thermal stability, specific surface area, and ease of separation (Han et al. 2016; Ferreira et al. 2009). The production of biodiesel from *Pistacia chinensis* seed oil was done through microwave-assisted transesterification catalyzed by the magnetic heteropolyacid catalyst. An optimal condition of 15 wt% catalyst loading, 10:1 methanol to oil ratio, 60 °C reaction temperature, and 80 minutes of reaction period has produced the highest biodiesel yield of 93.1%. The magnetic heteropolyacid catalyst's ability to yield 80.7% biodiesel on the fourth cycle has proved that the catalyst is hydrothermally stable and environmentally friendly (Han et al. 2016).

As can be seen from these works of literature, magnetic catalysts produce significant yields of biodiesel production. The usage of magnetic catalysts, especially those with biochar as the main catalyst or support for biodiesel production, is full of potential. Magnetic catalysts offer high-catalyst recovery rate, shorter separation time, and lower energy consumption. All these are financially favorable from the industrial viewpoint (F. Zhang et al. 2015; Atkinson et al. 2011). Table 2.7 shows a number of studies investigating magnetic catalysts for biodiesel production.

Table 2.7: Biodiesel production from magnetic catalyst.

Catalyst precursor	Magnetic component	Catalyst synthesis parameters	Biodiesel feedstock	CC (wt%)	M:O	RT (°C)	RP	Reusability	Yield (wt%)	Reference
Sawdust	Fe_3O_4	Precursor Fe-loaded via adsorption, carbonized at 600°C, 1h, sulfonated with H_2SO_4 at 150°C, 10h	Acetic acid	34.5	5:1	88	n/a	~90% on 5^{th} cycle	93	(W. J. Liu et al. 2013)
Glucose	Fe_3O_4	Precursor Fe-loaded via adsorption, carbonized at 700°C, 1.5h, sulfonated with H_2SO_4 at 150°C, 16h	Jatropha oil	10	24:1	200	10 h	3 cycles	90.5	(F. Zhang et al. 2015)
Bamboo	Ni	Precursor Ni-loaded via adsorption, carbonized at 700°C, 2h, doped with Na_2SiO_3, calcined at 400°C, 2h	Soybean oil	65	9:1	65	102 min.	80.9% on 5^{th} cycle	98.1	(F. Zhang et al. 2016)
Cotton	Fe_3O_4	Precursor sulfonated with CS_2, 10h, Fe ions co-precipitated, immobilized phosphotungstic acid	Pistacia chinensis seed oil	15	10:1	60	78 min.	80.7% on 4^{th} cycle	93.1	(Han et al. 2016)
$Al(NO_3)_3.9H_2O$	Fe_3O_4	Fe ions co-precipitated, doped onto precursor, calcined at 700°C, 2h	Microalgae	4	12:1	65	6 h	85.6% on 6^{th} cycle	95.6	(Kazemifard et al. 2019)

Table 2.7 continued.

Chitosan	Fe_3O_4	Fe ions co-precipitated, doped onto precursor, sulfonated with p-toluenesulfonic acid monohydrate	Oleic acid	4	15:1	80	3 h	84.3% on 5^{th} cycle	96.7	(A. Wang et al. 2018)
Bamboo	γ-Fe_2O_3	Fe ions co-precipitated, impregnated onto precursor along with KNO_3, calcined at 500°C, 3h	Soybean oil	2.5	8:1	60	60 min.	94% on 4^{th} cycle	98	(K. Liu et al. 2018)
Jatropha hull	Fe_3O_4	Precursor Fe-loaded via adsorption, carbonized at 700°C, 1.5h, sulfonated with H_2SO_4 at 150°C, 16h	Jatropha oil	10	12:1	90	2 h	92.4% on 3^{rd} cycle	92.44	(F. Zhang et al. 2017)
Jatropha hull	Ni	Precursor Ni-loaded via adsorption, calcined at 700°C, 2h, impregnated with Na_2SiO_3, calcined at 400°C, 2h	Jatropha oil	7	9:1	65	2 h	75.3% on 5^{th} cycle	96.7	(F. Zhang et al. 2017)
$Na_2O.3SiO_2$	Fe_3O_4	Fe ions co-precipitated, $Na_2O{\cdot}3SiO_2$ impregnated onto Fe_3O_4, calcined at 350°C, 2.5h	Cottonseed oil	5	6:1	60	100 min.	90% on 7^{th} cycle	99.6	(P. Guo et al. 2012)

CC = Catalyst Concentration, **M:O** = Methanol to oil ratio, **RT** = Reaction Temperature, **RP** = Reaction Period

2.5.3 Enzyme Catalyst

Enzyme catalyst, also known as biocatalyst, is developed to counter production problems caused by base and acid catalysts. It is usually produced via fermentation and originated from microbial (Semwal et al. 2011). Three main types of enzyme catalysts, namely extracellular lipases, intracellular lipases, and free enzymes, are used for biodiesel-producing applications (Bohlouli and Mahdavian 2019; Yan et al. 2014). Extracellular lipases, usually known as immobilization, are extracted and purified lipase enzymes from host microorganisms, immobilized on a carrier support material, and then used directly for transesterification (Ganesan et al. 2021). This type of enzyme catalyst offers high reaction stability and selectivity although it is costly to produce mainly due to its complicated synthesis process (Yan et al. 2014). *Candida rugosa* lipase is conjugated with magnetic nanoparticles and used as a catalyst for biodiesel transesterification from UCO and brown grease. The study managed to obtain 100% brown grease to biodiesel conversion under an optimum condition of 1:3 lipid-to-alcohol molar ratio, 1:0.1 lipid-to-enzyme weight ratio, 30 °C reaction temperature, and 35 h reaction time. In addition, due to the magnetic property of the catalyst, it can be reused up to five times while being stable operationally (R. K. Sharma et al. 2019). On the other hand, intracellular lipases, known as whole-cell lipases, are used directly as a catalyst for biodiesel transesterification from their lipases-producing microbial cells (Ganesan et al. 2021; Guldhe et al. 2016). Unlike extracellular lipases, this type of enzyme omits the need to perform extra steps, such as enzyme extraction and purification. This makes its production cost relatively lower than extracellular lipases. The simpler intracellular lipase synthesis also means that they can be produced in large amounts for a larger biodiesel production scale (Guldhe et al. 2016). Both extracellular lipases and intracellular lipases are limited by their mass transfer capability (J. Guo et al. 2020). Extracellular lipases also have a high affinity with glycerol (Pollardo et al. 2018). Free enzymes or liquid enzymes are reported to overcome these problems. At a relatively lower cost, free enzymes offer better miscibility and mass transfer compared to both extracellular lipases and intracellular lipases (Andrade et al. 2019). Genetically modified *Aspergillus oryzae,* a type of free liquid lipase, was reported to successfully yield 97% biodiesel from high FFA content low-quality feedstock (Chang et al. 2021). However, free liquid enzymes lack the ability to be reused (Yan et al. 2014).

Compared to heterogeneous and homogeneous catalysts, enzyme catalysts generally do not require high energy, have a simple process, and are reusable. Also, they are less susceptible to high FFA and moisture content. These traits can eliminate the saponification problem, which

usually occurs when the common base or acid catalysts are used. The biodiesel produced through enzymatically catalyzed transesterification is rather simpler to purify (Meher et al. 2006). However, the production cost for the enzyme is high. Also, the reaction parameters needed for the enzyme catalyst to produce an optimum amount of biodiesel are inflexible and generally have a long reaction time (Boey et al. 2011). Furthermore, the deactivation of enzyme catalyst triggered by methanol has caused the biodiesel yield to decline, as only a limited amount of methanol is allowed to exist during the reaction (Magner 2013). Table 2.8 shows the advantages and disadvantages of a common transesterification catalyst.

Table 2.8: Advantages and disadvantages of common transesterification catalyst.

Catalyst	Examples	Advantages	Limitations	References
Basic Homogeneous	NaOH, KOH	• Fast reaction • Inexpensive • Moderate condition requirement	• Low FFA feedstock requirement • Needs more water for purification • Non-reusable	(J. Zeng et al. 2009; M. N. Mohiddin et al. 2018)
Acidic Homogeneous	H_2SO_4, $C_2HF_3O_2$	• Suitable for feedstock with high FFA • Simultaneous esterification and transesterification • Moderate condition requirement	• Corrosive • Non-reusable • Slow reaction	(Haas and Wagner 2011; Miao et al. 2009)
Basic Heterogeneous	CaO, CaO/ZnO, CaO/Al_2O_3, Sodium silicate	• Fast reaction • Noncorrosive • Easy separation • Reusable	• Hygroscopic • Low FFA feedstock requirement • Needs more water for purification • Functional species leaching	(Mohd Nurfirdaus Mohiddin et al. 2020; Alba-Rubio et al. 2010; Zabeti et al. 2010; F. Guo et al. 2010)
Acidic Heterogeneous	ZS/Si, Zr0.7H0.2PW12O40, Zeolite-X	• Suitable for feedstock with high FFA • Simultaneous esterification and transesterification • Easy separation • Reusable	• Slow reaction • Functional species leaching • High condition requirement	(Ramos et al. 2008; X. Zhang et al. 2009; Jacobson et al. 2008)

Table 2.8 continued.

Enzyme	Immobilized Candida antarctica lipase, Rhizomucor mieheilipase, Immobilized Burkholderia cepacia lipase	• Suitable for feedstock with high FFA • Easy purification • Moderate condition requirement	• Expensive • Susceptible to alcohol denaturation	(X. Li et al. 2007; A. C. Oliveira and Rosa 2006; Jegannathan et al. 2010)

2.6 Modelling and Process Optimization

In a number of experimental settings, the design of the experiment (DOE) is a helpful technique for gathering and analyzing data to assess the connection between process parameters (factors) and their output (response). With the use of DOE, it is possible to examine the interactions between various factors and their effects on the response. By only conducting a limited amount of organized experiments, DOE also makes it possible to express the process factors mathematically (Rakić et al. 2014). Numerous statistical optimization methodologies, including the univariate, factorial, the Taguchi method, and response surface methodology (RSM), have been utilized in past literature in order to choose the optimal combination of most or all of the optimized process parameters (Okolie et al. 2021).

The Taguchi method is an eight-step process/product optimization method that involves designing, performing, and analyzing matrix experiment data to identify the optimal values of control variables. It is a factorial-based approach that assigns the factors (variables) chosen for an experiment using an orthogonal array (a sequence of trials in different conditions) (S. Salam et al. 2020). To evaluate the discrepancy between the experimental and intended values, the Taguchi method suggests using a loss function, which is then converted into a signal-to-noise (SN) ratio (Alavi-Borazjani et al. 2021). The main aim is to maintain the output variance as low as possible even though noise inputs exist. As a result, the processes/products are created to be impervious to all changes. The Taguchi method is often applied as an experimental design method for process optimization research and high-quality system design (Ahangari et al. 2021).

One of the benefits of utilizing the Taguchi method in an experimental design is it requires significantly fewer experimental runs. A reduction in the number of experiments also reduces the time taken for the whole analysis and the overall cost associated with it (Okolie et al. 2021). Compared to other experimental designs, such as RSM and genetic algorithm, the Taguchi method requires relatively fewer experimental runs due to it disregarding any interaction between factors (Patience and Bérard 2018). The Taguchi method has a comparable capability in process optimization compared to RSM. Studies by Awogbemi, Inambao, and Onuh (2019) reported the comparison study between the Taguchi method and RSM for the optimization of transesterification of waste sunflower oil to FAME. In this study, the Taguchi method was proven to perform comparably with RSM. Although RSM produced a more precise result, the Taguchi method can effectively optimize a model with fewer experimental runs (Awogbemi et al. 2019). Another study by Mia (2018) investigated the parametric optimization

of the machining process using RSM and the Taguchi method. The study concluded that both methods have justified adequacy for the process optimization (Mia 2018).

Optimal conditions for a combination of factors can be acquired via the Taguchi method by combined utilization of SN ratio and analysis of variance (ANOVA) (Alavi-Borazjani et al. 2021). Studies by Esan et al. (2021) and Helmi et al. (2021) investigated the optimization study of biodiesel production. The literatures reported successful biodiesel conversion optimization. Among the parameters studied are catalyst weight, methanol-to-oil ratio, reaction time, and reaction temperature (Esan, Olalere, et al. 2021; Helmi et al. 2021).

Nevertheless, one of the Taguchi method's limitations is the true optimal values for the factors are very hard to define. The pre-defined factorial levels in the Taguchi method are not necessarily the true optimal level. The method only considers the pre-defined factorial levels for the analysis and comparison (Okolie et al. 2021; Ravuri et al. 2021). One way to increase the accuracy of the optimization is to combine the Taguchi method with another method, such as RSM. W.-H. Chen et al. (2021) have acquired the optimized combination of reaction parameters of syngas production by applying two-stage optimization of the Taguchi method and RSM. Another study by T. S. Singh and Verma (2019) studied the conversion of waste cooking oil into methyl esters. The study also applied a combination of the Taguchi method and RSM to determine the optimized reaction parameters for the conversion reaction. In the literature, the combined optimization method was proven to be more efficient and increase the accuracy of the analysis (W.-H. Chen et al. 2021; T. S. Singh and Verma 2019).

2.7 Effect of Transesterification Parameters on Biodiesel Yield

2.7.1 Catalyst Concentration

Catalyst type and concentration are important parameters in transesterification. Acid catalyst tends to work better with high FFA content feedstocks, while base catalyst works better with low FFA content feedstocks. Regardless of its type, a catalyst speeds up a reaction by the mean of lowering the reaction's activation energy (Mansir et al. 2018). Different catalyst concentration is needed for a different type of catalyst. Though a catalyst is chemically similar to another catalyst, other factors may cause the biodiesel production reaction to take place in different catalyst concentrations in order to produce the same amount of biodiesel yield (Gondra 2010). Catalyst concentration is among the most influential parameters which affect biodiesel yield (Karmakar and Halder 2019). Therefore, most literature in catalytic studies includes catalyst concentration as one of the experimental parameters (Kirubakaran and Arul Mozhi Selvan 2018; Leung et al. 2010; Mardhiah et al. 2017; Niju et al. 2016).

Lower catalyst concentration usually yields less amount of biodiesel. One of the causes for the low yield is less amount of catalyst, leading to a less catalytic surface for the transesterification process to occur (Korkut and Bayramoglu 2018; Y. H. Tan, Abdullah, Nolasco-Hipolito, et al. 2015). Another basis for the yield reduction because of lower catalyst concentration is methanol solubility with the glycerol by-product of the reaction. Insufficient catalyst concentration creates a surplus amount of unreacted methanol, which dissolves into glycerol and hinders the overall biodiesel production process (Reddy, Saleh, et al. 2017b). Yield typically peaks and drops as the catalyst concentration increases. An increased amount of catalyst reduces biodiesel yield as it usually forms slurry, increases viscosity, and then increases soap formation (Reddy, Ahmed, et al. 2017; Mata et al. 2011; Korkut and Bayramoglu 2018). Increased soap formation causes the reduction of overall biodiesel yield (G. Chen et al. 2014; Tang, Gu, and Chen 2013). Therefore, an optimum amount of catalyst is usually studied in catalytic studies on the subject of biodiesel production via transesterification (Fayyazi et al. 2015).

2.7.2 Oil to Methanol Ratio

One of the most influential transesterification parameters is the oil-to-methanol molar ratio (Banković-Ilić et al. 2014). Other types of alcohol can also be used in order to produce biodiesel, such as ethanol, propanol, isopropyl alcohol, butanol, and pentanol (Rehan et al. 2018; Mansir et al. 2018; Alonzo 2007). However, methanol remains highly preferred for biodiesel production because its commercial significance is lower than other longer-chain alcohols, making it a cheaper option for the transesterification of biodiesel (Gopal and Sajitha 2013). Methanol also does not form an azeotrope with water. Therefore, it can be simply recycled for biodiesel production (Gerpen 2005). Hypothetically, three moles of triglycerides and one mole of methanol are needed to produce three moles of methyl esters and one mole of glycerin (Maneerung et al. 2016). However, a higher methanol portion is needed in order for the reaction to be optimal and produce the maximum quantity of biodiesel. The amount of methanol needed for optimized transesterification is vital to ensure biodiesel production is cost-effective (Gebremariam and Marchetti 2018).

The ratio of oil to methanol is linked to the type of catalyst used in the transesterification process. Acid catalysts generally require a higher oil-to-methanol ratio compared to base catalysts. As high as the 1:15 oil-to-methanol ratio is needed for acid-catalyzed transesterification, while base catalysts mostly only require a 1:6 oil-to-methanol ratio (Leung et al. 2010). Syazwani et al. (2017) successfully produced palm oil biodiesel from CaO catalyst

obtained from waste venus clamshells with an oil-to-methanol ratio of 1:15. Maneerung et al. (2016) also reported an optimum oil-to-methanol ratio of 1:15 on producing waste cooking oil biodiesel using CaO from calcined chicken manure. Wei et al. (2009) studied the production of soybean biodiesel from waste eggshell CaO and found that the optimized oil-to-methanol ratio for the production process to be 1:9. A study by Venkat Reddy et al. (2006) reported an optimum oil-to-methanol ratio of 3:10 on producing biodiesel from poultry fat at room temperature using neat CaO catalyst. Goli and Sahu (2018) reported an optimum oil-to-methanol ratio to be 1:10 in their study, which investigated the waste eggshell CaO catalyst for biodiesel production from soybean oil. From the literature, it was observed that though CaO catalyst is a type of base catalyst; thus, its requirement for the oil-to-methanol ratio usually exceeds 1:6 and is roughly within the range of 1:10 to 1:15.

Too little or too much methanol in a reaction produces a low biodiesel yield. If the oil-to-methanol ratio is too low, the reaction will not shift toward product formation. The transesterification reaction will reverse towards the reactants instead of producing biodiesel. This is a result of the reversible nature of the transesterification process (Reddy, Saleh, et al. 2017b; Çetinkaya and Karaosmanoğlu 2004). The lack amount of methanol also caused an incomplete reaction, where there was an excess of feedstock with an absence of methanol to produce more biodiesel (Rad et al. 2018).

Nonetheless, when too high of an oil-to-methanol ratio is utilized, the active sites of the catalyst are flooded by methanol, which decreases the chances for the catalyst-oil interaction (Lokman et al. 2014). Excessive use of methanol also has been associated with difficulty during glycerol separation (Ahmad et al. 2014). The overall density of glycerol is reduced when excessive methanol is used in a reaction; thus, this hinders its separation from the excess methanol (S. Sharma et al. 2018). Eventually, these two main causes result in a decrease in biodiesel yield. In addition, the cost of methanol recovery is higher when a higher oil-to-methanol ratio is used (Yan Li et al. 2010).

2.7.3 Reaction Temperature

Transesterification is an endothermic reaction (Baskar et al. 2018). Temperature evidently influences the amount of biodiesel produced in a transesterification reaction. Elevated temperature supports the feedstock to rise over the activation energy barrier (Hanif et al. 2018). The biodiesel yield generally increases as the reaction temperature rises as a result of the decrease in the viscosity of oil or fat (Encinar et al. 2010). Another reason why temperature affects biodiesel yield is that the transesterification reaction rate is controlled by

kinetic (Brucato et al. 2010). The lack of reaction temperature results in poor mixing between the reactants as the viscosity of the oil remains thick at a lower temperature (Takase et al. 2014).

Nevertheless, an increase in reaction temperature beyond the optimum temperature decreases the biodiesel yield (Abbah et al. 2016). Reaction temperature higher than the boiling point of the alcohol used for the transesterification causes the evaporation of the alcohol, reducing its availability; thus, this further decreases the methanol-oil contact time and eventually decreases the overall biodiesel yield (Dhawane et al. 2017; Zhao et al. 2013). A higher reaction temperature also expedites saponification between a base catalyst and FFA from the oil (Eevera et al. 2009; Leung et al. 2010). Baskar et al. (2018) discovered a decrease in the methanol polarity due to overheating the reactants of a transesterification process, which is one of the reasons for the lack of biodiesel yield for a higher reaction temperature.

Sharma and Singh (2010) reported an optimum reaction temperature of 55 °C for a biodiesel transesterification of Karanja oil with H_2SO_4. Another similar study by Ghadge and Raheman (2005) using the same catalyst, H_2SO_4, reported an optimum reaction temperature of 60 °C in producing biodiesel from Mahua oil. Gandhi et al. (2011) also reported an optimum reaction temperature of 60 °C. They studied the production of biodiesel from crude *Jatropha curcas* oil using KOH as a catalyst. Sirisomboonchai et al. (2015) studied biodiesel production from waste cooking oil via CaO synthesized from scallop shells. This study determined the reaction's optimum temperature to be 65 °C. Kabbashi et al. (2015) successfully produced biodiesel from Jatropha curcas oil using immobilized *Candida cylindracea* lipase, an enzyme catalyst. They recorded an optimum reaction temperature of 40°C. Another study by Suwanno et al. (2017) investigated biodiesel production using oil extracted from palm oil mill effluent. They also utilized an enzyme catalyst, crude lipase, and recorded an optimum reaction temperature of 35 °C. The range and optimum temperature of a reaction depend on the type of catalyst. Acid and base catalysts record an optimum temperature between 50 °C and 60 °C, while enzyme catalysts usually record an optimum temperature between 30 °C and 50 °C (K. A. Salam et al. 2016). Enzyme catalyst loses biodiesel yield beyond the reaction temperature of 50 °C because of lower enzymatic activity (Dhawane et al. 2018). Nevertheless, the reaction temperature also slightly depends on other factors, such as reaction time, type of oil used, and reaction pressure (Datta and Mandal 2016).

2.7.4 Reaction Period

In general, biodiesel yield increases with reaction time. However, the optimum reaction period for a transesterification process depends on the type of feedstock, the catalyst used, and

its concentration (Sharma et al., 2018). Base catalysts generally produced the maximum amount of biodiesel at 4000 times faster compared to acid catalysts. This is one of the reasons why acid catalysts are usually used as a pretreatment prior to and not in transesterification (K. A. Salam et al. 2016). Enzyme catalysts, on the other hand, need a relatively longer reaction time (Dhawane et al. 2018).

Mata et al. (2011) studied waste chicken fat biodiesel production using KOH as a catalyst. They successfully converted 76.8% of waste chicken fat into biodiesel for a reaction time of two hours. Another study by Felizardo et al. (2006) investigated biodiesel production from waste frying oil using a NaOH catalyst. They converted 98% of the waste frying oil into biodiesel under a reaction time of 40 minutes. Zhu et al. (2006) reported a biodiesel yield of 93% by transesterification of *Jatropha curcas* oil using a solid superbase CaO catalyst. They managed to do the reaction under a reaction time of 2.5 hours. Ramadhas et al. (2005) successfully produced biodiesel from rubber seed oil using a H_2SO_4 catalyst. Patil and Deng (2009) also utilized the same type of catalyst in producing biodiesel from Karanja oil. Both studies concluded that the optimum reaction time needed for a maximum biodiesel yield to be two hours. Naranjo et al. (2010) successfully converted palm oil into biodiesel using *Candida antarctica B* lipase, an enzyme catalyst with a 100% yield. However, the reaction time required to achieve this high yield was relatively longer, at 40 hours. Similarly, a study by Giraldo and Moreno-Piraján (2012) investigated biodiesel production via *Candida antarctica B* lipase catalyst with avocado oil as feedstock, and reported a biodiesel yield of 100% with the expense of a reaction time of 32 hours. From the literature, it is observed that the optimum reaction time for base and acid catalyst are generally within the range of 1-2 hours, while enzyme catalyst commonly requires more than 24 hours to obtain the maximum biodiesel yield.

Short reaction time resulted in the feedstock and methanol not mixing and dispersing properly (Tang, Gu, and Chen 2013). Syazwani et al. (2017) reported a low biodiesel yield at the beginning of a reaction. With time, the feedstock was converted to two main derivatives of triglyceride, namely monoglyceride and diglyceride, which facilitate biodiesel production. With enough amount of mono and diglycerides, the production reaction took off and achieved equilibrium at its optimum reaction time. However, when the reaction time was too long, the reaction was forced to maintain its equilibrium. Hydrolysis of ester then occurred, and so did saponification. Both of these situations eventually resulted in low biodiesel yield (Eevera et al. 2009). These situations happened because of the reversible nature of the transesterification reaction (Leung et al. 2010; Çetinkaya and Karaosmanoğlu 2004).

2.8 Kinetic Studies on Biodiesel Production

2.8.1 Mechanism for Transesterification

Transesterification is a series of three reversible reactions that convert triglycerides into diglycerides in the beginning in the presence of a catalyst and alcohol. Then, diglycerides are further converted into monoglycerides. Finally, monoglycerides are converted into glycerol. In each step of the reactions, one mole of fatty acid esters, known as biodiesel, is produced (Meher et al. 2006). This intermediate three-step mechanism is shown in Equations 2.1 – 2.3 using methanol as the alcohol. Transesterification can be catalyzed by either acidic or basic catalyst. Nonetheless, the chemical reactions of transesterification for producing biodiesel is the same for both types of catalyst (Koberg and Gedanken 2013). In terms of stoichiometry, one mole of triglyceride will react with three moles of alcohol to produce three moles of fatty acid esters and one mole of glycerol. This overall equation is shown in Equation 2.4 (Bashiri and Pourbeiram 2017).

$$\mathrm{TG} + \mathrm{CH_3OH} \rightleftarrows \mathrm{DG} + \mathrm{ME} \tag{2.1}$$

$$\mathrm{DG} + \mathrm{CH_3OH} \rightleftarrows \mathrm{MG} + \mathrm{ME} \tag{2.2}$$

$$\mathrm{MG} + \mathrm{CH_3OH} \rightleftarrows \mathrm{GL} + \mathrm{ME} \tag{2.3}$$

$$\mathrm{TG} + 3\ \mathrm{CH_3OH} \rightleftarrows 3\ \mathrm{ME} + \mathrm{GL} \tag{2.4}$$

where TG is the triglyceride, DG is the diglyceride, MG is the monoglyceride, ME is the methyl ester, and GL is the glycerol.

A limited amount of research has addressed kinetic studies for biodiesel production. Specific reaction conditions are needed for developing kinetic models and rate equations. For this reason, most studies made assumptions about some of the parameters of the reaction. The intermediate three steps reactions of diglyceride and monoglyceride are usually combined into a single step (Kusdiana and Saka 2001). Other than that, methanol was always used in excess; thus, its concentration was negligible. The amount of catalyst was sufficient in order to favor biodiesel production by shifting the equilibrium towards the product.

Booramurthy et al. (2020) investigated the optimization and kinetics of biodiesel production from tannery waste-derived fat using a magnetic nano-catalyst. The study revealed that the transesterification reaction obeyed the pseudo first-order kinetics. Another study by Deshmane and Adewuyi (2013) also reported a pseudo first-order kinetic mechanism for their two-step ultrasound-assisted transesterification. They studied biodiesel production from soybean oil using sodium methoxide as a base catalyst. In a study by Gurunathan and Ravi (2015), first-order kinetics was more fitting compared to pseudo first-order. In this study, neem

oil was converted to biodiesel through copper-doped zinc oxide-catalyzed transesterification. Nautiyal, Subramanian, and Dastidar (2014) also reported a transesterification reaction obeying first-order reaction kinetic in their research. They successfully converted *Spirulina platensis* algae biomass oil into biodiesel through an H_2SO_4 acid catalyst extraction-transesterification reaction. K. Singh, Kumar, and Blümich (2019) investigated biodiesel production from sunflower oil through a NaOH-catalyzed transesterification reaction. In their research, they concluded that the reaction obeyed second-order kinetics. They also reported the reaction rate increased with the catalyst loading, methanol ratio, and reaction temperature. Another study by Neeharika et al. (2017) also recorded a second-order reaction kinetic for their biodiesel production reaction. They converted jatropha oil into biodiesel using sulfonic acid as a catalyst. From the review of these past studies, it can be established that not all transesterification reaction obeys a single type of reaction kinetics.

2.8.2 Activation Energy

The minimum amount of kinetic energy needed for a reaction to take place is known as the activation energy. The frequency factor, also known as a pre-exponential factor, signifies the frequency at which the reactants molecules collide with one another. Arrhenius equation can show the relationship between activation energy, pre-exponential factor, and rate constant in a temperature-dependent formula, as shown in Equation 2.5.

$$k = Ae^{\frac{-E_a}{RT}} \tag{2.5}$$

where k is the rate constant, A is the pre-exponential factor, E_a is the activation energy, R is the universal gas constant, and T is the absolute temperature.

Ali, Elkatory, and Hamad (2020) reported an E_a and A value of 37.64 kJ mol^{-1} and 6.75×10^3 min^{-1}, respectively, for a transesterification reaction of waste frying oil catalyzed by magnetic $CuFe_2O_4$. Another study by Booramurthy et al. (2020) investigated biodiesel production from tannery waste-derived fat using a magnetic nano-catalyst. In their work, they recorded an E_a and A value of 43.8 kJ mol^{-1} and 7.5×10^4 min^{-1}. However, L. Zhang et al. (2010) recorded a higher E_a and A value of 79.1 kJ $mo1^{-1}$ and 1.26×10^9 min^{-1}, respectively, for a biodiesel transesterification of palm oil using KOH. The dissimilarities in the values of E_a and A in the literature show the different capabilities of catalysts in reducing the E_a and increasing the A during the transesterification reaction (Tang et al. 2018). Table 2.9 shows a lot of research work that carried out kinetic studies on the transesterification of biodiesel.

Table 2.9: Kinetic studies on transesterification of biodiesel.

Feedstock	Catalyst	Kinetic Model	E_a (kJ mol^{-1})	A (min^{-1})	References
Waste frying oil	$CuFe_2O_4$	Pseudo first-order	37.64	6.75×10^3	(Ali et al. 2020)
Tannery waste	Magnetic nano-catalyst	Pseudo first-order	43.8	7.5×10^4	(Booramurthy et al. 2020)
Palm oil	KOH	Pseudo first-order	79.1	1.26×10^9	(L. Zhang et al. 2010)
Waste cooking oil	NaOH	Irreversible-pseudo second-order	27.24	n/a	(Mercy Nisha Pauline et al. 2021)
Waste cooking oil	Calcined periwinkle shells	Pseudo first-order	16.47	n/a	(Okoye et al. 2020)
Tung nut oil	Solid acidic ionic liquid polymer catalyst	First-order	72.81	n/a	(Panchal et al. 2020)
Non-edible oils blend	Waste tires activated carbon	Pseudo first-order	19.01	4.10	(Ayoob and Fadhil 2019)
Waste cooking oil	CaO/SiO_2	Pseudo first-order	66.27	5.44×10^8	(Putra et al. 2018)
Soybean oil	Na-pumice catalyst	Pseudo first-order	n/a	n/a	(de Luna et al. 2017)
Sunflower oil	$MgO\text{-}La_2O_3$	Second-order	77.6	3.5×10^7	(Feyzi et al. 2017)
Sunflower oil	Al-Sr	Pseudo first-order	72.86	3.38×10^7	(Feyzi and Shahbazi 2017)
Nannochloropsis sp. algae	$Ca(OCH_3)_2$	Pseudo first-order	58.62	n/a	(Teo et al. 2016)
Palm oil	CaO	Second-order irreversible (conventional)	n/a	n/a	(Ye et al. 2016)
Palm oil	CaO	Second-order reversible (microwave)	n/a	n/a	(Ye et al. 2016)

2.9 Summary and Research Gap

Despite the commonly flooded biodiesel market with biodiesel based on edible oils, a lot of recent studies are focusing on making the transition from edible to non-edible biodiesel feedstocks. Biodiesel produced from edible oil sources has received great scrutiny due to its likelihood to cause environmental, social, economic, and in some countries, political problems.

For this research, transesterification has been chosen as the process to produce biodiesel. This choice was made due to the simplicity, energy efficiency, and the versatility of transesterification to accept wide range of oil feedstock. Feedstocks from waste UCO are both economic and ecological. The abundance and the ease of procurement of UCO made it a perfect choice as an oil feedstock for producing biodiesel with in this research. Additionally, this is also due to its utilization as a biodiesel feedstock reduced waste disposal landfill area, and it is readily available with low to no cost. The cost of biodiesel production can be reduced by sourcing the reactants and catalysts from inexpensive materials. From the reviewed literature, methanol has been recognized and used as an alcohol feedstock for biodiesel production in this research because of its superior reactivity and lower cost relative to other alcohol. A reusable catalyst further drives the production cost down and increases the sustainability of biodiesel production. Catalysts synthesized from biomass have been proven economic and sustainable. The mild FFA level of UCO that can cause saponification problem from the usage of basic catalyst can be avoided by utilizing acidic catalyst. The acidic sulfonated magnetic biochar catalyst (SMBC), made from PKS, EFB, and OPF, has great potential as catalysts for one step biodiesel production. However, the synthesis and the separation mechanism for this SMBC have not been widely studied. The optimum synthesis parameter of SMBC synthesized from PKS, EFB, and OPF biomass is still rarely studied.

The optimum reaction parameters for producing biodiesel from SMBC and its reusability are not widely studied. In addition, the mechanism and kinetics of biodiesel production using SMBC have not been studied.

The lack of research literature on the subject of magnetic catalysts has been realized. Therefore, this research addresses the research gap as follows:

i. The optimized reaction parameters for SMBC synthesis.
ii. The reaction mechanism and kinetic for transesterification of biodiesel using SMBC.

CHAPTER 3
METHODOLOGY

3.1 Overview

This research methodology started with the synthesis of sulfonated magnetic biochar catalyst (SMBC). The catalyst was then characterized in order to investigate its physicochemical properties. The SMBC was then utilized for biodiesel production through transesterification to investigate its catalytic performance. The results from these investigations were used to conduct a kinetic study of biodiesel production using SMBC. A general overview of the methodology is shown in Figure 3.1.

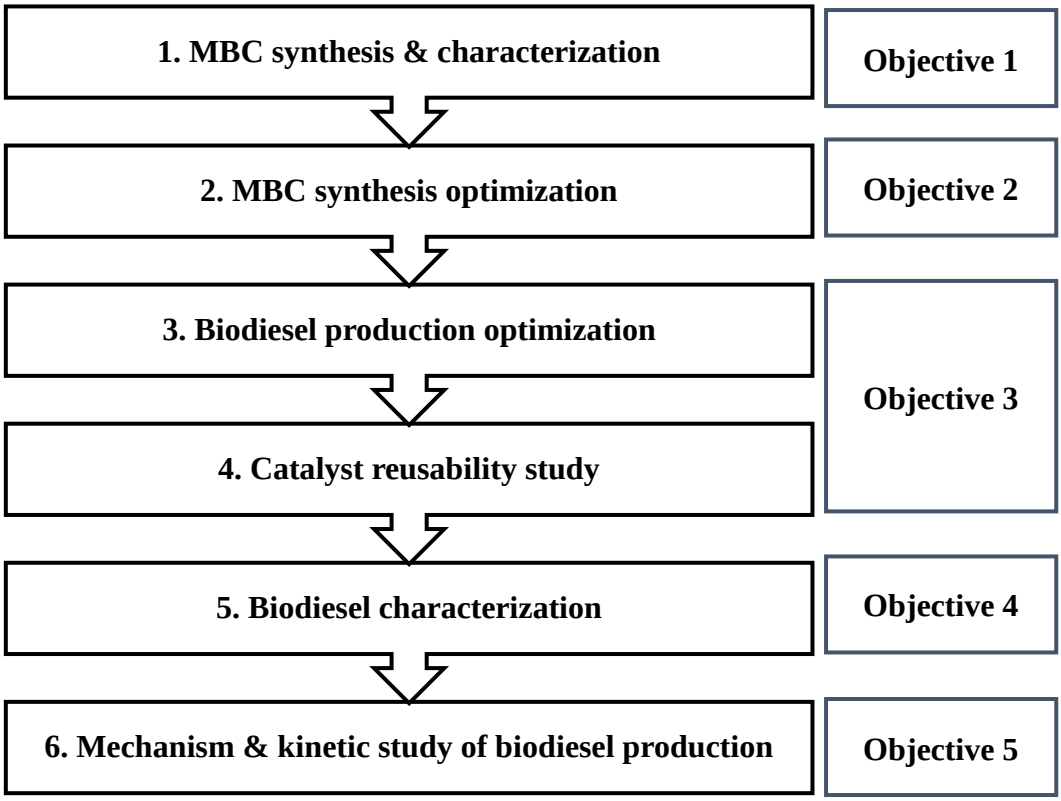

Figure 3.1: General overview of the methodology.

This chapter details the experimental methods, instrumentation, and materials used in this research. Section 3.2 describes the materials used in this research. Section 3.3 presents the method used to synthesize the SMBC. Section 3.4 describes in detail the methods for characterizing the SMBC. Section 3.5 describes the method for SMBC synthesis optimization. Section 3.6 presents the method of biodiesel production and optimization. Section 3.7 describes the SMBC reusability study method. Section 3.8 describes the methods to analyze the

physicochemical properties and the characteristics of biodiesel. Lastly, Section 3.9 describes the method for studying the kinetic of biodiesel production from SMBC.

3.2 Materials and Chemicals

Oil palm biomass, such as PKS, EFB, and OPF, were provided by Sarawak Oil Palms Berhad. Used cooking oil (UCO) was collected from a local restaurant in Miri, Sarawak, Malaysia. Laboratory grade chemicals, such as iron (III) chloride, sulfuric acid, methanol, ethanol, n-hexane, and methyl heptadecanoate, were supplied from Jaya Chemical Supplier. Table 3.1 shows the materials and chemicals used in this research.

Table 3.1: Materials and chemicals used in this research.

Materials / Chemicals (Purity)	Manufacturer (Supplier)	Purpose
Oil palm biomass (PKS, OPF, and EFB)	Sarawak Oil Palms Berhad	Catalyst raw material
Iron (III) chloride (97%)	Sigma-Aldrich (Jaya Chemical Supplier)	Catalyst iron impregnation
Sodium chloride (99.99%)	Merck (Jaya Chemical Supplier)	Catalyst characterization
Sodium hydroxide (97%)	Merck (Jaya Chemical Supplier)	Catalyst characterization
Sulfuric acid (95 – 98%)	Sigma-Aldrich (Jaya Chemical Supplier)	Catalyst sulfonation
Used cooking oil (FFA <1.5%)	Local restaurant in Miri, Sarawak	Biodiesel feedstock
Methanol (>99.9%)	Merck (Jaya Chemical Supplier)	Biodiesel production
Ethanol (99.98%)	Hmbg Chemicals (Jaya Chemical Supplier)	Biodiesel feedstock testing
n-hexane (99%)	Merck (Jaya Chemical Supplier)	Biodiesel feedstock testing
Methyl heptadecanoate (>99%)	Merck (Jaya Chemical Supplier)	Gas chromatography standard

3.3 Synthesis of Sulfonated Sulfonated Magnetic Biochar Catalyst

The synthesis method of the SMBC was modified from Mubarak et al. (2014) by utilizing a tube furnace for higher carbonization temperature instead of a microwave muffle

system oven. Some of the SMBC synthesis parameters, such as the type of oil palm biomass, the $FeCl_3 \cdot 6H_2O$ solution molarity, the carbonization temperature, and the sulfuric acid (H_2SO_4) molarity, were varied according to the experimental design, as shown in more detail in Section 3.5. The overview of the SMBC synthesis method is illustrated in Figure 3.2.

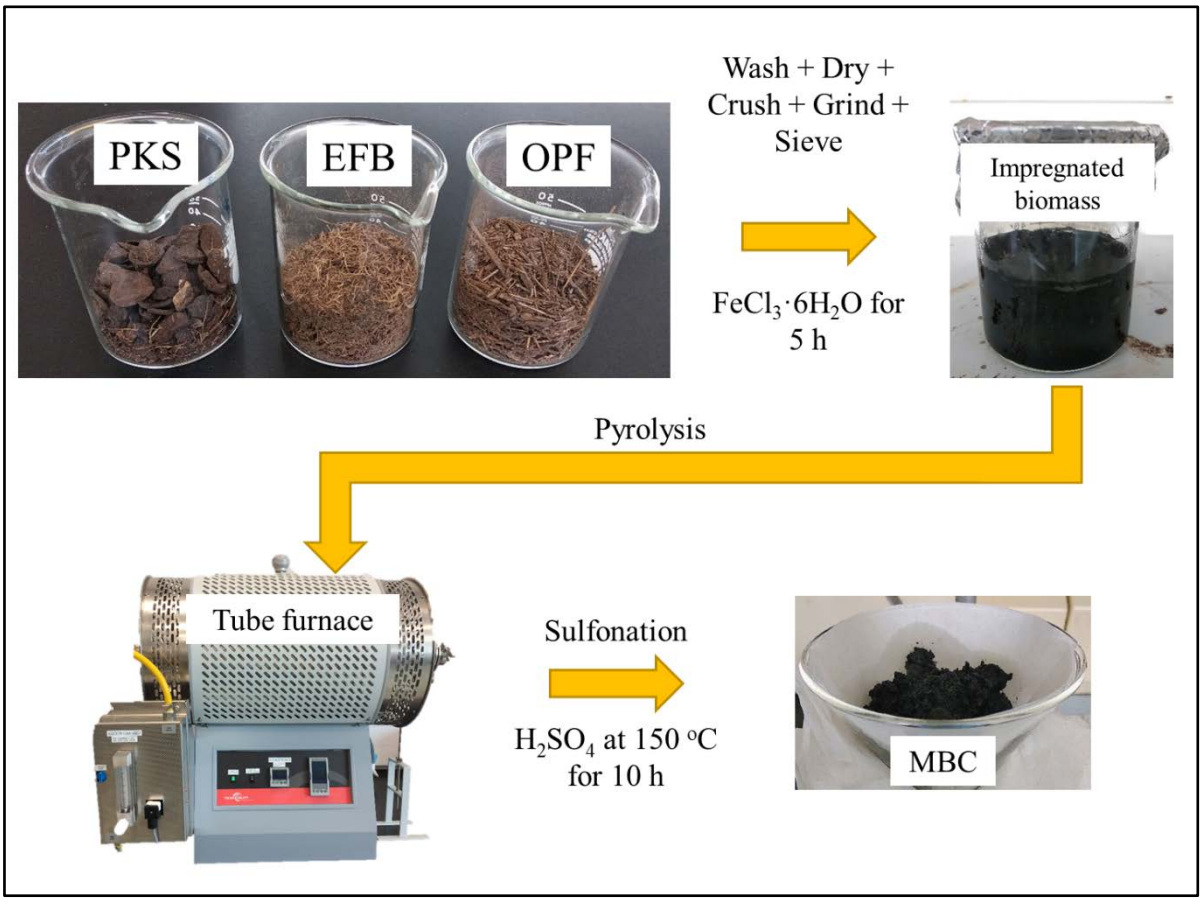

Figure 3.2: SMBC synthesis method.

The oil palm biomass (PKS, EFB, and OPF) was washed and dried. Then, they were impregnated with iron (III) chloride hexahydrate ($FeCl_3 \cdot 6H_2O$) solution. The $FeCl_3 \cdot 6H_2O$ solution molarity was varied from 1.5 M to 2.5 M. The ferrite ion-impregnated biomass was dried in an oven overnight at 110 °C using a lab drying oven (Binder ED240). The dried impregnated biomass was then carbonized by pyrolysis between 600 °C and 800 °C for 1 hour in argon gas flow with a flow rate of 200 mL min^{-1} using a high-temperature tube furnace (Thermconcept). The biochar then underwent sulfonation by immersion into 1.5M to 2.5M H_2SO_4 for 10 hours with constant stirring at 150 °C. The sulfonated magnetic biochar was dried in a lab drying oven (Binder ED240) at 80 °C overnight. After drying, the newly formed SMBC was stored in an airtight container prior to its usage.

3.4 Characterization of Sulfonated Magnetic Biochar Catalyst

3.4.1 Surface Morphology Determination

A surface morphology study was conducted to investigate the surface porosity of the SMBC. A field emission scanning electron microscope (FESEM) (FEI Quanta 400F) was utilized to study the morphology of the SMBC. The study was done between 100 and 100,000 times magnification and 20kV of accelerating voltage. The samples were tested one at a time. Prior to the test, a sample was mixed with ethanol to form a suspension. The suspension was dropped onto the sample holder and let sit for it to evaporate. The sample holder was then carefully put inside the FESEM for the analysis to begin.

3.4.2 Elemental Composition Determination

An Energy Dispersive X-Ray (EDX) analysis was done to study the elemental composition of SMBC. The target elements for the analysis were carbon, iron, and sulfur. Carbon was targeted for the comparison between the different types of oil palm biomass (PKS, OPF, and EFB). Iron was targeted for the confirmation of iron impregnation onto SMBC and the comparison of the impregnation ability of the different types of oil palm biomass. Similarly, sulfur was targeted for the confirmation of sulfonation of SMBC and the comparison of the sulfonation ability of the different types of oil palm biochar. This elemental analysis was done via an EDX analyzer (Oxford-Instruments INCA 400 with X-Max Detector) attached to a FESEM (FEI Quanta 400F). Each of the samples for the analysis was taken out at a time from its storing containers and then directly tested on the sample holder.

3.4.3 Specific Surface Area Determination

A specific surface area analysis was done to analyze the surface porosity and area availability for catalytic activity. The analysis was done using a gas sorption analyzer (TriStar II Plus). The Brunauer- Emmett-Teller (BET) equation was utilized to acquire the specific surface area. The samples were tested one at a time. Before each test, the samples had gone through degassing at 200 °C under vacuum for 12 hours and -195.8 °C for nitrogen gas adsorption.

3.4.4 Thermal Stability Determination

The thermal stability analysis of the oil palm biomass was analyzed to compare the lignocellulosic materials composition of the biomass. Raw PKS, raw OPF, and raw EFB were analyzed using a thermogravimetric analyzer (Mettler Toledo TGA/DSC1) under a flow of nitrogen at the flow rate of 50 mL min^{-1} and a temperature ramp from room temperature until

700 °C at 10 °C min^{-1}. From literature, oil palm biomass decomposition plateaued after 700 °C (Liew et al. 2018). As there was no significant weight reduction observed beyond 700 °C during the TGA analysis of the biomass, this research only investigated the thermal stability of the oil palm biomass until 700 °C.

3.4.5 Functional Group Determination

The functional groups' presence on the SMBC was studied via Fourier transform infrared (FTIR) spectroscopy analysis. The chemical analysis was done via an FTIR spectrophotometer (Perkin Elmer) using Attenuated Total Reflectance (ATR) sampling technique for a region of 4000 cm^{-1} to 400 cm^{-1}. The analysis was done in transmittance mode.

3.4.6 Acidity Determination

The acid density of SMBC, studied to evaluate the ability of the oil palm biochar to adsorb the sulfonic group during sulfonation, was calculated by performing neutralization titration. A fixed amount of SMBC was weighed and mixed with 0.1M NaCl solution. The mixture was left for 12 hours before it was filtered. Then, the filtrate was titrated with 0.01M NaOH solution with phenolphthalein as an indicator. The amount of 0.01M NaOH solution needed to turn the mixture pink for at least 10 seconds was noted for the calculation of the acid density of SMBC, as shown in Equation 3.1.

$$\text{Acid density (mmol g}^{-1}) = \frac{V_{NaOH} M_{NaOH}}{W_{SMBC}} \quad (3.1)$$

where V_{NaOH} = volume of NaOH solution needed for titration (mL), M_{NaOH} = molarity of NaOH solution (mol L^{-1}), W_{SMBC} = mass of SMBC (g). The experiment was repeated for every SMBC two more times, and the average acid density values were calculated and reported in terms of mmol g^{-1}.

3.4.7 Magnetic Properties Determination

The magnetic property of SMBC was studied using a vibrating sample magnetometer (VSM) (Lake Shore 7400 Series). The mass saturation magnetization (σ_s) was studied to investigate the ability of SMBC to be magnetically attracted for the product-catalyst separation during biodiesel production. The study was made at Sunway University Malaysia. The magnetic field was generated between -8000 Oe and 8000 Oe, and points were acquired continuously to generate a hysteresis loop.

3.5 Sulfonated Magnetic Biochar Catalyst Synthesis Optimization by the Taguchi Method

The Taguchi method was adopted to determine the optimized parameters for SMBC synthesis. This method was employed to reduce the number of experimental runs needed in order to find the optimal parameters for SMBC synthesis. Compared to other optimization methods, such as the full factorial method and response surface method, the Taguchi method requires significantly fewer experimental runs. Only four experimental runs were needed by this design to investigate three factors. A similar 3-factor design using the full factorial method will need eight runs, while the response surface method will need 20 runs. Therefore, the Taguchi method was chosen for the SMBC synthesis optimization analysis in this research in order to save the time and cost of running the catalyst characterization. In this research, each of the three parameters, also known as factors, was studied at two different levels. Therefore, the L4 Taguchi design (2-level, 3-factor) was used. The factors that were investigated are $FeCl_3 \cdot 6H_2O$ concentration, carbonization temperature, and H_2SO_4 concentration. Based on the studies by Santos et al. (2020), Quah et al. (2020), K. Liu, Wang, and Yu (2018), and Mubarak et al. (2014), the optimum levels for biochar synthesis were obtained. For $FeCl_3 \cdot 6H_2O$ and H_2SO_4 concentration, both of these factors were studied at 1.5M for level 1 and 2.5M for level 2. Meanwhile, the carbonization temperature was studied at 600 °C for level 1 and 800 °C for level 2. The responses that were considered for this analysis were the BET surface area, acid density, and the mass saturation magnetization of the produced catalyst. All of the factors and responses are shown in Table 3.2.

Table 3.2: The factors and responses for the Taguchi method optimization.

	Factors			**Responses**		
	$FeCl_3 \cdot 6H_2O$ Concentration	**Carbonization Temperature**	**H_2SO_4 Concentration**	**BET Surface Area**	**Acid Density**	**Mass saturation magnetization**
Symbol	FC	CT	HC	SA	AD	MM
Unit	M	°C	M	$m^2\ g^{-1}$	$mmol\ g^{-1}$	$Am^2\ kg^{-1}$
Level 1	1.5	600	1.5			
Level 2	2.5	800	2.5			

The computation for the Taguchi method was done on the MINITAB statistical software version 19. The software generated an experimental design matrix, as shown in Table 3.3, based on the L4 Taguchi design (2-level, 3-factor). The SMBC produce from PKS using the parameters from run 1 was denoted PKS1, run 2 was denoted PKS2, run 3 was denoted PKS3, and run 4 was denoted PKS4. The same denotation was done on the SMBC produced from OPF and EFB. From these experiments, the responses were analyzed through the SN ratio 'the larger is better' as the maximum value of responses was desired. The SN ratio was calculated, as shown in Equation 3.2.

Table 3.3: The design matrix for the Taguchi method optimization.

Design matrix			
Run	**$FeCl_3 \cdot 6H_2O$ Concentration (M)**	**Calcination (°C)**	**H_2SO_4 Concentration (M)**
1	1.5	800	2.5
2	2.5	800	1.5
3	1.5	600	1.5
4	2.5	600	2.5

$$\text{SN ratio (the larger is better)} = -10 \log_{10} \frac{1}{n} \sum \frac{1}{a_i^2} \quad (3.2)$$

where n = experiment count, a_i = response value.

3.6 Biodiesel Production

The reaction to produce fatty acid methyl ester (FAME), or generally known as biodiesel, was carried out, and the production began by mixing a fixed amount of methanol and SMBC in a 250 mL conical flask. The mixture was heated and shaken by a shaking incubator (LABNET-USA) at 200 rpm (Guldhe et al. 2017). UCO to be used in the reaction was filtered to remove any solid residue, and then used directly for the biodiesel production reaction. Transesterification was started by mixing filtered UCO with the heated and premixed methanol-SMBC mixture. The reaction parameters, such as the catalyst loading, oil to methanol molar ratio, reaction temperature, and reaction period, were determined by the values inserted into the response surface methodology - central composite design (RSM-CCD) module of the Design-Expert version 12 software. The response for the analysis is the biodiesel yield. Table

3.4 shows the actual levels of the parameters with respect to their coded values. The data for the design of experiment are shown in Appendix A. Figure 3.3 shows the overview of biodiesel synthesis. The biodiesel yield was determined through a gas chromatograph (GC) (Agilent 8890) equipped with a flame ionization detector (FID). The GC was fitted with a ZEBRON ZB-FAME capillary column (30 meters, 0.25 mm ID, 0.20 µm FT). Table 3.5 shows the oven program of the GC for the biodiesel yield analysis used for this study, as suggested by the capillary column manufacturer (Trass et al. 2017). The biodiesel sample was directly tested by the GC with n-hexane as a solvent and methyl heptadacenoate as an internal standard. Equation 3.3 was used to calculate the biodiesel yield using the data obtained from the GC biodiesel analysis (Patil et al. 2012). The biodiesel yield is the percentage of concentration of pure FAME in a crude biodiesel sample. Sample graph and yield calculation of GC result are shown in Appendix B.

Table 3.4: RSM factors and their respective levels with alpha value = 2.

Uncoded variables	**Symbol**	**Levels**				
		-2	**-1**	**0**	**1**	**2**
Catalyst loading (wt%)	A	4	7	10	13	16
Methanol-oil molar ratio	B	10	15	20	25	30
Temperature (°C)	C	50	55	60	65	70
Time (h)	D	2	4	6	8	10

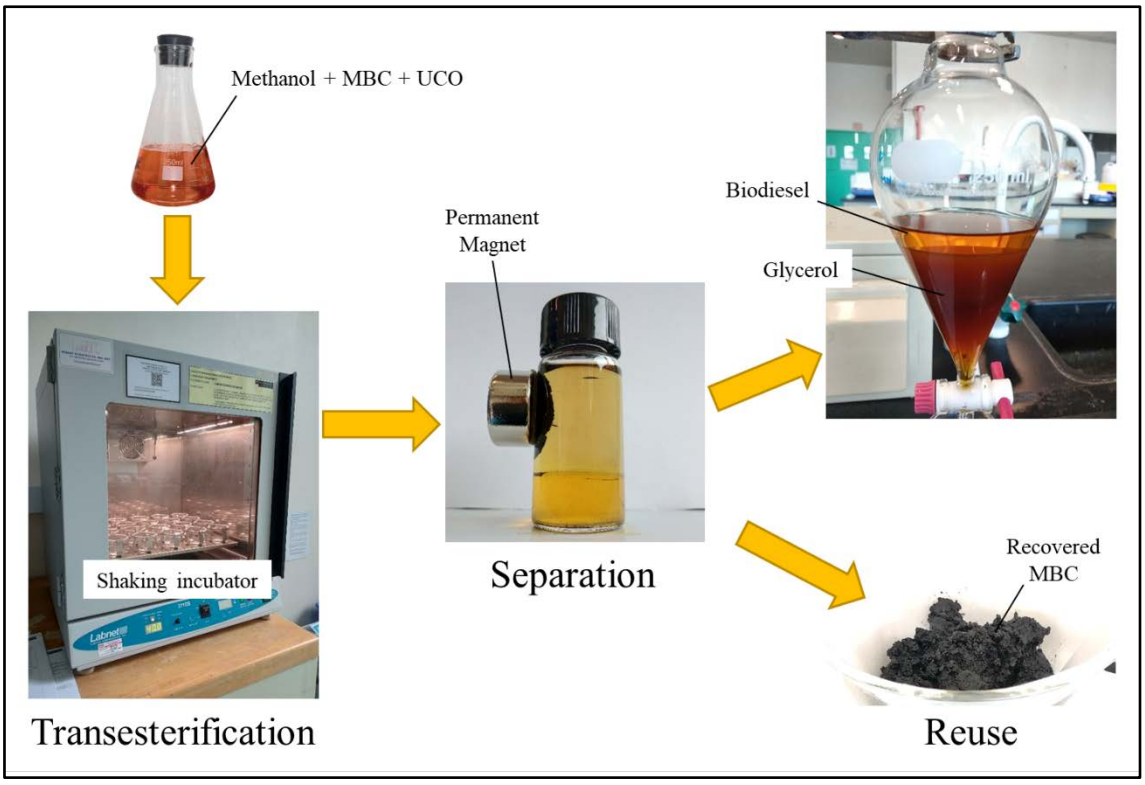

Figure 3.3: Biodiesel synthesis method.

Table 3.5: Gas chromatograph oven program for biodiesel analysis.

Event	Rate (°C min^{-1})	Value (°C)	Hold Time (min)	Total Time (min)
Initial	-	100	2	2
Ramp 1	10	140	0	6
Ramp 2	3	190	0	22.67
Ramp 3 (End)	30	260	2	27

$$Y = \frac{(\sum A) - A_{IS}}{A_{IS}} \times \frac{C_{IS} \times V_{IS}}{W} \times 100 \qquad (3.3)$$

where Y = biodiesel yield (%), $\sum A$ = total peak area, A_{IS} = peak area of internal standard, C_{IS} = concentration of internal standard (mg mL^{-1}), V_{IS} = volume of internal standard injected (mL), W = weight of crude biodiesel sample injected (mg).

3.7 Catalyst Reusability

After the optimum reaction parameters for biodiesel production were obtained from the previous experiments, the experiment was repeated using the optimum reaction parameters. The reaction was repeated for five cycles only as most literature that used a similar catalyst to

SMBC for biodiesel production reported significant deactivation of catalyst active sites after five cycles and needed to be reactivated (Roy et al. 2021). The SMBC was washed with n-hexane in a 250 mL conical flask, stirred at 200 rpm using an orbital shaker (IKA KS501) at room temperature in between cycles. The biodiesel yield was recorded in each cycle. The whole experiment was carried out in triplicate, and the average yield value was calculated and reported. The standard deviation (SD) of the data was calculated and served as an uncertainty level of the data. The error was represented by +/- one SD.

3.8 Characterization of Used Cooking Oil and Biodiesel

3.8.1 Physicochemical Properties Determination

The physicochemical properties of UCO and biodiesel, such as flash point, density at 15°C, specific gravity, API gravity at 60°C, kinematic viscosity at 40°C, cetane index, cloud point, and pour points, were determined by standard methods. The determination methods for each property are tabulated in Table 3.6.

Table 3.6: Biodiesel physicochemical properties determination standards.

Properties	Test method	Equipment
Flash point	ASTM D93	SYP1002B-IV Closed end flash point tester of petroleum products
Density at 15°C	ASTM D4052	DMA4500 M Laboratory Density Meter
Specific gravity	ASTM D4052	DMA4500 M Laboratory Density Meter
API gravity at 60°C	ASTM D4052	DMA4500 M Laboratory Density Meter
Kinematic viscosity at 40°C	ASTM D445	Cannon Viscometer
Cetane index	ASTM D976	Anton Paar ADU5 Automatic Distillation Unit
Cloud point	ASTM D2500	Manual apparatus for Cloud Point Test
Pour point	ASTM D97	Manual apparatus for Pour Point Test

3.8.2 Fatty Acid Profile Determination

The fatty acid profile of the biodiesel was determined through a gas chromatograph (GC) (Perkin Elmer Clarus 690 GC) equipped with a mass spectrometer detector (MSD). The

GC was fitted with a Perkin Elmer Elite-5MS capillary column (30 meters, 0.25 mm ID, 0.25 µm FT). The biodiesel sample was tested by the gas chromatograph diluted to 10 ng/mL with n-Hexane as a solvent.

3.9 Kinetic Study of Biodiesel Production

In this study, the kinetics of transesterification was studied. The effects of reaction temperature and time were investigated to establish the reaction's kinetics. The UCO was presumed mainly made up of triglyceride, as the FFA content of the UCO was less than 1.5%. Transesterification is a reversible reaction. This reaction may be divided into an intermediate three-step transesterification mechanism, as indicated in Equations 3.4 through 3.6. The overall transesterification process is shown in Equation 3.7 (Takase 2022).

$$\mathrm{TG} + \mathrm{ROH} \underset{k_2}{\overset{k_1}{\rightleftarrows}} \mathrm{DG} + \mathrm{ME} \tag{3.4}$$

$$\mathrm{DG} + \mathrm{ROH} \underset{k_4}{\overset{k_3}{\rightleftarrows}} \mathrm{MG} + \mathrm{ME} \tag{3.5}$$

$$\mathrm{MG} + \mathrm{ROH} \underset{k_6}{\overset{k_5}{\rightleftarrows}} \mathrm{GL} + \mathrm{ME} \tag{3.6}$$

$$\mathrm{TG} + 3\,\mathrm{ROH} \underset{k_8}{\overset{k_7}{\rightleftarrows}} 3\,\mathrm{ME} + \mathrm{GL} \tag{3.7}$$

where TG is the triglyceride, DG is the diglyceride, MG is the monoglyceride, ROH is the methanol, ME is the methyl ester, and GL is the glycerol. k1, k3, k5, k7 are the rate constants for forward reaction, while k2, k4, k6, k8 are the rate constants for backward reaction. The differential rate of reaction can be developed from Equations 3.4 – 3.6, as shown in Equations 3.8 – 3.13.

$$\frac{d[\mathrm{TG}]}{dt} = -k_1[\mathrm{TG}][\mathrm{ROH}] + k_2[\mathrm{DG}][\mathrm{ROH}] \tag{3.8}$$

$$\frac{d[\mathrm{DG}]}{dt} = k_1[\mathrm{TG}][\mathrm{ROH}] - k_2[\mathrm{DG}][\mathrm{ROH}] - k_3[\mathrm{DG}][\mathrm{ROH}] + k_4[\mathrm{MG}][\mathrm{ME}] \tag{3.9}$$

$$\frac{d[\mathrm{MG}]}{dt} = k_3[\mathrm{DG}][\mathrm{ROH}] - k_4[\mathrm{MG}][\mathrm{ROH}] - k_5[\mathrm{MG}][\mathrm{ROH}] + k_6[\mathrm{GL}][\mathrm{ME}] \tag{3.10}$$

$$\frac{d[\mathrm{GL}]}{dt} = k_5[\mathrm{MG}][\mathrm{ROH}] - k_6[\mathrm{GL}][\mathrm{ME}] \tag{3.11}$$

$$\frac{d[ME]}{dt} = k_1[TG][ROH] - k_2[DG][ME] + k_3[DG][ROH] - k_4[MG][ME] + k_5[MG][ROH] - k_6[GL][ME] \quad (3.12)$$

$$\frac{d[ROH]}{dt} = \frac{d[ME]}{dt} \quad (3.13)$$

From Equation 3.7, the overall rate of reaction can be written as in Equation 3.14.

$$-r_{TG} = -\frac{d[TG]}{dt} = -k_7[TG][ROH]^3 + k_8[GL][ME]^3 \quad (3.14)$$

where the bracketed species denote its molar concentration.

3.9.1 Pseudo-Irreversible First-Order Kinetic Model

The pseudo-irreversible first-order kinetic model assumes a sufficient catalyst is used with respect to the oil to tip the balance of the reaction in the direction of the synthesis of fatty acid methyl esters. As a result, it is possible to ignore the reverse reaction and consider the catalyst's concentration change to be negligible (Mercy Nisha Pauline et al. 2021). Considering the reaction is a single-step transesterification, Equation 3.15 may be used to express the rate law of the transesterification reaction for forward reactions.

$$-r_{TG} = -\frac{d[TG]}{dt} = k'[TG][ROH]^3 \quad (3.15)$$

where k' is the equilibrium rate constant. This reaction is governed by a fourth-order reaction rate law. The excess molar ratio of methanol to oil enables us to consider that the decrease in methanol concentration during the reaction is constant. The reaction can be assumed to exhibit as pseudo-irreversible first-order kinetics when methanol is reacted in excess. Its concentration behaves as a first-order reaction and does not change the order of the chemical reaction. The rate expression can finally be expressed, as shown in Equation 3.16.

$$-r_{TG} = -\frac{d[TG]}{dt} = k_{(1)}[TG] \quad (3.16)$$

where $k_{(1)}$ is the modified rate constant for pseudo-irreversible first-order reaction and $k_{(1)} = k'[ROH]^3$. At time t = 0, the initial triglyceride concentration was $[TG_0]$, and at time t, it reduced to [TG]. The integration of Equation 3.15 gives us Equation 3.17.

$$\ln[TG_0] - \ln[TG] = k_{(1)}t + C_1 \quad (3.17)$$

$$\ln\frac{[TG_0]}{[TG_t]} = k_{(1)}t + C_1 \quad (3.18)$$

From mass balance,

$$X_{ME} = 1 - \frac{[TG]}{[TG_0]} \quad (3.19)$$

where C_1 is the integration constant and X_{ME} is the methyl ester's production. Substituting Equation 3.19 for Equation 3.18 gives us Equation 3.20.

$$\ln \frac{1}{1-X_{ME}} = k_{(1)}t + C_1 \quad (3.20)$$

By simplifying Equation 3.20, we get the pseudo-irreversible first-order kinetic model Equation 3.21.

$$f(x_1) = -\ln(1 - X_{ME}) = k_{(1)}t + C_1 \quad (3.21)$$

The rate constant $k_{(1)}$ is acquired by plotting $f(x_1)$ versus t based on the optimum reaction parameters obtained from the biodiesel production optimization. The study was carried out at five different temperature readings, ranging from 50 °C - 70 °C. The gradient of the plot is the value of the rate constant at a respective temperature.

3.9.2 Pseudo-Irreversible Second-Order Kinetic Model

A transesterification of second-order reaction involves both of the reactants i.e. the methanol and oil. This ends up relatively hampering the reaction more compared to a first-order reaction. Nonetheless, for a pseudo-irreversible second-order reaction, the overall reaction is modelled with only the triglyceride as the methanol amount is assumed to be stoichiometrically in excess. As such, the rate law of the reaction is shown in Equation 3.22 (Stamenković et al. 2008).

$$-r_{TG} = -\frac{d[TG]}{dt} = k_{(2)}[TG]^2 \quad (3.22)$$

where $k_{(2)}$ is the pseudo-irreversible second-order reaction rate constant. Substituting Equation 3.22 for Equation 3.19, and assuming the chemical reaction is faster than the mass transfer $[TG_0] = 1$, we can turn the equation in terms of X_{ME} as shown in Equation 3.23.

$$-\frac{d[TG_0][1-X_{ME}]}{dt} = k_{(2)}[TG_0]^2(1 - X_{ME})^2 \quad (3.23)$$

$$-\frac{d[1-X_{ME}]}{(1-X_{ME})^2} = k_{(2)}dt \quad (3.24)$$

Integrating Equation 3.24 gives us the pseudo-irreversible second-order kinetic model Equation 3.25.

$$f(x_2) = \frac{1}{(1-X_{ME})} = k_{(2)}t + C_{(2)} \quad (3.25)$$

where $C_{(2)}$ is the integration constant. The rate constant $k_{(2)}$ is acquired by plotting $f(x_2)$ versus t based on the optimum reaction parameters obtained from the biodiesel production

optimization. The study was carried out at five different temperature readings, ranging from 50 °C - 70 °C. The gradient of the plot is the value of the rate constant at a respective temperature.

3.9.3 Pseudo-Reversible Second-Order Kinetic Model

The Langmuir-Hinshelwood-Hougen-Watson (LHHW) reaction mechanism was proposed for a heterogeneously catalyzed reaction. This mechanism states that the reactants molecule in this study, methanol, and triglyceride, are reacted at different catalytic sites on the catalyst surface through chemisorption (Sulaiman et al. 2020). For transesterification, nine steps of stepwise reactions are needed. Three steps involved are adsorption, reaction, and desorption (Feyzi et al. 2017). The stepwise reactions also describe the intermediate reactions that occur during transesterification. The stepwise reactions according to the LHHW mechanism are shown in Equations 3.26-3.34.

$$2 * + \mathrm{TG} + \mathrm{ROH} \underset{k_2}{\overset{k_1}{\rightleftarrows}} \mathrm{TG}^{*}\mathrm{ROH}^{*} \tag{3.26}$$

$$\mathrm{TG}^{*}\mathrm{ROH}^{*} \underset{k_4}{\overset{k_3}{\rightleftarrows}} \mathrm{DG}^{*}\mathrm{ME}^{*} \tag{3.27}$$

$$\mathrm{DG}^{*}\mathrm{ME}^{*} \underset{k_6}{\overset{k_5}{\rightleftarrows}} \mathrm{DG}^{*} + \mathrm{ME} + * \tag{3.28}$$

$$* + \mathrm{DG}^{*} + \mathrm{ROH} \underset{k_8}{\overset{k_7}{\rightleftarrows}} \mathrm{DG}^{*}\mathrm{ROH}^{*} \tag{3.29}$$

$$\mathrm{DG}^{*}\mathrm{ROH}^{*} \underset{k_{10}}{\overset{k_9}{\rightleftarrows}} \mathrm{MG}^{*}\mathrm{ME}^{*} \tag{3.30}$$

$$\mathrm{MG}^{*}\mathrm{ME}^{*} \underset{k_{12}}{\overset{k_{11}}{\rightleftarrows}} \mathrm{MG}^{*} + \mathrm{ME} + * \tag{3.31}$$

$$\mathrm{MG}^{*} + \mathrm{ROH} + * \underset{k_{14}}{\overset{k_{13}}{\rightleftarrows}} \mathrm{MG}^{*}\mathrm{ROH}^{*} \tag{3.32}$$

$$\mathrm{MG}^{*}\mathrm{ROH}^{*} \underset{k_{16}}{\overset{k_{15}}{\rightleftarrows}} \mathrm{GL}^{*}\mathrm{ME}^{*} \tag{3.33}$$

$$\mathrm{GL}^{*}\mathrm{ME}^{*} \underset{k_{18}}{\overset{k_{17}}{\rightleftarrows}} \mathrm{GL} + \mathrm{ME} + 2 * \tag{3.34}$$

where *, ROH*, TG*, DG*, MG*, GL*, and ME* are reaction intermediates between the catalyst surface and adsorbed ROH, TG, DG, MG, and ME.

Based on the stepwise reactions, Equations 3.26 and 3.27 are the rate limiting steps. From Equation 3.26, the rate law is shown in Equation 3.35.

$$r_{TG} = k_1[TG][ROH][*]^2 \tag{3.35}$$

where [*] is the catalytic active sites concentration. From Equation 3.27, the rate law is shown in Equation 3.36.

$$r_{TG} = k_3[TG^*ROH^*] \tag{3.36}$$

From Equation 3.26, we can derive Equation 3.37.

$$\frac{k_1}{k_2} = \frac{[TG^*ROH^*]}{[TG][ROH][*]^2} \tag{3.37}$$

Substituting Equation 3.37 for Equation 3.36, we get Equation 3.38.

$$r_{TG} = \frac{k_1 k_3}{k_2}[TG][ROH][*]^2 \tag{3.38}$$

Let, $$k' = \frac{k_1 k_3}{k_2} \tag{3.39}$$

The resulting rate law is shown in Equation 3.40.

$$r_{TG} = k'[TG][ROH][*]^2 \tag{3.40}$$

As both rate law derived from Equations 3.26 and 3.27 are similar, both are considered as rate determining step.

Let, $$k_{(3)} = k'[*] \tag{3.41}$$

where $k_{(3)}$ is the pseudo-reversible second-order reaction rate constant. Substituting Equation 3.41 for Equation 3.40, the resulting rate law is shown in Equation 3.42.

$$r_{TG} = k_{(3)}[TG][ROH] \tag{3.42}$$

From Equation 3.42, the overall chemical equation is shown in Equation 3.43.

$$TG + ROH \xrightarrow{k_{(3)}} Product \tag{3.43}$$

From Equation 3.43, only one mole from each reactant is needed for production. After substituting in Equation 3.19, the concentrations of reactants at any given time are calculated with Equations 3.44 and 3.45.

$$[\mathrm{TG}] = [\mathrm{TG_0}] - \mathrm{X_{ME}} \tag{3.44}$$

$$[\mathrm{ROH}] = [\mathrm{ROH_0}] - \mathrm{X_{ME}} \tag{3.45}$$

where $[ROH_0]$ is the methanol concentration at time t=0. By differentiating Equation 3.42 and substituting Equation 3.45 and Equation 3.44 for Equation 3.42, we get Equation 3.46.

$$\frac{\mathrm{dx}}{\mathrm{dt}} = \mathrm{k_{(3)}}([\mathrm{TG_0}] - \mathrm{X_{ME}})([\mathrm{ROH_0}] - \mathrm{X_{ME}}) \tag{3.46}$$

Integrating Equation 3.46 gives us the pseudo-reversible second-order kinetic model Equation 3.47.

$$\mathrm{f(x_3)} = \frac{1}{([\mathrm{ROH_0}]-[\mathrm{TG_0}])} \ln \frac{[\mathrm{TG_0}]([\mathrm{ROH_0}]-\mathrm{X_{ME}})}{[\mathrm{ROH_0}]([\mathrm{TG_0}]-\mathrm{X_{ME}})} = \mathrm{k_{(3)}t} \tag{3.47}$$

The rate constant $k_{(3)}$ is acquired by plotting $f(x_3)$ versus t based on the optimum reaction parameters obtained from the biodiesel production optimization. The study was carried out at five different temperature readings, ranging from 50 °C - 70 °C. The gradient of the plot is the value of the rate constant at a respective temperature.

3.9.4 Determination of Activation Energy and Reaction Kinetic

The Arrhenius equation was utilized as a tool to study the activation energy of the transesterification reaction to produce biodiesel. Equation 3.48 shows the Arrhenius equation in exponential form.

$$\mathrm{k} = \mathrm{A}e^{\frac{-E_a}{RT}} \tag{3.48}$$

where k is the rate constant (min^{-1}), A is the pre-exponential factor or frequency factor, E_a is the activation energy of reaction (J mol^{-1}), R is the gas constant (8.314 J mol^{-1} K^{-1}), and T is the absolute temperature (K). By linearizing Equation 3.48, taking a natural log at both sides, the transformed and rearranged linear form is shown in Equation 3.49.

$$ln\ \mathrm{k} = \ln\mathrm{A} - \frac{E_a}{RT} \tag{3.49}$$

By linear regression and plotting ln k versus 1/T based on the rate constant obtained through the kinetic modeling in Section 3.9.3, the E_a is derived from the gradient of the plot. The coefficient of determination (R^2) of the plot correlates the reaction rate with temperature (Gholipour Zanjani et al. 2020; Mani et al. 2020). In this study, this indicates that biodiesel transesterification fits to the proposed kinetic model, respectively (Putra et al. 2018; Gurunathan and Ravi 2015).

CHAPTER 4
RESULTS AND DISCUSSION

4.1 Overview

This chapter presents and discusses the findings of this research. First, the characterization of the sulfonated magnetic biochar catalyst (SMBC) via SEM, EDX, BET, TGA, FTIR, Neutralization Titration, and VSM is discussed in Section 4.2. In addition, the optimization of SMBC synthesis using the Taguchi method is discussed in Section 4.3. Section 4.4 presents the results from the biodiesel optimization. Section 4.5 presents the results from the catalyst reusability analysis. Section 4.6 discusses the physicochemical and fatty acid profile characterization of used cooking oil (UCO) biodiesel. The results from the kinetic study of the UCO biodiesel production are presented in Section 4.7. Lastly, Section 4.8 presents the summary of this chapter.

4.2 Characterization of Sulfonated Magnetic Biochar Catalyst

4.2.1 Surface Morphology of Sulfonated Magnetic Biochar Catalyst

As the performance of a catalyst can be generally defined by its surface morphology, the surface morphology of SMBC was analyzed using a FESEM. The SEM images shown in Figures 4.1 to 4.3 are for PKS, EFB, and OPF, respectively. Figure 4.1 (a) shows raw PKS and Figure 4.1 (b) shows PKS derived SMBC. From Figure 4.1, it can be observed that the surface of the PKS is smooth prior to carbonization. After carbonization, a porous surface is developed. Similarly, for EFB, in Figure 4.2, the smooth surface of EFB is turned to porous after the carbonization process. Figure 4.3 shows a similar trend for the OPF, in which its surface turns from smooth to porous. Figures 4.1 to 4.3 indicate that the smooth surface areas of the biomass are shown to have transformed as pores can be seen forming at the surface of the carbonized SMBC. Pore formation is one of the results of the production of volatile gas by biomass during the carbonization process. The remainder of the biomass that is non-volatile forms porous biochar, as can be observed from the SEM images (Liew et al. 2018). These results are also reported by Lim et al. (2020), in which EFB was carbonized, and rough surfaces with porosity were formed from the smooth-surfaced biomass. This study utilized EFB biochar as a catalyst for biodiesel production (Lim et al. 2020). Y. Wei et al. (2020) also reported pores formation and higher specific surface area for carbonized bamboo biochar. The study then utilized biochar as a catalyst for cellulose hydrolysis (Y. Wei et al. 2020).

Furthermore, it can be observed that the pore size developed on PKS is less apparent compared to EFB and OPF. The pores and channels developed on EFB and OPF are wider compared to PKS. The sulfonation treatment of the SMBC can also be acknowledged as another factor for the formation of the pores on the SMBC (Cheng and Li 2018). As the surface of the biochar exposed to the strong acid during sulfonation, more surface area was subjected to oxidation by the sulfonating agent. This gives the biochar a more open pore structure and at the same time increased the specific surface area (da Luz Corrêa et al. 2020; Ohra-aho et al. 2020).

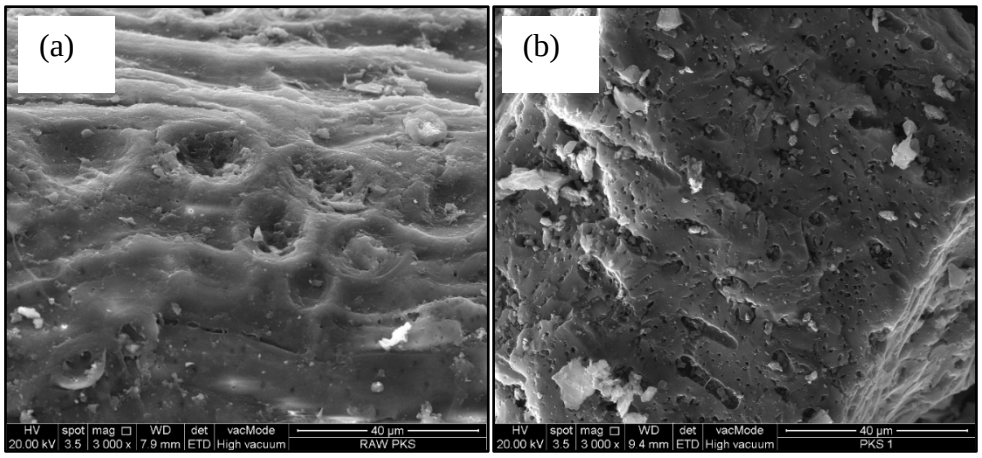

Figure 4.1: SEM images of (a) raw PKS, (b) PKS derived SMBC.

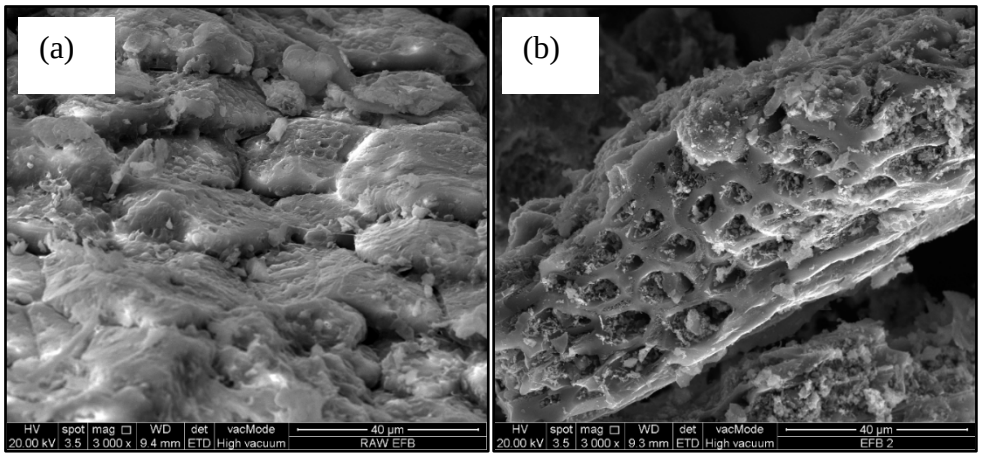

Figure 4.2: SEM images of (a) raw EFB, (b) EFB derived SMBC.

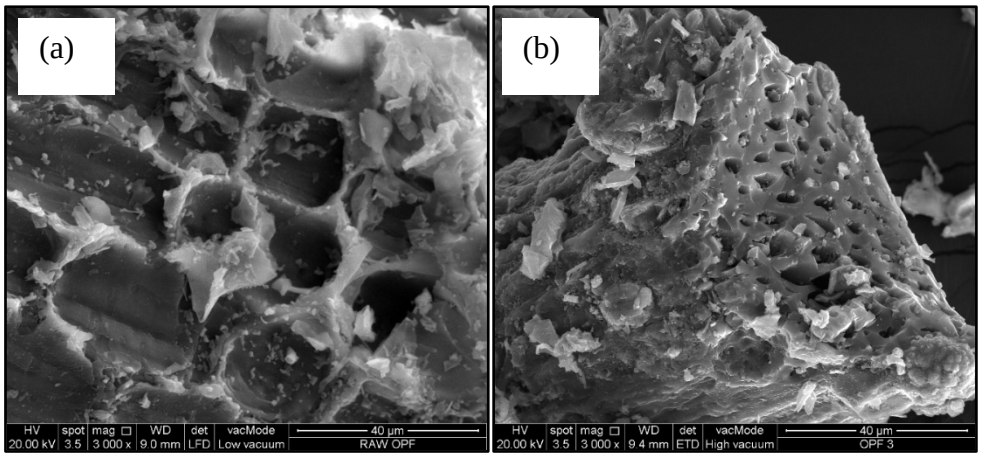

Figure 4.3: SEM images of (a) raw OPF, (b) OPF derived SMBC.

4.2.2 Energy Dispersive X-Ray Analysis of Sulfonated Magnetic Biochar Catalyst

EDX analysis was conducted to analyze the elemental composition of the SMBC. Figures 4.4, 4.5, and 4.6 show the spectra of PKS, EFB, and OPF, respectively. Table 4.1 summarizes the elemental composition of the analyzed samples. The iron peaks can be observed in all SMBC spectra with the exception of the raw biomass spectra, which is an indication of the magnetic iron impregnation to the SMBC. J. Dong et al. (2021) investigated a magnetic biochar catalyst for the adsorption of lead ions from an aqueous solution. The study reported an increase in iron content for an iron-impregnated catalyst compared to a non-impregnated catalyst (J. Dong et al. 2022). The relatively higher sulfur content on the other hand indicated the successful sulfonation of the SMBC. Q. Xie et al. (2020) prepared a sulfonated biochar catalyst for spiramycin hydrolysis. In this study, the elemental sulfur content of the sulfonated catalyst increased compared to the raw form of the biochar (Q. Xie et al. 2020).

As can be seen in Table 4.1, the composition of carbon in SMBC from PKS on average is higher compared to OPF and EFB. This can be attributed to the lower ability of PKS to be impregnated with iron and sulfur from the sulfonation process. The variation of iron and sulfur content between the biomass also indicates the variation of bonding strength of the functional group onto the biochar (W. Xie and Wang 2020). For PKS, less iron to sulfur content ratio was recorded compared to OPF and EFB. This is a result of the leaching of iron content during sulfonation (Quah et al. 2020). For OPF and EFB, this circumstance was less observed. The iron oxides formed during carbonation might be leached out through sulfuric acid solvation later during sulfonation. The severity of the leaching, however, depends on the capability of the biochar to bond with the functional groups (J. Lee et al. 2019). The leaching severity differs between the biomass, as each biomass was made from different lignocellulosic material

component and having different surface structure as discussed in much detailed in Section 4.2.4.

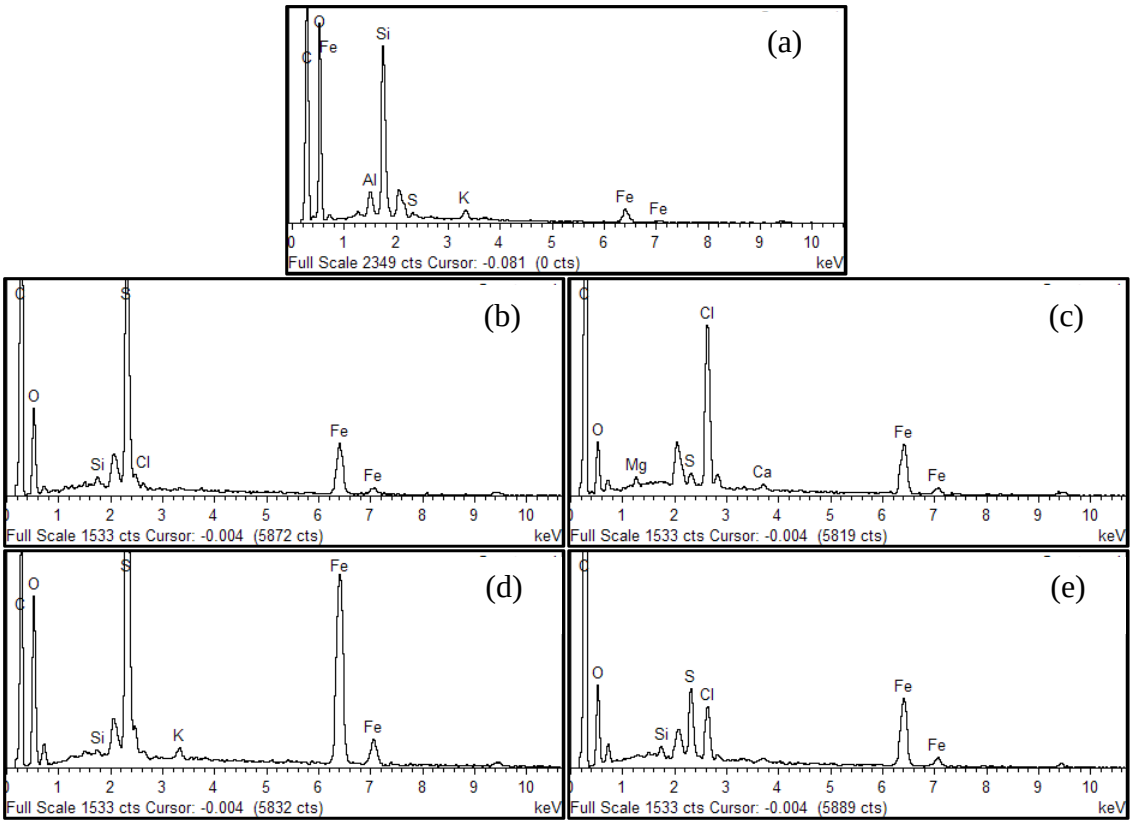

Figure 4.4: EDX spectra of (a) raw PKS, (b) PKS1, (c) PKS2, (d) PKS3, and (e) PKS4.

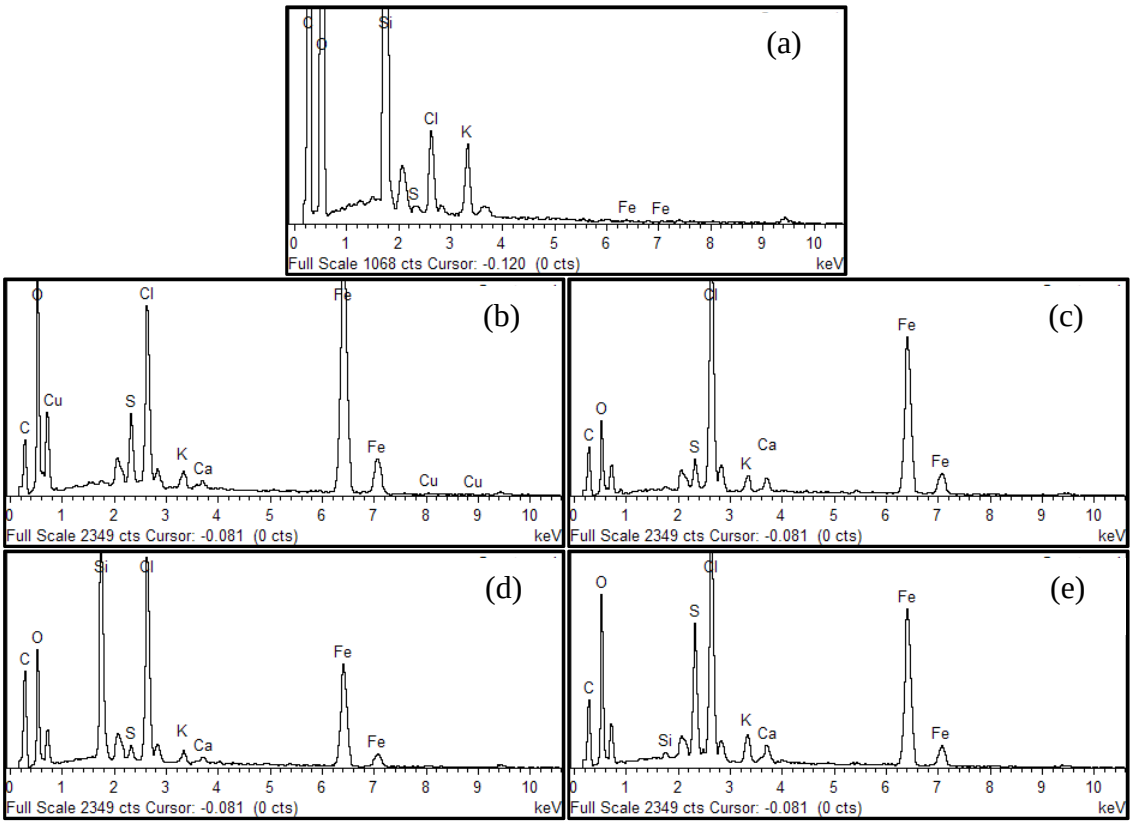

Figure 4.5: EDX spectra of (a) raw OPF, (b) OPF1, (c) OPF2, (d) OPF3, and (e) OPF4.

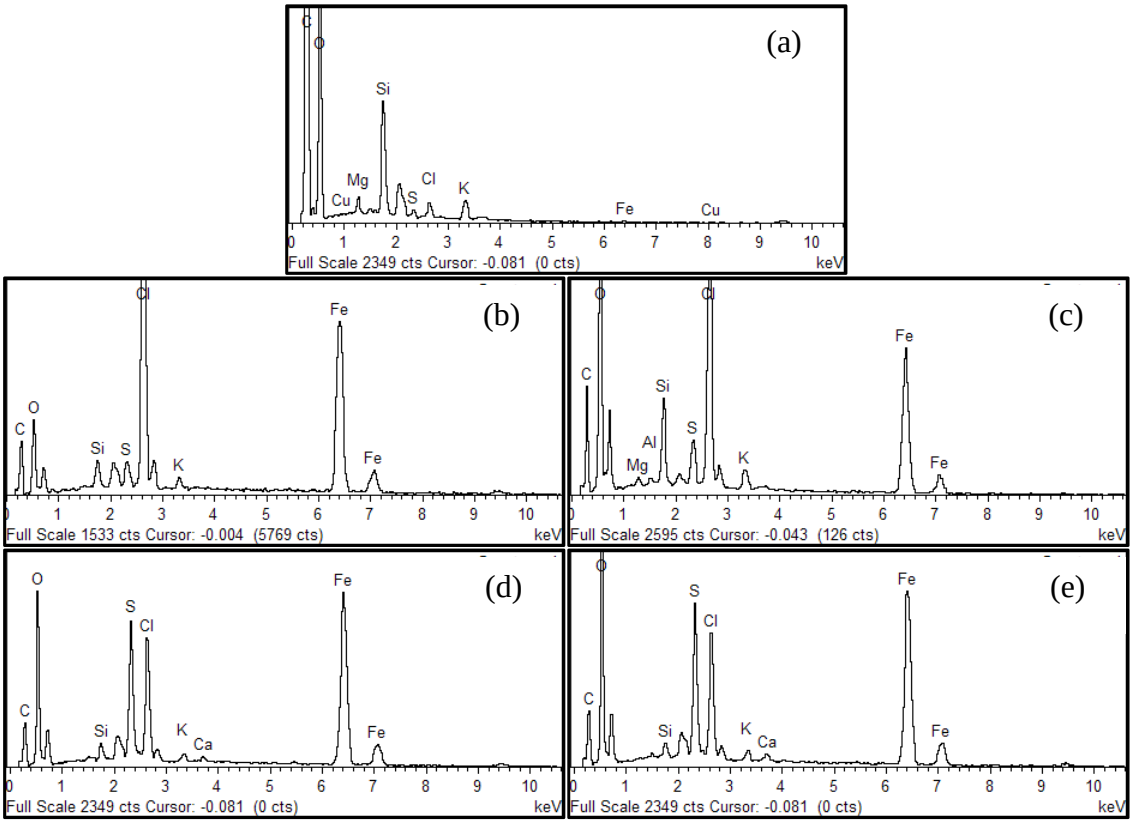

Figure 4.6: EDX spectra of (a) raw EFB, (b) EFB1, (c) EFB2, (d) EFB3, and (e) EFB4.

Table 4.1: Summary of elemental composition of raw biomass and SMBC.

	Weight%						
Element	**C**	**O**	**Si**	**S**	**Cl**	**K**	**Fe**
Raw PKS	51.76	39.29	5.49	0.24	0	0.43	2.04
PKS1	68.11	17.91	0.21	7.25	0.23	0	6.29
PKS2	73.55	12.75	0	0.42	5.90	0	6.86
PKS3	51.64	20.06	0.12	9.98	0.31	0	17.89
PKS4	72.26	15.78	0.25	1.96	1.75	0	7.99
Raw OPF	51.65	41.47	4.85	0.07	0.99	0.97	0
OPF1	24.83	27.34	0	2.70	7.44	0.78	36.09
OPF2	35.07	16.90	0	1.38	14.98	1.02	29.74
OPF3	45.04	22.67	6.77	0.59	8.81	0.56	15.22
OPF4	33.51	27.46	0.18	4.75	10.02	1.28	21.94
Raw EFB	56.83	39.73	1.88	0.20	0.32	0.52	0.07
EFB1	36.00	15.85	1.06	1.13	14.43	0.63	30.90
EFB2	35.97	33.99	2.16	1.35	8.50	0.76	16.87
EFB3	26.89	29.17	6.32	6.64	0.43	0.29	29.59
EFB4	25.94	34.83	0.50	5.85	5.72	0.48	26.30

4.2.3 Surface Area Analysis of Sulfonated Magnetic Biochar Catalyst

The surface and pore features of the SMBC are summarized in Table 4.2. The BET surface areas for PKS range from 0.94 $m^2 g^{-1}$ to 74.16 $m^2 g^{-1}$. Meanwhile, the BET surface areas for OPF range from 5.96 $m^2 g^{-1}$ to 23.27 $m^2 g^{-1}$, and the BET surface areas for EFB range from 6.58 $m^2 g^{-1}$ to 46.74 $m^2 g^{-1}$. Yunchao Li et al. (2020) reported a value of BET surface area between 19.1 $m^2 g^{-1}$ and 40.3 $m^2 g^{-1}$ for a biochar catalyst made from PKS and used in biodiesel production (Yunchao Li et al. 2020). This value is within the range of the current SMBC made from PKS. Lawal et al. (2021) prepared a PKS biochar catalyst with a higher BET surface area value at 377 $m^2 g^{-1}$ (Lawal et al. 2021). The higher BET surface area is caused by the difference in the biochar preparation method. The catalyst prepared in the literature was not impregnated with iron or treated chemically. Thus, the surface is free from any pore obstruction (Jenie et al. 2020). Another study by Lim et al. (2020) reported a BET surface area value of 2.851 $m^2 g^{-1}$ for a sulfonated EFB biochar catalyst. The study also highlighted the reduction of BET surface

area when comparing the sulfonated biochar catalyst to the non-sulfonated biochar catalyst. The surface area difference can also be associated with the different carbon feedstock for the catalyst synthesis (Lim et al. 2020).

On average, the BET surface area of EFB is higher than OPF and PKS. Meanwhile, the BET surface area of OPF is higher than PKS, except for PKS4. The high BET surface area for PKS4 is due to the formation of micropores, which can be observed from its average pore diameter of 2.83 nm. The average pore diameter of PKS4 is on the borderline between microporous and mesoporous structures. A mesoporous structure has an average pore diameter between 2 nm and 50 nm, while a microporous structure has an average pore diameter of less than 2 nm (Anto et al. 2019). Nevertheless, all of the SMBCs can be categorized as mesoporous based on their average pore diameters between 2.83 nm and 29.44 nm.

Table 4.2: BET surface area and porosity of SMBC.

Catalyst	BET Surface Area (m^2 g^{-1})	Pore Volume (cm^3 g^{-1})	Average Pore Diameter (nm)
PKS1	1.74	0.006	13.87
PKS2	1.45	0.011	29.44
PKS3	0.94	0.004	18.57
PKS4	74.16	0.053	2.83
OPF1	23.27	0.026	4.45
OPF2	8.10	0.024	11.95
OPF3	7.24	0.024	13.48
OPF4	5.96	0.018	12.48
EFB1	44.42	0.038	3.46
EFB2	46.74	0.040	3.44
EFB3	8.08	0.019	9.36
EFB4	6.58	0.016	9.48

4.2.4 Thermogravimetric Analysis of Sulfonated Magnetic Biochar Catalyst

TGA and differential thermal analysis (DTA) were done on the raw PKS, raw OPF, and raw EFB. Figure 4.7 show the thermograms of raw PKS, raw OPF, and raw EFB. Figures 4.7 (a) and 4.7 (b) represent the thermal decomposition of raw PKS and raw OPF, respectively. Both raw PKS and raw OPF show three decomposition peaks in both of their thermograms. The first peak that occurred around 80 °C represented the evaporation of moisture from the biomass (Dayang et al. 2017). The second peak that occurred around 280 °C represented the decomposition of hemicellulose to form biochar. The third peak that occurred around 350 °C represented the decomposition of cellulose to form biochar (Babinszki et al. 2021). Figure 4.7 (c) shows the thermograms for the thermal decomposition of raw EFB. For raw EFB, only two decomposition peaks can be observed. The first peak that occurred around 76 °C represented the evaporation of moisture from the raw EFB (Dayang et al. 2017). Meanwhile, the second peak that occurred around 320 °C represented the decomposition of cellulose to form biochar (Babinszki et al. 2021). The lignin component of the biomass decomposed from 150 °C to 600 °C at a slower rate compared to hemicellulose and cellulose (Y. Wei et al. 2020). From these

results, it can be concluded that raw EFB is mainly made up of cellulose and lignin. Meanwhile, both raw PKS and raw OPF have lignin and cellulose contents with a higher content of hemicellulose compared to raw EFB. The carbonization temperature of 600 °C and 800 °C chosen for SMBC synthesis was sufficient to form biochar from the oil palm biomass based on the observed weight change that plateaued after 500 °C. As there was no significant weight reduction that was observed beyond 500 °C during the TGA analysis of the biomass, the same is assumed for the catalyst. In addition, the reaction temperature for biodiesel production did not exceed 100 °C; thus, there is no concern about the stability of the catalyst.

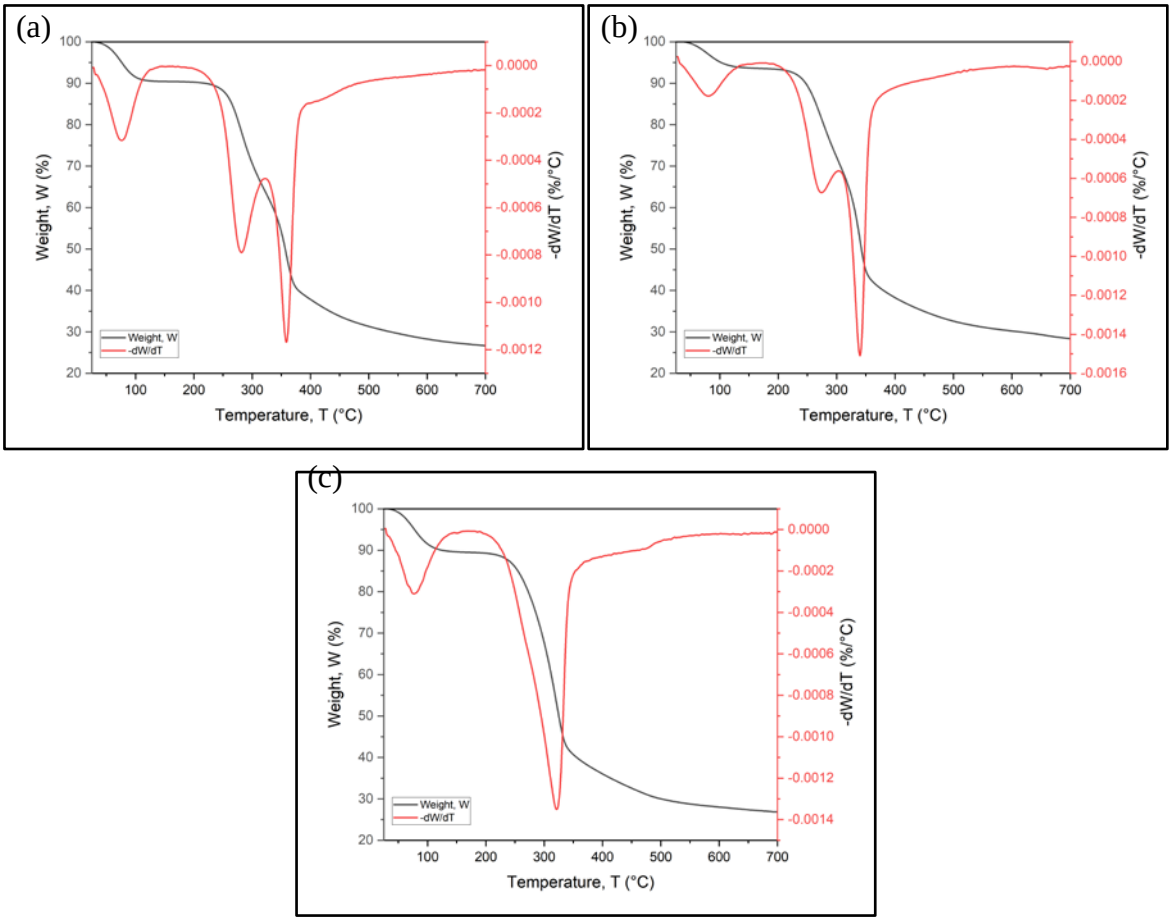

Figure 4.7: TGA- DTA curve of (a) raw PKS, (b) raw OPF, and (c) raw EFB at 10 °C min^{-1} heating rate.

4.2.5 FTIR Analysis of Sulfonated Magnetic Biochar Catalyst

FTIR was employed to study the functional groups present on the SMBC. Figures 4.8, 4.9, and 4.10 show the spectra of raw biomass and its respective SMBC. From Figures 4.8 to 4.10, it can be observed that the peaks in each spectrum between wavenumbers 3381 cm^{-1} and 3423 cm^{-1} correspond to O-H due to the hydration of the biomass and SMBC (Mateo et al. 2020). The peaks between 1569 cm^{-1} and 1597 cm^{-1} correspond to aromatic C=C bonds. The

peaks between 1081 cm^{-1} and 1136 cm^{-1} correspond to C-O group stretching, and the peaks between 1000 cm^{-1} and 1040 cm^{-1} corresponding to S=O bonds appeared after the sulfonation process of SMBC (Rocha et al. 2019). The peaks between 783 cm^{-1} and 808 cm^{-1} are attributed to the bending of aromatic C-H bonds (Jiang et al. 2020). The absorption peaks between 400 cm^{-1} and 600 cm^{-1} correspond to the Fe-O bonds as a result of the ferric ion impregnation on the SMBC (A. Wang et al. 2018). The peaks between 400 cm^{-1} and 600 cm^{-1} for all SMBC spectra are relatively higher than the raw biomass as a result of iron impregnation on the SMBC. Figure 4.11 shows the comparison of SMBC spectra synthesized from PKS, OPF, and EFB. Among the SMBC, OPF shows more significant S=O group peaks and higher Fe-O group peaks compared to EFB and PKS. From the EDX analysis in Section 4.2.2, the Fe and S content of OPF and EFB are comparable, and significantly higher than that of PKS. Table 4.3 shows the respective functional group of the biomass and SMBC.

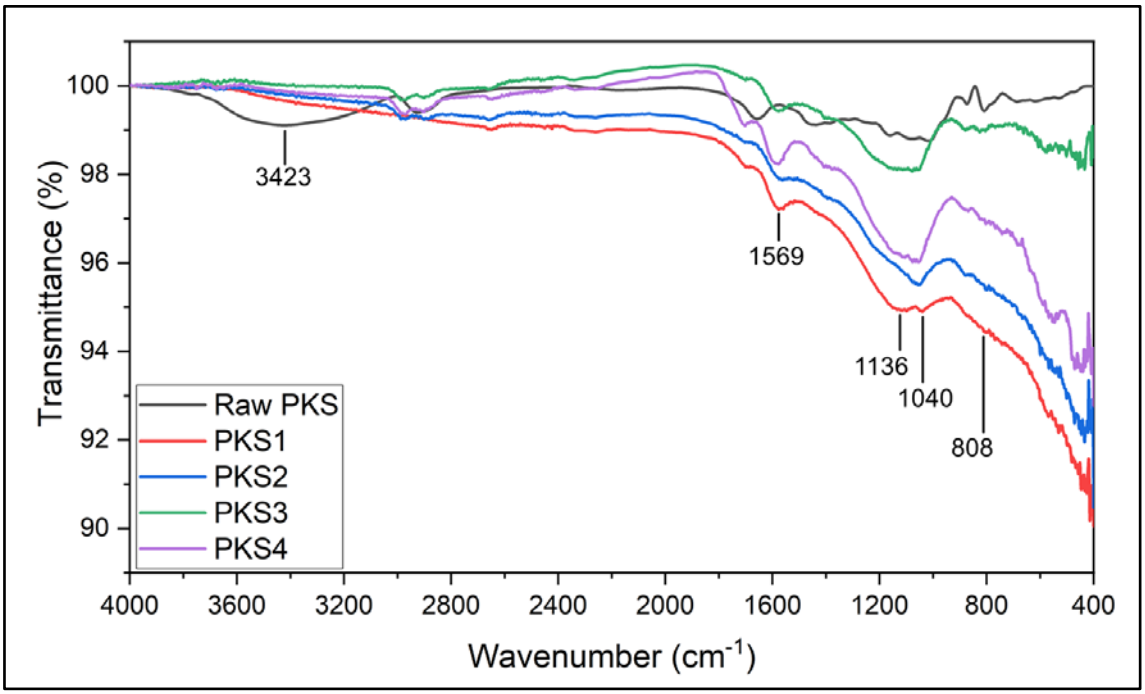

Figure 4.8: FTIR spectroscopy of raw PKS, PKS1, PKS2, PKS3, and PKS4.

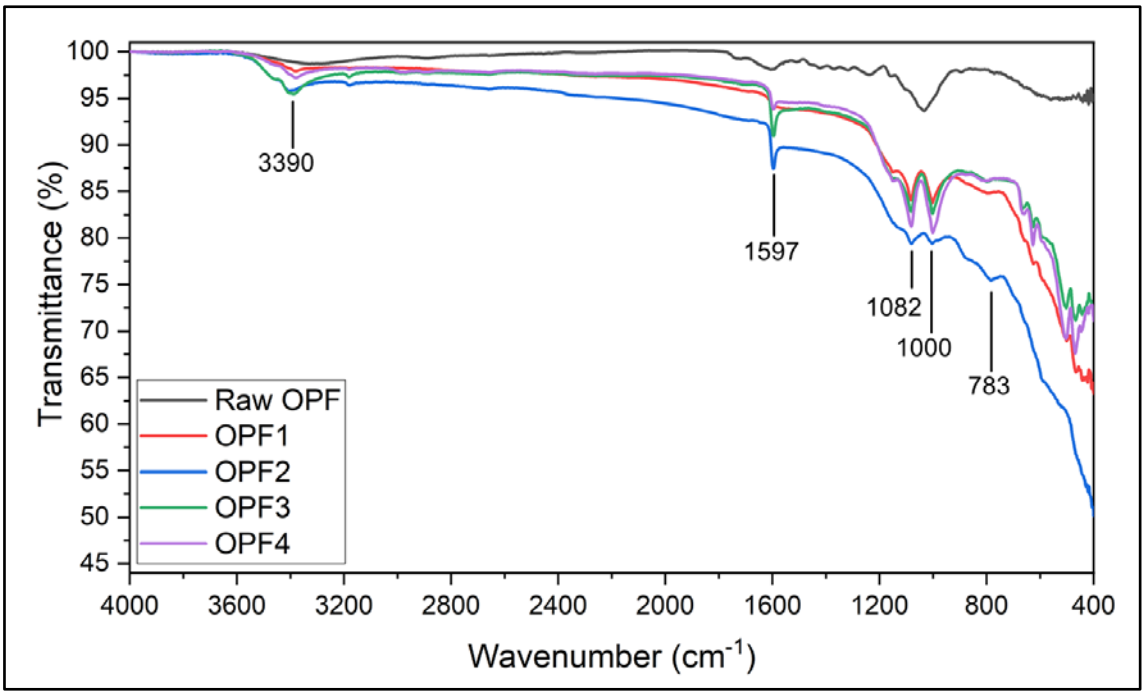

Figure 4.9: FTIR spectroscopy of raw OPF, OPF1, OPF2, OPF3, and OPF4.

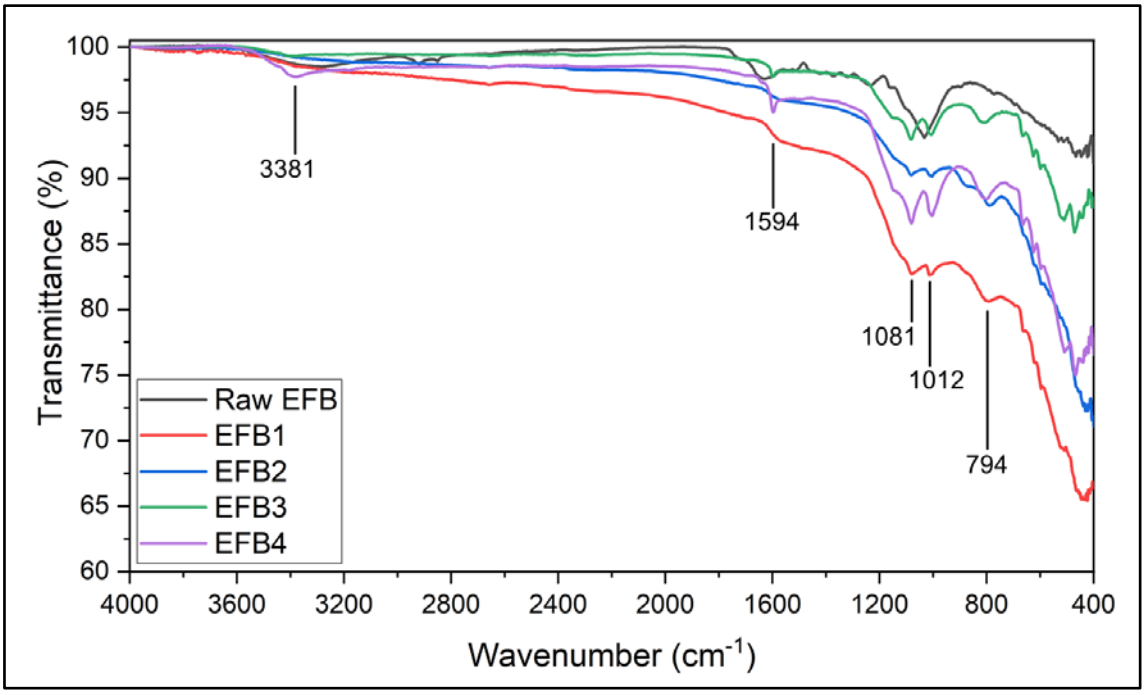

Figure 4.10: FTIR spectroscopy of raw EFB, EFB1, EFB2, EFB3, and EFB4.

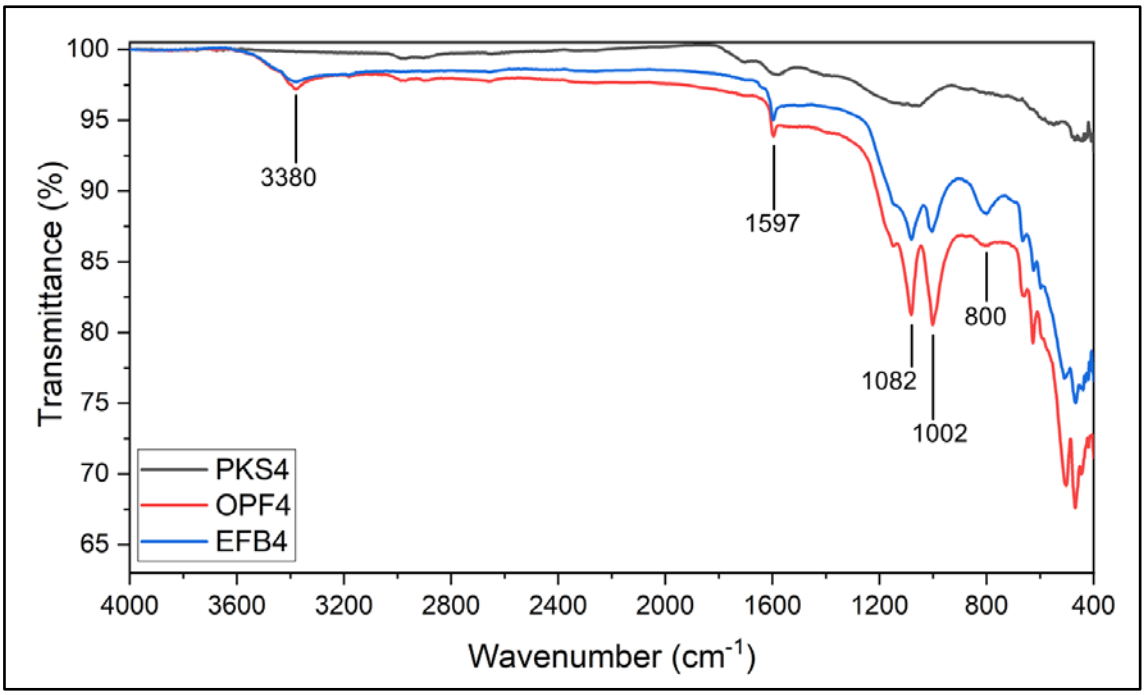

Figure 4.11: FTIR spectroscopy of PKS4, OPF4, and EFB4.

Table 4.3: Functional groups present on raw biomass and SMBC from FTIR analysis.

Functional Group	O-H (cm^{-1})	C=C (cm^{-1})	C-O (cm^{-1})	S=O (cm^{-1})	C-H (cm^{-1})	Fe-O (cm^{-1})
RAW PKS	3423	1569	1136	1040	808	-
PKS1-4	3423	1569	1136	1040	808	400-600
RAW OPF	3390	1597	1082	1000	783	-
OPF1-4	3390	1597	1082	1000	783	400-600
RAW EFB	3381	1594	1081	1012	794	-
EFB1-4	3381	1594	1081	1012	794	400-600

4.2.6 Acid Density of Sulfonated Magnetic Biochar Catalyst

The acid density of SMBC was calculated from the neutralization titration using Equation 4.1. Table 4.4 shows the calculated average acid density of SMBC and past literature for comparison. The acid density of the catalyst corresponds directly to its catalytic reactivity. The higher the acid density, the more active sites are available for the reactants to react with each other (Farabi et al. 2019). The values of the average acid density for SMBC from PKS range from 0.17 mmol g^{-1} to 0.74 mmol g^{-1}. For SMBC made from OPF, the average acid

density values range from 2.90 mmol g^{-1} to 4.41 mmol g^{-1}. Average acid values between 2.35 mmol g^{-1} and 4.55 mmol g^{-1} were recorded for SMBC made from EFB. Both OPF and EFB have comparable values of average acid density. However, PKS recorded significantly lower average acid density values. Farabi et al. (2019) studied the production of biodiesel from palm fatty acid distillate using sulfonated PKS biochar and reported a high catalyst acid density value of 14.4 mmol g^{-1} (Farabi et al. 2019). The significant difference in acid density value between the study by Farabi et al. (2019) and this current research was mainly due to the difference in sulfonating acid and its molarity. Farabi et al. (2019) used concentrated chlorosulfonic acid, while this research used 1.5M and 2.5M sulfuric acid as a sulfonating acid. Another study (Tang et al. 2020) investigated the use of sulfonated EFB biochar as a catalyst for biodiesel production, in which the catalyst's acid density value recorded was 2.24 mmol g^{-1} (Tang et al. 2020). This value is slightly lower compared to the ones of the SMBC from this current research.

The difference in the average acid values between the SMBC in this current research can be related to the surface porosity and the carbonization temperature of the biomass (D. Lee 2013; Y. W. Wang et al. 2021). Apart from that, the ability of the biochar to interact with the sulfonic group during the sulfonation process also plays a part in determining the acid density of a catalyst (Dawodu et al. 2014). From the SEM images in Figures 4.1 to 4.3 in Section 4.2.1 and the low specific surface area but high pore diameter of PKS in Section 4.2.3, we can deduce that PKS has less surface structure than EFB and OPF that can aid in the reaction with the sulfonating agent. This, combined with the higher carbon content for PKS from the EDX analysis in Section 4.2.2, proves that PKS is not as favorable as OPF and EFB in terms of sulfonation.

$$\text{Acid density (mmol g}^{-1}) = \frac{V_{NaOH} M_{NaOH}}{W_{SMBC}} \quad (4.1)$$

where V_{NaOH} = Volume of NaOH solution needed for titration in mL

M_{NaOH} = Molarity of NaOH solution in mol L^{-1}

W_{SMBC} = Mass of SMBC in g

Table 4.4: Average acid density of SMBC and past studies.

Catalyst / Precursor	Average acid density (mmol g^{-1})	References
PKS1	0.52	This study
PKS2	0.17	
PKS3	0.56	
PKS4	0.74	
OPF1	2.90	This study
OPF2	4.41	
OPF3	4.32	
OPF4	4.14	
EFB1	3.85	This study
EFB2	2.35	
EFB3	3.38	
EFB4	4.55	
PKS	14.40	(Farabi et al. 2019)
Palm seed cake	12.08	(Akinfalabi et al. 2017)
EFB	2.24	(Tang et al. 2020)
Bamboo	1.50	(B. Zhang et al. 2021)
Chitosan	1.20	(A. Wang et al. 2018)

4.2.7 Magnetic Analysis of Sulfonated Magnetic Biochar Catalyst

Figures 4.12, 4.13, and 4.14 illustrate the magnetic hysteresis loops of SMBC from PKS, OPF, and EFB, respectively. Similar to a past study, all SMBCs observed the ferromagnetic behavior at room temperature (Eltaweil et al. 2020). The mass saturation magnetization (σ_s) values of the SMBC indicate the capacity of the catalyst to be attracted toward a magnetic force. The higher the value of σ_s, the least magnetic force is needed in order to attract the catalyst (H. R. Khan 2003; Willard and Daniil 2013).

The σ_s values of PKS are between 0.25 $Am^2 kg^{-1}$ and 0.69 $Am^2 kg^{-1}$ with coercivity value (H_c) between 2.29 kA m^{-1} and 9.63 kA m^{-1}. For OPF, the σ_s values are between 2.99 $Am^2 kg^{-1}$ and 6.88 $Am^2 kg^{-1}$, with H_c values between 2.92 kA m^{-1} and 10.93 kA m^{-1}. Meanwhile, the σ_s values for EFB are between 1.88 $Am^2 kg^{-1}$ and 4.40 $Am^2 kg^{-1}$, with H_c values between 3.28 kA m^{-1} and 9.79 kA m^{-1}. Table 4.5 shows the σ_s value of SMBC and past literature for

comparison. A prior study by Hazmi et al. (2021) investigated the employment of magnetic rice husk biochar catalyst for biodiesel production. In this study, the σ_s value of the magnetic catalyst was found to be 3.779 $Am^2 kg^{-1}$ (Hazmi et al. 2021). Another study by Yi et al. (2021) used rice straw as a precursor of a magnetic biochar catalyst as an adsorbent. The study reported an σ_s value of 8.84 $Am^2 kg^{-1}$ for the magnetic biochar catalyst (Yi et al. 2021). In both studies, the magnetic components of the catalysts were different. The catalyst from Hazmi et al. (2021) had a nickel-based magnetic component, while the catalyst from Yi et al. (2021) had the iron-based magnetic component. The magnetic component of SMBC was presumed to be Fe_3O_4 based on past literature that synthesized magnetic biochar using similar method to this research (F. Zhang et al. 2017). The iron-based magnetic component were reported to demonstrate better magnetic quality than other magnetic metals. A study by H. Li et al. (2021) reported an σ_s value as high as 22 $Am^2 kg^{-1}$ for the iron-based magnetic catalyst used for biodiesel production (H. Li et al. 2021). σ_s values of PKS in this study are significantly lower than those in past studies. Meanwhile, the σ_s values of OPF and EFB correlate with the σ_s values of catalyst from the prior studies.

On average, SMBC from OPF showed better mass saturation magnetization compared to PKS and EFB. This result can be confirmed from the EDX analysis in Section 4.2.2, in which the iron content of OPF was observed to be higher than EFB and PKS. The same can be said for the FTIR analysis in Section 4.2.5, in which the spectra of OPF showed higher Fe-O peaks compared to EFB and PKS. The high pore diameter of OPF also helped with iron impregnation. Although PKS also had a high pore diameter as has been observed in Section 4.2.3, the same cannot be said regarding its ability for iron impregnation. The results from EDX showed that the ratio of iron to sulfur for PKS was lower than for OPF and EFB. This was due to the iron leaching during the sulfonation process.

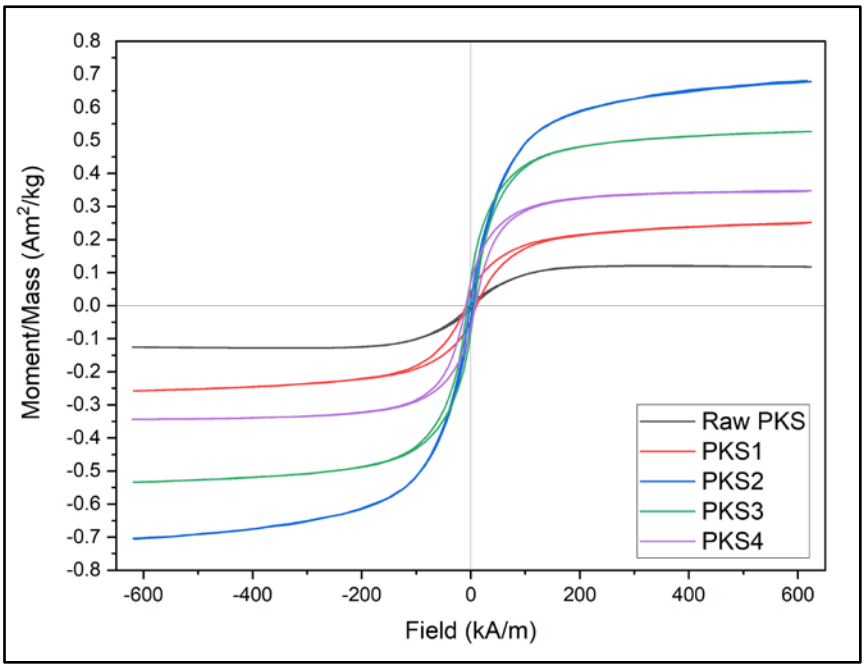

Figure 4.12: Magnetic hysteresis loops of PKS1, PKS2, PKS3, and PKS4.

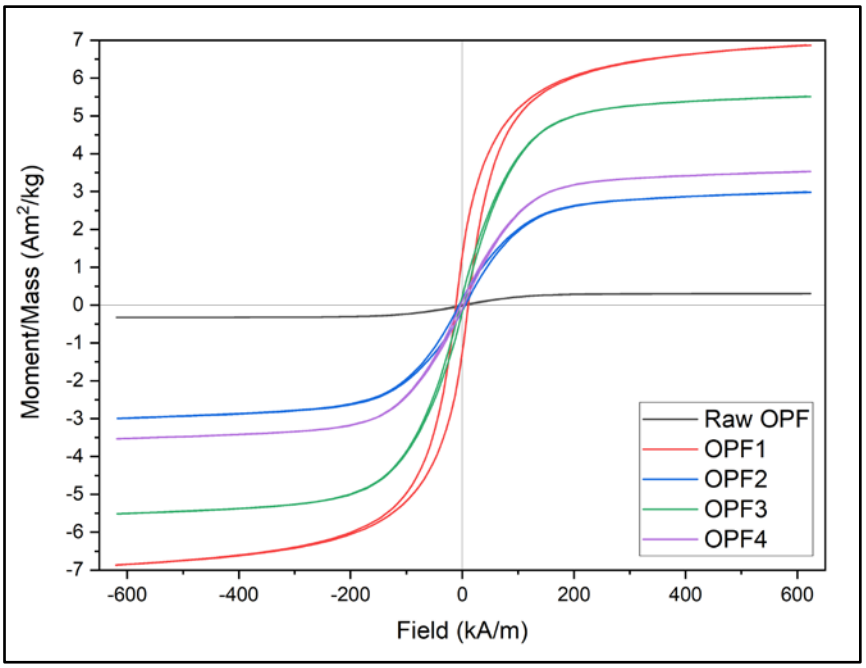

Figure 4.13: Magnetic hysteresis loops of OPF1, OPF2, OPF3, and OPF4.

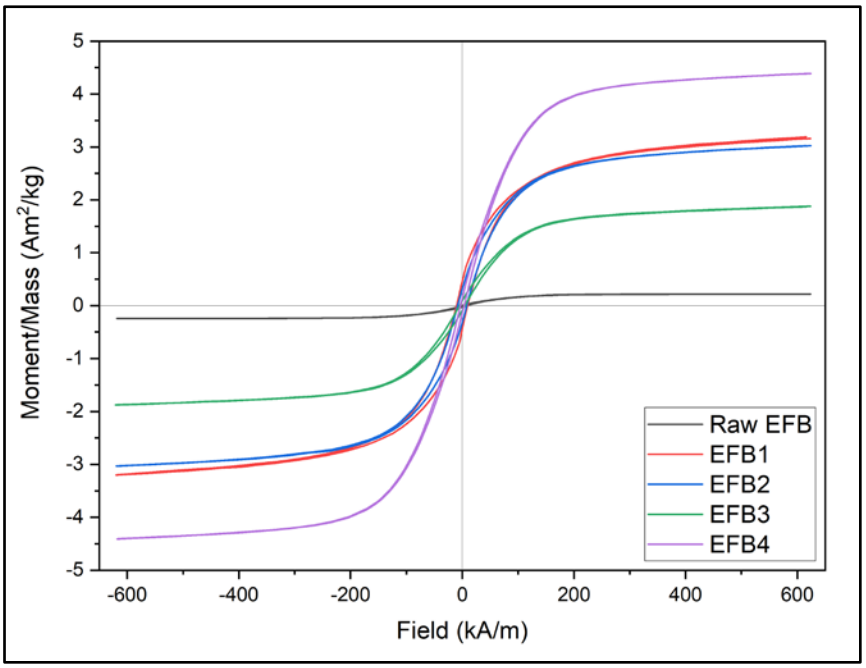

Figure 4.14: Magnetic hysteresis loops of EFB1, EFB2, EFB3, and EFB4.

Table 4.5: Mass saturation magnetization values of SMBC and past studies.

Catalyst / Precursor	Magnetic component	Mass saturation magnetization ($Am^2 kg^{-1}$)	References
PKS1	Fe_3O_4	0.2547	This study
PKS2	Fe_3O_4	0.6931	
PKS3	Fe_3O_4	0.5303	
PKS4	Fe_3O_4	0.3453	
OPF1	Fe_3O_4	6.8729	This study
OPF2	Fe_3O_4	2.9907	
OPF3	Fe_3O_4	5.5133	
OPF4	Fe_3O_4	3.5304	
EFB1	Fe_3O_4	3.1931	This study
EFB2	Fe_3O_4	3.0267	
EFB3	Fe_3O_4	1.8774	
EFB4	Fe_3O_4	4.3985	
Chitosan	Fe_3O_4	18.9	(A. Wang et al. 2018)
Rice husk	NiO	3.779	(Hazmi et al. 2021)
Rice straw	Fe_3O_4	8.84	(Yi et al. 2021)
MIL-100(Fe)	Fe_3O_4	22	(H. Li et al. 2021)

4.3 Sulfonated Magnetic Biochar Catalyst Synthesis Optimization

The best parameters to produce the SMBC were analyzed using the Taguchi experimental design method. This experimental design method was chosen because it requires relatively fewer experimental runs compared to other experimental design approaches. By having less experimental load, less time and less cost were needed for the analysis (Okolie et al. 2021). The analysis was carried out using the SN ratio criteria of 'the larger, the better'. The factors that were studied in this method were the $FeCl_3 \cdot 6H_2O$ concentration (FC), the carbonization temperature (CT), and the H_2SO_4 concentration (HC). These factors were studied at two levels which values based on prior literature. FC and HC were studied at 1.5 M and 2.5 M. Meanwhile, CT was studied at 600 °C and 800 °C. The responses that were considered for this method were the BET surface area (SA), the acid density (AD), and the mass saturation magnetization (MM). These responses were obtained from the characterization of the SMBC. Table 4.6 summarizes the factors and responses that were considered for the Taguchi analysis. Table 4.7 summarizes the SN ratio calculated from the responses of each SMBC.

Table 4.6: Summary of factors and responses for the Taguchi analysis on SMBC synthesis.

	Factors			**Responses**		
	$FeCl_3 \cdot 6H_2O$ Concentration	**Carbonization Temperature**	**H_2SO_4 Concentration**	**BET Surface Area**	**Acid Density**	**Mass saturation magnetization**
Symbol	**FC**	**CT**	**HC**	**SA**	**AD**	**MM**
Unit	**M**	**°C**	**M**	**$m^2\ g^{-1}$**	**mmol g^{-1}**	**$Am^2\ kg^{-1}$**
PKS1	1.5	800	2.5	1.74	0.52	0.25
PKS2	2.5	800	1.5	1.45	0.17	0.69
PKS3	1.5	600	1.5	0.94	0.56	0.53
PKS4	2.5	600	2.5	74.16	0.74	0.34
OPF1	1.5	800	2.5	23.27	2.90	6.88
OPF2	2.5	800	1.5	8.10	4.41	2.99
OPF3	1.5	600	1.5	7.24	4.32	5.51
OPF4	2.5	600	2.5	5.96	4.14	3.53
EFB1	1.5	800	2.5	44.42	3.85	3.19
EFB2	2.5	800	1.5	46.74	2.35	3.03

Table 4.6 continued.

EFB3	1.5	600	1.5	8.08	3.38	1.88
EFB4	2.5	600	2.5	6.58	4.55	4.40

Table 4.7: Summary of factors and SN ratios for the Taguchi analysis on SMBC synthesis.

Factors				**SN ratio**		
	$FeCl_3 \cdot 6H_2O$ Concentration	**Carbonization Temperature**	**H_2SO_4 Concentration**	**BET Surface Area**	**Acid Density**	**Mass saturation magnetization**
Symbol	**FC**	**CT**	**HC**	**SA**	**AD**	**MM**
Unit	**M**	**°C**	**M**	**-**	**-**	**-**
PKS1	1.5	800	2.5	4.79	-5.71	-11.88
PKS2	2.5	800	1.5	3.24	-15.20	-3.18
PKS3	1.5	600	1.5	-0.51	-4.97	-5.51
PKS4	2.5	600	2.5	37.40	-2.61	-9.24
OPF1	1.5	800	2.5	27.34	9.25	16.74
OPF2	2.5	800	1.5	18.17	12.89	9.52
OPF3	1.5	600	1.5	17.19	12.70	14.89
OPF4	2.5	600	2.5	15.51	12.34	10.96
EFB1	1.5	800	2.5	32.95	11.71	10.08
EFB2	2.5	800	1.5	33.39	7.42	9.62
EFB3	1.5	600	1.5	18.15	10.58	5.47
EFB4	2.5	600	2.5	16.37	13.17	12.87

Based on Table 4.8, the effect of all factors on the responses of PKS can be analyzed. The optimum parameters are given by the highest SN ratio for each factor. The optimum parameters to produce the SMBC from PKS with the best SA are at 2.5 M of FC, 600 °C of CT, and 2.5 M of HC. Table 4.8 also shows the ranking for the influence of the parameters on the responses for PKS. The most influential SMBC synthesis parameter on SA for PKS is HC, followed by FC and then CT. The optimum parameters to produce SMBC from PKS with the best AD are at 1.5 M of FC, 600 °C of CT, and 2.5 M of HC. The most influential SMBC synthesis parameter on AD for PKS is CT, followed by HC and then FC. The optimum

parameters to produce SMBC from PKS with the best MM are at 2.5 M of FC, 600 °C of CT, and 1.5 M of HC. The most influential SMBC synthesis parameter on MM for PKS is HC, followed by FC and then CT. Based on the literature review in Section 2.4, the predicted most influential factor for SA is CT; for AD, it was predicted to be HC, and for MM, it was predicted to be FC. Based on these predictions and the influential factors of PKS, PKS did not act as predicted. This is mainly due to the formation of micropores and the hard structure of PKS, as discussed in the EDX analysis in Section 4.2.2 and the VSM analysis in Section 4.2.7.

Table 4.8: The response table for SN ratios (larger is better) for PKS.

Response	Level	$FeCl_3 \cdot 6H_2O$ Concentration (FC)	Carbonization Temperature (CT)	H_2SO_4 Concentration (HC)
BET Surface Area (SA)	1	2.14	18.45	1.37
	2	20.32	4.02	21.10
	Delta	18.18	14.43	19.73
	Rank	2	3	1
Acid Density (AD)	1	-5.34	-3.79	-10.09
	2	-8.91	-10.46	-4.16
	Delta	3.57	6.66	5.93
	Rank	3	1	2
Mass saturation magnetization (MM)	1	-8.69	-7.37	-4.35
	2	-6.21	-7.53	-10.56
	Delta	2.48	0.16	6.21
	Rank	2	3	1

Table 4.9 shows the optimum parameters for the production of SMBC from OPF with the best SA are at 1.5 M of FC, 800 °C of CT, and 2.5 M of HC. The most influential SMBC synthesis parameter on SA for OPF is CT, followed by FC and then HC. The optimum parameters to produce SMBC from OPF with the best AD are at 2.5 M of FC, 600 °C of CT, and 1.5 M of HC. The most influential SMBC synthesis parameter on AD for OPF is HC, followed by FC and then CT. The optimum parameters to produce SMBC from OPF with the best MM are at 1.5 M of FC, 800 °C of CT, and 2.5 M of HC. The most influential SMBC synthesis parameter on MM for OPF is FC, followed by HC and then CT. Based on the previous predictions about the most influential factors, OPF behaves more predictably than PKS.

Based on Table 4.10, the optimum parameters to produce SMBC from EFB with the best SA are at 1.5 M of FC, 800 °C of CT, and 1.5 M of HC. The most influential SMBC synthesis parameter on SA for EFB is CT, followed by HC and then FC. The optimum

parameters to produce SMBC from EFB with the best AD are at 1.5 M of FC, 600 °C of CT, and 2.5 M of HC. The most influential SMBC synthesis parameter on AD for EFB is HC, followed by CT and then FC. The optimum parameters to produce SMBC from EFB with the best MM are at 2.5 M of FC, 800 °C of CT, and 2.5 M of HC. The most influential SMBC synthesis parameter on MM for EFB is HC, followed by FC and then CT. Based on the previous predictions about the most influential factors, EFB behaved not as predictable as OPF. The responses on SA and AD behaved as predicted but not the response on MM. MM is not as predictable because the EFB was susceptible to the leaching problems, as discussed in the EDX analysis Section 4.2.2.

Table 4.9: The response table for SN ratios on SA (larger is better) for OPF.

Response	Level	$FeCl_3 \cdot 6H_2O$ Concentration (FC)	Carbonization Temperature (CT)	H_2SO_4 Concentration (HC)
BET Surface Area (SA)	1	22.26	16.35	17.68
	2	16.84	22.75	21.42
	Delta	5.42	6.41	3.74
	Rank	2	1	3
Acid Density (AD)	1	10.98	12.52	12.80
	2	12.62	11.07	10.79
	Delta	1.64	1.45	2.01
	Rank	2	3	1
Mass saturation magnetization (MM)	1	15.79	12.89	12.17
	2	10.24	13.13	13.85
	Delta	5.55	0.24	1.68
	Rank	1	3	2

Table 4.10: The response table for SN ratios on SA (larger is better) for EFB.

Response	Level	$FeCl_3 \cdot 6H_2O$ Concentration (FC)	Carbonization Temperature (CT)	H_2SO_4 Concentration (HC)
BET Surface Area (SA)	1	25.55	17.26	25.77
	2	24.88	33.17	24.66
	Delta	0.67	15.91	1.11
	Rank	3	1	2
Acid Density (AD)	1	11.145	11.874	8.998
	2	10.291	9.563	12.439
	Delta	0.854	2.311	3.441
	Rank	3	2	1
Mass saturation magnetization (MM)	1	7.778	9.169	7.545
	2	11.243	9.852	11.475
	Delta	3.465	0.683	3.93
	Rank	2	3	1

By considering all three responses, the overall optimum parameters for SMBC synthesis were obtained by assigning all responses with importance weighting. In this research, all responses were assigned with equal importance. The overall optimum parameters for SMBC synthesis from PKS, OPF, and EFB from the analysis software are shown in Table 4.11. The overall optimum parameters for PKS are 2.5 M of FC, 600 °C of CT, and 2.5 M of HC. For OPF, the overall optimum SMBC synthesis parameters are 1.5 M of FC, 800 °C of CT, and 2.5 M of HC. Meanwhile, the overall optimum SMBC synthesis parameters for EFB are 1.5 M of FC, 800 °C of CT, and 2.5 M of HC. At the optimum synthesis parameter, the values of SA and AD of EFB are greater than that of OPF and PKS. Therefore, EFB1 has been chosen and utilized in the biodiesel optimization and kinetic study of this research. As a part of the Taguchi analysis' characteristics, one of the limitations of this method is the lack of precision. The optimum parameters established in this analysis rely on pre-determined values from prior literature (W.-H. Chen et al. 2021; T. S. Singh and Verma 2019). Thus, the value of the optimized parameters might not be exactly the same as the reported values, but it is still accurate enough for the purpose of the analysis of the pre-determined values which were chosen properly. Prior studies have proven that the ability of the Taguchi method is comparable to other optimization methods, such as RSM (Odiaka et al. 2021; W.-H. Chen et al. 2021). The studies have managed to identify the optimum parameters for their studies.

Table 4.11: The optimum parameters for SMBC synthesis by response and overall.

Biomass	Response	$FeCl_3 \cdot 6H_2O$ Concentration (M)	Carbonization Temperature (°C)	H_2SO_4 Concentration (M)
PKS	BET Surface Area (SA)	2.5	600	2.5
	Acid Density (AD)	1.5	600	2.5
	Mass saturation magnetization (MM)	2.5	600	1.5
	Overall	2.5	600	2.5
OPF	BET Surface Area (SA)	1.5	800	2.5
	Acid Density (AD)	2.5	600	1.5
	Mass saturation magnetization (MM)	1.5	800	2.5
	Overall	1.5	800	2.5
EFB	BET Surface Area (SA)	1.5	800	1.5
	Acid Density (AD)	1.5	600	2.5
	Mass saturation magnetization (MM)	2.5	800	2.5
	Overall	1.5	800	2.5

4.4 Biodiesel Production Optimization Analysis

The best parameters for biodiesel production were analyzed using the RSM based on the CCD design. Four factors were studied in this method: the catalyst loading (A), methanol to oil molar ratio (B), reaction temperature (C), and reaction time (D). Table 4.12 summarizes the uncoded factors and responses that were considered for the analysis.

Table 4.12: The CCD design matrix for biodiesel production optimization.

Run	Parameters				Biodiesel Yield (%)	
	A: Catalyst loading (wt%)	B: Methanol-oil molar ratio	C: Temperature (°C)	D: Time (h)	Prediction	Actual
1	10	20	60	10	84.98	84.22
2	10	20	60	6	89.00	90.19
3	7	15	55	4	76.20	74.79
4	10	10	60	6	73.36	74.02
5	7	15	55	8	76.20	77.17
6	10	20	60	6	89.00	90.68
7	13	25	65	8	88.62	90.06
8	10	20	50	6	79.24	78.47
9	10	20	70	6	91.44	91.74
10	10	20	60	6	89.00	91.30
11	13	15	65	8	75.24	76.08
12	10	20	60	6	89.00	88.87
13	10	20	60	6	89.00	85.47
14	10	30	60	6	91.70	90.57
15	7	25	55	4	81.17	80.77
16	7	15	65	8	82.71	82.31
17	16	20	60	6	62.71	61.55
18	13	15	55	8	67.59	66.29
19	13	15	65	4	73.56	72.67
20	7	25	65	4	85.72	87.05
21	7	25	65	8	90.08	88.67
22	4	20	60	6	72.61	73.31
23	7	25	55	8	83.68	84.59
24	13	15	55	4	67.77	69.62
25	10	20	60	6	89.00	87.51
26	13	25	65	4	84.43	83.90
27	13	25	55	8	81.08	82.03
28	7	15	65	4	80.86	80.35
29	13	25	55	4	78.74	79.17
30	10	20	60	2	80.79	81.08

4.4.1 Regression Analysis

A regression model was produced by the RSM analysis, and a quadratic model was suggested by the Design-Expert software. The developed equation fitting to the biodiesel yield from the parameters of transesterification is shown in Equation 4.2. The equation is presented in terms of the actual value of the parameters.

$$Y = -137.79944 + 7.93472\,A + 2.192\,B + 4.56158\,C + 1.1475\,D + 0.100167\,AB + 0.018917\,AC - 0.007083\,AD - 0.00105\,BC + 0.06275\,BD + 0.046375\,CD - 0.592778\,A^2 - 0.06475\,B^2 - 0.03665\,C^2 - 0.3825\,D^2 \quad (4.2)$$

where Y is the biodiesel yield (%). The sign preceding each term dictates its influence on the biodiesel yield (Reddy et al. 2017a). A positive term has a synergistic effect on the reaction, while a negative term has an antagonistic effect on the reaction. From Equation 4.2, all linear terms have a synergistic effect on the reaction. The other interaction terms have mixed effects on the reaction.

An analysis of variance (ANOVA) was also conducted through the Design-Expert software. Table 4.13 shows the data from the ANOVA on the developed model. From the ANOVA data, the developed model for this study is significant, which can be observed from the model's F-value of 39.90. From the F-value of the model terms, the importance of each model term can be shown as B, C, and A, in the order of importance. From the analyzed p-value, the model terms A, B, C, and A^2 are significant model terms as their p-values are less than 0.0001. The R^2 value of the model of 0.9739 indicates the fit of the model for associating the factors and response with the experimental response. The adequate precision value of 23.0811, which is a signal-to-noise ratio, is greater than 4, indicating that this model is fit for analysis.

Table 4.13: ANOVA for biodiesel production optimization.

Source	Sum of Squares	df	Mean Square	F-value	p-value	
Model	1762.22	14	125.87	39.90	< 0.0001	Significant
A-Catalyst loading	147.02	1	147.02	46.61	< 0.0001	Significant
B-Methanol-oil ratio	504.72	1	504.72	160.01	< 0.0001	Significant
C-Temperature	223.26	1	223.26	70.78	< 0.0001	Significant
D-Time	26.38	1	26.38	8.36	0.0112	Not significant
AB	36.12	1	36.12	11.45	0.0041	Not significant
AC	1.29	1	1.29	0.4084	0.5324	Not significant
AD	0.0289	1	0.0289	0.0092	0.925	Not significant
BC	0.011	1	0.011	0.0035	0.9536	Not significant
BD	6.30	1	6.30	2	0.178	Not significant
CD	3.44	1	3.44	1.09	0.3128	Not significant
A^2	780.68	1	780.68	247.49	< 0.0001	Significant
B^2	71.87	1	71.87	22.79	0.0002	Not significant
C^2	23.03	1	23.03	7.30	0.0164	Not significant
D^2	64.21	1	64.21	20.36	0.0004	Not significant
Residual	47.32	15	3.15			
Lack of Fit	23.09	10	2.31	0.4765	0.8509	Not significant
Std. Dev.	1.78					
Mean	81.48					
C.V. %	2.18					
R^2	0.9739					
Adjusted R^2	0.9494					
Predicted R^2	0.9072					
Adequate Precision	23.0811					

4.4.2 Effect of Catalyst Loading on Biodiesel Yield

Transesterification of UCO was carried out at catalyst loading value of between 4 wt% and 16 wt%. Figures 4.15 (a), 4.15 (b), and 4.15 (c) show the response surface contour plots of the interaction of catalyst loading with methanol to oil ratio, reaction temperature, and reaction time, respectively. In general, the highest biodiesel yield can be observed around 10 wt% catalyst loading. The biodiesel yield decreases by decreasing the catalyst amount away from this value. Insufficient use of a catalyst will decrease the sites for reactants to react, thus decreasing the biodiesel yield (Syazwani et al. 2017). Excessive use of catalyst increases the amount of by-product glycerol. In turn, this causes the viscosity of the reactants mixture to increase, thus hampering the mixing and mass transfer, decreasing the biodiesel yield (Bhatia et al. 2020). From Equation 4.2, we can observe a positive interaction between catalyst loading and methanol to oil molar ratio and temperature. However, catalyst loading has a negative effect on its interaction with reaction time. Among factors interaction, the interaction between catalyst loading and methanol to oil ratio highly influences biodiesel production. The increased amount of methanol in the reaction may also alleviate or increase the viscosity caused by higher catalyst loading. Thus, to some extent, this is beneficial to biodiesel production.

4.4.3 Effect of Methanol to Oil Ratio on Biodiesel Yield

The influence of methanol to oil molar ratio on biodiesel yield is shown in Figures 4.15 (a), 4.15 (d), and 4.15 (e). The methanol to oil molar ratios used for the transesterification varied from 10 to 30. The molar ratio of methanol to oil that worked best was approximately 30. Extra methanol has to be used in transesterification to achieve a thorough feedstock conversion (Helmi et al. 2021). On the other hand, if methanol is supplied to the transesterification reaction after it has reached its maximum level, it causes biodiesel to emulsify and byproduct glycerol to dissolve in methanol, blocking the reaction (Shankar and Jambulingam 2017).

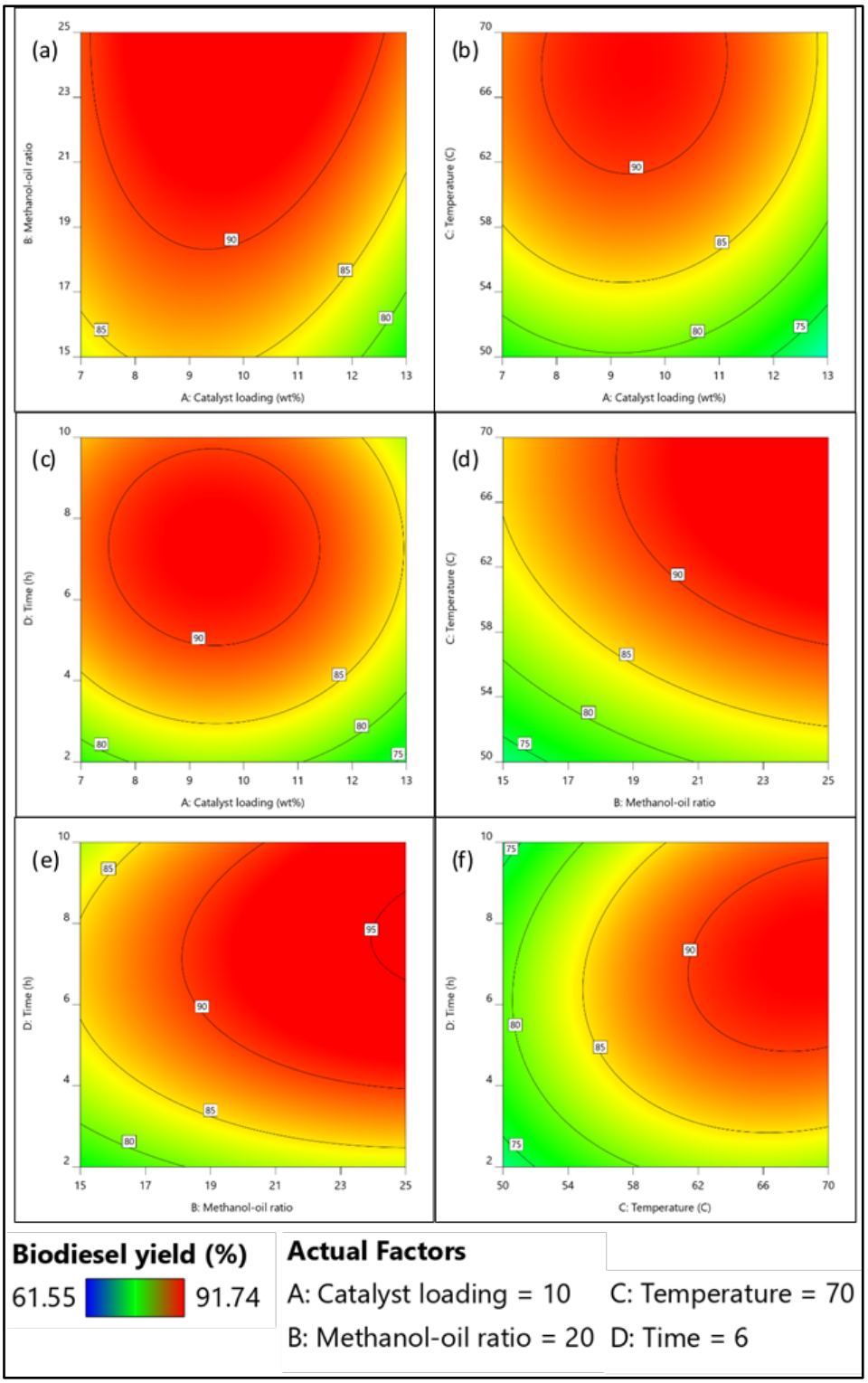

Figure 4.15: 2D contour plots of transesterification parameter's interaction between (a) catalyst loading and methanol to oil ratio, (b) catalyst loading and reaction temperature, (c) catalyst loading and reaction time, (d) methanol to oil ratio and reaction temperature, (e) methanol to oil ratio and reaction time, and (f) reaction temperature and reaction time.

The positive interaction of methanol to oil ratio with catalyst loading has been discussed in Section 4.4.2. The interaction of methanol to oil ratio with reaction time was observed to be positive, according to Equation 4.2. The increase in both the methanol to oil molar ratio and the reaction time enabled more biodiesel production reactions to occur. The methanol to oil molar ratio had a negative interaction with reaction temperature. This was caused by the evaporation of methanol at a higher reaction temperature that eventually hindered the transesterification forward reaction and decreased the biodiesel yield.

4.4.4 Effect of Reaction Temperature on Biodiesel Yield

UCO was converted to biodiesel at a reaction temperature between 50 °C and 70 °C. According to Figures 4.15 (b), 4.15 (d), and 4.15 (f), the reaction temperature of around 66 °C was when biodiesel production was at its peak. A lower or higher reaction temperature than 66 °C resulted in lower biodiesel yields. It has been demonstrated that raising the reaction temperature over the ideal temperature does not enhance the output of biodiesel (Kirubakaran and Arul Mozhi Selvan 2018). Higher reaction temperature accelerates the saponification of triglycerides, reducing biodiesel production (Ngige et al. 2023). As discussed in Section 4.4.2, reaction temperature has a positive interaction with catalyst loading. The negative interaction between reaction temperature and the methanol to oil molar ratio was discussed in Section 4.4.3. Reaction temperature has a positive interaction with reaction time. In an ideal setting, a higher reaction temperature and longer reaction time produce a greater amount of product. However, higher temperature doesn’t lead to the reactant loss because the entire experiment is conducted in closed system, the evaporated methanol will recirculate and dissolve in the biodiesel mixture.

4.4.5 Effect of Reaction Time on Biodiesel Yield

The transesterification of biodiesel from UCO was carried out at a reaction time between 2 h and 10 h. Figures 4.15 (c), 4.15 (e), and 4.15 (f) show the interaction of reaction time with catalyst loading, methanol to oil ratio, and reaction temperature, respectively. From these figures, the highest amount of biodiesel was produced at a reaction time of around 8 h. Transesterification must be allowed enough time to finish its reaction. Nevertheless, a longer reaction time reduces the output of biodiesel. This is consistent with the notion that transesterification is a reversible process (Baskar et al. 2018).

4.4.6 Biodiesel Yield Optimization

Combinations of reaction parameters were obtained through the optimization module in the Design-Expert software. These parameters were produced within the range of the value of factors that were studied while aiming to maximize the biodiesel yield. Figure 4.16 shows the criteria for each factor and the response, which is the biodiesel yield. Three sets of parameters were selected for validation. Table 4.14 shows the data sets from the optimization analysis along with the predicted biodiesel yield from the analysis and the actual biodiesel yield from the validation. The optimum biodiesel yield was produced at conditions catalyst loading (10.12 wt%), methanol to oil molar ratio (28), reaction temperature (70°C), and reaction time (8 h). The predicted optimal biodiesel yield was at 96.02%. Between the three optimization data sets, set 1 produced the highest biodiesel yield at 95.87%, with the least difference from the predicted yield of 0.16%.

F. Zhang, Fang, and Wang (2015) reported a maximum yield of 90.5% for biodiesel production from jatropha oil using magnetic catalyst synthesized from glucose. This study obtained the maximum biodiesel yield by using a catalyst loading of 10 wt%, methanol – oil ratio of 24:1, reaction temperature of 200°C, and a reaction time of 10 h. Another study by Kostić et al. (2016) obtained a maximum biodiesel yield of 99% from sunflower oil using palm kernel shell biochar catalyst with reaction parameters of 3 wt% catalyst loading, methanol – oil ratio of 9:1, reaction temperature of 65°C, and a reaction time of 6 h. Comparing with the published literature, the optimal transesterification parameters obtained in this research apparently conform to most studies utilizing similar type of catalyst. In the optimum reaction temperature of 70 °C in this research exceeds the boiling point of methanol at atmospheric pressure (64.7°C). This high temperature may cause the methanol to boil and reduce the reaction between the reactants and SMBC. However, higher temperature can lead to the increase in the biodiesel yield. This might have been due to decrease in oil viscosity with an elevation of reaction temperature, which resulted in an increase in the solubility of the oil in the methanol, leading to an improvement in the contact between the oil and the methanol. Therefore, with the combination of other reaction parameters such as the stirring rate, excess amount of methanol, and optimum amount of SMBC, the number reaction sites producing biodiesel can be kept optimum (Rahimi et al. 2021).

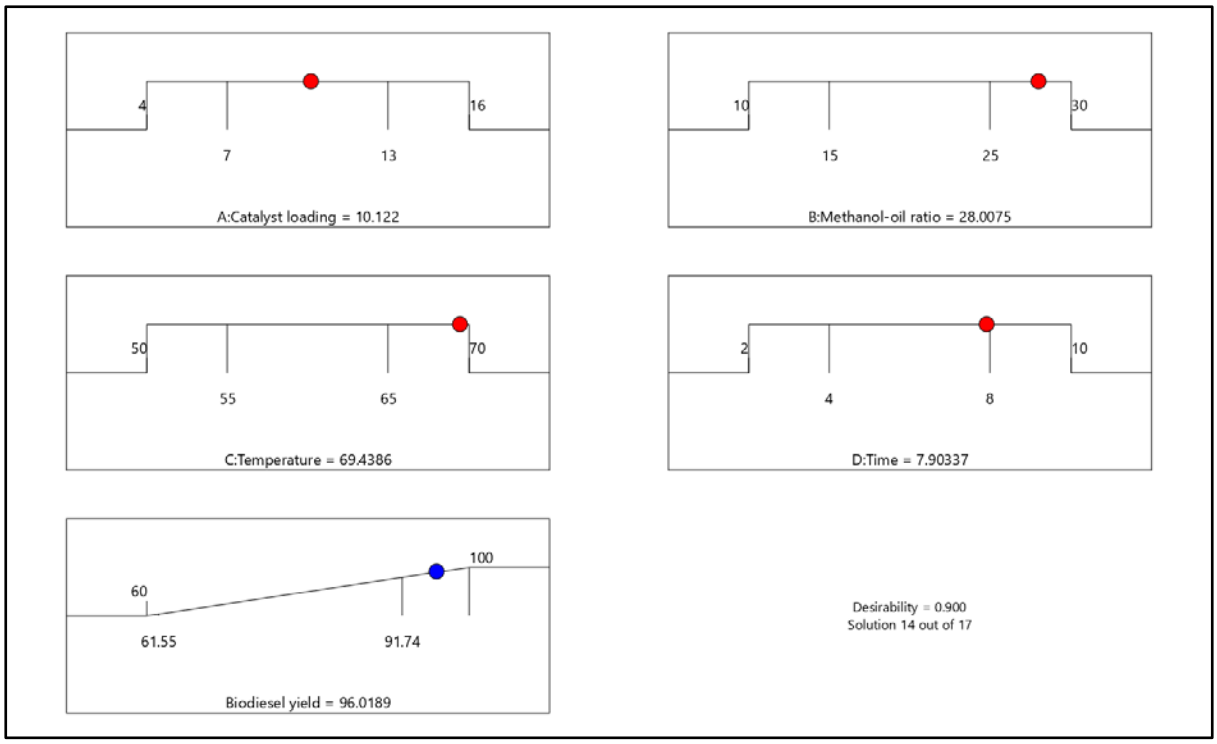

Figure 4.16: Optimized reaction parameters for biodiesel transesterification.

Table 4.14: Data sets for the validation of optimal reaction parameters for biodiesel transesterification.

Set	Parameters				Biodiesel Yield (%)		
	A: Catalyst loading (wt%)	B: Methanol-oil molar ratio	C: Temperature (°C)	D: Time (h)	Prediction	Actual	Error %
1	10.12	28	70	8	96.02	95.87	0.16
2	10.12	28	70	8	96.02	95.82	0.21
3	10.12	28	70	8	96.02	95.80	0.23

4.5 Catalyst Reusability

The transesterification of biodiesel with SMBC while utilizing the ideal reaction conditions discovered from prior experiments allowed the reusability of SMBC to be investigated. The conditions were: 10.12 wt% catalyst loading, a methanol to oil molar ratio of 28, a reaction temperature of 70 °C, and a reaction duration of 8 h. Five cycles of transesterification using SMBC were performed. Biodiesel production for each cycle of transesterification with SMBC is shown in Figure 4.17. In the first cycle, SMBC displays a biodiesel production of 95.84%. In the fifth cycle, the biodiesel output gradually decreased to 70.16%. Between the first cycle and the fifth cycle, the biodiesel yield decreased by 25.68%.

The depletion of active catalytic sites led to a rapid drop in biodiesel production cycle after cycle. The catalyst's surface morphology underwent structural alteration, which led to the depletion of SMBC's catalytic sites (Rahimi et al. 2021). Through repeated calcination or sintering, the catalyst surface deteriorated (Syazwani et al. 2017). Ion leaching into the biodiesel, which results in soap formation, is another factor affecting biodiesel production (Mazaheri et al. 2018). The blockage of catalytic active sites by absorbed glycerol and free fatty acids that cannot be dissolved by the solvent is also a reason for the loss of catalytic activity of the catalyst (Bhatia et al. 2020).

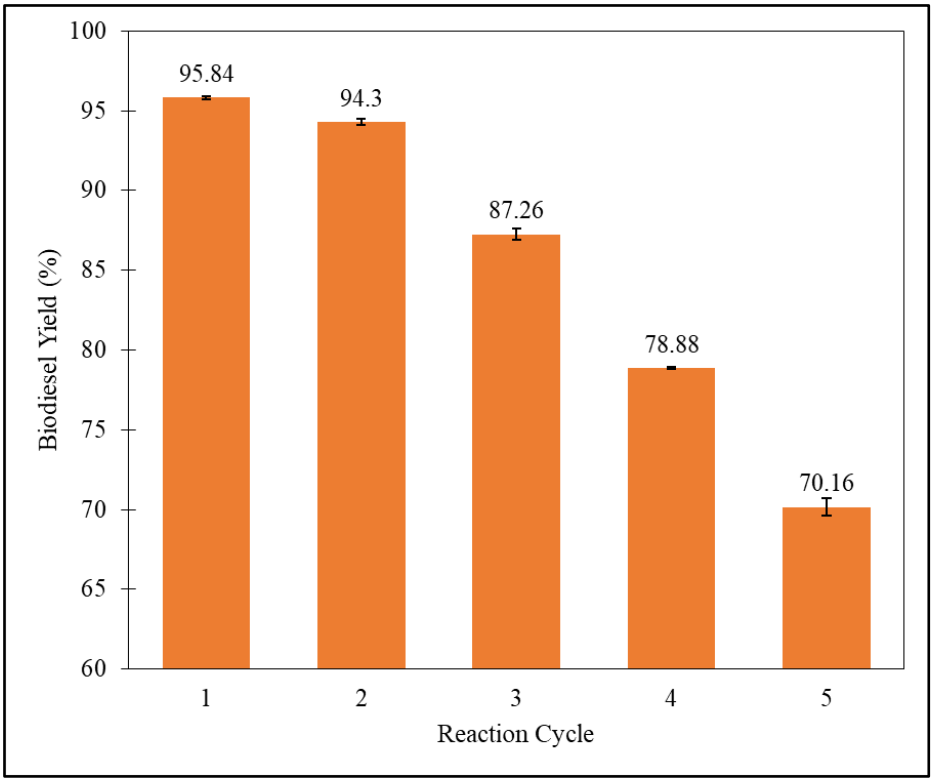

Figure 4.17: SMBC reusability after five reaction cycles.

4.6 Characterization of Used Cooking Oil and Used Cooking Oil Biodiesel

4.6.1 Physicochemical Properties of Used Cooking Oil and Used Cooking Oil Biodiesel

The physicochemical characteristics of UCO and the biodiesel produced from it are presented in Table 4.15, together with the biodiesel standards EN 14214 and ASTM D6751 (European Committee for Standardization 2010; ASTM International 2020). Biodiesel has the necessary physicochemical properties to be utilized as a vehicle diesel fuel. The density and specific gravity of biodiesel, 883.6 kg m^{-3} and 0.8841, respectively, are significantly within the limit. If the density of the diesel fuel is not within specifications, issues with fuel injection and thermal efficiency may occur in the engine (Sakthivel et al. 2018). The kinematic viscosity of biodiesel met the ASTM D6751 requirement but not the EN 14214 requirement.

The lowest limit defined by EN 14214 is greater than the flash point of biodiesel. In actuality, the biodiesel's flash point is greater than that of petrodiesel, which is often the case for biodiesel. High flash point fuel is less dangerous to handle, move, and store (Mat Yasin et al. 2017; Boey et al. 2011). Both the cloud and pour points of the biodiesel exceed the maximum limit required by both EN 14214 and ASTM D6751 standards. High pour point and cloud point values are characteristics of biodiesel produced from feedstock with high content of saturated fatty acids. Biodiesel with a high pour point and cloud point is unsuitable for use in low-temperature climates (Alptekin and Canakci 2011). The cetane index for UCO biodiesel slightly falls below the minimum requirement for both standards. A fuel's cetane number is a crucial factor in determining how well it will ignite. Better engine performance and emissions are made possible by higher cetane numbers, allowing for quieter and better engine operation. Lower cetane fuel requires more time to ignite and produces more HC and PM emissions (Mahmudul et al. 2017). The low cetane index of UCO biodiesel may be caused by its high density. The fatty acid profile of the biodiesel in Section 4.6.2 shows the biodiesel is mostly comprised of saturated fatty acid. Past literature has reported that biodiesel with higher content of saturated fatty acid tends to have a high cetane index (Senthur Prabu et al. 2017). However, this is not the case for UCO biodiesel.

Table 4.15: Physicochemical properties of UCO and produced biodiesel.

Property	EN 14214	ASTM D6751	UCO	Biodiesel
Density at 15 °C (kg m^{-3})	860 – 900	870 – 900	922.7	883.6
Specific Gravity	n/a	0.86 – 0.90	0.9233	0.8841
API Gravity at 60 °F	n/a	n/a	31.8	28.6
Kinematic Viscosity at 40 °C (cSt)	3.5 – 5.0	1.9 – 6.0	54.53	5.149
Flash Point (°C)	>101	>130	238	156
Cloud Point (°C)	n/a	-3 – 12	14	15
Pour Point (°C)	n/a	-15 – 10	9	12
Cetane Index	>51	48 – 65	n/a	46.7

4.6.2 Fatty Acid Profile of Used Cooking Oil Biodiesel

The chromatography of biodiesel produced from UCO with respect to its component peaks is shown in Figure 4.18. Table 4.16 shows the fatty acid profile of biodiesel produced from UCO. Biodiesel consists of long-chain fatty acids, having between 13 and 21 carbons. Biodiesel with long-chain fatty acids was reported as having a high calorific value (Muhammed Niyas and Shaija 2022b). Both saturated and unsaturated fats are observed in the UCO

biodiesel. Saturated fatty acid molecules include palmitic acid (C16:0), stearic acid (C18:0), and eicosanoic acid (C20:0) comprised 62.15wt% of the UCO biodiesel. Unsaturated fatty acids such as linoleic acid (C18:2) and oleic acid (C18:1) made up only 34.75 wt% of the UCO biodiesel while 3.10 wt% of biodiesel is made from traces of other fatty acids. The physicochemical properties of biodiesel are influenced by the amount of saturated and unsaturated fatty acids. It has been reported that biodiesel with a higher oxidation stability was generated from a feedstock with a greater concentration of saturated fat (S. S. Kulkarni 2022; Reddy et al. 2018). Nevertheless, biodiesel with higher content of saturated fatty acid is linked to higher cloud and pour points (Muhammed Niyas and Shaija 2022a). This can be observed from the high cloud and pour points of UCO biodiesel reported in Section 4.6.1.

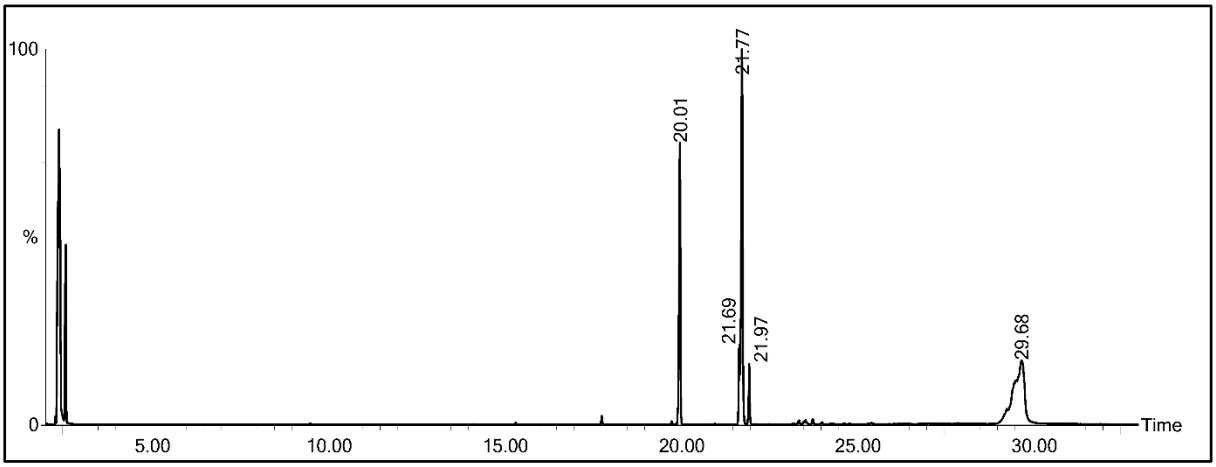

Figure 4.18: Chromatograph of biodiesel produced from UCO.

Table 4.16: Fatty acid profile of biodiesel produced from UCO.

Retention time (min.)	Area	Normalized concentration (wt%)	Fatty acid
20.007	827,594,368	21.67	C16:0 Palmitic acid
21.695	183,541,520	4.81	C18:2 Linoleic acid
21.765	1,143,294,848	29.94	C18:1 Oleic acid
21.969	128,521,000	3.37	C18:0 Stearic acid
29.682	1,417,041,664	37.11	C20:0 Eicosanoic acid
Others	118,270,549	3.10	
Total	3,818,263,949	100.00	

4.7 Biodiesel Synthesis Mechanism and Kinetic Study

In heterogeneously catalyzed transesterification, the reaction took place on the catalyst surface's active sites. Carbocation was formed when triglyceride linked with the proton present on the heterogeneous catalyst's surface. Oxygen from the methanol molecule attacked the nucleus of the carbocation and formed an unstable tetrahedral intermediate. The unstable tetrahedral intermediate simply disintegrated, resulting in a molecule of fatty acid methyl ester and a molecule of diglyceride (M. G. Kulkarni et al. 2006). The heterogeneous catalyst was also freed and ready for the following reaction. In a similar fashion, diglyceride went through the same process to produce a molecule of monoglyceride and a molecule of fatty acid methyl ester. The monoglyceride then also went through the same process to produce a molecule of glycerol and a molecule of fatty acid methyl ester. The proposed reaction mechanism of transesterification using SMBC is shown in Figure 4.19. The transesterification of triglyceride ultimately produced three molecules of fatty acid methyl esters and a molecule of glycerol.

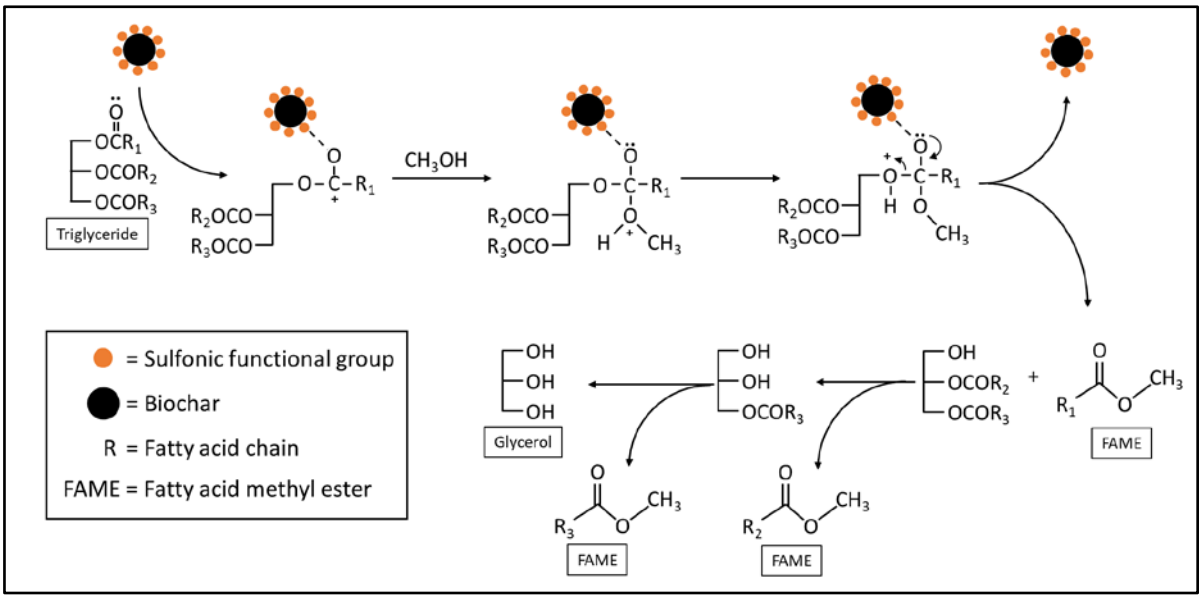

Figure 4.19: The proposed reaction mechanism of transesterification using SMBC.

Based on the optimum transesterification parameters obtained from Section 4.4.6, which are at catalyst loading (10.12 wt%), methanol to oil molar ratio (28), and reaction time (8 h), the kinetic study was carried out at five different reaction temperatures (50°C, 55°C, 60°C, 65°C, and 70°C) catalyzed by SMBC synthesized from EFB. Figure 4.20 shows the biodiesel yield at each temperature for the duration of the reaction. For each reaction, samples were collected at a pre-determined interval. Table 4.17 shows the biodiesel yield in decimal terms with respect to the reaction temperature.

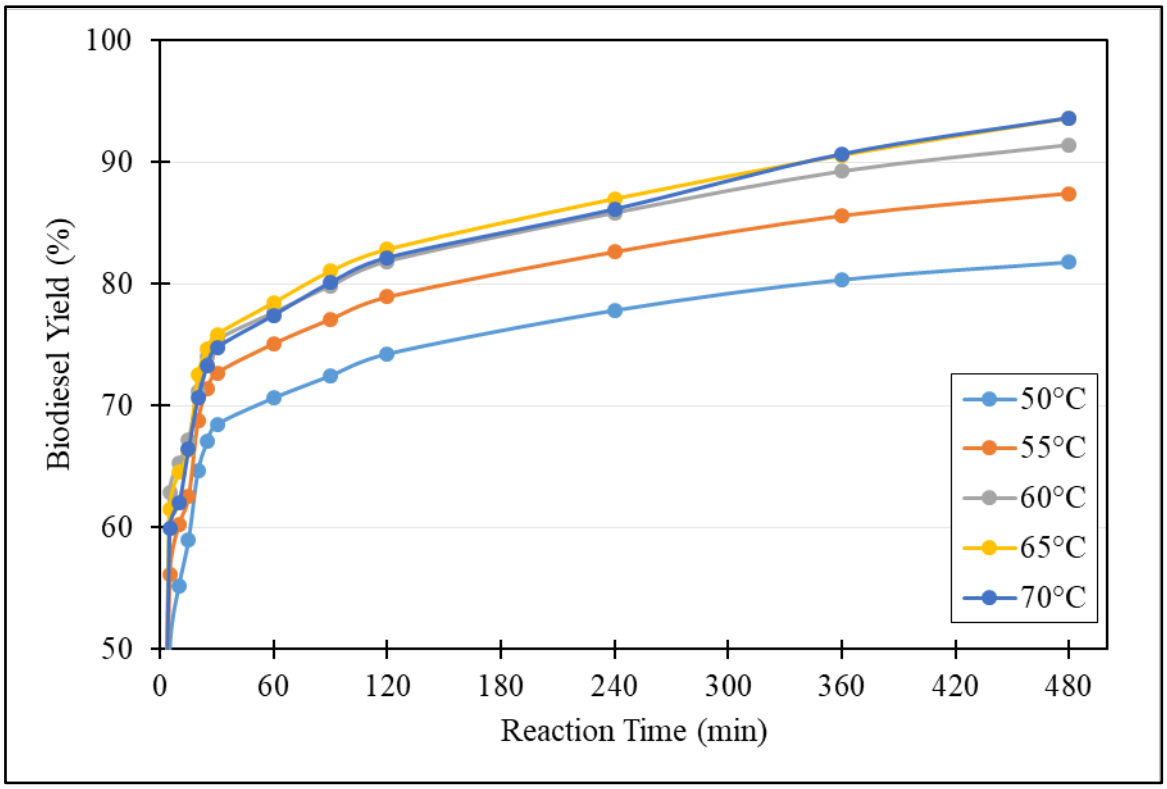

Figure 4.20: Biodiesel yield with respect to the reaction temperature at catalyst loading (10.12 wt%) and methanol to oil molar ratio (28).

Table 4.17: Biodiesel yield at catalyst loading (10.12 wt%) and methanol to oil molar ratio (28).

	X_{ME}				
	Temperature (°C)				
t (min)	**50**	**55**	**60**	**65**	**70**
5	0.4978	0.5610	0.6289	0.6151	0.5991
10	0.5518	0.6022	0.6529	0.6449	0.6197
15	0.5899	0.6249	0.6721	0.6635	0.6642
20	0.6463	0.6879	0.7118	0.7256	0.706
25	0.6701	0.7139	0.7397	0.7469	0.7331
30	0.6844	0.7268	0.7539	0.7584	0.7476
60	0.7062	0.7508	0.7766	0.7846	0.7743
90	0.7244	0.7708	0.7985	0.8104	0.8011
120	0.7424	0.7891	0.8185	0.8282	0.8215
240	0.7781	0.8262	0.8583	0.8698	0.8614
360	0.8033	0.8559	0.8925	0.9057	0.9066
480	0.8177	0.8743	0.9141	0.9361	0.9363

4.7.1 Pseudo-Irreversible First-Order Kinetic Model

Table 4.18 shows the calculated value for the pseudo-irreversible first-order kinetic model. Figure 4.21 shows the plot of this data along with the linear equation fitting of the plot. The gradients from the linear fitting are tabulated in Table 4.19 and derived into its natural logarithm (ln k). Figure 4.22 shows the plot of ln k versus 1/T. By linearizing this plot, the resulting gradient and intercept were used to calculate the E_a and A, respectively, using Equations 4.3 and 4.4.

Table 4.18: Derived biodiesel yield data for pseudo-irreversible first-order kinetic model at catalyst loading (10.12 wt%) and methanol to oil molar ratio (28).

	$\mathbf{f(x_1) = -\ln(1 - X_{ME})}$				
	Temperature (°C)				
t (min)	**50**	**55**	**60**	**65**	**70**
5	0.6888	0.8233	0.9913	0.9548	0.9140
10	0.8025	0.9218	1.0581	1.0354	0.9668
15	0.8914	0.9806	1.1150	1.0892	1.0912
20	1.0393	1.1644	1.2441	1.2932	1.2242
25	1.1090	1.2514	1.3459	1.3740	1.3209
30	1.1533	1.2976	1.402	1.4205	1.3767
60	1.2249	1.3895	1.4988	1.5353	1.4885
90	1.2888	1.4732	1.602	1.6628	1.6150
120	1.3563	1.5564	1.7065	1.7614	1.7232
240	1.5055	1.7499	1.9540	2.0387	1.9762
360	1.6261	1.9372	2.2303	2.3613	2.3709
480	1.7021	2.0739	2.4546	2.7504	2.7536

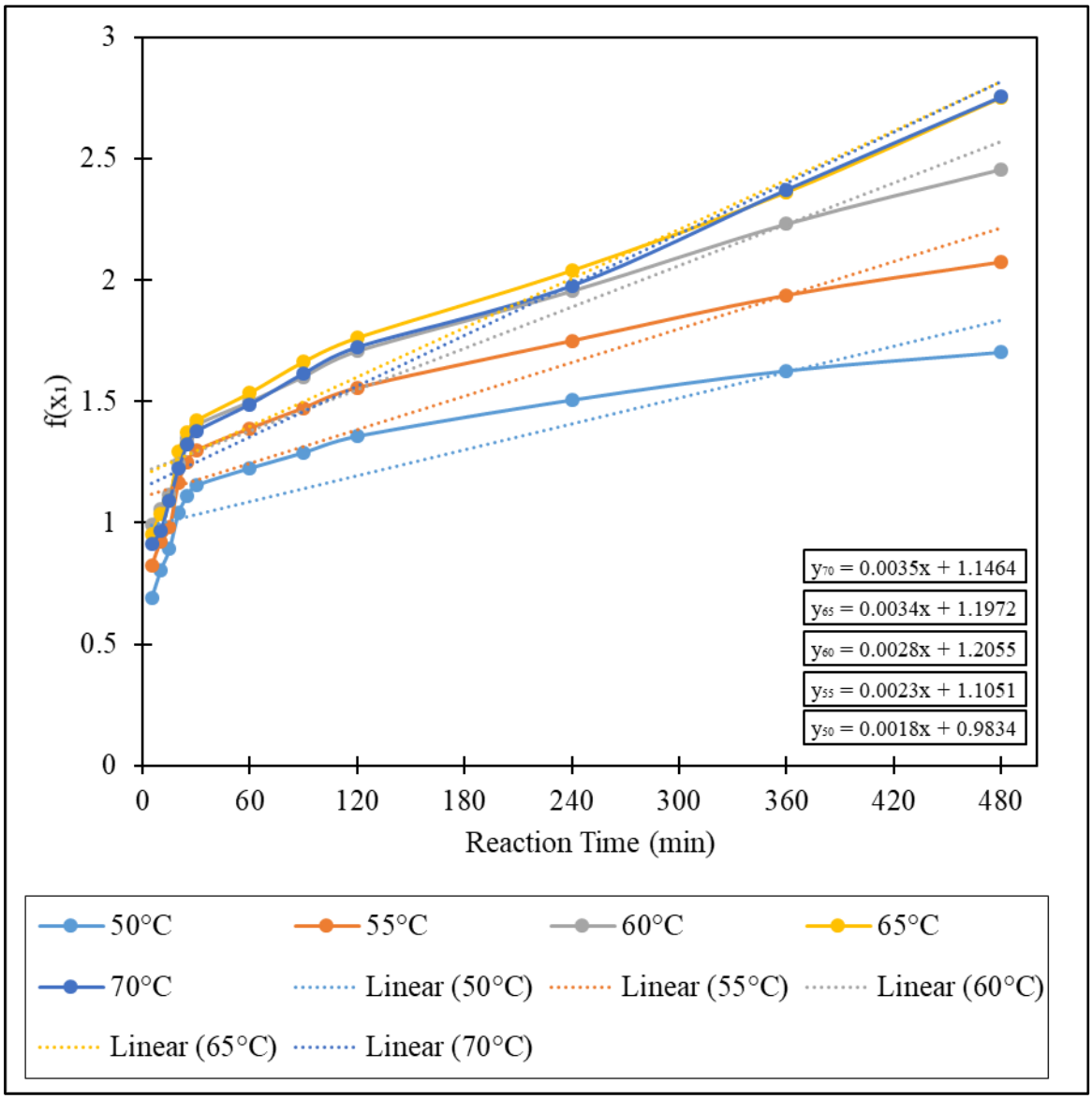

Figure 4.21: Pseudo-irreversible first-order kinetic model, $f(x_1)$ against reaction time plot with linearization.

Table 4.19: Kinetic data for pseudo-irreversible first-order kinetic model.

T (K)	1/T (K^{-1})	$k_{(1)}$	ln $k_{(1)}$
323.15	0.003095	0.0018	-6.32
328.15	0.003047	0.0023	-6.07
333.15	0.003002	0.0028	-5.88
338.15	0.002957	0.0034	-5.68
343.15	0.002914	0.0035	-5.65

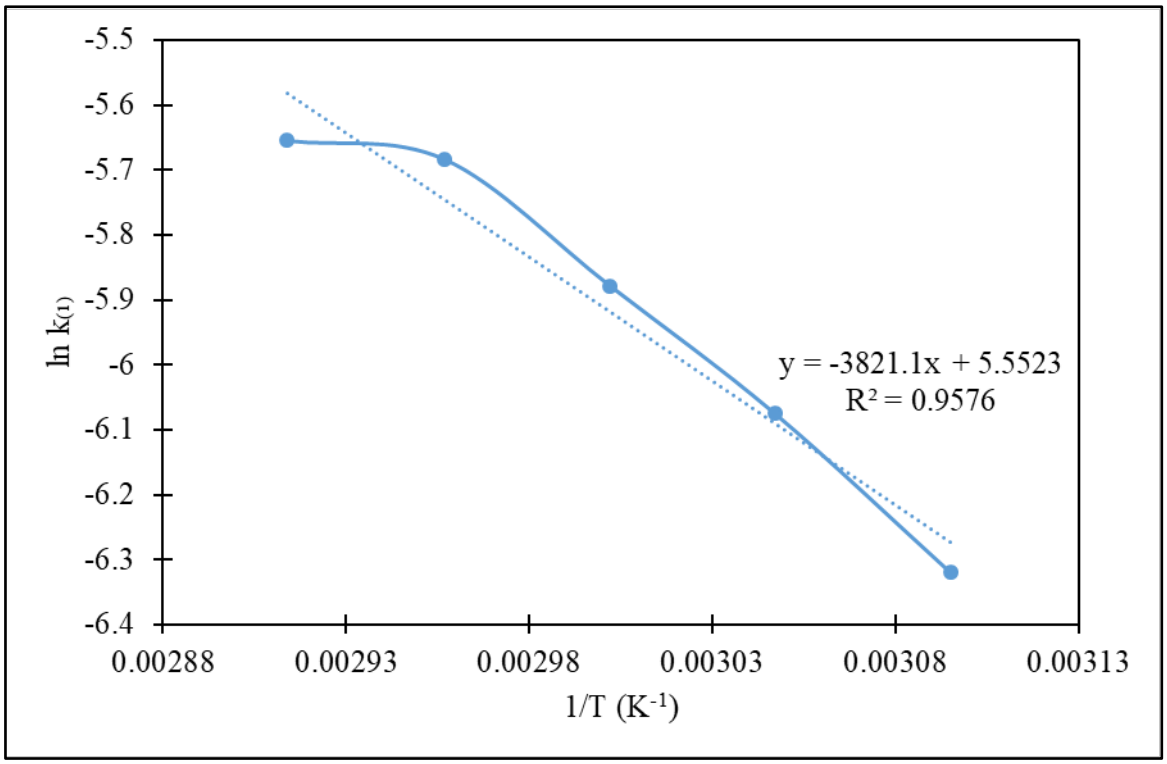

Figure 4.22: Plot of ln $k_{(1)}$ versus 1/T for pseudo-irreversible first-order kinetic model.

From Arrhenius equation, Equations 4.3 and 4.4 can be derived.

$$E_a = - Rm \tag{4.3}$$

$$A = e^c \tag{4.4}$$

where R is the gas constant, m is the gradient of the slope value, and c is the intercept value from the linearization of ln k vs. 1/T plot. From Equations 4.3 and 4.4, the values of E_a and A for the pseudo-irreversible first-order kinetic model are 31.77 kJ mol^{-1} and 257.83, respectively. The R^2 value of the linearization of ln k vs. 1/T plot, 0.9576, shows good conformity of the transesterification reaction to the pseudo-irreversible first-order kinetic model.

4.7.2 Pseudo-Irreversible Second-Order Kinetic Model

The computed value for the pseudo-irreversible second-order kinetic model is shown in Table 4.20. The plot of this data and the linear equation fitting of the plot are shown in Figure 4.23. The linear fitting's gradients are listed in Table 4.21 and converted to their natural logarithm (ln k). The ln k versus 1/T figure is shown in Figure 4.24. Equations 4.3 and 4.4 were used to determine the gradient and intercept after linearizing this plot in order to determine the Ea and A, respectively.

Table 4.20: Derived biodiesel yield data for the pseudo-irreversible second-order kinetic model at catalyst loading (10.12 wt%) and methanol to oil molar ratio (28).

	$\mathbf{f(x_2) = \frac{1}{(1 - X_{ME})}}$				
	Temperature (°C)				
t (min)	**50**	**55**	**60**	**65**	**70**
5	1.9912	2.2779	2.6947	2.5981	2.4944
10	2.2311	2.5138	2.8810	2.8161	2.6295
15	2.4384	2.666	3.0497	2.9718	2.9780
20	2.8273	3.2041	3.4698	3.6443	3.4014
25	3.0312	3.4953	3.8417	3.9510	3.7467
30	3.1686	3.6603	4.0634	4.1391	3.9620
60	3.4037	4.0128	4.4763	4.6425	4.4307
90	3.6284	4.3630	4.9628	5.2743	5.0277
120	3.8820	4.7416	5.5096	5.8207	5.6022
240	4.5065	5.7537	7.0572	7.6805	7.2150
360	5.0839	6.9396	9.3023	10.6045	10.7066
480	5.4855	7.9554	11.6414	15.6495	15.6986

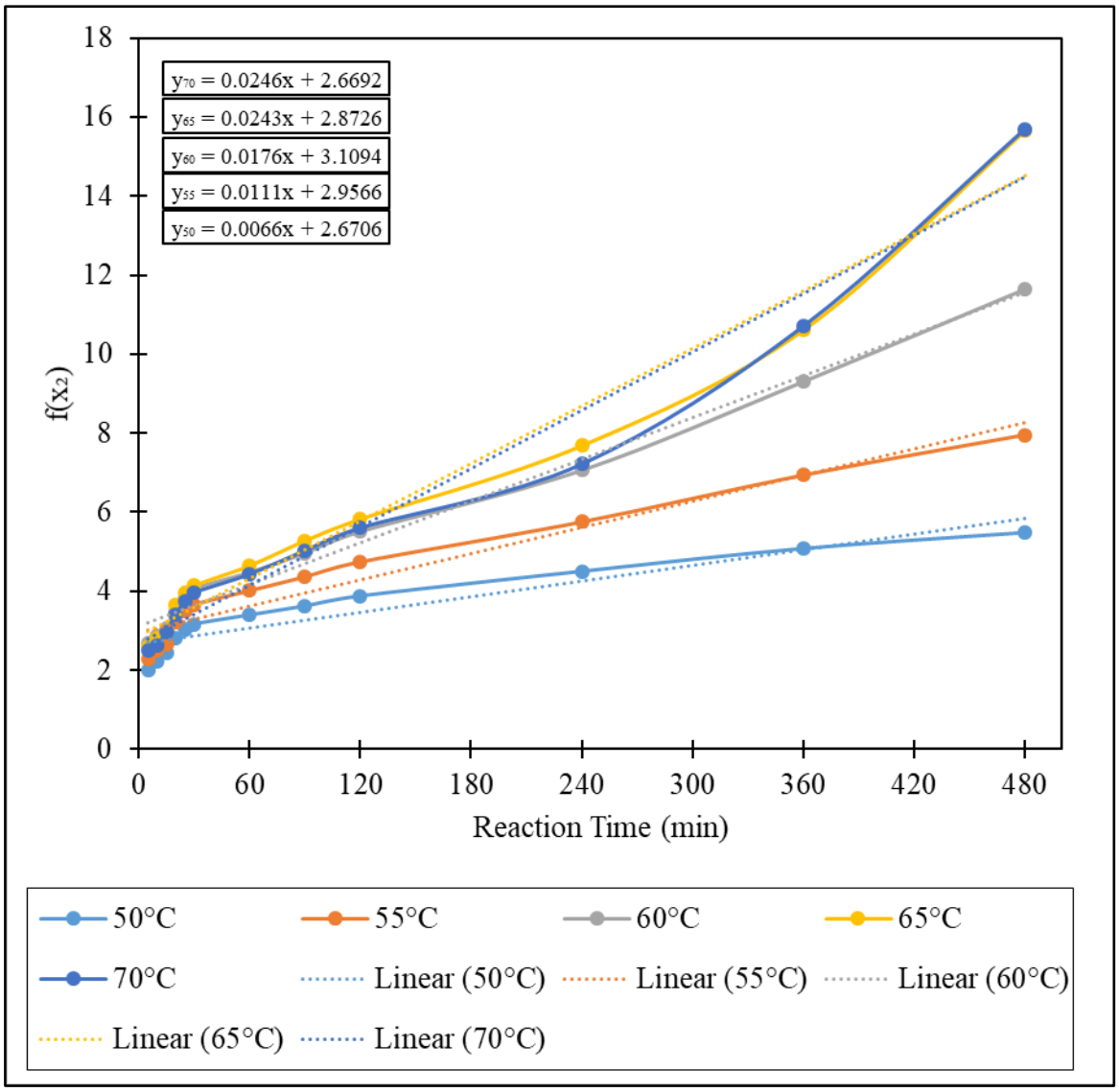

Figure 4.23: Pseudo-irreversible second-order kinetic model, $f(x_2)$ against reaction time plot with linearization.

Table 4.21: Kinetic data for pseudo-irreversible second-order kinetic model.

T (K)	1/T (K^{-1})	$k_{(2)}$	ln $k_{(2)}$
323.15	0.003095	0.0066	-5.02
328.15	0.003047	0.0111	-4.50
333.15	0.003002	0.0176	-4.04
338.15	0.002957	0.0243	-3.72
343.15	0.002914	0.0246	-3.71

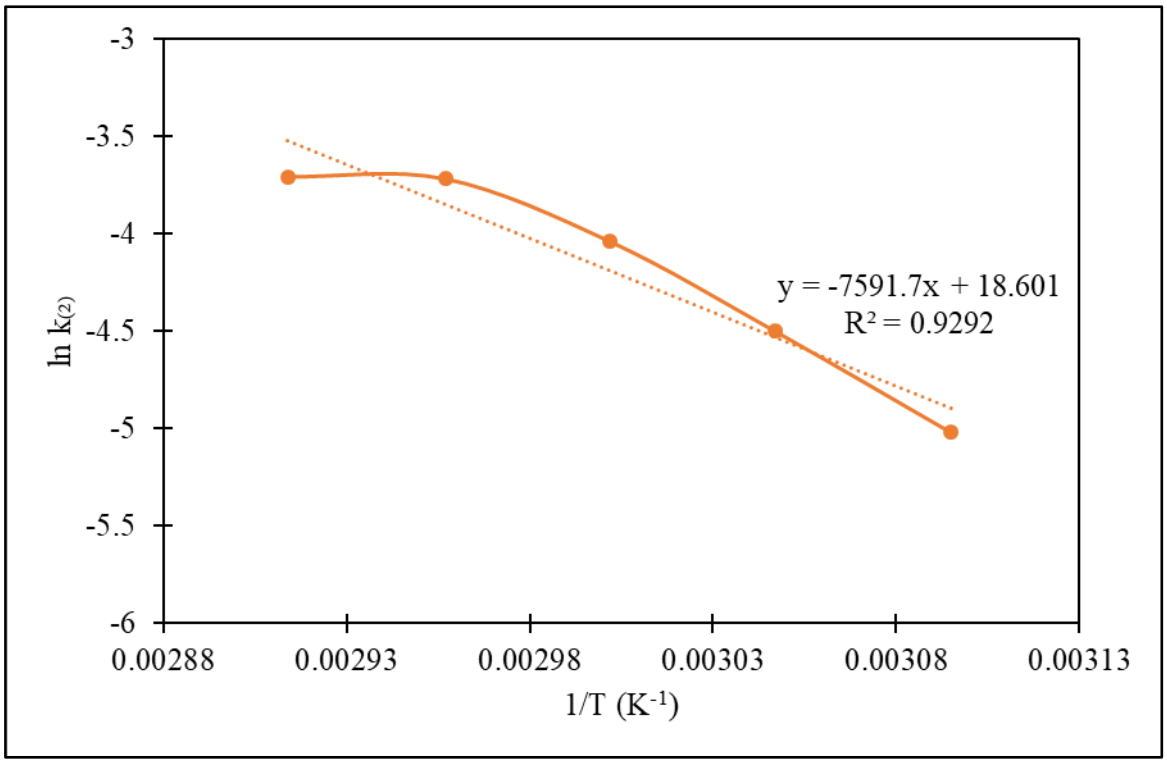

Figure 4.24: Plot of ln $k_{(2)}$ versus 1/T for pseudo-irreversible second-order kinetic model.

According to Equations 4.3 and 4.4, the values of E_a and A for the pseudo-irreversible second-order kinetic model are 63.12 kJ mol^{-1} and 1.20×10^{8}, respectively. The linearization of ln k vs. 1/T plot's R^2 value of 0.9292 demonstrates the transesterification reaction's agreement with the pseudo-irreversible second-order kinetic model.

4.7.3 Pseudo-Reversible Second-Order Kinetic Model

The computed value for the pseudo-reversible second-order kinetic model is shown in Table 4.22. Figure 4.25 displays the data plot and the linear equation fitting of the data. Table 4.23 lists and converts the gradients of the linear fitting to their natural logarithm (ln k). Figure 4.26 displays the ln k versus 1/T graph. After linearizing this figure, the gradient and intercept were considered for Ea and A calculation using equations 4.3 and 4.4, respectively.

Table 4.22: Derived biodiesel yield data for the pseudo-reversible second-order kinetic model at catalyst loading (10.12 wt%) and the methanol to oil molar ratio (28).

	$\mathbf{f(x_3) = \frac{1}{([ROH_0] - [TG_0])} \ln \frac{[TG_0]([ROH_0] - X_{ME})}{[ROH_0]([TG_0] - X_{ME})}}$				
	Temperature (°C)				
t (min)	**50**	**55**	**60**	**65**	**70**
5	0.0248	0.0297	0.0359	0.0345	0.0330
10	0.0290	0.0333	0.0383	0.0375	0.0350
15	0.0322	0.0355	0.0404	0.0394	0.0395
20	0.0376	0.0422	0.0451	0.0469	0.0444
25	0.0402	0.0454	0.0488	0.0499	0.0479
30	0.0418	0.0471	0.0509	0.0516	0.0500
60	0.0444	0.0504	0.0545	0.0558	0.0541
90	0.0467	0.0535	0.0582	0.0605	0.0587
120	0.0492	0.0566	0.0621	0.0641	0.0627
240	0.0547	0.0637	0.0712	0.0743	0.0720
360	0.0591	0.0706	0.0814	0.0862	0.0866
480	0.0619	0.0756	0.0897	0.1006	0.1007

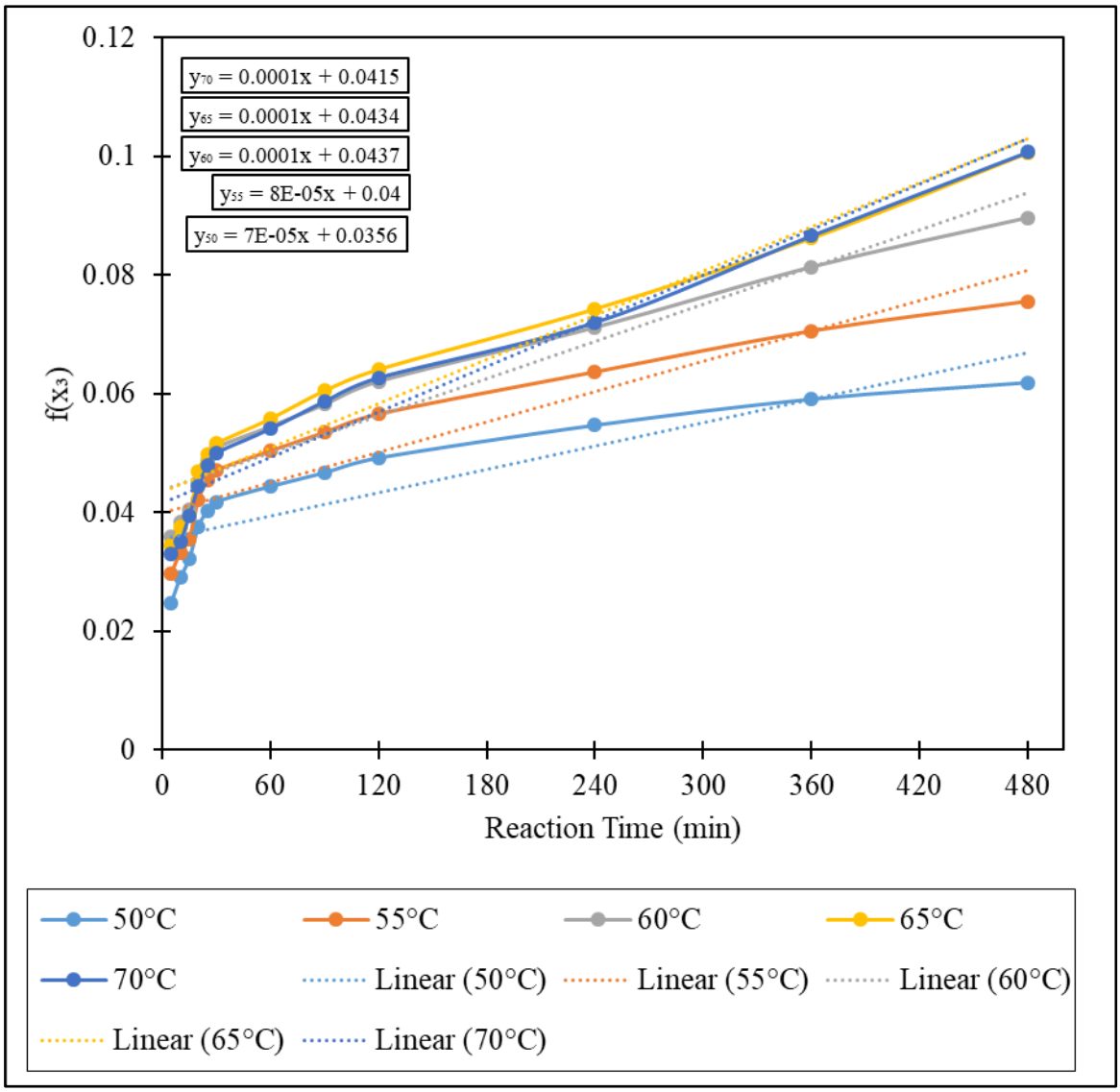

Figure 4.25: Pseudo-reversible second-order kinetic model, $f(x_3)$ against reaction time plot with linearization.

Table 4.23: Kinetic data for pseudo-reversible second-order kinetic model.

T (K)	1/T (K^{-1})	$k_{(3)}$	ln $k_{(3)}$
323.15	0.003095	0.00007	-9.57
328.15	0.003047	0.00008	-9.43
333.15	0.003002	0.00010	-9.21
338.15	0.002957	0.00010	-9.21
343.15	0.002914	0.00010	-9.21

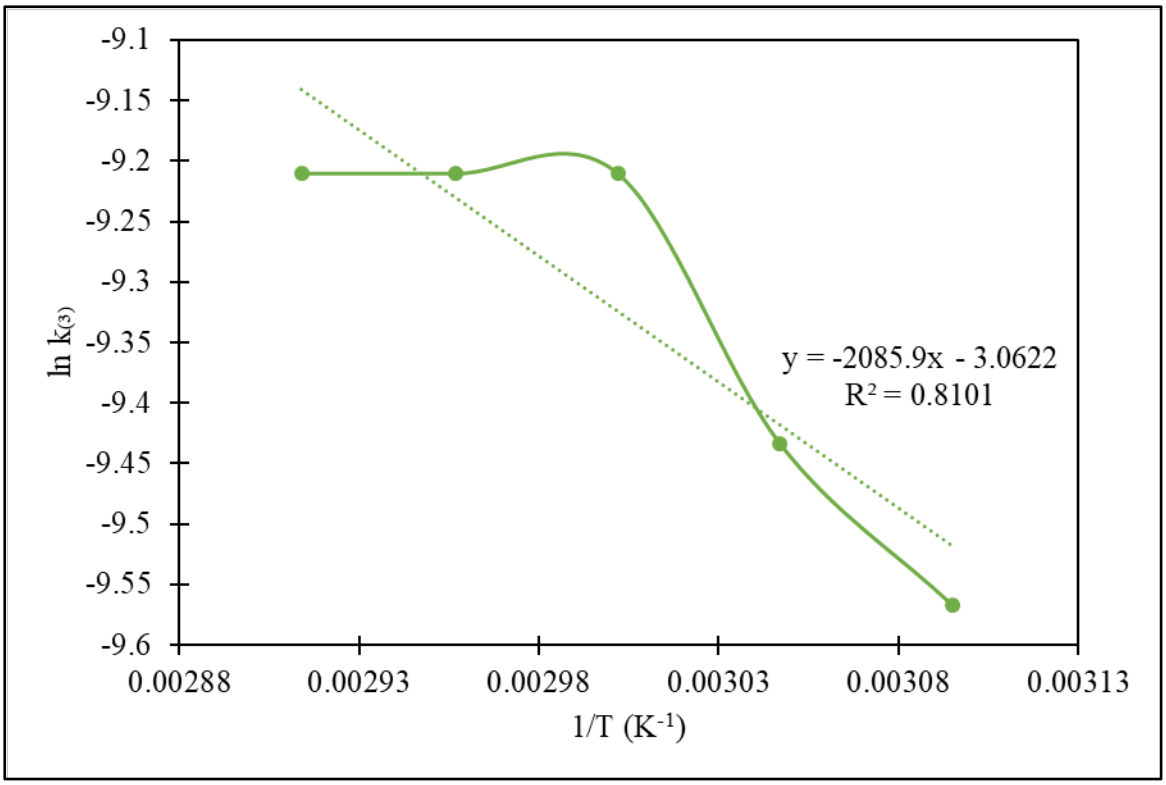

Figure 4.26: Plot of ln $k_{(3)}$ versus 1/T for pseudo-reversible second-order kinetic model.

From Equations 4.3 and 4.4, the values of E_a and A for the pseudo-reversible second-order kinetic model are 17.34 kJ mol^{-1} and 0.0467, respectively. The R^2 value of the linearization of ln k vs. 1/T plot, 0.8101, shows fair conformity of the transesterification reaction to the pseudo-reversible second-order kinetic model.

4.7.4 Kinetic Models Comparison

Table 4.24 summarizes the kinetic data for the three kinetic models investigated in this study. From these data, the presumed reaction kinetic for transesterification was mostly the pseudo-irreversible first-order kinetic based on its R^2 value, which is the closest to one. The E_a value for the pseudo-reversible second-order is lower than the pseudo-irreversible first-order and the pseudo-irreversible second-order kinetic models. However, this model is considered less suitable for the transesterification reaction kinetic modeling in this study due to its low R^2 value.

In this study, the E_a of the pseudo-irreversible first-order kinetic agrees with most literature. The typical E_a value for a first-order reaction ranges from as low as 21.47 kJ mol^{-1} for sulfonic acid catalyzed biodiesel production from jatropha oil (Neeharika et al. 2017) to as high as 77.6 kJ mol^{-1} for MgO-La_2O_3 catalyzed biodiesel production from sunflower oil (Feyzi et al. 2017). A reaction using a homogeneous catalyst typically requires a lower E_a compared

to the ones using a heterogeneous catalyst. A. Wang et al. (2018) reported E_a value of 37.5 kJ mol^{-1} for biodiesel production from oleic acid using sulfonated magnetic catalyst from chitosan. Another study by Putra et al. (2018) reported E_a value of 66.27 kJ mol^{-1} for biodiesel production from waste cooking oil using CaO/SiO_2 catalyst. Ali, Elkatory, and Hamad (2020) reported E_a value of 37.64 kJ mol^{-1} for biodiesel production from waste frying oil using $CuFe_2O_4$ catalyst. Compared with these literature, the E_a of the pseudo-irreversible first-order kinetic of this research is slightly lower. A reaction with lower E_a requires less energy to initiate, ultimately reduces the cost to produce the biodiesel.

Based on these data, the proposed mechanism of transesterification of UCO using SMBC shown in Figure 4.19 was deemed reasonable. The kinetic model implies that a sufficient catalyst is utilized in relation to the oil to shift the balance of the reaction in the direction of fatty acid methyl esters production. When methanol is reacted in excess, the reaction shows pseudo-irreversible first-order kinetics.

Table 4.24: Summary of evaluated data for kinetic study.

Kinetic Model	**Ea (kJ mol^{-1})**	**R^2**
Pseudo-irreversible first-order	31.77	0.9576
Pseudo-irreversible second-order	63.12	0.9292
Pseudo-reversible second-order	17.34	0.8101

4.8 Summary

This chapter partially presents in detail the results and discussions of this research. The results and discussions for the synthesis and characterization of SMBC from PKS, OPF, and EFB are presented in Section 4.2. From the characterization, SMBC based on OPF and EFB have been observed to have comparable properties and better compared to SMBC based on PKS. The results and discussions for the analysis of optimum SMBC synthesis parameters via the Taguchi method are presented in Section 4.3. From this analysis, EFB has been chosen as the best biomass to produce SMBC (variation EFB1) with optimum synthesis parameters of 1.5 M of FC, 800 °C of CT, and 2.5 M of HC. The UCO biodiesel production optimization is discussed in Section 4.4, in which the optimum reaction parameters were observed to be at conditions catalyst loading (10.12 wt%), methanol to oil molar ratio (28), reaction temperature (70°C), and reaction time (8 h). The experimental optimal biodiesel yield was at 95.87%. Section 4.5 presents the results from the SMBC reusability analysis. The catalyst was able to produce a biodiesel yield of 70.16% at the fifth cycle, which is a decrease of 25.68% between the first cycle and the fifth cycle. Section 4.6 discusses the characterization of UCO biodiesel. The UCO biodiesel was observed to be mostly consist of saturated fatty acids. Lastly, the results of the kinetic study of UCO biodiesel production using SMBC are presented in Section 4.7. The UCO biodiesel has been observed to correspond to a pseudo-irreversible first-order with Ea of 31.77 kJ mol^{-1}.

The whole results successfully fulfilled this research's five objectives. Objective 1: To synthesize and characterize the SMBC from PKS, OPF, and EFB. Objective 2: To optimize the synthesis of SMBC from PKS, OPF, and EFB. Objective 3: To study the catalytic activity, regeneration, and reusability of the SMBC in optimized biodiesel production from UCO. Objective 4: To characterize the biodiesel produced from UCO using SMBC. Lastly, objective 5: To investigate the mechanism and kinetics of SMBC-catalyzed biodiesel production.

The next chapter presents the conclusion and future recommendations of this research.

CHAPTER 5
CONCLUSION

5.1 Conclusion

In conclusion, this study has successfully synthesized sulfonated magnetic biochar catalyst (SMBC) from PKS, OPF, and EFB. The SMBC was characterized via FESEM, EDX, BET, TGA, FTIR, neutralization titration, and VSM. Through FESEM, the formation of a porous structure on the SMBC was observed. The EDX elemental analysis confirmed the presence of elemental iron and sulfur to correspond with iron impregnation and sulfonation on the SMBC, respectively. The BET surface area of the optimized SMBC based on EFB (EFB1 variation in the Taguchi analysis) was determined to be 44.42 m^2 g^{-1}. TGA visualized the release of the volatile compound during the carbonization process of SMBC synthesis. FTIR analysis distinguished the functional group of SMBC. The average acid density values of SMBC obtained through neutralization titration showed that optimized SMBC had an average acid density value of 3.85 mmol g^{-1}. VSM analysis showed the optimized SMBC had a σ_s value of 3.19 Am^2 kg^{-1}.

The Taguchi method was employed to investigate the optimum parameters for SMBC synthesis. Based on the Taguchi analysis and characterization results, EFB was chosen as the best biomass for SMBC synthesis with the optimum synthesis parameters of EFB1 variation at 1.5 M of FC, 800 °C of CT, and 2.5 M of HC.

The experimental design by RSM-CCD was used, and the optimum biodiesel production from UCO using the optimized SMBC was investigated. The SMBC was synthesized from EFB according to the optimized synthesis parameters from the Taguchi analysis. The optimum UCO biodiesel production parameters were obtained at a catalyst loading of 10.12 wt%, methanol to oil molar ratio of 28, reaction temperature of 70°C, and reaction time of 8 h. The maximum biodiesel yield was achieved at 95.87%. A biodiesel yield reduction to 70.16% was recorded after five cycles when SMBC was recycled for biodiesel production according to the optimum production parameters.

The produced UCO biodiesel was characterized by its physicochemical properties and fatty acid profile. The physicochemical characterization showed the UCO biodiesel has met the ASTM D6751 standard except for its cloud point, pour point, and cetane index. The fatty acid profile of UCO biodiesel obtained from the GC-MS analysis has shown the biodiesel produced majorly consists of saturated fatty acids.

Finally, this study also investigated the kinetics of biodiesel transesterification from UCO using SMBC. The same biodiesel production optimum parameters were adopted, and the reaction demonstrated a pseudo-irreversible first-order kinetic with an activation energy of 31.77 kJ mol^{-1}. These results showed that SMBC-catalyzed biodiesel production from UCO is a highly-potential way to produce biodiesel.

5.2 Future Recommendation

This study has investigated the SMBC synthesis, reaction, and separation mechanism in-depth in producing biodiesel from UCO. However, more studies should be done to encompass most catalysts and biodiesel synthesis topics. This study would like to convey the following recommendation for future research:

(a) Economic and environmental effects of the catalyst synthesis process can be studied through exergoeconomic and exergoenvironmental optimization. These methods of analysis can potentially reduce the cost and environmental impacts of a full-scale biodiesel production process.

(b) Optimization of the catalyst synthesis can be studied in more detail by applying full factorial or RSM for the synthesis parameters. Meanwhile, other types of biomass can be utilized as catalyst precursors or catalyst support.

(c) Reaction parameters for biodiesel production that might influence the biodiesel yield, such as reaction pressure, stirring rate, and stirring mode, can be studied. Different chemicals, such as another type of oil feedstock and alcohol other than methanol, can be used for biodiesel production investigation. Additional equipment, such as a reactor, can increase the reaction modeling accuracy.

(d) The catalyst reusability study can be extended and carried out extensively beyond five cycles to investigate the effects and causes of the biodiesel yield decrease over catalyst reuse cycle. Qualitative analysis like the characteristic tests of the spent catalyst can be carried out to investigate the cause and effect of the catalyst deactivation.

(e) Post-reaction processes such as oil pretreatment, separation, and product refining can be studied. The inclusion of these post-reaction steps can increase biodiesel quality and value. Among the biodiesel properties that can benefit from these processes are oxidation stability, product purity, cold flow characteristics, cloud, and pour point.

(f) For better understanding of the relation of energy and work in a transesterification using SMBC, thermodynamics study can be carried out in addition of the kinetics study.

Thermodynamics study can give more data on the characteristics of transesterification using SMBC.

(g) Data on kinetic study can be enhanced by integrating the catalyst deactivation rate due to contamination and loss of catalytic active sites. Consequently, the behavior and the reaction kinetics of the catalyst can be further understood. As a result, the kinetic model can be used more accurate and for longer reaction time.

(h) Quantitative study on the difference of energy and time consumed for catalyst-product separation between different types of separation means can justify the usage of magnetic catalyst over other non-magnetic catalyst by providing in detail the energy and time saving of using magnetic separation and magnetic catalyst over other non-magnetic catalyst.

(i) Further study on the scalability and economic viability of the process can be done to include a feasibility study on the scale-up of the biodiesel production process using the synthesized sulfonated magnetic biochar catalyst, considering the economic feasibility and sustainability of the process.

(j) To scale up biodiesel production in the industry, a cost estimate and life cycle assessment for the production can be developed. High-quality data is essential for a reliable evaluation in a life cycle assessment analysis, as this task can consume time and effort.

REFERENCES

Abbah, E.C., G.I. Nwandikom, C.C. Egwuonwu, and N.R. Nwakuba. 2016. “Effect of Reaction Temperature on the Yield of Biodiesel From Neem Seed Oil.” *American Journal of Energy Science* 3 (3): 16–20.

Abdalla, Ibrahim E. 2018. “Experimental Studies for the Thermo-Physiochemical Properties of Biodiesel and Its Blends and the Performance of Such Fuels in a Compression Ignition Engine.” *Fuel* 212 (x): 638–55. https://doi.org/10.1016/j.fuel.2017.10.064.

Abdulhussein Alsaedi, Alyaa, Md Sohrab Hossain, Venugopal Balakrishnan, Marwan Abdul Hakim Shaah, Muaz Mohd Zaini Makhtar, Norli Ismail, Mu Naushad, and Chinna Bathula. 2022. “Extraction and Separation of Lipids from Municipal Sewage Sludge for Biodiesel Production: Kinetics and Thermodynamics Modeling.” *Fuel* 325 (June): 124946. https://doi.org/10.1016/j.fuel.2022.124946.

Abdullah, Bawadi, Syed Anuar Faua’ad Syed Muhammad, Zahra Shokravi, Shahrul Ismail, Khairul Anuar Kassim, Azmi Nik Mahmood, and Md Maniruzzaman A. Aziz. 2019. “Fourth Generation Biofuel: A Review on Risks and Mitigation Strategies.” *Renewable and Sustainable Energy Reviews* 107 (February): 37–50. https://doi.org/10.1016/j.rser.2019.02.018.

Abdullah, Sharifah Hanis Yasmin Sayid, Nur Hanis Mohamad Hanapi, Azman Azid, Roslan Umar, Hafizan Juahir, Helena Khatoon, and Azizah Endut. 2017. “A Review of Biomass-Derived Heterogeneous Catalyst for a Sustainable Biodiesel Production.” *Renewable and Sustainable Energy Reviews* 70 (December): 1040–51. https://doi.org/10.1016/j.rser.2016.12.008.

Ahangari, Hossein, Jerry W. King, Ali Ehsani, and Mohammad Yousefi. 2021. “Supercritical Fluid Extraction of Seed Oils – A Short Review of Current Trends.” *Trends in Food Science & Technology* 111 (May 2020): 249–60. https://doi.org/10.1016/j.tifs.2021.02.066.

Ahmad, Junaid, Suzana Yusup, Awais Bokhari, and Ruzaimah Nik Mohammad Kamil. 2014. “Study of Fuel Properties of Rubber Seed Oil Based Biodiesel.” *Energy Conversion and Management* 78: 266–75. https://doi.org/10.1016/j.enconman.2013.10.056.

Ahmed, Rawaz, and Katherine Huddersman. 2022. “Review of Biodiesel Production by the Esterification of Wastewater Containing Fats Oils and Grease (FOGs).” *Journal of Industrial and Engineering Chemistry* 110 (June): 1–14. https://doi.org/10.1016/j.jiec.2022.02.045.

Ajorloo, Mojtaba, Maryam Ghodrat, Jason Scott, and Vladimir Strezov. 2022. “Recent

Advances in Thermodynamic Analysis of Biomass Gasification: A Review on Numerical Modelling and Simulation." *Journal of the Energy Institute* 102 (May): 395–419. https://doi.org/10.1016/j.joei.2022.05.003.

Akinfalabi, Shehu-Ibrahim, Umer Rashid, Robiah Yunus, and Yun Hin Taufiq-Yap. 2017. "Synthesis of Biodiesel from Palm Fatty Acid Distillate Using Sulfonated Palm Seed Cake Catalyst." *Renewable Energy* 111 (October): 611–19. https://doi.org/10.1016/j.renene.2017.04.056.

Akkarawatkhoosith, Nattee, Amaraporn Kaewchada, Chawalit Ngamcharussrivichai, and Attasak Jaree. 2020. "Biodiesel Production Via Interesterification of Palm Oil and Ethyl Acetate Using Ion-Exchange Resin in a Packed-Bed Reactor." *BioEnergy Research* 13 (2): 542–51. https://doi.org/10.1007/s12155-019-10051-4.

Al-Ameri, Mariam, and Sulaiman Al-Zuhair. 2019. "Using Switchable Solvents for Enhanced, Simultaneous Microalgae Oil Extraction-Reaction for Biodiesel Production." *Biochemical Engineering Journal* 141 (January): 217–24. https://doi.org/10.1016/j.bej.2018.10.017.

Al-Humairi, Shurooq T., Jonathan G.M. Lee, and Adam P. Harvey. 2022. "Direct and Rapid Production of Biodiesel from Algae Foamate Using a Homogeneous Base Catalyst as Part of an Intensified Process." *Energy Conversion and Management: X* 16 (August): 100284. https://doi.org/10.1016/j.ecmx.2022.100284.

Al-Jammal, Noor, Zayed Al-Hamamre, and Mohammad Alnaief. 2016. "Manufacturing of Zeolite Based Catalyst from Zeolite Tuft for Biodiesel Production from Waste Sunflower Oil." *Renewable Energy* 93 (August): 449–59. https://doi.org/10.1016/j.renene.2016.03.018.

Alavi-Borazjani, Seyedeh Azadeh, Luís António da Cruz Tarelho, and Maria Isabel Capela. 2021. "Parametric Optimization of the Dark Fermentation Process for Enhanced Biohydrogen Production from the Organic Fraction of Municipal Solid Waste Using Taguchi Method." *International Journal of Hydrogen Energy* 46 (41): 21372–82. https://doi.org/10.1016/j.ijhydene.2021.04.017.

Alba-Rubio, Ana C., José Santamaría-González, Josefa M. Mérida-Robles, Ramón Moreno-Tost, David Martín-Alonso, Antonio Jiménez-López, and Pedro Maireles-Torres. 2010. "Heterogeneous Transesterification Processes by Using CaO Supported on Zinc Oxide as Basic Catalysts." *Catalysis Today* 149 (3–4): 281–87. https://doi.org/10.1016/j.cattod.2009.06.024.

Ali, Rehab M., Marwa R. Elkatory, and Hesham A. Hamad. 2020. "Highly Active and Stable

Magnetically Recyclable CuFe2O4 as a Heterogenous Catalyst for Efficient Conversion of Waste Frying Oil to Biodiesel." *Fuel* 268 (January): 117297. https://doi.org/10.1016/j.fuel.2020.117297.

Alonzo, Dora E. López de. 2007. "Heterogeneous Catalysis and Biodiesel Forming Reactions." Clemson University.

Alptekin, Ertan, and Mustafa Canakci. 2011. "Optimization of Transesterification for Methyl Ester Production from Chicken Fat." *Fuel* 90 (8): 2630–38. https://doi.org/10.1016/j.fuel.2011.03.042.

Ambat, Indu, Varsha Srivastava, and Mika Sillanpää. 2018. "Recent Advancement in Biodiesel Production Methodologies Using Various Feedstock: A Review." *Renewable and Sustainable Energy Reviews* 90 (February 2017): 356–69. https://doi.org/10.1016/j.rser.2018.03.069.

Ambaye, Teklit Gebregiorgis, Mentore Vaccari, Adrián Bonilla-Petriciolet, Shiv Prasad, Eric D. van Hullebusch, and Sami Rtimi. 2021. "Emerging Technologies for Biofuel Production: A Critical Review on Recent Progress, Challenges and Perspectives." *Journal of Environmental Management* 290 (July): 112627. https://doi.org/10.1016/j.jenvman.2021.112627.

Andrade, Thalles A., Mariano Martín, Massimiliano Errico, and Knud V. Christensen. 2019. "Biodiesel Production Catalyzed by Liquid and Immobilized Enzymes: Optimization and Economic Analysis." *Chemical Engineering Research and Design* 141 (January): 1–14. https://doi.org/10.1016/j.cherd.2018.10.026.

Anto, Susaimanickam, Rathinasamy Karpagam, Ponnuswamy Renukadevi, Kalimuthu Jawaharraj, and Perumal Varalakshmi. 2019. "Biomass Enhancement and Bioconversion of Brown Marine Microalgal Lipid Using Heterogeneous Catalysts Mediated Transesterification from Biowaste Derived Biochar and Bionanoparticle." *Fuel* 255 (January): 115789. https://doi.org/10.1016/j.fuel.2019.115789.

Aro, Eva-Mari. 2016. "From First Generation Biofuels to Advanced Solar Biofuels." *Ambio* 45 (S1): 24–31. https://doi.org/10.1007/s13280-015-0730-0.

Arumugam, A., and V. Ponnusami. 2019. "Biodiesel Production from Calophyllum Inophyllum Oil a Potential Non-Edible Feedstock: An Overview." *Renewable Energy* 131 (February): 459–71. https://doi.org/10.1016/j.renene.2018.07.059.

ASTM International. 2010. *ASTM D6751 - 03a Standard Specification for Biodiesel Fuel Blend Stock (B100) for Middle Distillate Fuels*. Vol. i. West Conshohocken, PA: ASTM International. https://doi.org/10.1520/D6751-15CE01.

———. 2020. *ASTM D6751-20a, Standard Specification for Biodiesel Fuel Blend Stock (B100) for Middle Distillate Fuels*. West Conshohocken, PA: ASTM International. https://doi.org/10.1520/D6751-20A.

Atabani, A.E., A.S. Silitonga, Irfan Anjum Badruddin, T.M.I. Mahlia, H.H. Masjuki, and S. Mekhilef. 2012. "A Comprehensive Review on Biodiesel as an Alternative Energy Resource and Its Characteristics." *Renewable and Sustainable Energy Reviews* 16 (4): 2070–93. https://doi.org/10.1016/j.rser.2012.01.003.

Atkinson, John D., Maria E. Fortunato, Seyed A. Dastgheib, Massoud Rostam-Abadi, Mark J. Rood, and Kenneth S. Suslick. 2011. "Synthesis and Characterization of Iron-Impregnated Porous Carbon Spheres Prepared by Ultrasonic Spray Pyrolysis." *Carbon* 49 (2): 587–98. https://doi.org/10.1016/j.carbon.2010.10.001.

Attorney General's Chambers of Malaysia. 2019. *Malaysian Biofuel Industry (Blending Percentage and Mandatory Use) Regulations 2019*. Malaysia.

Awogbemi, Omojola, F. L. Inambao, and E. I. Onuh. 2019. "Modelling and Optimization of Transesterification of Waste Sunflower Oil to Fatty Acid Methyl Ester: A Case of Response Surface Methodology vs Taguchi Orthogonal Approach." *International Journal of Engineering Research and Technology* 12 (12): 2346–61.

Awogbemi, Omojola, and Daramy Vandi Von Kallon. 2023. "Application of Biochar Derived from Crops Residues for Biofuel Production." *Fuel Communications* 15 (March): 100088. https://doi.org/10.1016/j.jfueco.2023.100088.

Awogbemi, Omojola, Daramy Vandi Von Kallon, and Adefemi O. Owoputi. 2022. "Biofuel Generation from Potato Peel Waste: Current State and Prospects." *Recycling* 7 (2): 23. https://doi.org/10.3390/recycling7020023.

Ayoob, Arqam K., and Abdelrahman B. Fadhil. 2019. "Biodiesel Production through Transesterification of a Mixture of Non-Edible Oils over Lithium Supported on Activated Carbon Derived from Scrap Tires." *Energy Conversion and Management* 201 (October): 112149. https://doi.org/10.1016/j.enconman.2019.112149.

Azad, A. K., M. G. Rasul, M. M.K. Khan, Subhash C. Sharma, M. Mofijur, and M. M.K. Bhuiya. 2016. "Prospects, Feedstocks and Challenges of Biodiesel Production from Beauty Leaf Oil and Castor Oil: A Nonedible Oil Sources in Australia." *Renewable and Sustainable Energy Reviews* 61: 302–18. https://doi.org/10.1016/j.rser.2016.04.013.

Babinszki, Bence, Emma Jakab, Viktor Terjék, Zoltán Sebestyén, Gábor Várhegyi, Zoltán May, Aparat Mahakhant, et al. 2021. "Thermal Decomposition of Biomass Wastes Derived from Palm Oil Production." *Journal of Analytical and Applied Pyrolysis* 155

(February): 105069. https://doi.org/10.1016/j.jaap.2021.105069.

Banković-Ilić, Ivana B., Ivan J. Stojković, Olivera S. Stamenković, Vlada B. Veljkovic, and Yung-Tse Hung. 2014. "Waste Animal Fats as Feedstocks for Biodiesel Production." *Renewable and Sustainable Energy Reviews* 32 (April): 238–54. https://doi.org/10.1016/j.rser.2014.01.038.

Bargole, Swapnil Sukhadeo, Prakash Kumar Singh, Suja George, and Virendra Kumar Saharan. 2021. "Valorisation of Low Fatty Acid Content Waste Cooking Oil into Biodiesel through Transesterification Using a Basic Heterogeneous Calcium-Based Catalyst." *Biomass and Bioenergy* 146 (February): 105984. https://doi.org/10.1016/j.biombioe.2021.105984.

Bashir, Mohammed J.K., Lai Peng Wong, Dickens St Hilaire, Jihyun Kim, Oluwaseun Salako, Mith Jennifer Jean, Remi Adeyemi, Serena James, Tia Foster, and Lawrence M. Pratt. 2020. "Biodiesel Fuel Production from Brown Grease Produced by Wastewater Treatment Plant: Optimization of Acid Catalyzed Reaction Conditions." *Journal of Environmental Chemical Engineering* 8 (4): 103848. https://doi.org/10.1016/j.jece.2020.103848.

Bashiri, H., and N. Pourbeiram. 2017. "Kinetic Monte Carlo Study of Biodiesel Production through Transesterification of Brassica Carinata Oil." *Physical Chemistry Research* 5 (2): 329–38. https://doi.org/10.22036/PCR.2016.57445.1279.

Baskar, G., I. Aberna Ebenezer Selvakumari, and R. Aiswarya. 2018. "Biodiesel Production from Castor Oil Using Heterogeneous Ni Doped ZnO Nanocatalyst." *Bioresource Technology* 250 (December 2017): 793–98. https://doi.org/10.1016/j.biortech.2017.12.010.

Baskar, G, S Soumiya, and R Aiswarya. 2016. "Biodiesel Production from Pongamia Oil Using Magnetic Composite of Zinc Oxide Nanocatalyst." *International Journal of Modern Science and Technology* 1 (4): 129–37.

Bhatia, Shashi Kant, Ranjit Gurav, Tae-Rim Choi, Hyun Joong Kim, Soo-Yeon Yang, Hun-Suk Song, Jun Young Park, et al. 2020. "Conversion of Waste Cooking Oil into Biodiesel Using Heterogenous Catalyst Derived from Cork Biochar." *Bioresource Technology* 302 (January): 122872. https://doi.org/10.1016/j.biortech.2020.122872.

Boey, Peng-Lim, Gaanty Pragas Maniam, and Shafida Abd Hamid. 2011. "Performance of Calcium Oxide as a Heterogeneous Catalyst in Biodiesel Production: A Review." *Chemical Engineering Journal* 168 (1): 15–22. https://doi.org/10.1016/j.cej.2011.01.009.

Bohlouli, Ali, and Leila Mahdavian. 2019. "Catalysts Used in Biodiesel Production: A Review." *Biofuels* 0 (0): 1–14. https://doi.org/10.1080/17597269.2018.1558836.

Booramurthy, Vijaya Kumar, Ramesh Kasimani, Deepalakshmi Subramanian, and Sivakumar Pandian. 2020. “Production of Biodiesel from Tannery Waste Using a Stable and Recyclable Nano-Catalyst: An Optimization and Kinetic Study.” *Fuel* 260 (July 2019): 116373. https://doi.org/10.1016/j.fuel.2019.116373.

Brucato, A., A. Busciglio, F. Di Stefano, F. Grisafi, G. Micale, and F. Scargiali. 2010. “High Temperature Solid-Catalized Transesterification for Biodiesel Production.” *Chemical Engineering Transactions* 19: 31–36. https://doi.org/10.3303/CET1019006.

Cardoso, Raquel K.P., Gabriel V.A. Silva, Bruno T.S. Alves, Vitória A. Freire, José J.N. Alves, and Bianca V.S. Barbosa. 2022. “Evaluation of the Effect of Si/Mo and Oil/Alcohol Ratios in the Production of Biodiesel from Soybean Oil.” *Arabian Journal of Chemistry* 15 (9): 104074. https://doi.org/10.1016/j.arabjc.2022.104074.

Çetinkaya, Merve, and Filiz Karaosmanoğlu. 2004. “Optimization of Base-Catalyzed Transesterification Reaction of Used Cooking Oil.” *Energy & Fuels* 18 (6): 1888–95. https://doi.org/10.1021/ef049891c.

Chakraborty, R., and H. Sahu. 2014. “Intensification of Biodiesel Production from Waste Goat Tallow Using Infrared Radiation: Process Evaluation through Response Surface Methodology and Artificial Neural Network.” *Applied Energy* 114 (February): 827–36. https://doi.org/10.1016/j.apenergy.2013.04.025.

Chang, Mun Yuen, Eng-seng Chan, and Cher Pin Song. 2021. “Biodiesel Production Catalysed by Low-Cost Liquid Enzyme Eversa® Transform 2.0: Effect of Free Fatty Acid Content on Lipase Methanol Tolerance and Kinetic Model.” *Fuel* 283 (October 2020): 119266. https://doi.org/10.1016/j.fuel.2020.119266.

Changmai, Bishwajit, Ruma Rano, Chhangte Vanlalveni, and Lalthazuala Rokhum. 2021. “A Novel Citrus Sinensis Peel Ash Coated Magnetic Nanoparticles as an Easily Recoverable Solid Catalyst for Biodiesel Production.” *Fuel* 286 (P2): 119447. https://doi.org/10.1016/j.fuel.2020.119447.

Chellamuthu, Muthulakshmi, Kokiladevi Eswaran, and Selvi Subramanian. 2022. “Genetic Engineering for Oil Modification.” In *Genetically Modified Plants and Beyond*. IntechOpen. https://doi.org/10.5772/intechopen.101823.

Chen, Guanyi, Rui Shan, Jiafu Shi, and Beibei Yan. 2014. “Ultrasonic-Assisted Production of Biodiesel from Transesterification of Palm Oil over Ostrich Eggshell-Derived CaO Catalysts.” *Bioresource Technology* 171 (November): 428–32. https://doi.org/10.1016/j.biortech.2014.08.102.

Chen, Wei-Hsin, Guo-Lun Chiu, Hwai Chyuan Ong, Su Shiung Lam, Steven Lim, Yong Sik

Ok, and Eilhann E.Kwon. 2021. “Optimization and Analysis of Syngas Production from Methane and CO2 via Taguchi Approach, Response Surface Methodology (RSM) and Analysis of Variance (ANOVA).” *Fuel* 296 (February): 120642. https://doi.org/10.1016/j.fuel.2021.120642.

Chen, Yun-An, Pao-Wen Grace Liu, Liang-Ming Whang, Yi-Ju Wu, and Sheng-Shung Cheng. 2019. “Biodegradability and Microbial Community Investigation for Soil Contaminated with Diesel Blending with Biodiesel.” *Process Safety and Environmental Protection* 130 (October): 115–25. https://doi.org/10.1016/j.psep.2019.07.001.

Chen, Yurong, Xue-Rong Zhou, Zhi-Jun Zhang, Paul Dribnenki, Surinder Singh, and Allan Green. 2015. “Development of High Oleic Oil Crop Platform in Flax through RNAi-Mediated Multiple FAD2 Gene Silencing.” *Plant Cell Reports* 34 (4): 643–53. https://doi.org/10.1007/s00299-015-1737-5.

Cheng, Feng, and Xiuwei Li. 2018. “Preparation and Application of Biochar-Based Catalysts for Biofuel Production.” *Catalysts* 8 (9): 346. https://doi.org/10.3390/catal8090346.

Chi, Nguyen Thúy Lan, Susaimanickam Anto, Tharifkhan Shan Ahamed, Smita S. Kumar, Sabarathinam Shanmugam, Melvin S. Samuel, Thangavel Mathimani, Kathirvel Brindhadevi, and Arivalagan Pugazhendhi. 2021. “A Review on Biochar Production Techniques and Biochar Based Catalyst for Biofuel Production from Algae.” *Fuel* 287 (November 2020): 119411. https://doi.org/10.1016/j.fuel.2020.119411.

Chisholm, Hugh. 2018. “Entry for ‘Petroleum.’” In *1911 Encyclopedia Britanica*, 1–9.

Chopade, Shruti G., K. S. Kulkarni, A. D. Kulkarni, and Niraj S. Topare. 2013. “ChemInform Abstract: Solid Heterogeneous Catalysts for Production of Biodiesel from Trans-Esterification of Triglycerides with Methanol: A Review.” *ChemInform* 44 (47): 8–14. https://doi.org/10.1002/chin.201347225.

Chouhan, A. P Singh, and A. K. Sarma. 2011. “Modern Heterogeneous Catalysts for Biodiesel Production: A Comprehensive Review.” *Renewable and Sustainable Energy Reviews* 15 (9): 4378–99. https://doi.org/10.1016/j.rser.2011.07.112.

Chung, Kyong-Hwan, Jin Kim, and Ki-Young Lee. 2009. “Biodiesel Production by Transesterification of Duck Tallow with Methanol on Alkali Catalysts.” *Biomass and Bioenergy* 33 (1): 155–58. https://doi.org/10.1016/j.biombioe.2008.04.014.

Crabbe, Edward, Cirilo Nolasco-Hipolito, Genta Kobayashi, Kenji Sonomoto, and Ayaaki Ishizaki. 2001. “Biodiesel Production from Crude Palm Oil and Evaluation of Butanol Extraction and Fuel Properties.” *Process Biochemistry* 37 (1): 65–71. https://doi.org/10.1016/S0032-9592(01)00178-9.

Cunha, Michele Espinosa da, Laiza Canielas Krause, Maria Silvana Aranda Moraes, Candice Schmitt Faccini, Rosângela Assis Jacques, Suelen Rodrigues Almeida, Maria Regina Alves Rodrigues, and Elina Bastos Caramão. 2009. "Beef Tallow Biodiesel Produced in a Pilot Scale." *Fuel Processing Technology* 90 (4): 570–75. https://doi.org/10.1016/j.fuproc.2009.01.001.

Dafiqurrohman, Hafif, Kania Amelia Safitri, M. Ismail Bagus Setyawan, Adi Surjosatyo, and Muhammad Aziz. 2022. "Gasification of Rice Wastes toward Green and Sustainable Energy Production: A Review." *Journal of Cleaner Production* 366 (July): 132926. https://doi.org/10.1016/j.jclepro.2022.132926.

Dahdah, Eliane, Jane Estephane, Reem Haydar, Yara Youssef, Bilal El Khoury, Cedric Gennequin, Antoine Aboukaïs, Edmond Abi-Aad, and Samer Aouad. 2020. "Biodiesel Production from Refined Sunflower Oil over Ca–Mg–Al Catalysts: Effect of the Composition and the Thermal Treatment." *Renewable Energy* 146 (February): 1242–48. https://doi.org/10.1016/j.renene.2019.06.171.

Danane, Fetta, Rahma Bessah, Rhiad Alloune, Latifa Tebouche, Farid Madjene, Ahmed Yasser Kheirani, and Reda Bouabibsa. 2022. "Experimental Optimization of Waste Cooking Oil Ethanolysis for Biodiesel Production Using Response Surface Methodology (RSM)." *Science and Technology for Energy Transition* 77 (July): 14. https://doi.org/10.2516/stet/2022014.

Datta, Ambarish, and Bijan Kumar Mandal. 2016. "A Comprehensive Review of Biodiesel as an Alternative Fuel for Compression Ignition Engine." *Renewable and Sustainable Energy Reviews* 57 (May): 799–821. https://doi.org/10.1016/j.rser.2015.12.170.

Dawodu, Folasegun A., Olubunmi Ayodele, Jiayu Xin, Suojiang Zhang, and Dongxia Yan. 2014. "Effective Conversion of Non-Edible Oil with High Free Fatty Acid into Biodiesel by Sulphonated Carbon Catalyst." *Applied Energy* 114 (February): 819–26. https://doi.org/10.1016/j.apenergy.2013.10.004.

Dayang, Nuradila, Wan Ab Karim Ghani Wan Azlina, and Alias Azil Bahari. 2017. "PALM KERNEL SHELL-DERIVED BIOCHAR AND CATALYST FOR BIODIESEL PRODUCTION." *Malaysian Journal of Analytical Science* 21 (1): 197–203. https://doi.org/10.17576/mjas-2017-2101-23.

De, Arghyadeep, and Siddhartha Sankar Boxi. 2020. "Application of Cu Impregnated TiO2 as a Heterogeneous Nanocatalyst for the Production of Biodiesel from Palm Oil." *Fuel* 265 (October 2019): 117019. https://doi.org/10.1016/j.fuel.2020.117019.

Dehghani, Sahar, and Mohammad Haghighi. 2019. "Sono-Dispersed MgO over Cerium-Doped

MCM-41 Nanocatalyst for Biodiesel Production from Acidic Sunflower Oil: Surface Evolution by Altering Si/Ce Molar Ratios." *Waste Management* 95 (July): 584–92. https://doi.org/10.1016/j.wasman.2019.05.042.

Dehkhoda, Amir Mehdi, and Naoko Ellis. 2013. "Biochar-Based Catalyst for Simultaneous Reactions of Esterification and Transesterification." *Catalysis Today* 207 (May): 86–92. https://doi.org/10.1016/j.cattod.2012.05.034.

Dehkhoda, Amir Mehdi, Alex H. West, and Naoko Ellis. 2010. "Biochar Based Solid Acid Catalyst for Biodiesel Production." *Applied Catalysis A: General* 382 (2): 197–204. https://doi.org/10.1016/j.apcata.2010.04.051.

Department of Standards Malaysia. 2014. *MS 2008:2014 Automotive Fuels - Palm Methyl Esters (PME) for Diesel Engines - Requirements and Test Methods*. Department of Standards Malaysia.

Deshmane, Vishwanath Ganpat, and Yusuf Gbadebo Adewuyi. 2013. "Synthesis and Kinetics of Biodiesel Formation via Calcium Methoxide Base Catalyzed Transesterification Reaction in the Absence and Presence of Ultrasound." *Fuel* 107 (May): 474–82. https://doi.org/10.1016/j.fuel.2012.12.080.

Dey, S., N.M. Reang, P.K. Das, and M. Deb. 2021. "A Comprehensive Study on Prospects of Economy, Environment, and Efficiency of Palm Oil Biodiesel as a Renewable Fuel." *Journal of Cleaner Production* 286 (March): 124981. https://doi.org/10.1016/j.jclepro.2020.124981.

Dhawane, Sumit H., Akash Pratim Bora, Tarkeshwar Kumar, and Gopinath Halder. 2017. "Parametric Optimization of Biodiesel Synthesis from Rubber Seed Oil Using Iron Doped Carbon Catalyst by Taguchi Approach." *Renewable Energy* 105 (May): 616–24. https://doi.org/10.1016/j.renene.2016.12.096.

Dhawane, Sumit H., Tarkeshwar Kumar, and Gopinath Halder. 2018. "Recent Advancement and Prospective of Heterogeneous Carbonaceous Catalysts in Chemical and Enzymatic Transformation of Biodiesel." *Energy Conversion and Management* 167 (April): 176–202. https://doi.org/10.1016/j.enconman.2018.04.073.

Dong, Jun, Lingfang Shen, Shengdao Shan, Wanpeng Liu, Zhifu Qi, Chunhong Liu, and Xiang Gao. 2022. "Optimizing Magnetic Functionalization Conditions for Efficient Preparation of Magnetic Biochar and Adsorption of Pb(II) from Aqueous Solution." *Science of The Total Environment* 806 (xxxx): 151442. https://doi.org/10.1016/j.scitotenv.2021.151442.

Dong, Tao, Difeng Gao, Chao Miao, Xiaochen Yu, Charles Degan, Manuel Garcia-Pérez, Barbara Rasco, Shyam S. Sablani, and Shulin Chen. 2015. "Two-Step Microalgal

Biodiesel Production Using Acidic Catalyst Generated from Pyrolysis-Derived Bio-Char." *Energy Conversion and Management* 105 (November): 1389–96. https://doi.org/10.1016/j.enconman.2015.06.072.

Duangdee, Bheechanat, Dussadee Rattanaphra, Sasikarn Nuchdang, Anusith Thanapimmetha, Maythee Saisriyoot, and Penjit Srinophakun. 2022. "Bifunctional Mixed Rare Earth Solid Catalyst for Biodiesel Production from Acid Palm Oil." *Journal of Rare Earths*, no. xxxx (February). https://doi.org/10.1016/j.jre.2022.02.007.

Dutta, Kasturi, Achlesh Daverey, and Jih-Gaw Lin. 2014. "Evolution Retrospective for Alternative Fuels: First to Fourth Generation." *Renewable Energy* 69 (September): 114–22. https://doi.org/10.1016/j.renene.2014.02.044.

Eevera, T., K. Rajendran, and S. Saradha. 2009. "Biodiesel Production Process Optimization and Characterization to Assess the Suitability of the Product for Varied Environmental Conditions." *Renewable Energy* 34 (3): 762–65. https://doi.org/10.1016/j.renene.2008.04.006.

Eltaweil, A.S., H. Ali Mohamed, Eman M. Abd El-Monaem, and G.M. El-Subruiti. 2020. "Mesoporous Magnetic Biochar Composite for Enhanced Adsorption of Malachite Green Dye: Characterization, Adsorption Kinetics, Thermodynamics and Isotherms." *Advanced Powder Technology* 31 (3): 1253–63. https://doi.org/10.1016/j.apt.2020.01.005.

Encinar, J M, J F González, A Pardal, and G Martínez. 2010. "Transesterification of Rapeseed Oil with Methanol in the Presence of Various Co-Solvents." *Proceedings Venice 2010 Third International Symposium on Energy from Biomass and Waste Venice Italy*, no. November 2010.

Endut, Azizah, Sharifah Hanis Yasmin Sayid Abdullah, Nur Hanis Mohamad Hanapi, Siti Hajar Abdul Hamid, Fathurrahman Lananan, Mohd Khairul Amri Kamarudin, Roslan Umar, Hafizan Juahir, and Helena Khatoon. 2017. "Optimization of Biodiesel Production by Solid Acid Catalyst Derived from Coconut Shell via Response Surface Methodology." *International Biodeterioration & Biodegradation* 124 (October): 250–57. https://doi.org/10.1016/j.ibiod.2017.06.008.

Esan, Akintomiwa O., Ojeyemi M. Olabemiwo, Siwaporn M. Smith, and Shangeetha Ganesan. 2021. "A Concise Review on Alternative Route of Biodiesel Production via Interesterification of Different Feedstocks." *International Journal of Energy Research* 45 (9): 12614–37. https://doi.org/10.1002/er.6680.

Esan, Akintomiwa O., Olusegun A. Olalere, Chee-Yuen Gan, Siwaporn M. Smith, and Shangeetha Ganesan. 2021. "Synthesis of Biodiesel from Waste Palm Fatty Acid

Distillate (PFAD) and Dimethyl Carbonate (DMC) via Taguchi Optimisation Method." *Biomass and Bioenergy* 154 (April): 106262. https://doi.org/10.1016/j.biombioe.2021.106262.

Estevez, Rafael, Laura Aguado-Deblas, Felipa M. Bautista, Diego Luna, Carlos Luna, Juan Calero, Alejandro Posadillo, and Antonio A. Romero. 2019. "Biodiesel at the Crossroads: A Critical Review." *Catalysts* 9 (12). https://doi.org/10.3390/catal9121033.

European Committee for Standardization. 2010. *BS EN 14214:2008+A1:2009 Automotive Fuels — Fatty Acid Methyl Esters (FAME) for Diesel Engines — Requirements and Test Methods*. *British Standard Institution*. 2009th ed. London: British Standard Institution.

Fadhil, Abdelrahman B., and Latif H. Ali. 2013. "Alkaline-Catalyzed Transesterification of Silurus Triostegus Heckel Fish Oil: Optimization of Transesterification Parameters." *Renewable Energy* 60 (December): 481–88. https://doi.org/10.1016/j.renene.2013.04.018.

Farabi, M.S. Ahmad, M. Lokman Ibrahim, Umer Rashid, and Yun Hin Taufiq-Yap. 2019. "Esterification of Palm Fatty Acid Distillate Using Sulfonated Carbon-Based Catalyst Derived from Palm Kernel Shell and Bamboo." *Energy Conversion and Management* 181 (September 2018): 562–70. https://doi.org/10.1016/j.enconman.2018.12.033.

Farooq, Muhammad, Anita Ramli, and Duvvuri Subbarao. 2013. "Biodiesel Production from Waste Cooking Oil Using Bifunctional Heterogeneous Solid Catalysts." *Journal of Cleaner Production* 59 (November): 131–40. https://doi.org/10.1016/j.jclepro.2013.06.015.

Fassinou, Wanignon Ferdinand, Aboubakar Sako, Alhassane Fofana, Kamenan Blaise Koua, and Siaka Toure. 2010. "Fatty Acids Composition as a Means to Estimate the High Heating Value (HHV) of Vegetable Oils and Biodiesel Fuels." *Energy* 35 (12): 4949–54. https://doi.org/10.1016/j.energy.2010.08.030.

Fassinou, Wanignon Ferdinand, Laurent Van De Steene, Siaka Toure, and Eric Martin. 2011. "What Correlation Is Appropriate to Evaluate Biodiesels and Vegetable Oils Higher Heating Value (HHV)?" *Fuel* 90 (11): 3398–3403. https://doi.org/10.1016/j.fuel.2011.04.025.

Fayyazi, E., B. Ghobadian, G. Najafi, B. Hosseinzadeh, R. Mamat, and J. Hosseinzadeh. 2015. "An Ultrasound-Assisted System for the Optimization of Biodiesel Production from Chicken Fat Oil Using a Genetic Algorithm and Response Surface Methodology." *Ultrasonics Sonochemistry* 26: 312–20. https://doi.org/10.1016/j.ultsonch.2015.03.007.

Felizardo, Pedro, M. Joana Neiva Correia, Idalina Raposo, João F. Mendes, Rui Berkemeier,

and João Moura Bordado. 2006. “Production of Biodiesel from Waste Frying Oils.” *Waste Management* 26 (5): 487–94. https://doi.org/10.1016/j.wasman.2005.02.025.

Ferreira, P, I Fonseca, A Ramos, J Vital, and J Castanheiro. 2009. “Esterification of Glycerol with Acetic Acid over Dodecamolybdophosphoric Acid Encaged in USY Zeolite.” *Catalysis Communications* 10 (5): 481–84. https://doi.org/10.1016/j.catcom.2008.10.015.

Ferrero, Gabriel O., Edgar M. Sánchez Faba, Adriana A. Rickert, and Griselda A. Eimer. 2020. “Alternatives to Rethink Tomorrow: Biodiesel Production from Residual and Non-Edible Oils Using Biocatalyst Technology.” *Renewable Energy* 150 (May): 128–35. https://doi.org/10.1016/j.renene.2019.12.114.

Feyzi, Mostafa, Nahid Hosseini, Nakisa Yaghobi, and Rohollah Ezzati. 2017. “Preparation, Characterization, Kinetic and Thermodynamic Studies of MgO-La2O3 Nanocatalysts for Biodiesel Production from Sunflower Oil.” *Chemical Physics Letters* 677 (June): 19–29. https://doi.org/10.1016/j.cplett.2017.03.014.

Feyzi, Mostafa, and Zahra Shahbazi. 2017. “Preparation, Kinetic and Thermodynamic Studies of Al–Sr Nanocatalysts for Biodiesel Production.” *Journal of the Taiwan Institute of Chemical Engineers* 71: 145–55. https://doi.org/10.1016/j.jtice.2016.11.023.

Firth, Ben. 2014. “Biodiesel Production in Fixed-Bed Monolithic Reactors.” University of Bath.

Gaide, Ieva, Violeta Makareviciene, Egle Sendzikiene, and Milda Gumbyte. 2022. “Application of Dolomite as Solid Base Catalyst for Transesterification of Rapeseed Oil with Butanol.” *Sustainable Energy Technologies and Assessments* 52 (PC): 102278. https://doi.org/10.1016/j.seta.2022.102278.

Gandhi, B. Sanjay, S. Sam Chelladurai, and D. Senthil Kumaran. 2011. “Process Optimization for Biodiesel Synthesis From Jatropha Curcas Oil.” *Distributed Generation & Alternative Energy Journal* 26 (4): 6–16. https://doi.org/10.1080/21563306.2011.10462201.

Ganesan, Ramya, S. Manigandan, Sabarathinam Shanmugam, V.P. Chandramohan, Raveendran Sindhu, Sang-hyoun Kim, Kathirvel Brindhadevi, and Arivalagan Pugazhendhi. 2021. “A Detailed Scrutinize on Panorama of Catalysts in Biodiesel Synthesis.” *Science of The Total Environment* 777 (July): 145683. https://doi.org/10.1016/j.scitotenv.2021.145683.

Gaurav, Aashish, Stéphane Dumas, Chau T.Q. Mai, and Flora T.T. Ng. 2019. “A Kinetic Model for a Single Step Biodiesel Production from a High Free Fatty Acid (FFA) Biodiesel Feedstock over a Solid Heteropolyacid Catalyst.” *Green Energy and Environment* 4 (3): 328–41. https://doi.org/10.1016/j.gee.2019.03.004.

Gebremariam, S. N., and J. M. Marchetti. 2018. “Economics of Biodiesel Production: Review.” *Energy Conversion and Management* 168 (May): 74–84. https://doi.org/10.1016/j.enconman.2018.05.002.

Gerpen, Jon Van. 2005. “Biodiesel Processing and Production.” *Fuel Processing Technology* 86 (10): 1097–1107. https://doi.org/10.1016/j.fuproc.2004.11.005.

Ghadge, Shashikant Vilas, and Hifjur Raheman. 2005. “Biodiesel Production from Mahua (Madhuca Indica) Oil Having High Free Fatty Acids.” *Biomass and Bioenergy* 28 (6): 601–5. https://doi.org/10.1016/j.biombioe.2004.11.009.

Gholipour Zanjani, Nooshin, Arash Kamran Pirzaman, and Elmira Yazdanian. 2020. “Biodiesel Production in the Presence of Heterogeneous Catalyst of Alumina: Study of Kinetics and Thermodynamics.” *International Journal of Chemical Kinetics* 52 (7): 472–84. https://doi.org/10.1002/kin.21363.

Ghosh, Nabanita, and Gopinath Halder. 2022. “Current Progress and Perspective of Heterogeneous Nanocatalytic Transesterification towards Biodiesel Production from Edible and Inedible Feedstock: A Review.” *Energy Conversion and Management* 270 (July): 116292. https://doi.org/10.1016/j.enconman.2022.116292.

Giraldo, Liliana, and Juan Carlos Moreno-Piraján. 2012. “Lipase Supported on Mesoporous Materials as a Catalyst in the Synthesis of Biodiesel from Persea Americana Mill Oil.” *Journal of Molecular Catalysis B: Enzymatic* 77 (May): 32–38. https://doi.org/10.1016/j.molcatb.2012.01.001.

Givord, D., and T. Takabatake. 2016. “Magnetic Order.” In *Reference Module in Materials Science and Materials Engineering*, 1–10. Elsevier. https://doi.org/10.1016/B978-0-12-803581-8.01109-7.

Goli, Jibril, and Omprakash Sahu. 2018. “Development of Heterogeneous Alkali Catalyst from Waste Chicken Eggshell for Biodiesel Production.” *Renewable Energy* 128 (December): 142–54. https://doi.org/10.1016/j.renene.2018.05.048.

Gondra, Zaloa Ares. 2010. “Study of Factors Influencing the Quality and Yield of Biodiesel Produced by Transesterification of Vegetable Oils.” UNIVERSITY OF GAVLE.

González, M.E., M. Cea, D. Reyes, L. Romero-Hermoso, P. Hidalgo, S. Meier, N. Benito, and R. Navia. 2017. “Functionalization of Biochar Derived from Lignocellulosic Biomass Using Microwave Technology for Catalytic Application in Biodiesel Production.” *Energy Conversion and Management* 137 (April): 165–73. https://doi.org/10.1016/j.enconman.2017.01.063.

Gopal, Sruthi, and C.M Sajitha. 2013. “Production of Biodiesel from Vegetable Oil Using CaO

Catalyst & Analysis of Its Performance in Four Stroke Diesel Engine." *International Journal of Scientific and Research Publications* 3 (11): 1–6.

Gotovuša, Mia, Mihovil Medić, Fabio Faraguna, Matea Šibalić, Lucija Konjević, Jelena Parlov Vuković, and Marko Racar. 2022. "Fatty Acids Propyl Esters: Synthesis Optimization and Application Properties of Their Blends with Diesel and 1-Propanol." *Renewable Energy* 185 (February): 655–64. https://doi.org/10.1016/j.renene.2021.12.088.

Gouran, Ashkan, Babak Aghel, and Farzad Nasirmanesh. 2021. "Biodiesel Production from Waste Cooking Oil Using Wheat Bran Ash as a Sustainable Biomass." *Fuel* 295 (February): 120542. https://doi.org/10.1016/j.fuel.2021.120542.

Guldhe, Abhishek, Bhaskar Singh, Ismail Rawat, and Faizal Bux. 2014. "Synthesis of Biodiesel from Scenedesmus Sp. by Microwave and Ultrasound Assisted in Situ Transesterification Using Tungstated Zirconia as a Solid Acid Catalyst." *Chemical Engineering Research and Design* 92 (8): 1503–11. https://doi.org/10.1016/j.cherd.2014.05.012.

Guldhe, Abhishek, Poonam Singh, Faiz Ahmad Ansari, Bhaskar Singh, and Faizal Bux. 2017. "Biodiesel Synthesis from Microalgal Lipids Using Tungstated Zirconia as a Heterogeneous Acid Catalyst and Its Comparison with Homogeneous Acid and Enzyme Catalysts." *Fuel* 187 (January): 180–88. https://doi.org/10.1016/j.fuel.2016.09.053.

Guldhe, Abhishek, Poonam Singh, Sheena Kumari, Ismail Rawat, Kugen Permaul, and Faizal Bux. 2016. "Biodiesel Synthesis from Microalgae Using Immobilized Aspergillus Niger Whole Cell Lipase Biocatalyst." *Renewable Energy* 85: 1002–10. https://doi.org/10.1016/j.renene.2015.07.059.

Günay, M. Erdem, Lemi Türker, and N. Alper Tapan. 2019. "Significant Parameters and Technological Advancements in Biodiesel Production Systems." *Fuel* 250 (April): 27–41. https://doi.org/10.1016/j.fuel.2019.03.147.

Guo, Feng, Zhen-Gang Peng, Jian-Ying Dai, and Zhi-Long Xiu. 2010. "Calcined Sodium Silicate as Solid Base Catalyst for Biodiesel Production." *Fuel Processing Technology* 91 (3): 322–28. https://doi.org/10.1016/j.fuproc.2009.11.003.

Guo, Feng, Zhi-Long Xiu, and Zhi-Xia Liang. 2012. "Synthesis of Biodiesel from Acidified Soybean Soapstock Using a Lignin-Derived Carbonaceous Catalyst." *Applied Energy* 98 (October): 47–52. https://doi.org/10.1016/j.apenergy.2012.02.071.

Guo, Jingjing, Shangde Sun, and Jingming Liu. 2020. "Conversion of Waste Frying Palm Oil into Biodiesel Using Free Lipase A from Candida Antarctica as a Novel Catalyst." *Fuel* 267 (December 2019): 117323. https://doi.org/10.1016/j.fuel.2020.117323.

Guo, Mengli, Weiqiang Jiang, Chao Chen, Shaokang Qu, Jie Lu, Weiming Yi, and Jincheng Ding. 2021. “Process Optimization of Biodiesel Production from Waste Cooking Oil by Esterification of Free Fatty Acids Using La3+/ZnO-TiO2 Photocatalyst.” *Energy Conversion and Management* 229 (December 2020): 113745. https://doi.org/10.1016/j.enconman.2020.113745.

Guo, Pingmei, Fenghong Huang, Mingming Zheng, Wenlin Li, and Qingde Huang. 2012. “Magnetic Solid Base Catalysts for the Production of Biodiesel.” *Journal of the American Oil Chemists’ Society* 89 (5): 925–33. https://doi.org/10.1007/s11746-011-1979-5.

Gurunathan, Baskar, and Aiswarya Ravi. 2015. “Process Optimization and Kinetics of Biodiesel Production from Neem Oil Using Copper Doped Zinc Oxide Heterogeneous Nanocatalyst.” *Bioresource Technology* 190 (August): 424–28. https://doi.org/10.1016/j.biortech.2015.04.101.

Haagenson, Darrin M., Rachel L. Brudvik, Hongjian Lin, and Dennis P. Wiesenborn. 2010. “Implementing an In Situ Alkaline Transesterification Method for Canola Biodiesel Quality Screening.” *Journal of the American Oil Chemists’ Society* 87 (11): 1351–58. https://doi.org/10.1007/s11746-010-1607-9.

Haas, Michael J., and Karen M. Scott. 1996. “Combined Nonenzymatic-Enzymatic Method for the Synthesis of Simple Alkyl Fatty Acid Esters from Soapstock.” *Journal of the American Oil Chemists’ Society* 73 (11): 1393–1401. https://doi.org/10.1007/BF02523502.

Haas, Michael J., and Karen Wagner. 2011. “Simplifying Biodiesel Production: The Direct or in Situ Transesterification of Algal Biomass.” *European Journal of Lipid Science and Technology* 113 (10): 1219–29. https://doi.org/10.1002/ejlt.201100106.

Hajjari, Masoumeh, Meisam Tabatabaei, Mortaza Aghbashlo, and Hossein Ghanavati. 2017. “A Review on the Prospects of Sustainable Biodiesel Production: A Global Scenario with an Emphasis on Waste-Oil Biodiesel Utilization.” *Renewable and Sustainable Energy Reviews* 72 (November 2016): 445–64. https://doi.org/10.1016/j.rser.2017.01.034.

Han, Ying-Zhi, Li Hong, Xi-Qing Wang, Ju-Zhao Liu, Jiao Jiao, Meng Luo, and Yu-Jie Fu. 2016. “Biodiesel Production from Pistacia Chinensis Seed Oil via Transesterification Using Recyclable Magnetic Cellulose-Based Catalyst.” *Industrial Crops and Products* 89 (October): 332–38. https://doi.org/10.1016/j.indcrop.2016.05.015.

Hanif, Muhammad Asif, Shafaq Nisar, Muhammad Nadeem Akhtar, Numra Nisar, and Nosheen Rashid. 2018. “Optimized Production and Advanced Assessment of Biodiesel: A Review.” *International Journal of Energy Research*, no. October 2017: 1–14.

https://doi.org/10.1002/er.3990.

Hariprasath, P., S.T. Selvamani, M. Vigneshwar, K. Palanikumar, and D. Jayaperumal. 2019. "Comparative Analysis of Cashew and Canola Oil Biodiesel with Homogeneous Catalyst by Transesterification Method." *Materials Today: Proceedings* 16: 1357–62. https://doi.org/10.1016/j.matpr.2019.05.236.

Hasan, M.M., and M.M. Rahman. 2017. "Performance and Emission Characteristics of Biodiesel–Diesel Blend and Environmental and Economic Impacts of Biodiesel Production: A Review." *Renewable and Sustainable Energy Reviews* 74 (February): 938–48. https://doi.org/10.1016/j.rser.2017.03.045.

Hashmi, Sidra, Sumbal Gohar, Tariq Mahmood, Umar Nawaz, and Hadayatullah Farooqi. 2016. "Biodiesel Production by Using CaO-Al2O3 Nano Catalyst." *International Journal of Engineering Research & Science* 2 (3): 2395–6992.

Hazmi, Balkis, Umer Rashid, Mohd Lokman Ibrahim, Imededdine Arbi Nehdi, Mohammad Azam, and Saud Ibrahim Al-Resayes. 2021. "Synthesis and Characterization of Bifunctional Magnetic Nano-Catalyst from Rice Husk for Production of Biodiesel." *Environmental Technology & Innovation* 21 (February): 101296. https://doi.org/10.1016/j.eti.2020.101296.

Hazrat, M. A., Mohammad G. Rasul, Mohammad M. K. Khan, Nanjappa Ashwath, Arridina S. Silitonga, I. M. R. Fattah, and T. M. Indra Mahlia. 2022. "Kinetic Modelling of Esterification and Transesterification Processes for Biodiesel Production Utilising Waste-Based Resource." *Catalysts* 12 (11): 1472. https://doi.org/10.3390/catal12111472.

Helmi, Maryam, Mahdi Ghadiri, Kambiz Tahvildari, and Alireza Hemmati. 2021. "Biodiesel Synthesis Using Clinoptilolite-Fe3O4-Based Phosphomolybdic Acid as a Novel Magnetic Green Catalyst from Salvia Mirzayanii Oil via Electrolysis Method: Optimization Study by Taguchi Method." *Journal of Environmental Chemical Engineering* 9 (5): 105988. https://doi.org/10.1016/j.jece.2021.105988.

Hredzak, Tammy L., and Quynh Le. 2012. "Challenges to Achieving Food Security in APEC." Singapore.

Hu, Lei, Xing Tang, Zhen Wu, Lu Lin, Jiaxing Xu, Ning Xu, and Benlin Dai. 2015. "Magnetic Lignin-Derived Carbonaceous Catalyst for the Dehydration of Fructose into 5-Hydroxymethylfurfural in Dimethylsulfoxide." *Chemical Engineering Journal* 263 (March): 299–308. https://doi.org/10.1016/j.cej.2014.11.044.

Hughes, Michael. 2017. "GC-MS Characterization of Sulfur Species in Low Temperature Distillates of Biodiesel from Waste Grease." Delaware State University.

Hums, Megan E., Richard A. Cairncross, and Sabrina Spatari. 2016. “Life-Cycle Assessment of Biodiesel Produced from Grease Trap Waste.” *Environmental Science & Technology* 50 (5): 2718–26. https://doi.org/10.1021/acs.est.5b02667.

International Energy Agency. 2017. “Key World Energy Statistics 2017.” International Energy Agency.

Ismail, S., S. A. Abu, R. Rezaur, and H. Sinin. 2014. “Biodiesel Production from Castor Oil and Its Application in Diesel Engine.” *Journal on Science and Technology for Development* 31 (2): 91–101.

Iwuozor, Kingsley O., Ebuka Chizitere Emenike, Ebenezer O. Omonayin, Joy O. Bamigbola, Happiness T. Ojo, Adeolu A. Awoyale, Omodele A.A. Eletta, and Adewale George Adeniyi. 2023. “Unlocking the Hidden Value of Pods: A Review of Thermochemical Conversion Processes for Biochar Production.” *Bioresource Technology Reports* 22 (March): 101488. https://doi.org/10.1016/j.biteb.2023.101488.

Jacobson, K, R Gopinath, L Meher, and A Dalai. 2008. “Solid Acid Catalyzed Biodiesel Production from Waste Cooking Oil.” *Applied Catalysis B: Environmental* 85 (1–2): 86–91. https://doi.org/10.1016/j.apcatb.2008.07.005.

Jafari, Naser. 2010. “Review of Polution Sources and Controls in Caspian Sea Region.” *Journal of Ecology and the Natural Environment* 2 (2): 25–29.

Jaroszewska, Karolina, Janusz Nowicki, Hanna Nosal-Kovalenko, Jolanta Grzechowiak, Katarzyna Pstrowska, Rafał Łużny, Marek Lewandowski, et al. 2022. “Selected Acid and Basic Functionalized Ordered Mesoporous Materials as Solid Catalysts for Transesterification of Canola Oil: A Comparative Study.” *Fuel* 325 (June): 124902. https://doi.org/10.1016/j.fuel.2022.124902.

Jayakumar, Saravanan, Mashitah M. Yusoff, Mohd Hasbi Ab Rahim, Gaanty Pragas Maniam, and Natanamurugaraj Govindan. 2017. “The Prospect of Microalgal Biodiesel Using Agro-Industrial and Industrial Wastes in Malaysia.” *Renewable and Sustainable Energy Reviews* 72 (January): 33–47. https://doi.org/10.1016/j.rser.2017.01.002.

Jegannathan, Kenthorai Raman, Leong Jun-Yee, Eng-Seng Chan, and Pogaku Ravindra. 2010. “Production of Biodiesel from Palm Oil Using Liquid Core Lipase Encapsulated in κ-Carrageenan.” *Fuel* 89 (9): 2272–77. https://doi.org/10.1016/j.fuel.2010.03.016.

Jenie, S.N. Aisyiyah, Anis Kristiani, Sudiyarmanto, Deni S. Khaerudini, and Kaoru Takeishi. 2020. “Sulfonated Magnetic Nanobiochar as Heterogeneous Acid Catalyst for Esterification Reaction.” *Journal of Environmental Chemical Engineering* 8 (4): 103912. https://doi.org/10.1016/j.jece.2020.103912.

Jeong, Gwi-Taek, Hee-Seung Yang, and Don-Hee Park. 2009. “Optimization of Transesterification of Animal Fat Ester Using Response Surface Methodology.” *Bioresource Technology* 100 (1): 25–30. https://doi.org/10.1016/j.biortech.2008.05.011.

Jiang, Qimeng, Guihua Yang, Fangong Kong, Pedram Fatehi, and Xiaoying Wang. 2020. “High Acid Biochar-Based Solid Acid Catalyst from Corn Stalk for Lignin Hydrothermal Degradation.” *Polymers* 12 (7): 1623. https://doi.org/10.3390/polym12071623.

Jung, Jong-Min, Jeong-Ik Oh, Kitae Baek, Jechan Lee, and Eilhann E. Kwon. 2018. “Biodiesel Production from Waste Cooking Oil Using Biochar Derived from Chicken Manure as a Porous Media and Catalyst.” *Energy Conversion and Management* 165 (February): 628–33. https://doi.org/10.1016/j.enconman.2018.03.096.

Kabbashi, Nassereldeen Ahmed, Nurudeen Ishola Mohammed, Md Zahangir Alam, and Mohamed Elwathig Saeed Mirghani. 2015. “Hydrolysis of Jatropha Curcas Oil for Biodiesel Synthesis Using Immobilized Candida Cylindracea Lipase.” *Journal of Molecular Catalysis B: Enzymatic* 116 (June): 95–100. https://doi.org/10.1016/j.molcatb.2015.03.009.

Karmakar, Bisheswar, and Gopinath Halder. 2019. “Progress and Future of Biodiesel Synthesis: Advancements in Oil Extraction and Conversion Technologies.” *Energy Conversion and Management* 182 (December 2018): 307–39. https://doi.org/10.1016/j.enconman.2018.12.066.

Kastner, James R., Joby Miller, Daniel P. Geller, Jason Locklin, Lawrence H. Keith, and Tyson Johnson. 2012. “Catalytic Esterification of Fatty Acids Using Solid Acid Catalysts Generated from Biochar and Activated Carbon.” *Catalysis Today* 190 (1): 122–32. https://doi.org/10.1016/j.cattod.2012.02.006.

Kaur, Mandeep, and Amjad Ali. 2011. “Lithium Ion Impregnated Calcium Oxide as Nano Catalyst for the Biodiesel Production from Karanja and Jatropha Oils.” *Renewable Energy* 36 (11): 2866–71. https://doi.org/10.1016/j.renene.2011.04.014.

Kavindi, Gajasinghe Arachchige Ganga, and Zhongfang Lei. 2019. “Development of Activated Hydrochar from Paddy Straw for Nutrient Adsorption and Crop Water Management.” In *WIT Transactions on Ecology and the Environment*, 229:67–77. https://doi.org/10.2495/WRM190071.

Kazemifard, Sina, Hamed Nayebzadeh, Naser Saghatoleslami, and Ebrahim Safakish. 2019. “Application of Magnetic Alumina-Ferric Oxide Nanocatalyst Supported by KOH for in-Situ Transesterification of Microalgae Cultivated in Wastewater Medium.” *Biomass and Bioenergy* 129 (October 2018): 105338. https://doi.org/10.1016/j.biombioe.2019.105338.

Khan, H.R. 2003. “Ferromagnetism.” In *Encyclopedia of Physical Science and Technology*, 759–68. Elsevier. https://doi.org/10.1016/B0-12-227410-5/00240-4.

Khan, Haris Mahmood, Chaudhry Haider Ali, Tanveer Iqbal, Saima Yasin, Muhammad Sulaiman, Hamayoun Mahmood, Muhammad Raashid, Mohsin Pasha, and Bozhong Mu. 2019. “Current Scenario and Potential of Biodiesel Production from Waste Cooking Oil in Pakistan: An Overview.” *Chinese Journal of Chemical Engineering* 27 (10): 2238–50. https://doi.org/10.1016/j.cjche.2018.12.010.

Khatibi, Maryam, Farhad Khorasheh, and Afsanehsadat Larimi. 2021. “Biodiesel Production via Transesterification of Canola Oil in the Presence of Na–K Doped CaO Derived from Calcined Eggshell.” *Renewable Energy* 163 (January): 1626–36. https://doi.org/10.1016/j.renene.2020.10.039.

Kim, Dong Shik;, Mohammadmatin; Hanifzadeh, and Ashok Kumar. 2018. “Trend of Biodiesel Feedstock and Its Impact on Biodiesel Emission Characteristics.” *Environmental Progress and Sustainable Energy* 37 (1): 7–19. https://doi.org/10.1002/ep.12800.

Kim, Keon Hee, Ok Kyung Lee, Chul Ho Kim, Jeong-Woo Seo, Baek-Rock Oh, and Eun Yeol Lee. 2016. “Lipase-Catalyzed in-Situ Biosynthesis of Glycerol-Free Biodiesel from Heterotrophic Microalgae, Aurantiochytrium Sp. KRS101 Biomass.” *Bioresource Technology* 211 (July): 472–77. https://doi.org/10.1016/j.biortech.2016.03.092.

Kirubakaran, M, and V. Arul Mozhi Selvan. 2018. “A Comprehensive Review of Low Cost Biodiesel Production from Waste Chicken Fat.” *Renewable and Sustainable Energy Reviews* 82 (July 2017): 390–401. https://doi.org/10.1016/j.rser.2017.09.039.

Knothe, Gerhard, Jürgen Krahl, and Jon Van Gerpen. 2010. *The Biodiesel Handbook*. Edited by Gerhard Knothe, Jürgen Krahl, and Jon Van Gerpen. 2nd Editio. Urbana, Illinois: AOCS Press.

Koberg, Miri, and Aharon Gedanken. 2013. “Using Microwave Radiation and SrO as a Catalyst for the Complete Conversion of Oils, Cooked Oils, and Microalgae to Biodiesel.” In *New and Future Developments in Catalysis*, 209–27. Elsevier. https://doi.org/10.1016/B978-0-444-53878-9.00010-2.

Kolobeng, Rebaone, Clever Ketlogetswe, Mbako Jonas, and Dimpho Mautle. 2022. “Effects of Moisture Content on Biodiesel (B100) Properties during Storage: A Comparative Analysis between Biodiesel Produced from Used Cooking Oil and Beef Tallow.” *Sustainable Energy Technologies and Assessments* 54 (July): 102844. https://doi.org/10.1016/j.seta.2022.102844.

Korkut, Ibrahim, and Mahmut Bayramoglu. 2018. “Selection of Catalyst and Reaction Conditions for Ultrasound Assisted Biodiesel Production from Canola Oil.” *Renewable Energy* 116 (February): 543–51. https://doi.org/10.1016/j.renene.2017.10.010.

Kostić, Milan D., Alireza Bazargan, Olivera S. Stamenković, Vlada B. Veljković, and Gordon McKay. 2016. “Optimization and Kinetics of Sunflower Oil Methanolysis Catalyzed by Calcium Oxide-Based Catalyst Derived from Palm Kernel Shell Biochar.” *Fuel* 163 (January): 304–13. https://doi.org/10.1016/j.fuel.2015.09.042.

Krishnan, Shamala Gowri, Fei-ling Pua, and Fan Zhang. 2021. “A Review of Magnetic Solid Catalyst Development for Sustainable Biodiesel Production.” *Biomass and Bioenergy* 149 (December 2020): 106099. https://doi.org/10.1016/j.biombioe.2021.106099.

Krstić, Jugoslav B., Zvonko B. Nježić, Milan D. Kostić, Boško D. Marić, Olivera D. Šimurina, Olivera S. Stamenković, and Vlada B. Veljković. 2022. “Biodiesel Production from Rapeseed Oil over Calcined Waste Filter Cake from Sugar Beet Processing.” *Process Safety and Environmental Protection* 168 (July): 463–73. https://doi.org/10.1016/j.psep.2022.10.021.

Kulkarni, Mangesh G., Rajesh Gopinath, Lekha Charan Meher, and Ajay Kumar Dalai. 2006. “Solid Acid Catalyzed Biodiesel Production by Simultaneous Esterification and Transesterification.” *Green Chemistry* 8 (12): 1056. https://doi.org/10.1039/b605713f.

Kulkarni, Sneha S. 2022. “Optimization of Fatty Acid Profile and Synthesis of Biodiesel from Mixing Salvodara Persica and Leucas Aspera Seed Oils: Critical Analysis of Fuel Properties.” *Materials Today: Proceedings* 49: 665–75. https://doi.org/10.1016/j.matpr.2021.05.166.

Kusdiana, D., and S. Saka. 2001. “Kinetics of Transesterification in Rapeseed Oil to Biodiesel Fuel as Treated in Supercritical Methanol.” *Fuel* 80 (5): 693–98. https://doi.org/10.1016/S0016-2361(00)00140-X.

Laksmono, Nino, Maria Paraschiv, Khaled Loubar, and Mohand Tazerout. 2013. “Biodiesel Production from Biomass Gasification Tar via Thermal/Catalytic Cracking.” *Fuel Processing Technology* 106 (February): 776–83. https://doi.org/10.1016/j.fuproc.2012.10.016.

Lawal, Abubakar Abdullahi, Mohd Ali Hassan, Mohd Rafein Zakaria, Mohd Zulkhairi Mohd Yusoff, Mohd Nor Faiz Norrrahim, Mohd Noriznan Mokhtar, and Yoshihito Shirai. 2021. “Effect of Oil Palm Biomass Cellulosic Content on Nanopore Structure and Adsorption Capacity of Biochar.” *Bioresource Technology* 332 (March): 125070. https://doi.org/10.1016/j.biortech.2021.125070.

Lee, Duckhee. 2013. “Preparation of a Sulfonated Carbonaceous Material from Lignosulfonate and Its Usefulness as an Esterification Catalyst.” *Molecules* 18 (7): 8168–80. https://doi.org/10.3390/molecules18078168.

Lee, Jechan, Ajit K. Sarmah, and Eilhann E. Kwon. 2019. “Production and Formation of Biochar.” In *Biochar from Biomass and Waste*, 3–18. Elsevier. https://doi.org/10.1016/B978-0-12-811729-3.00001-7.

Lee, Roland Arthur, and Jean-Michel Lavoie. 2013. “From First- to Third-Generation Biofuels: Challenges of Producing a Commodity from a Biomass of Increasing Complexity.” *Animal Frontiers* 3 (2): 6–11. https://doi.org/10.2527/af.2013-0010.

Leung, Dennis Y.C., Xuan Wu, and M.K.H. Leung. 2010. “A Review on Biodiesel Production Using Catalyzed Transesterification.” *Applied Energy* 87 (4): 1083–95. https://doi.org/10.1016/j.apenergy.2009.10.006.

Li, Hui, Junchi Wang, Xiaoling Ma, Yangyang Wang, Guoning Li, Min Guo, Ping Cui, Wanpeng Lu, Shoujun Zhou, and Mingzhi Yu. 2021. “Carbonized MIL−100(Fe) Used as Support for Recyclable Solid Acid Synthesis for Biodiesel Production.” *Renewable Energy* 179 (December): 1191–1203. https://doi.org/10.1016/j.renene.2021.07.122.

Li, Penglin, Xiaoling Miao, Rongxiu Li, and Jianjiang Zhong. 2011. “In Situ Biodiesel Production from Fast-Growing and High Oil Content Chlorella Pyrenoidosa in Rice Straw Hydrolysate.” *Journal of Biomedicine and Biotechnology* 2011: 1–8. https://doi.org/10.1155/2011/141207.

Li, Xiufeng, Han Xu, and Qingyu Wu. 2007. “Large-Scale Biodiesel Production from MicroalgaChlorella Protothecoides through Heterotrophic Cultivation in Bioreactors.” *Biotechnology and Bioengineering* 98 (4): 764–71. https://doi.org/10.1002/bit.21489.

Li, Yan, Xiao-Dong Zhang, Li Sun, Jie Zhang, and Hai-Peng Xu. 2010. “Fatty Acid Methyl Ester Synthesis Catalyzed by Solid Superacid Catalyst /ZrO2–TiO2/La3+.” *Applied Energy* 87 (1): 156–59. https://doi.org/10.1016/j.apenergy.2009.06.030.

Li, Yunchao, Bo Xing, Yan Ding, Xinhong Han, and Shurong Wang. 2020. “A Critical Review of the Production and Advanced Utilization of Biochar via Selective Pyrolysis of Lignocellulosic Biomass.” *Bioresource Technology* 312 (May): 123614. https://doi.org/10.1016/j.biortech.2020.123614.

Liang, Yanna, Nicolas Sarkany, and Yi Cui. 2009. “Biomass and Lipid Productivities of Chlorella Vulgaris under Autotrophic, Heterotrophic and Mixotrophic Growth Conditions.” *Biotechnology Letters* 31 (7): 1043–49. https://doi.org/10.1007/s10529-009-9975-7.

Liew, Rock Keey, Wai Lun Nam, Min Yee Chong, Xue Yee Phang, Man Huan Su, Peter Nai Yuh Yek, Nyuk Ling Ma, Chin Kui Cheng, Cheng Tung Chong, and Su Shiung Lam. 2018. “Oil Palm Waste: An Abundant and Promising Feedstock for Microwave Pyrolysis Conversion into Good Quality Biochar with Potential Multi-Applications.” *Process Safety and Environmental Protection* 115 (April): 57–69. https://doi.org/10.1016/j.psep.2017.10.005.

Likozar, Blaž, and Janez Levec. 2014. “Transesterification of Canola, Palm, Peanut, Soybean and Sunflower Oil with Methanol, Ethanol, Isopropanol, Butanol and Tert-Butanol to Biodiesel: Modelling of Chemical Equilibrium, Reaction Kinetics and Mass Transfer Based on Fatty Acid Composition.” *Applied Energy* 123 (June): 108–20. https://doi.org/10.1016/j.apenergy.2014.02.046.

Lim, Steven, Chin Yi Yap, Yean Ling Pang, and Kam Huei Wong. 2020. “Biodiesel Synthesis from Oil Palm Empty Fruit Bunch Biochar Derived Heterogeneous Solid Catalyst Using 4-Benzenediazonium Sulfonate.” *Journal of Hazardous Materials* 390 (October 2019): 121532. https://doi.org/10.1016/j.jhazmat.2019.121532.

Lima, Ana Carolina, Khadidja Hachemane, António E. Ribeiro, Ana Queiroz, Maria Carolina Sérgi Gomes, and Paulo Brito. 2022. “Evaluation and Kinetic Study of Alkaline Ionic Liquid for Biodiesel Production through Transesterification of Sunflower Oil.” *Fuel* 324 (January): 124586. https://doi.org/10.1016/j.fuel.2022.124586.

Liu, Bo, and Zongbao (Kent) Zhao. 2007. “Biodiesel Production by Direct Methanolysis of Oleaginous Microbial Biomass.” *Journal of Chemical Technology & Biotechnology* 82 (8): 775–80. https://doi.org/10.1002/jctb.1744.

Liu, Junheng, Xuchao Zhang, Cheng Tang, Lejian Wang, Ping Sun, and Pan Wang. 2023. “Effects of Palm Oil Biodiesel Addition on Exhaust Emissions and Particle Physicochemical Characteristics of a Common-Rail Diesel Engine.” *Fuel Processing Technology* 241 (December 2022): 107606. https://doi.org/10.1016/j.fuproc.2022.107606.

Liu, Kang, Rui Wang, and Meiqing Yu. 2018. “An Efficient, Recoverable Solid Base Catalyst of Magnetic Bamboo Charcoal: Preparation, Characterization, and Performance in Biodiesel Production.” *Renewable Energy* 127 (November): 531–38. https://doi.org/10.1016/j.renene.2018.04.092.

Liu, Wu Jun, Ke Tian, Hong Jiang, and Han Qing Yu. 2013. “Facile Synthesis of Highly Efficient and Recyclable Magnetic Solid Acid from Biomass Waste.” *Scientific Reports* 3 (1): 2419. https://doi.org/10.1038/srep02419.

Ljupkovic, Radomir, Radoslav Micic, Milan Tomic, Niko Radulovic, Aleksandar Bojic, and Aleksandra Zarubica. 2014. “Significance of the Structural Properties of CaO Catalyst in the Production of Biodiesel: An Effect on the Reduction of Greenhouse Gases Emission.” *Hemijska Industrija* 68 (4): 399–412. https://doi.org/10.2298/HEMIND130612063L.

Lokman, Ibrahim M., Umer Rashid, Robiah Yunus, and Yun Hin Taufiq-Yap. 2014. “Carbohydrate-Derived Solid Acid Catalysts for Biodiesel Production from Low-Cost Feedstocks: A Review.” *Catalysis Reviews - Science and Engineering* 56 (2): 187–219. https://doi.org/10.1080/01614940.2014.891842.

Luna, Mark Daniel G. de, Jodel L. Cuasay, Nolan C. Tolosa, and Tsair Wang Chung. 2017. “Transesterification of Soybean Oil Using a Novel Heterogeneous Base Catalyst: Synthesis and Characterization of Na-Pumice Catalyst, Optimization of Transesterification Conditions, Studies on Reaction Kinetics and Catalyst Reusability.” *Fuel* 209 (July): 246–53. https://doi.org/10.1016/j.fuel.2017.07.086.

Luz Corrêa, Ana Paula da, Rafael Roberto Cardoso Bastos, Geraldo Narciso da Rocha Filho, José Roberto Zamian, and Leyvison Rafael Vieira da Conceição. 2020. “Preparation of Sulfonated Carbon-Based Catalysts from Murumuru Kernel Shell and Their Performance in the Esterification Reaction.” *RSC Advances* 10 (34): 20245–56. https://doi.org/10.1039/D0RA03217D.

Luz Martínez, Sandra, Rubi Romero, José Carlos López, Amaya Romero, Víctor Sánchez Mendieta, and Reyna Natividad. 2011. “Preparation and Characterization of CaO Nanoparticles/NaX Zeolite Catalysts for the Transesterification of Sunflower Oil.” *Industrial & Engineering Chemistry Research* 50 (5): 2665–70. https://doi.org/10.1021/ie1006867.

Ma, Guixia, Wenrong Hu, Haiyan Pei, Liqun Jiang, Mingming Song, and Ruimin Mu. 2015. “In Situ Heterogeneous Transesterification of Microalgae Using Combined Ultrasound and Microwave Irradiation.” *Energy Conversion and Management* 90 (January): 41–46. https://doi.org/10.1016/j.enconman.2014.10.061.

Madhuvilakku, Rajesh, and Shakkthivel Piraman. 2013. “Biodiesel Synthesis by TiO2–ZnO Mixed Oxide Nanocatalyst Catalyzed Palm Oil Transesterification Process.” *Bioresource Technology* 150 (December): 55–59. https://doi.org/10.1016/j.biortech.2013.09.087.

Magner, Edmond. 2013. “Immobilisation of Enzymes on Mesoporous Silicate Materials.” *Chemical Society Reviews* 42 (15): 6213. https://doi.org/10.1039/c2cs35450k.

Mahayuddin, Nurul Eza Maisara Mohd, Sharifah Nur Afiqah Syed Mustaffa, Hafiza Shukor, Jennifer Patero Tamayo, and Farizul Hafiz Kasim. 2022. “Biodiesel Production in

Malaysia: Current Status and Challenges." In *AIP Conference Proceedings*, 2541:020005. https://doi.org/10.1063/5.0113176.

Mahdi, Hilman Ibnu, Nurfadhila Nasya Ramlee, José Leandro da Silva Duarte, Yu-Shen Cheng, Rangabhashiyam Selvasembian, Faisal Amir, Leonardo Hadlich de Oliveira, Nur Izyan Wan Azelee, Lucas Meili, and Gayathri Rangasamy. 2023. "A Comprehensive Review on Nanocatalysts and Nanobiocatalysts for Biodiesel Production in Indonesia, Malaysia, Brazil and USA." *Chemosphere* 319 (January): 138003. https://doi.org/10.1016/j.chemosphere.2023.138003.

Mahloujifar, Maliheh, and Mohammadreza Mansournia. 2021. "A Comparative Study on the Catalytic Performances of Alkali Metals-Loaded KAlSiO4 for Biodiesel Production from Sesame Oil." *Fuel* 291 (March 2020): 120145. https://doi.org/10.1016/j.fuel.2021.120145.

Mahmudul, H.M., F.Y. Hagos, R. Mamat, A. Abdul Adam, W.F.W. Ishak, and R. Alenezi. 2017. "Production, Characterization and Performance of Biodiesel as an Alternative Fuel in Diesel Engines – A Review." *Renewable and Sustainable Energy Reviews* 72 (November 2016): 497–509. https://doi.org/10.1016/j.rser.2017.01.001.

Malaysian Biodiesel Association. 2018. "Malaysian Biodiesel Association - Timeline." Malaysian Biodiesel Association. 2018. http://www.mybiodiesel.org.my/index.php/biodiesel-industry/biodiesel-factsheet.

———. 2023. "About Malaysian Biodiesel." Malaysian Biodiesel Association. 2023. http://www.mybiodiesel.org.my/index.php/biodiesel-industry/about-biodiesel 2/2.

Maleki, Fatemeh, Rezvan Torkaman, Meisam Torab-Mostaedi, and Mehdi Asadollahzadeh. 2022. "Optimization of Grafted Fibrous Polymer Preparation Procedure as a New Solid Basic Catalyst for Biodiesel Fuel Production from Palm Oil." *Fuel* 329 (July): 125015. https://doi.org/10.1016/j.fuel.2022.125015.

Maneerung, Thawatchai, Sibudjing Kawi, Yanjun Dai, and Chi Hwa Wang. 2016. "Sustainable Biodiesel Production via Transesterification of Waste Cooking Oil by Using CaO Catalysts Prepared from Chicken Manure." *Energy Conversion and Management* 123: 487–97. https://doi.org/10.1016/j.enconman.2016.06.071.

Mani, Yuvarani, Thiruselvi Devaraj, Kubendran Devaraj, Salma Aathika AbdurRawoof, and Sivanesan Subramanian. 2020. "Experimental Investigation of Biodiesel Production from Madhuca Longifolia Seed through in Situ Transesterification and Its Kinetics and Thermodynamic Studies." *Environmental Science and Pollution Research* 27 (29): 36450–62. https://doi.org/10.1007/s11356-020-09626-y.

Mansir, Nasar, Siow Hwa Teo, Umer Rashid, Mohd Izham Saiman, Yen Ping Tan, G. Abdulkareem Alsultan, and Yun Hin Taufiq-Yap. 2018. “Modified Waste Egg Shell Derived Bifunctional Catalyst for Biodiesel Production from High FFA Waste Cooking Oil. A Review.” *Renewable and Sustainable Energy Reviews* 82 (November 2017): 3645–55. https://doi.org/10.1016/j.rser.2017.10.098.

Mardhiah, H. Haziratul, Hwai Chyuan Ong, H. H. Masjuki, Steven Lim, and H. V. Lee. 2017. “A Review on Latest Developments and Future Prospects of Heterogeneous Catalyst in Biodiesel Production from Non-Edible Oils.” *Renewable and Sustainable Energy Reviews* 67: 1225–36. https://doi.org/10.1016/j.rser.2016.09.036.

Marinković, Miloš, Hadi Waisi, Stevan Blagojević, Aleksandra Zarubica, Radomir Ljupković, Aleksandra Krstić, and Bojan Janković. 2022. “The Effect of Process Parameters and Catalyst Support Preparation Methods on the Catalytic Efficiency in Transesterification of Sunflower Oil over Heterogeneous KI/Al2O3-Based Catalysts for Biodiesel Production.” *Fuel* 315 (November 2021): 123246. https://doi.org/10.1016/j.fuel.2022.123246.

Marjadi, Darshan, and Nishith Dharaiya. 2010. “Analysis of Edible Oil Contaminated Soil Within North Gujarat Region.” *Life Sciences Leaflets* 10: 287–91.

Martinez-Guerra, Edith, Veera Gnaneswar Gude, Andro Mondala, William Holmes, and Rafael Hernandez. 2014. “Extractive-Transesterification of Algal Lipids under Microwave Irradiation with Hexane as Solvent.” *Bioresource Technology* 156 (March): 240–47. https://doi.org/10.1016/j.biortech.2014.01.026.

Mat Yasin, Mohd Hafizil, Rizalman Mamat, G. Najafi, Obed Majeed Ali, Ahmad Fitri Yusop, and Mohd Hafiz Ali. 2017. “Potentials of Palm Oil as New Feedstock Oil for a Global Alternative Fuel: A Review.” *Renewable and Sustainable Energy Reviews* 79 (May): 1034–49. https://doi.org/10.1016/j.rser.2017.05.186.

Mata, Teresa M., Nelson Cardoso, Mariana Ornelas, Soraia Neves, and Nídia S. Caetano. 2011. “Evaluation of Two Purification Methods of Biodiesel from Beef Tallow, Pork Lard, and Chicken Fat.” *Energy & Fuels* 25 (10): 4756–62. https://doi.org/10.1021/ef2010207.

Mateo, Wendy, Hanwu Lei, Elmar Villota, Moriko Qian, Yunfeng Zhao, Erguang Huo, Qingfa Zhang, Xiaona Lin, Chenxi Wang, and Zhiyang Huang. 2020. “Synthesis and Characterization of Sulfonated Activated Carbon as a Catalyst for Bio-Jet Fuel Production from Biomass and Waste Plastics.” *Bioresource Technology* 297: 122411. https://doi.org/10.1016/j.biortech.2019.122411.

Math, M.C., Sudheer Prem Kumar, and Soma V. Chetty. 2010. “Technologies for Biodiesel

Production from Used Cooking Oil — A Review." *Energy for Sustainable Development* 14 (4): 339–45. https://doi.org/10.1016/j.esd.2010.08.001.

Mathew, Gincy Marina, Diksha Raina, Vivek Narisetty, Vinod Kumar, Saurabh Saran, Arivalagan Pugazhendi, Raveendran Sindhu, Ashok Pandey, and Parameswaran Binod. 2021. "Recent Advances in Biodiesel Production: Challenges and Solutions." *Science of The Total Environment* 794 (November): 148751. https://doi.org/10.1016/j.scitotenv.2021.148751.

Mazaheri, Hoora, Hwai Chyuan Ong, H H Masjuki, Zeynab Amini, Mark D Harrison, Chin-TsanWang, Fitranto Kusumo, and Azham Alwi. 2018. "Rice Bran Oil Based Biodiesel Production Using Calcium Oxide Catalyst Derived from Chicoreus Brunneus Shell." *Energy* 144: 10–19. https://doi.org/https://doi.org/10.1016/j.energy.2017.11.073.

Meher, L. C., D. Vidya Sagar, and S. N. Naik. 2006. "Technical Aspects of Biodiesel Production by Transesterification - A Review." *Renewable and Sustainable Energy Reviews* 10 (3): 248–68. https://doi.org/10.1016/j.rser.2004.09.002.

Mercy Nisha Pauline, J., Ramachandran Sivaramakrishnan, Arivalagan Pugazhendhi, T. Anbarasan, and Anant Achary. 2021. "Transesterification Kinetics of Waste Cooking Oil and Its Diesel Engine Performance." *Fuel* 285 (April 2020): 119108. https://doi.org/10.1016/j.fuel.2020.119108.

Mguni, LL, Reinout Meijboom, and Kalala Jalama. 2012. "Biodiesel Production over Nano-MgO Supported on Titania." *Proceedings of World Academy of …* 5592367 (4): 1155–59.

Mia, Mozammel. 2018. "Mathematical Modeling and Optimization of MQL Assisted End Milling Characteristics Based on RSM and Taguchi Method." *Measurement* 121 (December 2017): 249–60. https://doi.org/10.1016/j.measurement.2018.02.017.

Miao, Xiaoling, Rongxiu Li, and Hongyan Yao. 2009. "Effective Acid-Catalyzed Transesterification for Biodiesel Production." *Energy Conversion and Management* 50 (10): 2680–84. https://doi.org/10.1016/j.enconman.2009.06.021.

Mohadesi, Majid, Ashkan Gouran, and Amir Dehghan Dehnavi. 2021. "Biodiesel Production Using Low Cost Material as High Effective Catalyst in a Microreactor." *Energy* 219 (March): 119671. https://doi.org/10.1016/j.energy.2020.119671.

Mohibbe Azam, M, A Waris, and N Nahar. 2005. "Prospects and Potential of Fatty Acid Methyl Esters of Some Non-Traditional Seed Oils for Use as Biodiesel in India." *Biomass and Bioenergy* 29 (4): 293–302. https://doi.org/10.1016/j.biombioe.2005.05.001.

Mohiddin, M. N., A. A. Saleh, A. N. R. Reddy, and S. Hamdan. 2018. "A Study on Chicken

Fat as an Alternative Feedstock: Biodiesel Production, Fuel Characterisation, and Diesel Engine Performance Analysis." *International Journal of Automotive and Mechanical Engineering* 15 (3): 5535–46. https://doi.org/10.15282/ijame.15.3.2018.10.0425.

Mohiddin, Mohd Nurfirdaus, A.A. Saleh, Amarnadh N.R. Reddy, and Sinin Hamdan. 2020. "Turritella Terebra Shell Synthesized Calcium Oxide Catalyst for Biodiesel Production from Chicken Fat." *Materials Science Forum* 997 (June): 93–101. https://doi.org/10.4028/www.scientific.net/MSF.997.93.

Molaei Dehkordi, Asghar, and Mohammad Ghasemi. 2012. "Transesterification of Waste Cooking Oil to Biodiesel Using Ca and Zr Mixed Oxides as Heterogeneous Base Catalysts." *Fuel Processing Technology* 97 (May): 45–51. https://doi.org/10.1016/j.fuproc.2012.01.010.

Montefrio, Marvin Joseph, Tai Xinwen, and Jeffrey Philip Obbard. 2010. "Recovery and Pre-Treatment of Fats, Oil and Grease from Grease Interceptors for Biodiesel Production." *Applied Energy* 87 (10): 3155–61. https://doi.org/10.1016/j.apenergy.2010.04.011.

Mubarak, N.M., A. Kundu, J.N. Sahu, E.C. Abdullah, and N.S. Jayakumar. 2014. "Synthesis of Palm Oil Empty Fruit Bunch Magnetic Pyrolytic Char Impregnating with FeCl3 by Microwave Heating Technique." *Biomass and Bioenergy* 61 (February): 265–75. https://doi.org/10.1016/j.biombioe.2013.12.021.

Muhammed Niyas, M., and A. Shaija. 2022a. "Performance Evaluation of Diesel Engine Using Biodiesels from Waste Coconut, Sunflower, and Palm Cooking Oils, and Their Hybrids." *Sustainable Energy Technologies and Assessments* 53 (PC): 102681. https://doi.org/10.1016/j.seta.2022.102681.

———. 2022b. "Effect of Repeated Heating of Coconut, Sunflower, and Palm Oils on Their Fatty Acid Profiles, Biodiesel Properties and Performance, Combustion, and Emission, Characteristics of a Diesel Engine Fueled with Their Biodiesel Blends." *Fuel* 328 (July): 125242. https://doi.org/10.1016/j.fuel.2022.125242.

Mujtaba, M.A., H.H. Masjuki, M.A. Kalam, Hwai Chyuan Ong, M. Gul, M. Farooq, Manzoore Elahi M. Soudagar, Waqar Ahmed, M.H. Harith, and M.N.A.M. Yusoff. 2020. "Ultrasound-Assisted Process Optimization and Tribological Characteristics of Biodiesel from Palm-Sesame Oil via Response Surface Methodology and Extreme Learning Machine - Cuckoo Search." *Renewable Energy* 158 (October): 202–14. https://doi.org/10.1016/j.renene.2020.05.158.

Mujtaba, M.A., Haeng Muk Cho, H.H. Masjuki, M.A. Kalam, M. Farooq, Manzoore Elahi M. Soudagar, M. Gul, et al. 2021. "Effect of Alcoholic and Nano-Particles Additives on

Tribological Properties of Diesel–Palm–Sesame–Biodiesel Blends." *Energy Reports* 7 (November): 1162–71. https://doi.org/10.1016/j.egyr.2020.12.009.

Murguía-Ortiz, D., I. Cordova, M.E. Manriquez, E. Ortiz-Islas, R. Cabrera-Sierra, J.L. Contreras, B. Alcántar-Vázquez, M. Trejo-Rubio, J.T. Vázquez-Rodríguez, and L.V. Castro. 2021. "Na-CaO/MgO Dolomites Used as Heterogeneous Catalysts in Canola Oil Transesterification for Biodiesel Production." *Materials Letters* 291 (May): 129587. https://doi.org/10.1016/j.matlet.2021.129587.

Musil, Martin, Frantisek Skopal, Martin Hájek, and Ales Vavra. 2018. "Butanolysis: Comparison of Potassium Hydroxide and Potassium Tert-Butoxide as Catalyst for Biodiesel Preparing from Rapeseed Oil." *Journal of Environmental Management* 218 (July): 555–61. https://doi.org/10.1016/j.jenvman.2018.04.100.

Nahas, Lea, Eliane Dahdah, Samer Aouad, Bilal El Khoury, Cedric Gennequin, Edmond Abi Aad, and Jane Estephane. 2023. "Highly Efficient Scallop Seashell-Derived Catalyst for Biodiesel Production from Sunflower and Waste Cooking Oils: Reaction Kinetics and Effect of Calcination Temperature Studies." *Renewable Energy* 202 (December 2022): 1086–95. https://doi.org/10.1016/j.renene.2022.12.020.

Nambiappan, Balu. 2018. "Malaysia: 100 Years of Resilient Palm Oil Economic Performance." *Journal of Oil Palm Research* 30 (1): 13–25. https://doi.org/10.21894/jopr.2018.0014.

Naranjo, Juan Camilo, Andrés Córdoba, Liliana Giraldo, Vanessa S. García, and Juan Carlos Moreno-Piraján. 2010. "Lipase Supported on Granular Activated Carbon and Activated Carbon Cloth as a Catalyst in the Synthesis of Biodiesel Fuel." *Journal of Molecular Catalysis B: Enzymatic* 66 (1–2): 166–71. https://doi.org/10.1016/j.molcatb.2010.05.002.

Nautiyal, Piyushi, K.A. Subramanian, and M.G. Dastidar. 2014. "Kinetic and Thermodynamic Studies on Biodiesel Production from Spirulina Platensis Algae Biomass Using Single Stage Extraction–Transesterification Process." *Fuel* 135 (July): 228–34. https://doi.org/10.1016/j.fuel.2014.06.063.

Naylor, Rosamond L., and Matthew M. Higgins. 2017. "The Political Economy of Biodiesel in an Era of Low Oil Prices." *Renewable and Sustainable Energy Reviews* 77 (April): 695–705. https://doi.org/10.1016/j.rser.2017.04.026.

Neeharika, T. S.V.R., Vidhi H. Bhimjiyani, Bhushan R. Dole, K. N. Prasanna Rani, V. Y. Karadbhajne, and R. B.N. Prasad. 2017. "Esterification of Free Fatty Acids Present in Jatropha Oil: A Kinetic Study." *Indian Journal of Chemical Technology* 24 (2): 213–17.

Ngige, Godswill Adizue, Prosper Eguono Ovuoraye, Chinenye Adaobi Igwegbe, Endrit Fetahi, Jones A. Okeke, Alfred D. Yakubu, and Pius Chukwukelue Onyechi. 2023. "RSM

Optimization and Yield Prediction for Biodiesel Produced from Alkali-Catalytic Transesterification of Pawpaw Seed Extract: Thermodynamics, Kinetics, and Multiple Linear Regression Analysis." *Digital Chemical Engineering* 6 (October 2022): 100066. https://doi.org/10.1016/j.dche.2022.100066.

Niju, S., K.M. Meera Sheriffa Begum, and N. Anantharaman. 2016. "Enhancement of Biodiesel Synthesis over Highly Active CaO Derived from Natural White Bivalve Clam Shell." *Arabian Journal of Chemistry* 9 (5): 633–39. https://doi.org/10.1016/j.arabjc.2014.06.006.

Nježić, Zvonko B., Milan D. Kostić, Boško D. Marić, Olivera S. Stamenković, Olivera D. Šimurina, Jugoslav Krstić, and Vlada B. Veljković. 2023. "Kinetics and Optimization of Biodiesel Production from Rapeseed Oil over Calcined Waste Filter Cake from Sugar Beet Processing Plant." *Fuel* 334 (July 2022): 126581. https://doi.org/10.1016/j.fuel.2022.126581.

No, Soo-Young. 2011. "Inedible Vegetable Oils and Their Derivatives for Alternative Diesel Fuels in CI Engines: A Review." *Renewable and Sustainable Energy Reviews* 15 (1): 131–49. https://doi.org/10.1016/j.rser.2010.08.012.

Odetoye, T.E., J.O. Agu, and E.O. Ajala. 2021. "Biodiesel Production from Poultry Wastes: Waste Chicken Fat and Eggshell." *Journal of Environmental Chemical Engineering* 9 (4): 105654. https://doi.org/10.1016/j.jece.2021.105654.

Odiaka, Timothy, Stephen A. Akinlabi, Nkosinathi Madushele, Olawale S. Fatoba, Surnir Hassan, and Esther T. Akinlabi. 2021. "Statistical Analysis of the Effect of Welding Parameters on the Tensile Strength of Titanium Reinforced Mild Steel Joints Using Taguchi's DoE." *Materials Today: Proceedings* 44: 1202–6. https://doi.org/10.1016/j.matpr.2020.11.240.

Ohra-aho, Taina, Christian Lindfors, Juha Lehtonen, Tarja Tamminen, and Virpi Siipola. 2020. "Activated Carbons from Fast Pyrolysis Biochar as Novel Catalysts for the Post-Treatment of Pyrolysis Vapors, Studied by Analytical Pyrolysis." *C* 6 (4): 65. https://doi.org/10.3390/c6040065.

Okolie, Jude A., Emmanuel I. Epelle, Sonil Nanda, Daniele Castello, Ajay K. Dalai, and Janusz A. Kozinski. 2021. "Modeling and Process Optimization of Hydrothermal Gasification for Hydrogen Production: A Comprehensive Review." *The Journal of Supercritical Fluids* 173 (January): 105199. https://doi.org/10.1016/j.supflu.2021.105199.

Okoye, C. C., C. F. Okey-Onyesolu, I. C. Nwokedi, O. C. Eije, and E. I. Asimobi. 2020. "Biodiesel Synthesis from Waste Cooking Oil Using Periwinkle Shells as Catalyst."

Journal of Energy Research and Reviews 4 (4): 32–43. https://doi.org/10.9734/jenrr/2020/v4i430135.

Oliveira, A. C., and M. F. Rosa. 2006. “Enzymatic Transesterification of Sunflower Oil in an Aqueous-Oil Biphasic System.” *Journal of the American Oil Chemists’ Society* 83 (1): 21–25. https://doi.org/10.1007/s11746-006-1170-6.

Oliveira, J. P., P. W. P. Antunes, T. Z. Mordente, A. R. Santos, L. M. Pinotti, and S. T. A. Cassini. 2017. “Biodiesel Production from Scum of Grease Traps and Sludge from Septic Tanks.” *Clean Technologies and Environmental Policy* 19 (4): 1231–37. https://doi.org/10.1007/s10098-016-1308-7.

Olkiewicz, Magdalena, Natalia V. Plechkova, Martyn J. Earle, Azael Fabregat, Frank Stüber, Agustí Fortuny, Josep Font, and Christophe Bengoa. 2016. “Biodiesel Production from Sewage Sludge Lipids Catalysed by Brønsted Acidic Ionic Liquids.” *Applied Catalysis B: Environmental* 181 (February): 738–46. https://doi.org/10.1016/j.apcatb.2015.08.039.

Opara, Karol R., and Pin Pin Oh. 2022. “Regularization and Concave Loss Functions for Estimation of Chemical Kinetic Models.” *Applied Soft Computing* 116 (February): 108286. https://doi.org/10.1016/j.asoc.2021.108286.

Ophardt, Charles. 2003. “What Are Mixtures and Solutions ?” In *Virtual Chembook*, 1–3. Elmhurst, Illinois: Elmhurst College.

Panchal, Balaji, Tao Chang, Shenjun Qin, Yuzhuang Sun, Jinxi Wang, and Kai Bian. 2020. “Optimization and Kinetics of Tung Nut Oil Transesterification with Methanol Using Novel Solid Acidic Ionic Liquid Polymer as Catalyst for Methyl Ester Synthesis.” *Renewable Energy* 151: 796–804. https://doi.org/10.1016/j.renene.2019.11.066.

Patience, G.S., and A. Bérard. 2018. “Experimental Planning.” In *Experimental Methods and Instrumentation for Chemical Engineers*, 65–106. Elsevier. https://doi.org/10.1016/B978-0-44-463782-6.00003-3.

Patil, Prafulla D., and Shuguang Deng. 2009. “Optimization of Biodiesel Production from Edible and Non-Edible Vegetable Oils.” *Fuel* 88 (7): 1302–6. https://doi.org/10.1016/j.fuel.2009.01.016.

Patil, Prafulla D, Veera Gnaneswar Gude, Harvind K. Reddy, Tapaswy Muppaneni, and Shuguang Deng. 2012. “Biodiesel Production from Waste Cooking Oil Using Sulfuric Acid and Microwave Irradiation Processes.” *Journal of Environmental Protection* 03 (01): 107–13. https://doi.org/10.4236/jep.2012.31013.

Pauline, A. Leena, and Kurian Joseph. 2020. “Hydrothermal Carbonization of Organic Wastes to Carbonaceous Solid Fuel – A Review of Mechanisms and Process Parameters.” *Fuel*

279 (July): 118472. https://doi.org/10.1016/j.fuel.2020.118472.

Pollardo, Aldricho Alpha, Hong-shik Lee, Dohoon Lee, Sangyong Kim, and Jaehoon Kim. 2018. “Solvent Effect on the Enzymatic Production of Biodiesel from Waste Animal Fat.” *Journal of Cleaner Production* 185 (June): 382–88. https://doi.org/10.1016/j.jclepro.2018.02.210.

Ponnusamy, Vinoth Kumar, Senthil Nagappan, Rahul R. Bhosale, Chyi-How Lay, Dinh Duc Nguyen, Arivalagan Pugazhendhi, Soon Woong Chang, and Gopalakrishnan Kumar. 2020. “Review on Sustainable Production of Biochar through Hydrothermal Liquefaction: Physico-Chemical Properties and Applications.” *Bioresource Technology* 310 (March): 123414. https://doi.org/10.1016/j.biortech.2020.123414.

Prasertsan, S., and P. Prasertsan. 1996. “Biomass Residues from Palm Oil Mills in Thailand: An Overview on Quantity and Potential Usage.” *Biomass and Bioenergy* 11 (5): 387–95. https://doi.org/10.1016/S0961-9534(96)00034-7.

Putra, Meilana Dharma, Chairul Irawan, Udiantoro, Yuli Ristianingsih, and Iryanti Fatyasari Nata. 2018. “A Cleaner Process for Biodiesel Production from Waste Cooking Oil Using Waste Materials as a Heterogeneous Catalyst and Its Kinetic Study.” *Journal of Cleaner Production* 195: 1249–58. https://doi.org/10.1016/j.jclepro.2018.06.010.

Qin, Fanzhi, Chen Zhang, Guangming Zeng, Danlian Huang, Xiaofei Tan, and Abing Duan. 2022. “Lignocellulosic Biomass Carbonization for Biochar Production and Characterization of Biochar Reactivity.” *Renewable and Sustainable Energy Reviews* 157 (September 2021): 112056. https://doi.org/10.1016/j.rser.2021.112056.

Qiu, Fengxian, Yihuai Li, Dongya Yang, Xiaohua Li, and Ping Sun. 2011. “Heterogeneous Solid Base Nanocatalyst: Preparation, Characterization and Application in Biodiesel Production.” *Bioresource Technology* 102 (5): 4150–56. https://doi.org/10.1016/j.biortech.2010.12.071.

Qu, Jing, Hui-Zhu Mao, Wen Chen, Shi-Qiang Gao, Ya-Nan Bai, Yan-Wei Sun, Yun-Feng Geng, and Jian Ye. 2012. “Development of Marker-Free Transgenic Jatropha Plants with Increased Levels of Seed Oleic Acid.” *Biotechnology for Biofuels* 5 (1): 10. https://doi.org/10.1186/1754-6834-5-10.

Qu, Tongxin, Shengli Niu, Xiangyu Zhang, Kuihua Han, and Chunmei Lu. 2021. “Preparation of Calcium Modified Zn-Ce/Al2O3 Heterogeneous Catalyst for Biodiesel Production through Transesterification of Palm Oil with Methanol Optimized by Response Surface Methodology.” *Fuel* 284 (August 2020): 118986. https://doi.org/10.1016/j.fuel.2020.118986.

Quah, Ray Vern, Yie Hua Tan, N. M. Mubarak, Jibrail Kansedo, Mohammad Khalid, E. C. Abdullah, and Mohammad Omar Abdullah. 2020. “Magnetic Biochar Derived from Waste Palm Kernel Shell for Biodiesel Production via Sulfonation.” *Waste Management* 118: 626–36. https://doi.org/10.1016/j.wasman.2020.09.016.

Rabiah Nizah, M.F., Y.H. Taufiq-Yap, Umer Rashid, Siow Hwa Teo, Z.A. Shajaratun Nur, and Aminul Islam. 2014. “Production of Biodiesel from Non-Edible Jatropha Curcas Oil via Transesterification Using Bi 2 O 3 –La 2 O 3 Catalyst.” *Energy Conversion and Management* 88 (December): 1257–62. https://doi.org/10.1016/j.enconman.2014.02.072.

Racar, Marko, Ivana Šoljić Jerbić, Zoran Glasovac, and Ante Jukić. 2023. “Guanidine Catalysts for Biodiesel Production: Activity, Process Modelling and Optimization.” *Renewable Energy* 202 (October 2022): 1046–53. https://doi.org/10.1016/j.renene.2022.11.044.

Rad, Ali Shokuhi, Mahtab Hoseini Nia, Fatemeh Ardestani, and Hamed Nayebzadeh. 2018. “Esterification of Waste Chicken Fat: Sulfonated MWCNT Toward Biodiesel Production.” *Waste and Biomass Valorization* 9 (4): 591–99. https://doi.org/10.1007/s12649-016-9732-9.

Rahimi, Tahereh, Danial Kahrizi, Mostafa Feyzi, Hossein Rostami Ahmadvandi, and Mostafa Mostafaei. 2021. “Catalytic Performance of MgO /Fe2O3-SiO2 Core-Shell Magnetic Nanocatalyst for Biodiesel Production of Camelina Sativa Seed Oil: Optimization by RSM-CCD Method.” *Industrial Crops and Products* 159 (October 2020): 113065. https://doi.org/10.1016/j.indcrop.2020.113065.

Rakić, Tijana, Irena Kasagić-Vujanović, Marko Jovanović, Biljana Jančić-Stojanović, and Darko Ivanović. 2014. “Comparison of Full Factorial Design, Central Composite Design, and Box-Behnken Design in Chromatographic Method Development for the Determination of Fluconazole and Its Impurities.” *Analytical Letters* 47 (8): 1334–47. https://doi.org/10.1080/00032719.2013.867503.

Ramadhas, A, S Jayaraj, and C Muraleedharan. 2005. “Biodiesel Production from High FFA Rubber Seed Oil.” *Fuel* 84 (4): 335–40. https://doi.org/10.1016/j.fuel.2004.09.016.

Ramos, María Jesús, Abraham Casas, Lourdes Rodríguez, Rubí Romero, and Ángel Pérez. 2008. “Transesterification of Sunflower Oil over Zeolites Using Different Metal Loading: A Case of Leaching and Agglomeration Studies.” *Applied Catalysis A: General* 346 (1–2): 79–85. https://doi.org/10.1016/j.apcata.2008.05.008.

Rashtizadeh, Elnaz, Faezeh Farzaneh, and Zahra Talebpour. 2014. “Synthesis and Characterization of Sr3Al2O6 Nanocomposite as Catalyst for Biodiesel Production.” *Bioresource Technology* 154 (February): 32–37.

https://doi.org/10.1016/j.biortech.2013.12.014.

Ravuri, Manu, Y. Santhosh Kumar Reddy, and D. Harsha Vardhan. 2021. “Parametric Optimization of Face Turning Parameters for Surface Roughness on EN 31 Material Using RSM and Taguchi Method.” *Materials Today: Proceedings* 37 (Part 2): 769–74. https://doi.org/10.1016/j.matpr.2020.05.816.

Rechnia-Gorący, Paulina, Anna Malaika, and Mieczysław Kozłowski. 2020. “Effective Conversion of Rapeseed Oil to Biodiesel Fuel in the Presence of Basic Activated Carbon Catalysts.” *Catalysis Today* 357 (September 2018): 102–12. https://doi.org/10.1016/j.cattod.2019.05.055.

Reddy, A. N. R., A. A. Saleh, M. S. Islam, S. Hamdan, Md. Rezaur Rahman, and H. H. Masjuki. 2018. “Experimental Evaluation of Fatty Acid Composition Influence on Jatropha Biodiesel Physicochemical Properties.” *Journal of Renewable and Sustainable Energy* 10 (1): 013103. https://doi.org/10.1063/1.5018743.

Reddy, A.N.R., A.S. Ahmed, M.D. Islam, and S. Hamdan. 2017. “Methanolysis of Crude Jatropha Oil Using Heterogeneous Catalyst from the Seashells and Eggshells as Green Biodiesel.” *ASEAN Journal on Science and Technology for Development* 32 (1): 16. https://doi.org/10.29037/ajstd.9.

Reddy, A.N.R., A.A. Saleh, M.S. Islam, and S. Hamdan. 2017a. “Active Razor Shell CaO Catalyst Synthesis for Jatropha Methyl Ester Production via Optimized Two-Step Transesterification.” *Journal of Chemistry* 2017 (1). https://doi.org/10.1155/2017/1489218.

———. 2017b. “Active Heterogeneous CaO Catalyst Synthesis from Anadara Granosa (Kerang) Seashells for Jatropha Biodiesel Production.” Edited by A. Hasan, A.A. Khan, Md. A. Mannan, C.N. Hipolito, N. Mohamed Sutan, Al-K. Hj. Othman, M.R. Kabit, and N. Abdul Wahab. *MATEC Web of Conferences* 87 (02008): 02008. https://doi.org/10.1051/matecconf/20178702008.

Rehan, M., J. Gardy, A. Demirbas, U. Rashid, W. M. Budzianowski, Deepak Pant, and A. S. Nizami. 2018. “Waste to Biodiesel: A Preliminary Assessment for Saudi Arabia.” *Bioresource Technology* 250 (August 2017): 17–25. https://doi.org/10.1016/j.biortech.2017.11.024.

Reusch, William. 2023. “Nomenclature of Alcohols.” Virtual Textbook of Organic Chemistry. 2023. http://chemwiki.ucdavis.edu/Organic_Chemistry/Alcohols/Nomenclature_of_Alcohols.

Rezaei, R., M. Mohadesi, and G.R. Moradi. 2013. “Optimization of Biodiesel Production Using

Waste Mussel Shell Catalyst." *Fuel* 109 (July): 534–41. https://doi.org/10.1016/j.fuel.2013.03.004.

Rezania, Shahabaldin, Muhammad Afzal Kamboh, Sadaf Sadia Arian, Naif Abdullah Al-Dhabi, Mariadhas Valan Arasu, Galal Ali Esmail, and Krishna Kumar Yadav. 2021. "Conversion of Waste Frying Oil into Biodiesel Using Recoverable Nanocatalyst Based on Magnetic Graphene Oxide Supported Ternary Mixed Metal Oxide Nanoparticles." *Bioresource Technology* 323 (December 2020): 124561. https://doi.org/10.1016/j.biortech.2020.124561.

Rocha, Pablo D., Leandro S. Oliveira, and Adriana S. Franca. 2019. "Sulfonated Activated Carbon from Corn Cobs as Heterogeneous Catalysts for Biodiesel Production Using Microwave-Assisted Transesterification." *Renewable Energy* 143: 1710–16. https://doi.org/10.1016/j.renene.2019.05.070.

Rokhum, Samuel Lalthazuala, Bishwajit Changmai, Thomas Kress, and Andrew E.H. Wheatley. 2022. "A One-Pot Route to Tunable Sugar-Derived Sulfonated Carbon Catalysts for Sustainable Production of Biodiesel by Fatty Acid Esterification." *Renewable Energy* 184 (January): 908–19. https://doi.org/10.1016/j.renene.2021.12.001.

Roschat, Wuttichai, Theeranun Siritanon, Boonyawan Yoosuk, Taweesak Sudyoadsuk, and Vinich Promarak. 2017. "Rubber Seed Oil as Potential Non-Edible Feedstock for Biodiesel Production Using Heterogeneous Catalyst in Thailand." *Renewable Energy* 101: 937–44. https://doi.org/10.1016/j.renene.2016.09.057.

Roy, Anupam Singha, Aby Cheruvathoor Poulose, Aristides Bakandritsos, Rajender S. Varma, and Michal Otyepka. 2021. "2D Graphene Derivatives as Heterogeneous Catalysts to Produce Biofuels via Esterification and Trans-Esterification Reactions." *Applied Materials Today* 23 (June): 101053. https://doi.org/10.1016/j.apmt.2021.101053.

Sadhukhan, Jhuma, Elias Martinez-Hernandez, Richard J. Murphy, Denny K.S. Ng, Mimi H. Hassim, Kok Siew Ng, Wan Yoke Kin, Ida Fahani Md Jaye, Melissa Y. Leung Pah Hang, and Viknesh Andiappan. 2018. "Role of Bioenergy, Biorefinery and Bioeconomy in Sustainable Development: Strategic Pathways for Malaysia." *Renewable and Sustainable Energy Reviews* 81 (April 2017): 1966–87. https://doi.org/10.1016/j.rser.2017.06.007.

Safarian, Sahar. 2023. "Performance Analysis of Sustainable Technologies for Biochar Production: A Comprehensive Review." *Energy Reports* 9 (December): 4574–93. https://doi.org/10.1016/j.egyr.2023.03.111.

Sakthivel, R, K Ramesh, R Purnachandran, and P. Mohamed Shameer. 2018. "A Review on the Properties, Performance and Emission Aspects of the Third Generation Biodiesels."

Renewable and Sustainable Energy Reviews 82 (5): 2970–92. https://doi.org/10.1016/j.rser.2017.10.037.

Salam, Kamoru A., Sharon B. Velasquez-Orta, and Adam P. Harvey. 2016. "A Sustainable Integrated in Situ Transesterification of Microalgae for Biodiesel Production and Associated Co-Product-a Review." *Renewable and Sustainable Energy Reviews* 65: 1179–98. https://doi.org/10.1016/j.rser.2016.07.068.

Salam, Satishchandra, Tushar Choudhary, Arivalagan Pugazhendhi, Tikendra Nath Verma, and Abhishek Sharma. 2020. "A Review on Recent Progress in Computational and Empirical Studies of Compression Ignition Internal Combustion Engine." *Fuel* 279 (May): 118469. https://doi.org/10.1016/j.fuel.2020.118469.

Salehi Jouzani, Gholamreza, Reza Sharafi, and Saeed Soheilivand. 2018. "Fueling the Future; Plant Genetic Engineering for Sustainable Biodiesel Production." *Biofuel Research Journal* 5 (3): 829–45. https://doi.org/10.18331/BRJ2018.5.3.3.

Salimi, Zahra, and Seyed Ali Hosseini. 2019. "Study and Optimization of Conditions of Biodiesel Production from Edible Oils Using ZnO/BiFeO3 Nano Magnetic Catalyst." *Fuel* 239 (April 2018): 1204–12. https://doi.org/10.1016/j.fuel.2018.11.125.

Santos, Jose Luis, Päivi Mäki-Arvela, Antonio Monzón, Dmitry Yu Murzin, and Miguel Ángel Centeno. 2020. "Metal Catalysts Supported on Biochars: Part I Synthesis and Characterization." *Applied Catalysis B: Environmental* 268 (July): 118423. https://doi.org/10.1016/j.apcatb.2019.118423.

Semwal, Surbhi, Ajay K. Arora, Rajendra P. Badoni, and Deepak K. Tuli. 2011. "Biodiesel Production Using Heterogeneous Catalysts." *Bioresource Technology* 102 (3): 2151–61. https://doi.org/10.1016/j.biortech.2010.10.080.

Senthur Prabu, S., M.A. Asokan, Rahul Roy, Steff Francis, and M.K. Sreelekh. 2017. "Performance, Combustion and Emission Characteristics of Diesel Engine Fuelled with Waste Cooking Oil Bio-Diesel/Diesel Blends with Additives." *Energy* 122 (March): 638–48. https://doi.org/10.1016/j.energy.2017.01.119.

Shah, Syed Hasnain, Iftikhar Ahmed Raja, Muhammad Rizwan, Naim Rashid, Qaisar Mahmood, Fayyaz Ali Shah, and Arshid Pervez. 2018. "Potential of Microalgal Biodiesel Production and Its Sustainability Perspectives in Pakistan." *Renewable and Sustainable Energy Reviews* 81 (June 2016): 76–92. https://doi.org/10.1016/j.rser.2017.07.044.

Shan, Rui, Lili Lu, Yueyue Shi, Haoran Yuan, and Jiafu Shi. 2018. "Catalysts from Renewable Resources for Biodiesel Production." *Energy Conversion and Management* 178 (July): 277–89. https://doi.org/10.1016/j.enconman.2018.10.032.

Shankar, Vijayalakshmi, and Ranjitha Jambulingam. 2017. “Waste Crab Shell Derived CaO Impregnated Na-ZSM-5 as a Solid Base Catalyst for the Transesterification of Neem Oil into Biodiesel.” *Sustainable Environment Research* 27 (6): 273–78. https://doi.org/10.1016/j.serj.2017.06.006.

Sharma, Rohit Kumar, Crystal A. O’Neill, Hector A.R. Ramos, Bibek Thapa, Vanessa C. Barcelo-Bovea, Kavita Gaur, and Kai Griebenow. 2019. “Candida Rugosa Lipase Nanoparticles as Robust Catalyst for Biodiesel Production in Organic Solvents.” *Biofuel Research Journal* 6 (3): 1025–38. https://doi.org/10.18331/BRJ2019.6.3.3.

Sharma, Swati, Varun Saxena, Anupriya Baranwal, Pranjal Chandra, and Lalit Mohan Pandey. 2018. “Engineered Nanoporous Materials Mediated Heterogeneous Catalysts and Their Implications in Biodiesel Production.” *Materials Science for Energy Technologies* 1 (1): 11–21. https://doi.org/10.1016/j.mset.2018.05.002.

Sharma, Y.C., and Bhaskar Singh. 2010. “A Hybrid Feedstock for a Very Efficient Preparation of Biodiesel.” *Fuel Processing Technology* 91 (10): 1267–73. https://doi.org/10.1016/j.fuproc.2010.04.008.

Shen, Shiquan, Kai Sun, Zhizhao Che, Tianyou Wang, and Ming Jia. 2020. “Puffing and Micro-Explosion of Heated Droplets for Homogeneous Ethanol-Propanol-Hexadecane Fuel and Micro-Emulsified Ethanol-Biodiesel-Hexadecane Fuel.” *Applied Thermal Engineering* 165 (October 2019): 114537. https://doi.org/10.1016/j.applthermaleng.2019.114537.

Shokravi, Hoofar, Zahra Shokravi, Mahshid Heidarrezaei, Hwai Chyuan Ong, Seyed Saeid Rahimian Koloor, Michal Petrů, Woei Jye Lau, and Ahmad Fauzi Ismail. 2021. “Fourth Generation Biofuel from Genetically Modified Algal Biomass: Challenges and Future Directions.” *Chemosphere* 285 (July). https://doi.org/10.1016/j.chemosphere.2021.131535.

Shrivastava, Sakshi, Pooja Prajapati, Virendra, Priyanka Srivastava, Ajay P.S. Lodhi, Deepak Kumar, Varsha Sharma, S.K. Srivastava, and D.D. Agarwal. 2023. “Chemical Transesterification of Soybean Oil as a Feedstock for Stable Biodiesel and Biolubricant Production by Using Zn Al Hydrotalcites as a Catalyst and Perform Tribological Assessment.” *Industrial Crops and Products* 192 (December 2022): 116002. https://doi.org/10.1016/j.indcrop.2022.116002.

Shu, Qing, Jixian Gao, Zeeshan Nawaz, Yuhui Liao, Dezheng Wang, and Jinfu Wang. 2010. “Synthesis of Biodiesel from Waste Vegetable Oil with Large Amounts of Free Fatty Acids Using a Carbon-Based Solid Acid Catalyst.” *Applied Energy* 87 (8): 2589–96.

https://doi.org/10.1016/j.apenergy.2010.03.024.

Silva, J.S., J.S. Mendes, J.A.C. Correia, M.V.P. Rocha, and L. Micoli. 2018. “Cashew Apple Bagasse as New Feedstock for the Hydrogen Production Using Dark Fermentation Process.” *Journal of Biotechnology* 286 (April): 71–78. https://doi.org/10.1016/j.jbiotec.2018.09.004.

Silva, Rondinelly Brandão da, Alcides Fernandes Lima Neto, Lucas Samuel Soares dos Santos, José Renato de Oliveira Lima, Mariana Helena Chaves, José Ribeiro dos Santos, Geraldo Magela de Lima, Edmilson Miranda de Moura, and Carla Verônica Rodarte de Moura. 2008. “Catalysts of Cu(II) and Co(II) Ions Adsorbed in Chitosan Used in Transesterification of Soy Bean and Babassu Oils – A New Route for Biodiesel Syntheses.” *Bioresource Technology* 99 (15): 6793–98. https://doi.org/10.1016/j.biortech.2008.01.047.

Singh, B., Faizal Bux, and Y.C. Sharma. 2011. “Comparison of Homogeneous and Heterogeneous Catalysis for Synthesis of Biodiesel from M. Indica Oil.” *Chemical Industry and Chemical Engineering Quarterly* 17 (2): 117–24. https://doi.org/10.2298/CICEQ100902061S.

Singh, Digambar, Dilip Sharma, S.L. Soni, Chandrapal Singh Inda, Sumit Sharma, Pushpendra Kumar Sharma, and Amit Jhalani. 2021. “A Comprehensive Review of Physicochemical Properties, Production Process, Performance and Emissions Characteristics of 2nd Generation Biodiesel Feedstock: Jatropha Curcas.” *Fuel* 285 (April 2020): 119110. https://doi.org/10.1016/j.fuel.2020.119110.

Singh, Digambar, Dilip Sharma, S.L. Soni, Sumit Sharma, Pushpendra Kumar Sharma, and Amit Jhalani. 2020. “A Review on Feedstocks, Production Processes, and Yield for Different Generations of Biodiesel.” *Fuel* 262 (October): 116553. https://doi.org/10.1016/j.fuel.2019.116553.

Singh, Kawarpal, Sharoff Pon Kumar, and Bernhard Blümich. 2019. “Monitoring the Mechanism and Kinetics of a Transesterification Reaction for the Biodiesel Production with Low Field 1H NMR Spectroscopy.” *Fuel* 243 (January): 192–201. https://doi.org/10.1016/j.fuel.2019.01.084.

Singh, Thokchom Subhaschandra, and Tikendra Nath Verma. 2019. “Taguchi Design Approach for Extraction of Methyl Ester from Waste Cooking Oil Using Synthesized CaO as Heterogeneous Catalyst: Response Surface Methodology Optimization.” *Energy Conversion and Management* 182 (December 2018): 383–97. https://doi.org/10.1016/j.enconman.2018.12.077.

Sirisomboonchai, Suchada, Maidinamu Abuduwayiti, Guoqing Guan, Chanatip Samart, Shawket Abliz, Xiaogang Hao, Katsuki Kusakabe, and Abuliti Abudula. 2015. “Biodiesel Production from Waste Cooking Oil Using Calcined Scallop Shell as Catalyst.” *Energy Conversion and Management* 95 (May): 242–47. https://doi.org/10.1016/j.enconman.2015.02.044.

Siva, S., and C. Marimuthu. 2015. “Production of Biodiesel by Transesterification of Algae Oil with an Assistance of Nano-CaO Catalyst Derived from Egg Shell.” *International Journal of ChemTech Research* 7 (4): 2112–16.

Soares, Diniara, Andrei Ferreira Pinto, Alan Guilherme Gonçalves, David Alexander Mitchell, and Nadia Krieger. 2013. “Biodiesel Production from Soybean Soapstock Acid Oil by Hydrolysis in Subcritical Water Followed by Lipase-Catalyzed Esterification Using a Fermented Solid in a Packed-Bed Reactor.” *Biochemical Engineering Journal* 81 (December): 15–23. https://doi.org/10.1016/j.bej.2013.09.017.

Soly Peter, Alex, Mathews P. Alias, Mildo P. Iype, Jerin Jolly, Vishnu Sankar, K. Joseph Babu, and Deepa K. Baby. 2021. “Optimization of Biodiesel Production by Transesterification of Palm Oil and Evaluation of Biodiesel Quality.” *Materials Today: Proceedings* 42: 1002–7. https://doi.org/10.1016/j.matpr.2020.11.995.

Stamenković, Olivera S., Zoran B. Todorović, Miodrag L. Lazić, Vlada B. Veljković, and Dejan U. Skala. 2008. “Kinetics of Sunflower Oil Methanolysis at Low Temperatures.” *Bioresource Technology* 99 (5): 1131–40. https://doi.org/10.1016/j.biortech.2007.02.028.

Su, Erzheng, and Dongzhi Wei. 2014. “Improvement in Biodiesel Production from Soapstock Oil by One-Stage Lipase Catalyzed Methanolysis.” *Energy Conversion and Management* 88 (December): 60–65. https://doi.org/10.1016/j.enconman.2014.08.041.

Su, Guangcan, Nurin Wahidah Mohd Zulkifli, Hwai Chyuan Ong, Shaliza Ibrahim, Quan Bu, and Ruonan Zhu. 2022. “Pyrolysis of Oil Palm Wastes for Bioenergy in Malaysia: A Review.” *Renewable and Sustainable Energy Reviews* 164 (April): 112554. https://doi.org/10.1016/j.rser.2022.112554.

Sulaiman, Nur Fatin, Siew Ling Lee, Susilawati Toemen, and Wan Azelee Wan Abu Bakar. 2020. “Physicochemical Characteristics of Cu/Zn/γ-Al2O3 Catalyst and Its Mechanistic Study in Transesterification for Biodiesel Production.” *Renewable Energy* 156 (August): 142–57. https://doi.org/10.1016/j.renene.2020.04.021.

Sun, Xiao, Hasan K. Atiyeh, Mengxing Li, and Yan Chen. 2020. “Biochar Facilitated Bioprocessing and Biorefinery for Productions of Biofuel and Chemicals: A Review.” *Bioresource Technology* 295 (August 2019): 122252.

https://doi.org/10.1016/j.biortech.2019.122252.

Sun, Yingqiang, Harvind K. Reddy, Tapaswy Muppaneni, Sundaravadivelnathan Ponnusamy, Prafulla D. Patil, Changzhu Li, Lijuan Jiang, and Shuguang Deng. 2014. "A Comparative Study of Direct Transesterification of Camelina Oil under Supercritical Methanol, Ethanol and 1-Butanol Conditions." *Fuel* 135 (November): 530–36. https://doi.org/10.1016/j.fuel.2014.06.070.

Suwanno, Saowakon, Thanaphorn Rakkan, Tewan Yunu, Nisa Paichid, Pattarawadee Kimtun, Poonsuk Prasertsan, and Kanokphorn Sangkharak. 2017. "The Production of Biodiesel Using Residual Oil from Palm Oil Mill Effluent and Crude Lipase from Oil Palm Fruit as an Alternative Substrate and Catalyst." *Fuel* 195 (May): 82–87. https://doi.org/10.1016/j.fuel.2017.01.049.

Syazwani, O. N., Siow Hwa Teo, Aminul Islam, and Yun Hin Taufiq-Yap. 2017. "Transesterification Activity and Characterization of Natural CaO Derived from Waste Venus Clam (Tapes Belcheri S.) Material for Enhancement of Biodiesel Production." *Process Safety and Environmental Protection* 105: 303–15. https://doi.org/10.1016/j.psep.2016.11.011.

Tahvildari, Kambiz, Yasaman Naghavi Anaraki, Reza Fazaeli, Sogol Mirpanji, and Elham Delrish. 2015. "The Study of CaO and MgO Heterogenic Nano-Catalyst Coupling on Transesterification Reaction Efficacy in the Production of Biodiesel from Recycled Cooking Oil." *Journal of Environmental Health Science and Engineering* 13 (1): 1–9. https://doi.org/10.1186/s40201-015-0226-7.

Takase, Mohammed. 2022. "Biodiesel Yield and Conversion Percentage from Waste Frying Oil Using Fish Shell at Elmina as a Heterogeneous Catalyst and the Kinetics of the Reaction." Edited by Nour Sh. El-Gendy. *International Journal of Chemical Engineering* 2022 (August): 1–9. https://doi.org/10.1155/2022/8718638.

Takase, Mohammed, Min Zhang, Weiwei Feng, Yao Chen, Ting Zhao, Samuel J. Cobbina, Liuqing Yang, and Xiangyang Wu. 2014. "Application of Zirconia Modified with KOH as Heterogeneous Solid Base Catalyst to New Non-Edible Oil for Biodiesel." *Energy Conversion and Management* 80 (April): 117–25. https://doi.org/10.1016/j.enconman.2014.01.034.

Tamjidi, Sajad, Hossein Esmaeili, and Bahareh Kamyab Moghadas. 2021. "Performance of Functionalized Magnetic Nanocatalysts and Feedstocks on Biodiesel Production: A Review Study." *Journal of Cleaner Production* 305 (July): 127200. https://doi.org/10.1016/j.jclepro.2021.127200.

Tan, E. S., P. Kumaran, T. M. Indra, and K. Yoshikawa. 2017. “Effect of Non-Edible Biodiesel Physical and Chemical Properties as Microturbine Fuel.” *Energy Procedia* 142: 413–18. https://doi.org/10.1016/j.egypro.2017.12.065.

Tan, Yie Hua, Mohammad Omar Abdullah, and Cirilo Nolasco-Hipolito. 2015. “The Potential of Waste Cooking Oil-Based Biodiesel Using Heterogeneous Catalyst Derived from Various Calcined Eggshells Coupled with an Emulsification Technique: A Review on the Emission Reduction and Engine Performance.” *Renewable and Sustainable Energy Reviews* 47: 589–603. https://doi.org/10.1016/j.rser.2015.03.048.

Tan, Yie Hua, Mohammad Omar Abdullah, Cirilo Nolasco-Hipolito, and Yun Hin Taufiq-Yap. 2015. “Waste Ostrich- and Chicken-Eggshells as Heterogeneous Base Catalyst for Biodiesel Production from Used Cooking Oil: Catalyst Characterization and Biodiesel Yield Performance.” *Applied Energy* 160: 58–70. https://doi.org/10.1016/j.apenergy.2015.09.023.

Tang, Ying, Xuefan Gu, and Gang Chen. 2013. “99 % Yield Biodiesel Production from Rapeseed Oil Using Benzyl Bromide-CaO Catalyst.” *Environmental Chemistry Letters* 11 (2): 203–8. https://doi.org/10.1007/s10311-013-0403-9.

Tang, Zo Ee, Steven Lim, Yean-Ling Pang, Hwai-Chyuan Ong, and Keat-Teong Lee. 2018. “Synthesis of Biomass as Heterogeneous Catalyst for Application in Biodiesel Production: State of the Art and Fundamental Review.” *Renewable and Sustainable Energy Reviews* 92 (March): 235–53. https://doi.org/10.1016/j.rser.2018.04.056.

Tang, Zo Ee, Steven Lim, Yean-Ling Pang, Siew-Hoong Shuit, and Hwai-Chyuan Ong. 2020. “Utilisation of Biomass Wastes Based Activated Carbon Supported Heterogeneous Acid Catalyst for Biodiesel Production.” *Renewable Energy* 158 (October): 91–102. https://doi.org/10.1016/j.renene.2020.05.119.

Tarigan, Juliati Br, Haryo Tejo Prakoso, Donald Siahaan, and Jamaran Kaban. 2017. “Rapid Biodiesel Production From Palm Kernel Through In Situ Transesterification Reaction Using Cao As Catalyst.” *International Journal of Applied Chemistry* 13 (3): 631–46.

Temur Ergan, Başak, Gizem Yılmazer, and Mahmut Bayramoğlu. 2022. “Fast, High Quality and Low-Cost Biodiesel Production Using Dolomite Catalyst in an Enhanced Microwave System with Simultaneous Cooling.” *Cleaner Chemical Engineering* 3 (April): 100051. https://doi.org/10.1016/j.clce.2022.100051.

Teo, Siow Hwa, Motonobu Goto, and Yun Hin Taufiq-Yap. 2015. “Biodiesel Production from Jatropha Curcas L. Oil with Ca and La Mixed Oxide Catalyst in near Supercritical Methanol Conditions.” *The Journal of Supercritical Fluids* 104 (September): 243–50.

https://doi.org/10.1016/j.supflu.2015.06.023.

Teo, Siow Hwa, Aminul Islam, and Yun Hin Taufiq-Yap. 2016. “Algae Derived Biodiesel Using Nanocatalytic Transesterification Process.” *Chemical Engineering Research and Design* 111 (July): 362–70. https://doi.org/10.1016/j.cherd.2016.04.012.

Teoh, Y.H., H. Yaqoob, H.G. How, T.D. Le, and H.T. Nguyen. 2022. “Comparative Assessment of Performance, Emissions and Combustion Characteristics of Tire Pyrolysis Oil-Diesel and Biodiesel-Diesel Blends in a Common-Rail Direct Injection Engine.” *Fuel* 313 (October 2020): 123058. https://doi.org/10.1016/j.fuel.2021.123058.

Thitsartarn, Warintorn, and Sibudjing Kawi. 2011. “Transesterification of Oil by Sulfated Zr-Supported Mesoporous Silica.” *Industrial & Engineering Chemistry Research* 50 (13): 7857–65. https://doi.org/10.1021/ie1022817.

Tien Thanh, Nguyen, Marhaini Mostapha, Man Kee Lam, Syukriyah Ishak, Yaleeni Kanna Dasan, Jun Wei Lim, Inn Shi Tan, Sie Yon Lau, Bridgid Lai Fui Chin, and Tony Hadibarata. 2022. “Fundamental Understanding of In-Situ Transesterification of Microalgae Biomass to Biodiesel: A Critical Review.” *Energy Conversion and Management* 270 (August): 116212. https://doi.org/10.1016/j.enconman.2022.116212.

Tran, Nguyen Phuong Lan, Lu Ki Ong, and Yi-Hsu Ju. 2019. *Biodiesel Production From Waste Oils*. *Biofuels: Alternative Feedstocks and Conversion Processes for the Production of Liquid and Gaseous Biofuels*. 2nd ed. Elsevier Inc. https://doi.org/10.1016/b978-0-12-816856-1.00024-5.

Tran, Thi Tuong Vi, Sunanta Kaiprommarat, Suwadee Kongparakul, Prasert Reubroycharoen, Guoqing Guan, Manh Huan Nguyen, and Chanatip Samart. 2016. “Green Biodiesel Production from Waste Cooking Oil Using an Environmentally Benign Acid Catalyst.” *Waste Management* 52 (June): 367–74. https://doi.org/10.1016/j.wasman.2016.03.053.

Trass, Matthew, Abraham Becerra, and Kristen Parnell. 2017. “37 FAMEs In Under 25 Minutes by GC / FID Using Zebron ™ ZB-FAME.” Torrance, USA.

Unnithan, Unnikrishnan. 2022. “Status and Challenges Of Biodiesel Programme Implementation In Malaysia.” In *3rd Palm Biodiesel Conference*. Yogyakarta, Indonesia: Council of Palm Oil Producing Countries.

Uprety, Bijaya K., Wittavat Chaiwong, Chinomnso Ewelike, and Sudip K. Rakshit. 2016. “Biodiesel Production Using Heterogeneous Catalysts Including Wood Ash and the Importance of Enhancing Byproduct Glycerol Purity.” *Energy Conversion and Management* 115 (May): 191–99. https://doi.org/10.1016/j.enconman.2016.02.032.

Varkkey, Helena, Adam Tyson, and Shofwan Al Banna Choiruzzad. 2018. “Palm Oil

Intensification and Expansion in Indonesia and Malaysia: Environmental and Socio-Political Factors Influencing Policy." *Forest Policy and Economics* 92 (April): 148–59. https://doi.org/10.1016/j.forpol.2018.05.002.

Velasquez-Orta, S.B., J.G.M. Lee, and A. Harvey. 2012. "Alkaline in Situ Transesterification of Chlorella Vulgaris." *Fuel* 94 (April): 544–50. https://doi.org/10.1016/j.fuel.2011.11.045.

Venkat Reddy, Chinta Reddy, Reed Oshel, and John G. Verkade. 2006. "Room-Temperature Conversion of Soybean Oil and Poultry Fat to Biodiesel Catalyzed by Nanocrystalline Calcium Oxides." *Energy & Fuels* 20 (3): 1310–14. https://doi.org/10.1021/ef050435d.

Vieira, Fábio Roberto, Carlos M. Romero Luna, Gretta L.A.F. Arce, and Ivonete Ávila. 2020. "Optimization of Slow Pyrolysis Process Parameters Using a Fixed Bed Reactor for Biochar Yield from Rice Husk." *Biomass and Bioenergy* 132 (November 2019): 105412. https://doi.org/10.1016/j.biombioe.2019.105412.

Wahab, Abdul Ghani. 2022. "Malaysia: Biofuels Annual." Kuala Lumpur.

Wahlen, Bradley D., Robert M. Willis, and Lance C. Seefeldt. 2011. "Biodiesel Production by Simultaneous Extraction and Conversion of Total Lipids from Microalgae, Cyanobacteria, and Wild Mixed-Cultures." *Bioresource Technology* 102 (3): 2724–30. https://doi.org/10.1016/j.biortech.2010.11.026.

Wan Ghazali, Wan Nor Maawa, Rizalman Mamat, H. H. Masjuki, and Gholamhassan Najafi. 2015. "Effects of Biodiesel from Different Feedstocks on Engine Performance and Emissions: A Review." *Renewable and Sustainable Energy Reviews* 51: 585–602. https://doi.org/10.1016/j.rser.2015.06.031.

Wang, Anping, Hu Li, Hu Pan, Heng Zhang, Fusheng Xu, Zhaozhuo Yu, and Song Yang. 2018. "Efficient and Green Production of Biodiesel Catalyzed by Recyclable Biomass-Derived Magnetic Acids." *Fuel Processing Technology* 181 (October): 259–67. https://doi.org/10.1016/j.fuproc.2018.10.003.

Wang, Shuxiao, Haoran Yuan, Yazhuo Wang, and Rui Shan. 2017. "Transesterification of Vegetable Oil on Low Cost and Efficient Meat and Bone Meal Biochar Catalysts." *Energy Conversion and Management* 150 (June): 214–21. https://doi.org/10.1016/j.enconman.2017.08.020.

Wang, Xiaohang, Kun Yang, Rui Cai, Yujie ChenYang, Zhixing Huang, and Benyong Han. 2022. "Optimization and Kinetics of Biodiesel Production from Soybean Oil Using New Tetraethylammonium Ionic Liquids with Amino Acid-Based Anions as Catalysts." *Fuel* 324 (PA): 124510. https://doi.org/10.1016/j.fuel.2022.124510.

Wang, Ying Wen, Ya Jing Zhang, Kang Jun Wang, Li Mei Tan, and Shu Ying Chen. 2021. "Preparation of Ni/SiO2 by Ammonia Evaporation Method for Synthesis of 2-MTHF from 2-MF Hydrogenation." *Ranliao Huaxue Xuebao/Journal of Fuel Chemistry and Technology* 49 (1): 97–103. https://doi.org/10.1016/S1872-5813(21)60007-5.

Wei, Yi, Chaoyue Shen, Jiale Xie, and Quan Bu. 2020. "Study on Reaction Mechanism of Superior Bamboo Biochar Catalyst Production by Molten Alkali Carbonates Pyrolysis and Its Application for Cellulose Hydrolysis." *Science of The Total Environment* 712 (April): 136435. https://doi.org/10.1016/j.scitotenv.2019.136435.

Wei, Ziku, Chunli Xu, and Baoxin Li. 2009. "Application of Waste Eggshell as Low-Cost Solid Catalyst for Biodiesel Production." *Bioresource Technology* 100 (11): 2883–85. https://doi.org/10.1016/j.biortech.2008.12.039.

Willard, Matthew A., and Maria Daniil. 2013. "Nanocrystalline Soft Magnetic Alloys Two Decades of Progress." In *Handbook of Magnetic Materials*, 1st ed., 21:173–342. Elsevier B.V. https://doi.org/10.1016/B978-0-444-59593-5.00004-0.

Williams, Lauren. 2015. "Synthesis and Characterization of Biodiesel Fuels by Clay-Catalyzed Transesterifications." Stephen F. Austin State University.

Wong, Pak Kin, Meisam Ahmadi Ghadikolaei, Shou Hao Chen, Adebayo Afolabi Fadairo, Kar Wei Ng, Simon Ming Yuen Lee, Jin Cheng Xu, et al. 2022. "Physicochemical and Cell Toxicity Properties of Particulate Matter (PM) from a Diesel Vehicle Fueled with Diesel, Spent Coffee Ground Biodiesel, and Ethanol." *Science of The Total Environment* 824 (June): 153873. https://doi.org/10.1016/j.scitotenv.2022.153873.

Xia, Shaige, Jian Li, Guanyi Chen, Junyu Tao, Wanqing Li, and Guangbin Zhu. 2022. "Magnetic Reusable Acid-Base Bifunctional Co Doped Fe2O3–CaO Nanocatalysts for Biodiesel Production from Soybean Oil and Waste Frying Oil." *Renewable Energy* 189 (April): 421–34. https://doi.org/10.1016/j.renene.2022.02.122.

Xie, Qianqian, Xiao Yang, Kangning Xu, Zheng Chen, Binoy Sarkar, and Xiaomin Dou. 2020. "Conversion of Biochar to Sulfonated Solid Acid Catalysts for Spiramycin Hydrolysis: Insights into the Sulfonation Process." *Environmental Research* 188 (July): 109887. https://doi.org/10.1016/j.envres.2020.109887.

Xie, Wenlei, and Hao Wang. 2020. "Synthesis of Heterogenized Polyoxometalate-Based Ionic Liquids with Brönsted-Lewis Acid Sites: A Magnetically Recyclable Catalyst for Biodiesel Production from Low-Quality Oils." *Journal of Industrial and Engineering Chemistry* 87 (July): 162–72. https://doi.org/10.1016/j.jiec.2020.03.033.

Xu, Ruoyu, and Yongli Mi. 2011. "Simplifying the Process of Microalgal Biodiesel Production

Through In Situ Transesterification Technology." *Journal of the American Oil Chemists' Society* 88 (1): 91–99. https://doi.org/10.1007/s11746-010-1653-3.

Yaakob, Zahira, Masita Mohammad, Mohammad Alherbawi, Zahangir Alam, and Kamaruzaman Sopian. 2013. "Overview of the Production of Biodiesel from Waste Cooking Oil." *Renewable and Sustainable Energy Reviews* 18 (February): 184–93. https://doi.org/10.1016/j.rser.2012.10.016.

Yameen, Muhammad Zubair, Hamad AlMohamadi, Salman Raza Naqvi, Tayyaba Noor, Wei-Hsin Chen, and Nor Aishah Saidina Amin. 2023. "Advances in Production & Activation of Marine Macroalgae-Derived Biochar Catalyst for Sustainable Biodiesel Production." *Fuel* 337 (December 2022): 127215. https://doi.org/10.1016/j.fuel.2022.127215.

Yan, Jinyong, Xianliang Zheng, and Shengying Li. 2014. "A Novel and Robust Recombinant Pichia Pastoris Yeast Whole Cell Biocatalyst with Intracellular Overexpression of a Thermomyces Lanuginosus Lipase: Preparation, Characterization and Application in Biodiesel Production." *Bioresource Technology* 151: 43–48. https://doi.org/10.1016/j.biortech.2013.10.037.

Yang, Jong, AS Ahmed, and Sinin Hamdan. 2012. "Production of Biodiesel From Waste Deep Frying Oils As a Renewable Energy Source." *Asian Journal of Science and Technology* 4 (11): 54–57.

Yang‡, Dan, Huaiyun Zhang, Kuan Peng, Lili Chen, Hanjie He, Xiaoxi Huang, Jieming Qin, Gongxiu He, and Dangquan Zhang. 2016. "Differential Gene Regulation of Lipid Synthesis in the Developing Seeds of Two Biodiesel Tree Species, Jatropha and Vernicia." *International Journal of Agriculture and Biology* 18 (06): 1143–52. https://doi.org/10.17957/IJAB/15.0218.

Yari, Neda, Mostafa Mostafaei, Leila Naderloo, and Seyed Mohammad Safieddin Ardebili. 2022. "Energy Indicators for Microwave-Assisted Biodiesel Production from Waste Fish Oil." *Energy Sources, Part A: Recovery, Utilization, and Environmental Effects* 44 (1): 2208–19. https://doi.org/10.1080/15567036.2019.1649324.

Ye, Wei, Yujie Gao, Hui Ding, Mingchao Liu, Shejiang Liu, Xu Han, and Jinlong Qi. 2016. "Kinetics of Transesterification of Palm Oil under Conventional Heating and Microwave Irradiation, Using CaO as Heterogeneous Catalyst." *Fuel* 180: 574–79. https://doi.org/10.1016/j.fuel.2016.04.084.

Yepes Maya, Diego Mauricio, Electo Eduardo Silva Lora, Rubenildo Vieira Andrade, Albert Ratner, and Juan Daniel Martínez Angel. 2021. "Biomass Gasification Using Mixtures of Air, Saturated Steam, and Oxygen in a Two-Stage Downdraft Gasifier. Assessment Using

a CFD Modeling Approach." *Renewable Energy* 177 (November): 1014–30. https://doi.org/10.1016/j.renene.2021.06.051.

Yi, Yunqiang, Guoquan Tu, Guangguo Ying, Zhanqiang Fang, and Eric Pokeung Tsang. 2021. "Magnetic Biochar Derived from Rice Straw and Stainless Steel Pickling Waste Liquor for Highly Efficient Adsorption of Crystal Violet." *Bioresource Technology* 341 (August): 125743. https://doi.org/10.1016/j.biortech.2021.125743.

You, Siming, Yong Sik Ok, Daniel C. W. Tsang, Eilhann E. Kwon, and Chi-Hwa Wang. 2018. "Towards Practical Application of Gasification: A Critical Review from Syngas and Biochar Perspectives." *Critical Reviews in Environmental Science and Technology* 48 (22–24): 1165–1213. https://doi.org/10.1080/10643389.2018.1518860.

Yu, Hewei, Yunlong Cao, Heyao Li, Gaiju Zhao, Xingyu Zhang, Shen Cheng, and Wei Wei. 2021. "An Efficient Heterogeneous Acid Catalyst Derived from Waste Ginger Straw for Biodiesel Production." *Renewable Energy* 176 (October): 533–42. https://doi.org/10.1016/j.renene.2021.05.098.

Zabeti, Masoud, Wan Mohd Ashri Wan Daud, and Mohamed Kheireddine Aroua. 2010. "Biodiesel Production Using Alumina-Supported Calcium Oxide: An Optimization Study." *Fuel Processing Technology* 91 (2): 243–48. https://doi.org/10.1016/j.fuproc.2009.10.004.

Zaharin, M. S.M., N. R. Abdullah, G. Najafi, H. Sharudin, and T. Yusaf. 2017. "Effects of Physicochemical Properties of Biodiesel Fuel Blends with Alcohol on Diesel Engine Performance and Exhaust Emissions: A Review." *Renewable and Sustainable Energy Reviews* 79 (April 2016): 475–93. https://doi.org/10.1016/j.rser.2017.05.035.

Zama, Eric F., Yong-Guan Zhu, Brian J. Reid, and Gou-Xin Sun. 2017. "The Role of Biochar Properties in Influencing the Sorption and Desorption of Pb(II), Cd(II) and As(III) in Aqueous Solution." *Journal of Cleaner Production* 148 (April): 127–36. https://doi.org/10.1016/j.jclepro.2017.01.125.

Zeng, Danlin, Shenglan Liu, Wanjun Gong, Guanghui Wang, Jianghua Qiu, and Hongxiang Chen. 2014. "Synthesis, Characterization and Acid Catalysis of Solid Acid from Peanut Shell." *Applied Catalysis A: General* 469 (January): 284–89. https://doi.org/10.1016/j.apcata.2013.09.038.

Zeng, Jianli, Xiaodong Wang, Bing Zhao, Jingcan Sun, and Yuchun Wang. 2009. "Rapid In Situ Transesterification of Sunflower Oil." *Industrial & Engineering Chemistry Research* 48 (2): 850–56. https://doi.org/10.1021/ie8008956.

Zhang, Bingxin, Ming Gao, Jiayu Geng, Yuwei Cheng, Xiaona Wang, Chuanfu Wu, Qunhui

Wang, Shu Liu, and Siu Ming Cheung. 2021. “Catalytic Performance and Deactivation Mechanism of a One-Step Sulfonated Carbon-Based Solid-Acid Catalyst in an Esterification Reaction.” *Renewable Energy* 164 (February): 824–32. https://doi.org/10.1016/j.renene.2020.09.076.

Zhang, Fan, Zhen Fang, and Yi-Tong Wang. 2015. “Biodiesel Production Direct from High Acid Value Oil with a Novel Magnetic Carbonaceous Acid.” *Applied Energy* 155 (October): 637–47. https://doi.org/10.1016/j.apenergy.2015.06.044.

Zhang, Fan, Xiao-Fei Tian, Zhen Fang, Mazloom Shah, Yi-Tong Wang, Wen Jiang, and Min Yao. 2017. “Catalytic Production of Jatropha Biodiesel and Hydrogen with Magnetic Carbonaceous Acid and Base Synthesized from Jatropha Hulls.” *Energy Conversion and Management* 142 (June): 107–16. https://doi.org/10.1016/j.enconman.2017.03.026.

Zhang, Fan, Xue-Hua Wu, Min Yao, Zhen Fang, and Yi-Tong Wang. 2016. “Production of Biodiesel and Hydrogen from Plant Oil Catalyzed by Magnetic Carbon-Supported Nickel and Sodium Silicate.” *Green Chemistry* 18 (11): 3302–14. https://doi.org/10.1039/C5GC02680F.

Zhang, Junsong. 2017. “Utilization of Fats , Oils and Grease in Biodiesel Production : From Market Study to Technical Feasibility.” University of Cincinnati.

Zhang, Liping, Boyang Sheng, Zhong Xin, Qun Liu, and Shuzhen Sun. 2010. “Kinetics of Transesterification of Palm Oil and Dimethyl Carbonate for Biodiesel Production at the Catalysis of Heterogeneous Base Catalyst.” *Bioresource Technology* 101 (21): 8144–50. https://doi.org/10.1016/j.biortech.2010.05.069.

Zhang, Xia, Jing Li, Yang Chen, Jianghua Wang, Laughlin Feng, Xiaohong Wang, and Fenghua Cao. 2009. “Heteropolyacid Nanoreactor with Double Acid Sites as a Highly Efficient and Reusable Catalyst for the Transesterification of Waste Cooking Oil.” *Energy & Fuels* 23 (9): 4640–46. https://doi.org/10.1021/ef900396a.

Zhang, Yunhua, Diming Lou, Piqiang Tan, Zhiyuan Hu, and Liang Fang. 2022. “Effects of Waste-Cooking-Oil Biodiesel Blends on Diesel Vehicle Emissions and Their Reducing Characteristics with Exhaust after-Treatment System.” *Journal of Cleaner Production* 381 (P1): 135190. https://doi.org/10.1016/j.jclepro.2022.135190.

Zhao, Lina, Zheyan Qiu, and Susan M. Stagg-Williams. 2013. “Transesterification of Canola Oil Catalyzed by Nanopowder Calcium Oxide.” *Fuel Processing Technology* 114 (October): 154–62. https://doi.org/10.1016/j.fuproc.2013.03.027.

Zhou, Wenguang, Paul Chen, Min Min, Xiaochen Ma, Jinghan Wang, Richard Griffith, Fida Hussain, et al. 2014. “Environment-Enhancing Algal Biofuel Production Using

Wastewaters." *Renewable and Sustainable Energy Reviews* 36 (August): 256–69. https://doi.org/10.1016/j.rser.2014.04.073.

Zhu, Huaping, Zongbin Wu, Yuanxiong Chen, Ping Zhang, Shijie Duan, Xiaohua Liu, and Zongqiang Mao. 2006. "Preparation of Biodiesel Catalyzed by Solid Super Base of Calcium Oxide and Its Refining Process." *Chinese Journal of Catalysis* 27 (5): 391–96. https://doi.org/10.1016/S1872-2067(06)60024-7.

Zillillah, Toh Ann Ngu, and Zhi Li. 2014. "Phosphotungstic Acid-Functionalized Magnetic Nanoparticles as an Efficient and Recyclable Catalyst for the One-Pot Production of Biodiesel from Grease via Esterification and Transesterification." *Green Chemistry* 16 (3): 1202. https://doi.org/10.1039/c3gc41379a.

Zohuri, Bahman, and Patrick McDaniel. 2021. "Population Growth Driving Energy Demand." In *Introduction to Energy Essentials*, 1–42. Elsevier. https://doi.org/10.1016/B978-0-323-90152-9.00001-3.

APPENDICES

Appendix A: Data for the design of experiment using RSM-CCD module of Design-Expert version 12 software.

Standard Order	Run Order	Space Point Type	Catalyst loading (wt%)	Methanol-oil molar ratio	Temperature (°C)	Time (h)	Biodiesel Yield	
							Predicted	Experimental
1	3	Factorial	7	15	55	4	76.20	74.79
2	24	Factorial	13	15	55	4	67.77	69.62
3	15	Factorial	7	25	55	4	81.17	80.77
4	29	Factorial	13	25	55	4	78.74	79.17
5	28	Factorial	7	15	65	4	80.86	80.35
6	19	Factorial	13	15	65	4	73.56	72.67
7	20	Factorial	7	25	65	4	85.72	87.05
8	26	Factorial	13	25	65	4	84.43	83.90
9	5	Factorial	7	15	55	8	76.20	77.17
10	18	Factorial	13	15	55	8	67.59	66.29
11	23	Factorial	7	25	55	8	83.68	84.59
12	27	Factorial	13	25	55	8	81.08	82.03
13	16	Factorial	7	15	65	8	82.71	82.31
14	11	Factorial	13	15	65	8	75.24	76.08
15	21	Factorial	7	25	65	8	90.08	88.67
16	7	Factorial	13	25	65	8	88.62	90.06
17	22	Axial	4	20	60	6	72.61	73.31
18	17	Axial	16	20	60	6	62.71	61.55
19	4	Axial	10	10	60	6	73.36	74.02
20	14	Axial	10	30	60	6	91.70	90.57
21	8	Axial	10	20	50	6	79.24	78.47
22	9	Axial	10	20	70	6	91.44	91.74

Appendix A continued.

23	30	Axial	10	20	60	2	80.79	81.08
24	1	Axial	10	20	60	10	84.98	84.22
25	10	Center	10	20	60	6	89.00	91.30
26	2	Center	10	20	60	6	89.00	90.19
27	13	Center	10	20	60	6	89.00	85.47
28	6	Center	10	20	60	6	89.00	90.68
29	25	Center	10	20	60	6	89.00	87.51
30	12	Center	10	20	60	6	89.00	88.87

Appendix B: Sample graph and calculation of GC result.

Single Injection Report

Agilent

Data file:	2022-11-02 15-09-53+08-00-13.dx		
Sequence Name:	8890GC-2022-11-02 08-32-17+08-00	**Project Name:**	Firdaus
Sample name:		**Operator:**	SYSTEM
Instrument:	8890GC	**Injection date:**	2022-11-02 15:15:41+08:00
Inj. volume:	1.000	**Location:**	10
Acq. method:	FAME Phenomenex + IS Layer.amx	**Type:**	Sample
Processing method:	*GC_LC Quantitative_DefaultMethod_NoSolvent+BlankSubtraction.pmx	**Sample amount:**	0.00
Manually modified:	None		

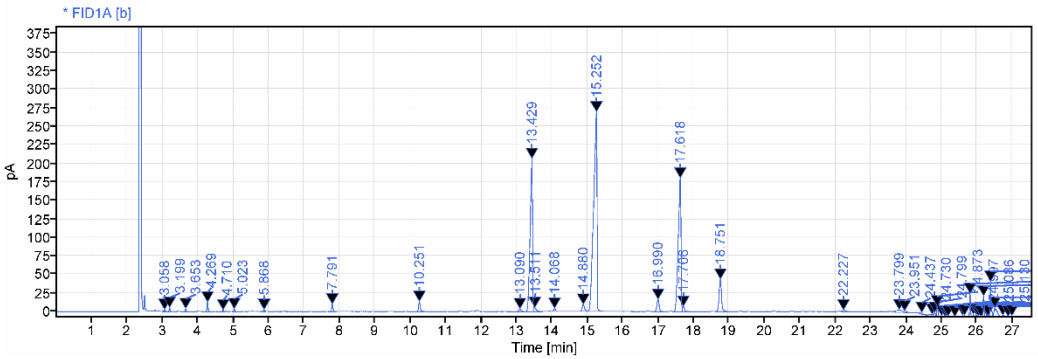

Signal: * FID1A [b]

RT [min]	Type	Width [min]	Area	Height	Area%	Name
3.058	BB	0.14	5.54	2.44	0.11	
3.199	BV	0.12	9.58	5.21	0.20	
3.653	BV	0.18	7.32	3.72	0.15	
4.269	BV	0.23	26.67	12.68	0.55	Methyl octanoate (C8:0)
4.710	BV	0.11	4.66	1.99	0.10	
5.023	VB	0.16	7.63	3.47	0.16	
5.868	BV	0.10	4.98	2.34	0.10	Methyl decanoate (C10:0)
7.791	VV	0.22	24.99	9.80	0.51	Methyl laurate (C12:0)
10.251	BV	0.31	43.72	13.50	0.89	Methyl myristate (C14:0)
13.090	BB	0.25	15.10	3.59	0.31	
13.429	BV	0.24	976.17	206.42	19.97	
13.511	VB	0.31	22.64	5.14	0.46	
14.068	VV	0.26	15.71	4.00	0.32	Methyl palmitoleate (C16:1)
14.880	BV	0.29	43.12	9.15	0.88	
15.252	VV	0.50	1764.06	269.39	36.09	Methyl heptadecanoate (C17:0)
16.990	VV	0.36	75.15	16.44	1.54	
17.618	BV	0.25	973.10	180.51	19.91	
17.706	VV	0.24	28.23	7.09	0.58	

C:\CDSProjects\Firdaus\Report Templates\01_ShortArea_CroppedSolvent.rdl [Rev. 8] Printed: 2022-11-03 10:54:16+08:00 Page 23 of 24

Single Injection Report

Agilent

RT [min]	Type	Width [min]	Area	Height	Area%	Name
18.751	VB	0.58	208.23	43.79	4.26	Methyl linoleate (C18:2)
22.227	VV	0.28	15.56	2.00	0.32	
23.799	VV	0.32	40.10	3.33	0.82	Methyl behenate (C22:0)
23.951	VB	0.23	9.57	1.83	0.20	Methyl erucate (C22:1)
24.437	VB	0.17	10.06	2.19	0.21	
24.730	VV	0.06	6.10	2.17	0.12	
24.799	VB	0.08	15.24	4.98	0.31	
24.873	BV	0.13	34.67	14.18	0.71	
24.997	VB	0.06	4.20	2.23	0.09	
25.086	BB	0.08	3.36	1.88	0.07	
25.130	BV	0.05	5.52	2.50	0.11	Methyl lignocerate (C24:0)
25.177	VB	0.11	10.87	2.77	0.22	
25.369	VB	0.11	10.88	3.06	0.22	
25.590	BV	0.11	15.87	4.71	0.32	
25.642	VB	0.07	11.20	4.67	0.23	
25.800	BB	0.11	65.50	33.24	1.34	
25.891	BV	0.08	14.09	5.89	0.29	
25.974	VV	0.06	16.25	6.05	0.33	
26.027	VB	0.07	17.44	5.79	0.36	
26.103	BV	0.06	11.13	3.93	0.23	
26.182	VB	0.11	82.62	31.46	1.69	
26.267	BV	0.06	6.97	3.88	0.14	
26.303	VB	0.04	3.80	2.52	0.08	
26.378	BV	0.11	109.16	48.83	2.23	
26.497	VV	0.20	85.70	13.62	1.75	
26.724	BB	0.14	16.10	3.23	0.33	
26.873	BV	0.07	5.29	1.93	0.11	
26.983	VBA	0.05	4.61	2.48	0.09	
		Sum	**4888.45**			

$$Y = \frac{(\sum A) - A_{IS}}{A_{IS}} \times \frac{C_{IS} \times V_{IS}}{W} \times 100$$

where Y = biodiesel yield (%)

From GC result, $\sum A$ = total peak area, A_{IS} = peak area of internal standard

From sample preparation, C_{IS} = concentration of internal standard (mg mL^{-1}), V_{IS} = volume of internal standard injected (mL), W = weight of crude biodiesel sample injected (mg)

$\sum A = 4888.45$

$A_{IS} = 1764.06$

$C_{IS} = 5$ mg mL^{-1}

$V_{IS} = 0.001$ mL

W = 0.0097 mg

$$Y = \frac{4888.45 - 1764.06}{1764.06} \times \frac{5 \times 0.001}{0.0097} \times 100$$

= 91.30 %